Development and Uses of a Primary Fish Gill Cell Culture System to investigate the Uptake, Efflux and Metabolism of Pharmaceuticals in Ecotoxicology

Stott, Lucy Claire

Awarding institution:
King's College London

Development and Uses of a Primary Fish Gill Cell Culture System to investigate the Uptake, Efflux and Metabolism of Pharmaceuticals in Ecotoxicology

Lucy C. Stott

SANCTE ET SAPIENTER

King's College London

A thesis submitted in fulfilment of the requirements for the degree of
Doctor of Philosophy

2016

I. Abstract

Worldwide, many animals are used in regulatory and academic studies to determine the environmental fate and impact of xenobiotic compounds that may be released into the environment. Fish are commonly used in these tests as they inhabit the aquatic environment, the sink into which many pharmaceuticals eventually enter. Fish gills are the primary site of xenobiotic uptake. In line with the replacement, reduction and refinement (3Rs) of the use of animals in scientific practices, alternative methods to *in vivo* fish testing are required. For rainbow trout (*Oncorhynchus mykiss*), a commonly used species in European and American *in vivo* regulatory testing, two gill epithelial models exist – primary gill cells cultured in a two compartment model (termed DSI – double seeded inserts) and the immortalised gill cell line RTgill-W1. This work uses these gill cell models to characterise the physiology of the *in vitro* gill epithelium and assess their suitability as epithelial gill surrogates. DSI cultures were found to have characteristics similar to the in tact gill, whilst experiments investigating the co-culture of RTgill-W1 with primary gill cells failed to produce epithelia with such features, like high TER and low paracellular permeability. The DSI cell culture system was used to investigate the uptake and efflux of pharmaceuticals over the gill and found that for some, active uptake plays a small but significant role. This work further investigates the metabolism of pharmaceuticals at the gill and shows the relevance of the primary gill cell DSI technique as an appropriate *in vitro* model, as the metabolite hydroxypropranolol was detected, which in single-seeded primary cultures (SSI) and RTgill-W1, it was not. This work is an important step forward in the development of alternative *in vitro* methods to assess the ecotoxicology of xenobiotic compounds in fish and provides evidence that the primary gill cell DSI technique provides the most accurate *in vitro* gill model. Experimental information obtained from DSI uptake, efflux and metabolism assays has the potential to be incorporated into and supplement *in vivo* regulatory studies, therefore reducing the numbers of fish used in such tests.

II. Table of Contents

III. List of Figures

IV. List of Tables

V. List of Abbreviations

β   Beta

Ω   Ohms

μm   Micrometres

^{o}C   Degrees Celsius

%   Percent

3D   Three-dimensional

3Rs   Replace, reduce, refine

A   Apical

ABC   ATP-binding cassette

ADME   Absorption, distribution, metabolism and excretion

AhR   Aryl hydrocarbon receptors

AnF   Alpha-naphthoflavone

ANOVA Analysis of variance

API   Active pharmaceutical ingredients

ARNT   Aryl hydrocarbon nuclear translocation

ATP   Adenosine triphosphate

B   Basal

BBB   Blood brain barrier

BCF   Bioconcentration Factor

BCRP   Breast cancer resistance protein

BFCOD Benzyloxy-4-trifluoromethylcoumarin-*O*-debenzyloxylase

BioP   Biocidal Products

BnF   Beta-naphthoflavone

BSA   Bovine serum albumin

BSEP   Bile salt export pump

BTA   Bi-directional transport assay

C   Carbon

Ca^{2+} Calcium ion

cAMP   Cyclic adenosine monophosphate

CC   Chloride cell

CEC   Contaminants of emerging concern

CETA   Concentration equilibrated transport assay

Ci   Curie

Cl^- Chloride ion

cm   Centimetre

CO_2 Carbon dioxide

Ctl   Control

CYP   Cytochrome P450

DAPSEI   2-(4-(dimethylamino)styryl) -N-ethylpyridinium iodide

DMSO   Dimethyl sulfoxide

dpm   Disintegrations per minute

Dr   Doctor

DSI   Double seeded insert

DSII   Double seeded inverted insert

EA   Environment Agency

ECHA   The European Chemicals Agency

EDTA	Ethylenediaminetetraacetic acid
EGF	Epidermal growth factor
EMEA	European Agency for the Evaluation of Medicinal Products
EROD	7-ethoxy-resorufin-O-deethylase
EU	European Union
FBS	Fetal bovine serum
FIFRA	The Federal Insecticide, Fungicide and Rodenticide Act
Fig	Figure
FW	Freshwater
g	Gram
GLP	Good laboratory practice
h	Hours
H^+	Hydrogen ion
HBSS	Hank's balanced salt solution
HCO_3^-	Bicarbonate ion
HOP	Hydroxypropranolol
HPLC	High-performance liquid chromatography
HSD	Honest significance test
JAM	Junction adhesion molecules
K^+	Potassium ion
kΩ	Kilohms
Kg	Kilogram
K_{ow}	Octanol-water partitioning coefficient
L	Litre
L-15	Leibovitz-15 cell culture medium

LDH	Lactose dehydrogenase
LOD	Limit of detection
LOQ	Limit of quantification
m	Minute
MDR	Multidrug resistance
MDCK	Madin-Darby canine kidney
MFO	Mixed-function oxidase
mg	Milligram
mL	Millilitre
mmol	Millimoles
MO	Monooxygenase
mOsm	Milliosmoles
mr	Microridges
MRC	Mitochondria-rich cell
MRP	Multidrug resistance protein
MTT	3-(4,5-Dimethylthiazol-2-Yl)-2,5-diphenyltetrazolium bromide
mV	Millivolt
MW	Molecular weight
MXR	Multixenobiotic resistance
n	Number
Na^+	Sodium ion
NBD	Nucleotide binding domain
ng	Nanogram
NH_3	Ammonia
NH_4^+	Ammonium ion

nm   Nanometre

nmol   Nanomoles

OCT   Organic cation transporter

OECD   Organisation for Economic Co-operation and Development

P   Passage

P   Probability

PAH   polycyclic aromatic hydrocarbon

P_{app} Apparent permeability coefficient

PBS   Phosphate buffered saline

PCB   Polychlorinated biphenols

PCDF   Polychlorinated dibenzofurans

PEG   Polyethylene glycol

PET   Polyethylene terephthalate

PgP   Permeability glycoprotein

pHEMA Poly(2-hydroxyethylmethacrylate)

pK_a Dissociation constant

pm   Plasma membrane

pmol   Picomoles

PPP   Plant protection products

PPR   Propranolol

Prof   Professor

psi   Pounds per square inch

PVC   Pavement cell

qRT-PCR Quantitative real time polymerase chain reaction

QSARs Quantitative structure activity relationships

REACH Registration, Evaluation, Authorisation & Restriction of Chemicals

Rh   Rhesus

Rpm   Rotations per minute

s   Second

SD   Standard deviation

SEM   Standard error of the mean

SLC   Solute carrier

SPE   Solid phase extraction

SSI   Single seeded insert

TCDD   Tetrachlorodibenzodioxin

TEP   Transepithelial potential

TER   Transepithelial resistance

TJ   Tight junction

TMD   Transmembrane domain

TR   Transport ratio

TSCA   The Toxic Substances Control Act

UPLC/MS Ultra-performance liquid chromatography tandem mass spectrometry

UWL   Unstirred water layer

v/v   Volume per volume

WWTP Waste water treatment plants

ZO-1   Zonula occludin

VI. Acknowledgements

Chapter 1

General Introduction

1.1   Introduction

The objectives of this work are to develop and assess the suitability of a primary fish gill cell culture system for characterising the transport and metabolism of xenobiotics, namely pharmaceuticals, at the rainbow trout (*Oncorhynchus mykiss*) gill. Through the development of this *in vitro* gill model there is the potential to replace fish in toxicological studies, which fulfils the UK government's current aims to reduce, replace and refine (3Rs) the use of animals in scientific research (Gov.UK, 2014). The freshwater teleost fish gill is a multifunctional organ. It is the primary site of respiratory gas exchange, ionic and osmotic regulation and nitrogenous waste excretion (Evans et al., 2005). The gill is adapted to maximise diffusive gas exchange whilst regulating the influx and efflux of water, ions and compounds and because of its constant contact with the aquatic environment, it is also the primary site of xenobiotic uptake from water (Bury et al., 2014).

1.2   Gill physiology and anatomy

Four gill arches lie beneath the operculum on either lateral side of the rainbow trout head. The filament abductor and adductor muscles control the positioning of the arches dependent on oxygen requirement from exercise, stress or hypoxia. Each gill arch bears hundreds of gill filaments lined in two hemibranch rows, each possessing thousands of leaf-like respiratory lamellae (Fig 1.1). The positioning of the lamellae with respect to the flow of water through the mouth and over the gills (Fig 1.2A) creates a counter-current flow system whereby blood flow through the lamellae is

opposite to that of the water over the gills (Fig 1.2B). This maintains a high oxygen concentration gradient between the blood and the water, even to near-fully oxygenated blood, maximising the efficiency of blood oxygenation (Wood, 2001).
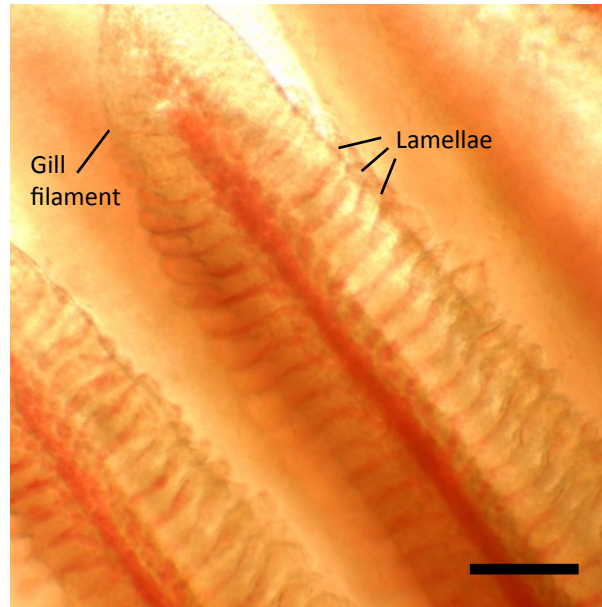
Fig 1.1 The gill filaments are made up of thousands of finger-like structures called lamellae. Bar = 0.5 mm.

The osmotic concentration of freshwater trout blood is in the range of 260-330 mOsm Kg^{-1}, whilst that of freshwater is typically less than 20 mOsm Kg^{-1} (Jobling, 1995). This osmotic gradient has profound effects on the fish's ability to maintain ionic homeostasis. Firstly, it means freshwater teleosts will absorb water across the gills, which is then excreted via the kidney as dilute urine. Secondly, fish will lose ions across the gill, which is compensated for by active ion uptake at the gill and intestine and efficient ionic reabsorption from the urine by the kidneys. Ions taken up at the gill and via food are reabsorbed in the kidney nephrons to counteract the high water excretion rate (approximately 4 mL. Kg^{-1} h^{-1}; Jobling, 1995).
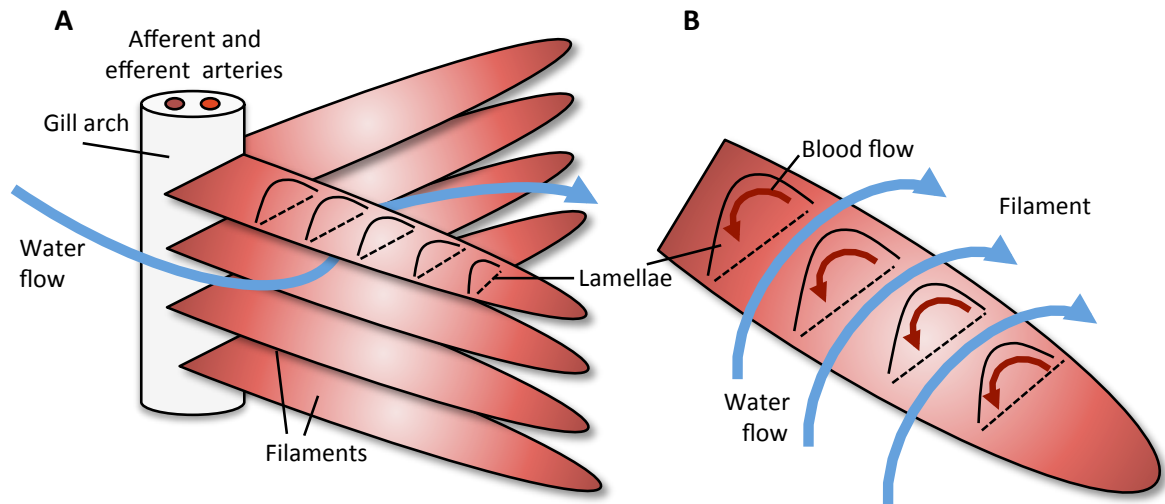
Fig 1.2 The counter current of blood flow to water flow in the teleost gill. Water flows between the gill filaments attached to the gill arch (A). Each filament possesses many leaf-like processes called lamellae, in which the blood flows in the opposite direction to the water flowing between them (B).

Nitrogen excretion in rainbow trout is mostly through the elimination of ammonium ions (NH_4^+), which constitute around 90% of nitrogenous waste in freshwater rainbow trout (McDonald & Wood, 2004). Oxygen crosses the branchial epithelium by diffusion and is used in cellular metabolism, producing water and carbon dioxide. These are diffusively excreted via the partial pressure gradient set up at the gill. Carbonic anhydrase may also convert carbon dioxide (CO_2) and water to bicarbonate ions (HCO_3^-) (excreted by a chloride, Cl^-/HCO_3^- exchanger) and hydrogen ions (H^+), which form ammonium ions (NH_4^+) that are excreted via a sodium/ammonium (Na^+/NH_4^+) exchanger (Wood, 2001). Ammonia (NH_3) may also be excreted via Rhesus (Rh) ammonia transport proteins (Wright & Wood, 2009). In the water most adjacent to the branchial epithelium, termed the unstirred water layer (UWL; a boundary layer), ions excreted undergo further reactions, such as the conversion of CO_2 back to HCO_3^- and H^+, which further maintains the partial pressure gradients required for these transport processes to occur (Wood, 2001).
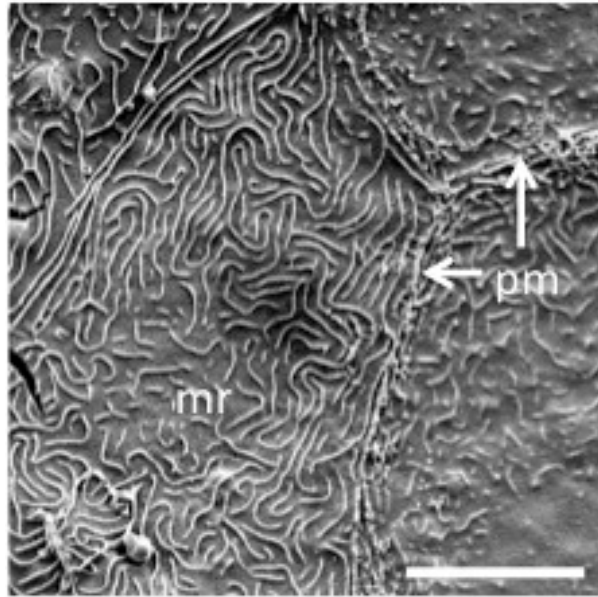
Fig 1.3 Scanning electron micrograph of the apical gill cell surface *in vitro*. The irregularly shaped epithelial cells with

microridges (mr) and plasma membrane (pm) can be observed. Bar = 20 µm. Reproduced with permission from Dr

Sabine Schnell.

The branchial epithelium is composed of four differentiated cell types: pavement cells (PVCs),

mitochondria-rich cells (MRCs), mucous cells and neuro-epithelial cells (Wood, 2001). Internally,

collagen and pillar cells channel blood flow from afferent lamellar arterioles to efferent along the

leading margin of each filament (Penrice & Eddy, 1993).

PVCs are polygonal cells, comprising at least 80% of the trout gill epithelium and are thought to be

responsible for diffusive gas exchange (Leguen et al., 2001; Wood, 2001). Microridges can be

observed on the apical surface (Fig 1.3) and function to increase the surface area and maintain the

UWL (Wood, 2001). A glycocalyx mucus layer produced by the mucous cells covers this. MRCs are

fewer, covering less than 15% of the epithelium and were first documented by Keys and Willmer

(1932) when describing the cells responsible for chloride ion excretion in seawater teleosts; hence

their initial terming as chloride cells (CCs). MRCs are the main site of active Cl^-, calcium ion (Ca^{2+})

and Na^+ exchange (Wood, 2001), and so possess many mitochondria to provide the energy for

these processes to occur (Perry, 1997). Histology shows that the MRCs are indented and more

rounded due to their partial covering by PVCs, with deep tight junctions and desmosomes between cells (Evans et al., 2005; Wood, 2001).
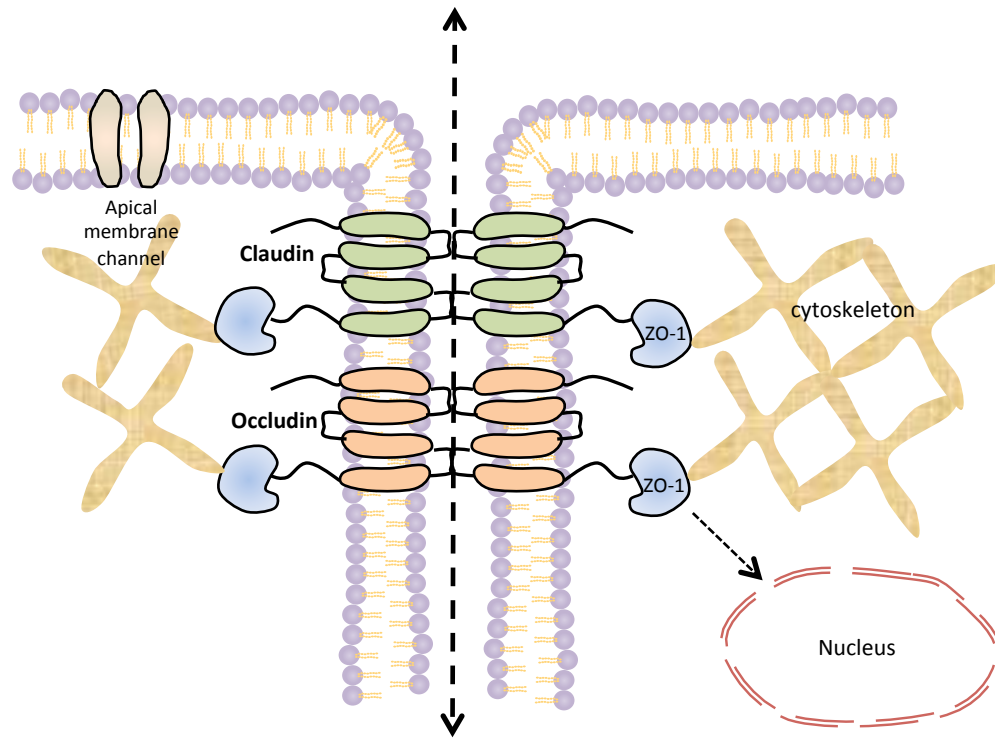
Fig 1.4 The tight junction complex of the teleost fish gill. Claudins and occludins constitute a network of proteins that act to gate keep the paracellular transport pathway. ZO-1 proteins link the external TJ complex to the internal actin cytoskeleton, whilst also acting to transduce signals to the nucleus about TJ formation and cell proliferation.

Tight junctions (TJs) and interconnecting desmosomes are present in the gill epithelium; their formation and relative impermeability are integral to the proper barrier functioning of the gill epithelium and its physiological pathways (Chasiotis & Kelly, 2011; Sandbichler et al., 2011a). Transmembrane proteins are held by cytoplasmic protein networks at the sides of epithelial cells (Fig 1.4) and act to limit the paracellular movement of water and ions. Communication between exposed transmembrane proteins and the internal actin cytoskeleton allows information about the external environment to be relayed to inside the cell, affecting transcriptional pathways regulating membrane permeability (Chasiotis et al., 2012).

1.3   Requirement for *in vitro* methods

Whole animal studies using rainbow trout provide information about the effects of pharmaceuticals and other chemicals on fish at the organism level. In order to understand individual organ functionality and physiology, it is necessary to develop an *in vitro* cell system (Baron et al., 2012; Murer & Kinne, 1980; Uchea et al., 2013). *In vitro* gill cell cultures offer a more detailed description of the transport properties of the gill, and to date there has been no gill cell culture model for assessing pharmaceutical uptake, efflux and metabolism by this organ. Furthermore, an *in vitro* method offers a reduction in the number of animals used in scientific research, as the gill cells obtained from two organisms can be used to create many individual gill epithelia for assaying, thus providing an alternative to whole-animal methods in line with the replacement, reduction and refinement (3Rs) of the use of animals in scientific research.

The gill cell line, RTgill-W1, offers an alternative model to whole-animal experiments and studies using cells obtained from live fish, that can be supplied conveniently and maintained in long-term culture (Bols et al., 1994). This cell line exhibits the PVC, MRC and goblet cells present in primary cells (Lee et al., 2009) but fails to form a tight epithelium (Trubitt et al., 2015) and enzymes essential for xenobiotic metabolism such as CYP1A are absent (Schirmer et al., 1998).

Other alternative freshwater gill surrogates have been identified, such as flat opercula or jaw skin preparations of freshwater adapted killifish (Wood & Marshall, 1994) or Nile tilapia (Burgess et al., 1998) that contain freshwater type MRCs and can be used to assess ion transport (Wood et al., 2002). However, these preparations very slowly, or completely lack the ability to, take up Cl^- or Na^+ when exposed to apical freshwater. This initiated the development of a suitable reconstructed freshwater gill epithelial model.
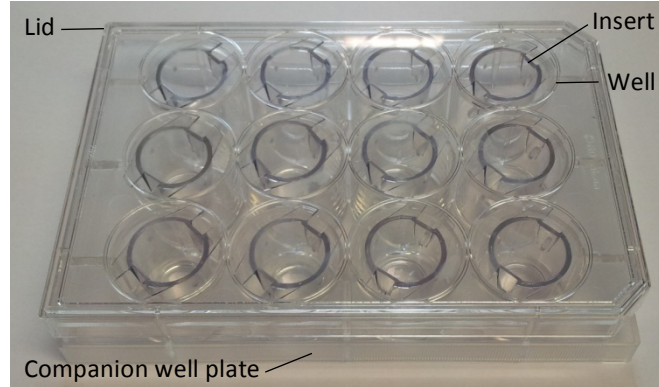
Fig 1.5 Permeable membrane cell culture inserts in a companion well plate.

Pärt et al. (1993) first documented the success of primary cell cultures of isolated rainbow trout epithelial cells on plates and demonstrated the best conditions for cell growth and attachment efficiency. This was later developed through the seeding of primary cells onto permeable membrane supports, termed single seeded inserts (SSI) (Fig 1.5) (Wood & Pärt, 1997). For SSI preparations, cells were grown in cell culture medium supplemented with fetal bovine serum (FBS) and formed an epithelial sheet on inserts (Fig 1.6A). SSI epithelia showed a gradual rise in transepithelial resistance (TER), which was indicative of the formation of intercellular tight junctions and a tight epithelium (Wood & Pärt, 1997). Epithelia could sustain apical freshwater exposure whilst cells remained bathed in the body fluid-like cell culture medium in the basolateral compartment (Fig 1.6B). Apical water exposure showed a 6-11 fold increase in TER and the creation of a basolaterally negative transepithelial potential (TEP), owing to the differential permeability of the epithelium to ions, which is similar to the TEP observed *in vivo* (Wood, 2001). Despite showing a developed apical glycocalyx and abundant rough endoplasmic reticulum, the SSI primary cultured cells showed no differentiation, and DASPEI staining revealed low mitochondrial activity indicating the presence of only PVCs (Wood et al., 1998).
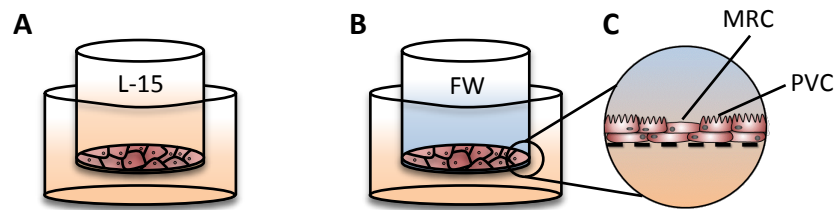
Fig 1.6 Representation of the *in vitro* gill in (A) symmetrical conditions with cell culture medium (orange; L-15) with FBS

and with or without antibiotics both sides of the epithelium, (B) asymmetrical conditions with freshwater (blue; FW) in

the apical chamber whilst the basolateral remains bathed in L-15 and (C) the gill epithelium growing multiple cell types

(PVCs and an MRC) in layers on the permeable membrane cell culture inserts.

Fletcher et al. (2000) later employed the double seeded insert (DSI) technique whereby primary

cells were seeded over two consecutive days. This provided a carpet of PVCs on the first day that

enables MRCs to attach during the second seed on day 2 (Fig 1.6C) (Wood et al., 2002). Using the

DSI technique produced epithelia with greater numbers of MRCs of around 15% of total cell

numbers, similar to the proportion observed *in vivo*, and higher TER values of up to 34,000 Ω cm^2,

typical of an electrically tight epithelium (Kelly et al., 2000). Furthermore, this reconstructed

epithelium exhibited transport properties of the intact freshwater gill such as active Cl$^-$ and Ca$^+$

uptake, and responded to hormone treatments such as cortisol and thyroid hormone (Wood et al.,

2002). However, despite the presence of active Na$^+$/K$^+$ATPase, the cell cultures did not

demonstrate discernible Na$^+$ or Cl$^-$ net uptake to values seen *in vivo* (Wood et al., 2002).

The development of a suitable *in vitro* gill epithelial model has allowed for the investigation of

other transport properties of this organ. The potential uses for this system are many (Wood et al.,

2002) particularly in the field of aquatic toxicology (Bury et al., 2014). This model has been used as

an *in vitro* method to assess the toxicity of waterborne metals to fish (Walker et al., 2008), for

environmental water monitoring (Minghetti et al., 2014) and most recently, as a system to assess

the uptake, efflux (Stott et al., 2015) and metabolism of xenobiotics such as pharmaceuticals at the gill.

Owing to its intimate contact with the water, the gill is the first point of contact of the organism to xenobiotics in the aquatic environment (Laurent & Perry, 1991; McKim & Erickson, 1991). The most common initial lesions at the gill after exposure to high concentrations of toxicants are lifting of the PVCs (causing TJ disruption), PVC and MRC hypertrophy, necrosis or apoptosis), fusion of neighbouring lamellae (reducing surface area) and PVC, MRC and mucous cell proliferation (Wood, 2001).

1.4   Pharmaceuticals in the aquatic environment

Pharmaceuticals are used in the therapy and treatment of numerous diseases and include many thousands of compounds, which are derived from natural sources or are synthetically produced. Recently, the production, availability and use of pharmaceuticals have increased, and so understanding the fate and implications of these compounds in the environment is necessary (Kümmerer, 2008). Moreover, all chemical products manufactured or imported into the EU in quantities of 1 tonne or more per year require environmental risk assessment to determine their safety (REACH, 2009).

Pharmaceuticals have become a class of contaminants of emerging concern (CECs) (Ashton et al., 2004; Kümmerer, 2008). This is owing to their specific design; their ability to cross biological membranes and remain stable makes them well designed for their desired use, but biologically detrimental when exposed to non-target organisms (Gunnarsson et al., 2008). Pharmaceuticals present in the environment include anti-depressants, antibiotics, anti-cancer drugs, beta-blockers, lipid regulators and oral contraceptives (Daughton & Ternes, 1999).

Wastewater treatment plants (WWTPs) process sewage water that contains unmetabolised active pharmaceutical ingredients (APIs) and their conjugate metabolites excreted from human drug use. Here, they may not be fully removed or degraded, or are further transformed by sewage microbial systems to other compounds that may ultimately enter environmental water systems. For example, the effect of increased environmental levels of synthetic oestrogens and their metabolites from excreted human usage not adequately removed by WWTPs has caused feminised male fish and altered sexual behaviours (Sumpter & Jobling, 2013). Veterinary medicines may enter ecosystems by excretion directly onto pastures used for animal husbandry or through the spreading of manure containing APIs and their metabolites on agricultural land, which will eventually enter surface and ground waters. Environmental levels of pharmaceuticals are in the ng-µg L^{-1} range. Their effect on human health specifically is unlikely because therapeutic doses are many orders of magnitude higher (Thomas & Klaper, 2012), although these low doses are a cause for concern for early life stages (i.e. pregnant women) and for chemicals with carcinogenic or chemotherapeutic properties.

Despite the detection of many types of pharmaceutical compounds in the environment, research into the effects to aquatic organisms has focused predominantly on single-substance exposures. In reality, wild organisms are probably exposed to mixtures of compounds and their metabolites (Khetan & Collins, 2007), thus risk assessments are therefore likely to underestimate the actual environmental impact imposed by the presence of many active pharmaceutical ingredients with similar or much different modes of action to one another.

The octanol-water partitioning coefficient (K_{ow}) is used as an indicator to predict the behaviour of compounds in the environment, based on the way it partitions between the phases of two immiscible liquids (Hermens et al., 2013). It is the ratio of the concentration of a chemical in octanol to water, often logged to create a Log K_{ow} scale for which different compounds can be

compared in terms of lipophilicity (the octanol phase) or hydrophilicity (the water phase), as shown in the following equation

$$K_{ow} = \frac{[solute]_{octanol}}{[solute]_{unionised\ water}}$$

The partition coefficient is calculated experimentally using the shake-flask method (OECD$_{107}$, 1995) or predicted using Quantitative Structure Activity Relationship algorithms (QSAR) (Hansch et al., 1995). Computer-based models (e.g. Parameter Client, Tetko et al., 2005) can make an interpretation of K_{ow} from the apparent functional groups within a chemical, based on those from a fixed set of known compounds. The values modelled in this way may therefore be different to figures obtained experimentally.

Log K_{ow} assumes a compound is non-ionisable and at constant temperature and pressure. For pharmaceuticals, many of which are ionisable and polar, the pH-corrected octanol-water distribution coefficient D_{ow} is preferred (Hermens et al., 2013). For both Log K_{ow} and Log D_{ow} a value of more than 3 indicates the likelihood that a compound will partition into the hydrophobic phase and accumulate in organisms, whilst a value of less than 1 predicts that a compound will remain in the environment or in the water phase. However, both these coefficients fail to take into account other interactions such as hydrogen bonding and van der Waals forces, or uptake via carrier-mediated processes (Dobson & Kell, 2008; Sugano et al., 2010).

The bioconcentration factor (BCF) is a measure of the ability of a compound to accumulate into an organism from the aquatic environment (i.e. the hydrophobic phase) or remain in the environment (i.e. the aqueous phase). It is calculated at steady state using the following equation

$$BCF = \frac{[compound]_{organism}}{[compound]_{environment}}$$

The determination of fish BCF follows guidelines standardised by the Organisation of Economic Co-operation and Development (OECD), using test guideline OECD$_{305}$, 'Bioaccumulation in Fish: Aqueous and Dietary Exposure' (OECD$_{305}$, 2012). During the uptake phase, fish are exposed to at least two concentrations and a water control (and a solvent control if required) of test compound. The internal compound concentrations are monitored throughout the exposure (for 28-60 days, depending on how long it takes for internal steady-state concentrations to be reached) and the depuration phase in substance-free conditions. BCF is then expressed normalised to a fish with a 5% lipid content (based on wet weight). The OECD$_{305}$ guidelines have recently been modified and for highly lipophilic (Log K_{ow} > 5 and solubility below 0.1 mg L^{-1}) compounds, fish are exposed via the diet in a different test protocol.

As well as OECD$_{305}$, BCF formulations for less hydrophobic compounds (Log K_{ow} < 5) can also be calculated using fish compartment models that incorporate the absorption, distribution, metabolism and excretion (ADME) of a compound, as represented by the following equation (Gobas, 1993; Gomez et al., 2010)

$$BCF = \frac{k_1 + k_U}{k_2 + k_G + k_M + k_E}$$

where k_1 is the uptake across gills, k_U is dietary ingestion, and k_2, k_G, k_M, k_E are rate constants representing elimination from across the gills (k_2), growth (k_G), metabolic biotransformation (k_M) and faecal egestion (k_E). Using this, *in vitro* assays could provide the inputs required in order to calculate the BCF of a compound, thus complementing information obtained from *in vivo* studies.

There are currently over 140,000 compounds registered with The European Chemicals Agency (ECHA), of which 30,000 compounds are being reassessed for their bioconcentrative properties as part of the EU Registration, Evaluation, Authorisation & restriction of Chemicals (REACH) (REACH,

2009). REACH aims to provide the protection of human health and the environment through the controlling of chemicals, and promotes the minimisation of animal testing.

Typically, each compound evaluated by $OECD_{305}$ uses at least 108 fish, and many thousands of fish are used worldwide for this test every year (Scholz et al., 2013). There is currently a desire to develop alternative methods to reduce, refine and replace (3Rs) the use of whole-animal studies such as $OECD_{305}$ to recognise and classify environmental hazards (Creton et al., 2013; Wolf et al., 2007). This requires the identification and validation of appropriate *in vitro* systems that could replace such studies (Stott et al., 2015). To find alternatives to the $OECD_{305}$ water exposure it is necessary to identify a suitable fish gill model that mimics the intact organ because the gill, being constantly and continuously exposed to substances in water, is the principle site of xenobiotic uptake (Bury et al., 2014).

1.5   Xenobiotic uptake

Entry into a biological system involves movement across cell membranes. In rainbow trout gill cells, this will firstly involve the influx of water into the buccal cavity by depression of the jaw, then over the gills as the operculum opens. Other routes of xenobiotic uptake are by ingestion or over the dermis. At the gill surface, xenobiotic compounds will come into contact with the plasma membranes of the gill epithelial cells (McKim & Erickson, 1991). The cell membranes of gill epithelial cells are amphiphilic phospholipid bilayers 5 nm thick, with a hydrophobic internal compartment composed of fatty acid tails lined by hydrophilic polar phospholipid heads. Cholesterol and membrane anchored proteins determine membrane fluidity. The main driving force dictating how a compound transfers from the aquatic environment into gill epithelial cells is determined by its lipophilicity (Log K_{ow}) (Huggett et al., 2003). This transport can be via passive diffusion across the lipid bilayer or by carrier-mediated transport using membrane protein transporters. It is thought that the two processes coexist together by an interplay of mechanisms

allowing for the transport of xenobiotics such as pharmaceuticals (Dobson & Kell, 2008; Sugano et al., 2010).

The transport of molecules at the apical surface of cells assumes free diffusion through the water most adjacent to the cell membrane (Fig 1.7) (Dobson & Kell, 2008). The chemistry of this unstirred water layer (UWL) may be altered from that of the rest of the bulk water due to cellular processes occurring at the gill cell apical surface such as ionic efflux of HCO_3^-, OH^- and H^+ and NH_3 excretion (Wood, 2001), which affects how xenobiotic compounds permeate this layer. Mucous produced by mucous cells to form the glycocalyx further presents another boundary layer that affects gas diffusion (Laurent & Perry, 1991) and therefore xenobiotic uptake. Mucus cells produce the glycoprotein mucin, which is thought to aid defense at the gill by reducing metal bioavailability via complexation or increasing Na^+, K^+, and Ca^{2+} concentrations, thereby increasing competition between these cations and metal uptake routes (Wood, 2001). The pH and chemistry of these boundary layers will affect the ionisation of pharmaceutical compounds and influence their transport across the gill.

Paracellular diffusion describes the transport of compounds between gill epithelial cells (Fig 1.7A), which depends on the formation of tight junctions (TJs). These are a vital feature of gill epithelia as they constitute the main barrier required between the freshwater and organism, and control the passage of water and ions via the paracellular transport pathway in fish (González-Mariscal et al., 2003). In general, the tighter and deeper the TJ, the less paracellular transport can occur. Transmembrane and cytosolic proteins constitute TJs and appear to 'stitch' cells together (Fig 1.3), whilst being anchored to the internal cytoskeleton of cells. This forms a belt at which the movement of apical membrane bound proteins and channels cannot pass to basolateral, and vice versa (Fig 1.4) (Chasiotis et al., 2012).
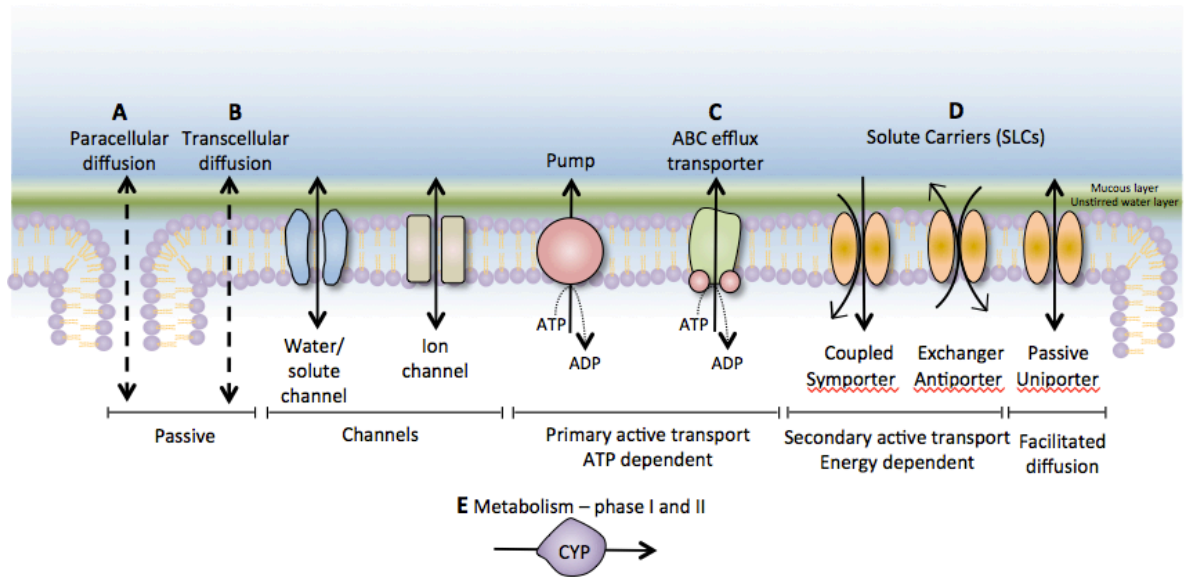
Fig 1.7 Transport processes at the apical gill epithelium. Xenobiotics in the water first penetrate the mucus layer and the

unstirred water layer (UWL). Uptake may occur via the paracellular route between epithelial cells (A) or transcellularly

through the phospholipid bilayer (B). ATP-binding cassette (ABC) transporters may be present on the cell membrane (C)

as well as members of the solute carrier (SLC) superfamily (D). Inside the cells of the gill epithelium, xenobiotics may

undergo metabolism by cytochrome P450 enzymes (E).

The TJs of freshwater teleosts are deeper and more complex than the more leaky TJs of seawater

fish, owing to the differences in osmotic gradient between the blood and external water that has

to be maintained. Furthermore, accessory cells with leakier cell junctions are absent in freshwater

fish species (Chasiotis et al., 2012). Therefore, the TJs of freshwater teleosts render the epithelium

more impermeable to paracellular transport. Cortisol plays an important role in regulating tight

junction formation, decreasing paracellular permeability and passive ion efflux in rainbow trout

gills (Chasiotis et al., 2010; Sandbichler et al., 2011b) and increasing cultured gill cell epithelial

tightening (Wood et al., 2002).

Over 40 vertebrate TJ proteins involved in the paracellular transport pathway have been identified

(González-Mariscal et al., 2003). The proteins occludin and claudin are integral to the TJ backbone

(González-Mariscal et al., 2003), as well as cadherins, zonula occludin (ZO-1) and junction adhesion molecules (JAMs) (Chasiotis et al., 2012). Occludin is a tetraspan protein involved specifically in the external TJ formation. It is anchored in the cell membrane by 4 transmembrane domains (Fig 1.4) and has been fully characterised in rainbow trout (Chasiotis & Kelly, 2011; Chasiotis et al., 2010). Claudins are a superfamily of tetraspan proteins, likewise anchored in the cell membrane, but appearing to be more associated with the facilitation of paracellular transport. Different subtypes aid the movement of different solutes in specific tissue regions, therefore acting as paracellular gatekeepers (Chasiotis et al., 2012). Many claudins have been identified in fish species – more so than in mammalian, and claudin expression is elevated in freshwater acclimatised fish, as would be expected in 'tighter' freshwater epithelia. In rainbow trout, claudin-12, -28b, -30 and -31 have been identified in whole gill tissue samples and PVCs (Chasiotis et al., 2012). Other TJ proteins include the ZO-1 proteins that are present inside gill cells (Fig 1.4), linking the external TJ proteins such as claudin and occludins to the internal actin cytoskeleton, whilst also acting to transduce signals to the nucleus about TJ formation and cell proliferation (Bauer et al., 2010).

In cultured rainbow trout epithelial cell cultures, 5 genes encoding for proteins involved in TJ formation, including claudin 28b, were identified when cells were exposed to freshwater (Sandbichler et al., 2011a). Occludin is expressed in whole gill tissue samples, as well as in PVCs in culture (Chasiotis et al., 2010). Staining of ZO-1 shows its location on the periphery of cultured rainbow trout PVCs (Walker et al., 2007).

Transcellular diffusion involves the movement of molecules into cells by permeating the phospholipid membrane down a concentration gradient (Fig 1.7B) (Sugano et al., 2010). This process will not reach saturation or be subject to inhibition and is concentration dependent. It is mainly driven by how easily a compound can permeate the hydrophobic region of the membrane and it being uncharged (Sugano et al., 2010). Therefore passive diffusion is governed by a compounds charge and lipophilicity, Log K_{ow} and Log D_{ow}. The characteristics of a compounds

passive transcellular transport can be assessed using octanol-water partitioning (OECD$_{107}$, 1995) or artificial membranes without transporters, such as black lipid membranes and liposomes, and parallel artificial membrane permeability assays (PAMPA) (Sugano et al., 2010). PAMPA studies have been shown to provide accurate information about drug partitioning across biological membranes in line with Log D_{ow} values (Galinis-Luciani et al., 2007), although others dispute this, due to their lacking the true structure of a biological membrane that performs paracellular or facilitated transport with proteins (Sugano et al., 2010).

Facilitated transport uses membrane bound protein carriers that act as gatekeepers to a cell, controlling the movement of water, ions, solutes and xenobiotics by passive (down a concentration gradient) or active (requiring energy) processes (Fig 1.7) (Hediger et al., 2004). Active transporters move substrates using energy obtained directly from the hydrolysis of ATP in primary active transport or indirectly in secondary active transport through the electrochemical gradient set up by pumping hydrogen ions into or out of cells (Hediger et al., 2004). Facilitated transporters include water, ion and solute channels (Fig 1.7), that allow passive movement by osmosis or down the electrochemical or concentration gradient, and that may open via gating mechanisms or changes in membrane conductance (Hediger et al., 2004). Ion pumps use energy to actively pump out ions such as Na^+, K^+, H^+ and Ca^{2+} to create electrochemical gradients that other secondary active transporters can use. Other carriers such as the efflux ATP-binding cassette (ABC) transporters also require energy to move substrates out of cells (Fig 1.7C).

The solute carrier (SLC) group of membrane transporters is a superfamily of carrier proteins involved in the movement of endogenous and exogenous substrates. SLCs are expressed on the apical, basolateral and organelle membrane of cells as passive transporters (uniporters), cotransporters (symporters) and exchangers (antiporters) (Fig 1.7D) (Dobson & Kell, 2008; Hediger et al., 2004). Symporters and exchangers are likely to utilise electrochemical gradients set up by the primary active transport of ions by pumps, and hence are termed secondary active

transporters (Sugano et al., 2010). In humans, 398 SLC genes have been grouped into one of 52 families (Bioparadigms, 2015). Certain carriers of SLC15 (the proton oligopeptide cotransporter family), SLCO (the organic anion transporter family), SLC22 (the organic cation/anion/zwitterion transporter family) and SLC47 (the multidrug and toxin extrusion family) appear to be involved in the uptake of xenobiotics (Daniel & Kottra, 2004; Dobson & Kell, 2008; Giacomini et al., 2010; Hagenbuch & Meier, 2003; Koepsell & Endou, 2004).

The SLC15 family contains 4 members including the PEPT1 and PEPT2 transporters, which mediate peptide substrate uptake through proton cotransport. They transport charged and uncharged di- and tri- peptides based on their stereospecificity, and because of this, will transport xenobiotics with similar structures (Daniel & Kottra, 2004). The SLCO family of carriers is named so due to their ability to transport organic anions (organic anion transporting proteins, OATPs), and is further divided into species-specific subfamilies (Hagenbuch & Meier, 2003). A total of 52 members have so far been identified, and in general they comprise 12 transmembrane domains. They transport by an anion exchange system, whereby the substrate is transported during the efflux of an endogenous substance in an electroneutral process (Giacomini et al., 2010). The SLC22 family comprises carriers concerned with the transport of organic cations and anions, with the general structure of 12 transmembrane domains (Koepsell & Endou, 2004). SLC22A1 (Organic cation transporter 1; OCT1) and SLC22A2 (OCT2) are uniporters that transport substrates in either direction with wide and overlapping substrate specificities, whilst SLC22A6 (Organic anion transporter 1; OAT1) and SLC22A8 (OAT3) are anion (or dicarboxylate) exchangers utilising electrochemical membrane gradients to drive transport (Koepsell & Endou, 2004).

Currently, representatives of 50 of the 52 human SLC families have been established in teleost fish (SLC28 remains undetected and SLC52 is newly identified; Yonezawa & Inui, 2013) comprising 338 members, most extensively so in zebrafish (*Dario rerio*) (Romano et al., 2014; Verri et al., 2012). In this species 304 out of 338 SLC genes have been identified, whilst in rainbow trout, this totals 22

(Verri et al., 2012). The difference is likely due to zebrafish being a popular teleost fish model used for functional studies, probably due to the annotation of its genes and genome and it is regarded as the reference teleost fish model in the solute carriers field to date (Romano et al., 2014).

Transporters analogous to human SLC15A1 and 2, peptide transporter 1 and 2 (PEPT1 and PEPT2) (slc15a1b and slc15a2) as well as another novel peptide transporter (zgc:63767) were identified in zebrafish, and their function has been tested through the transport of di- and tripeptides in a number of species (Verri et al., 2012). Of the SLCO family of solute carriers, 14 organic anion-transporting polypeptides (Oatps) have been identified in zebrafish (Popovic et al., 2010). In the gills of zebrafish, Oatp2b1 expression is highest, followed by Oatp3a1, Oatp1d1 and Oatp2a1. In humans, the SLCO2B1 (analogous to Oatp2b1 in fish) transports various drug types and is concerned with drug-drug interactions (Giacomini et al., 2010).

Eight members of the SLC22 family have been discovered in teleosts, mostly in zebrafish and Atlantic salmon (*Salmo salar*), but none so far in rainbow trout (Verri et al., 2012). Transporters analogous to mammalian SLC22A1 and 2 (OAT1 and OAT3) have been suggested in winter flounder (*Pseudopleuronectes americanus*) (fOat), zebrafish (zfOat) and puffer fish (pfOat) (Aslamkhan et al., 2006). The flounder SLC22 (Oat) transporter was tested for functionality and found to have the same substrates as mammalian OAT1 and OAT3 (Aslamkhan et al., 2006). Proteins analogous to mammalian SLC22A6 and 7 (OCT1 and OCT2) transporters that are involved in xenobiotic uptake are yet to be confirmed in teleost fish (Giacomini et al., 2010). slc47a1 and slc47a2 are the two members akin to the multidrug and toxin extrusion family in mammals, SLC47. Messenger RNA transcripts of both proteins have been identified in zebrafish, yet testing of the functionality of these transporters is yet to be confirmed (Giacomini et al., 2010).

1.6 Xenobiotic metabolism

Trout possess a suite of biotransformation enzymes that detoxify xenobiotics through phase I metabolism, and then conjugate these functional groups by further addition of endogenous molecules to add polarity in phase II. These compounds may then be excreted or further catabolised and broken down into smaller products involving enzymes such as proteases and hydrolases (Xu et al., 2005).

Phase I of xenobiotic metabolism involves the reduction, oxidation or hydrolysis of lipophilic compounds to more water-soluble by the mixed-function oxidase (MFO) or microsomal monooxygenase (MO) enzymes, which include the cytochrome P450 (CYP) superfamily of enzymes (Meunier et al., 2004). These are a collection of isoenzymes possessing an iron protoporphyrin IX prosthetic group and classified into families based on their primary amino acid sequences. They are termed microsomal due to suspension in the microsomal fraction after cell homogenisation, and are membrane bound in large numbers in the rough and smooth endoplasmic reticulum in cells, especially in the liver but also intestinal tract and gills of rainbow trout (Andersson & Förlin, 1992).

CYP proteins are induced in response to xenobiotic exposure. Xenobiotics that have entered cells bind to cytosolic aryl hydrocarbon receptors (AhR), which cause the release of bound proteins involved in a signal transduction cascade. The AhR-ligand complex enters the nucleus and binds to the aryl hydrocarbon nuclear translocation (ARNT) protein forming an activated transcription factor which is able to bind to certain segments of DNA resulting in the transcription of CYP proteins in the cell (Whyte et al., 2000).

CYP enzymes are closely associated with other MO enzymes present within the endoplasmic reticulum involved in metabolism, chiefly the flavoprotein nicotinamide adenine di-nucleotide phosphate (NADPH) and cytochrome P450 reductase, which transfers electrons to cytochrome

P450 during the step-by-step sequence of reactions. A substrate will bind to the hydrophobic site on P450 when the iron present in the enzyme is oxidised, ferric and in the low spin state. The binding site is close enough to the haem group present on the CYP molecule to interact with oxygen, causing a conformational change to the high spin state. This causes the first reduction of iron from its ferric to ferrous state, by an electron transfer from NADPH via cytochrome P450 reductase. The addition of molecular oxygen follows, before adding another electron via the same pathway to create a short term intermediate complex. This is rapidly protonated, releasing a molecule of water, whilst the other oxygen atom is inserted into the substrate complex to make it hydroxylated. After the product is released, the P450 enzyme returns to its active state (Meunier et al., 2004; Timbrell, 2000; van der Oost et al., 2003).

The families of Cytochrome P450 associated with xenobiotic metabolism in humans are CYP1, CYP2, CYP3 and CYP4 (Timbrell, 2000). They have broad and overlapping substrate specificity and different CYPs may metabolise the same substrate differently. For example propranolol is metabolised to 4-hydroxypropranolol by CYP2D6 and to napthoxylacetic acid by CYP2C19 (Timbrell, 2000).

In fish, 137 genes have been identified that are classified into 18 CYP families (Uno et al., 2012). In rainbow trout the CYP isoforms identified are CYP1A, CYP2K CYP2M, CYP3A27, CYP3A45, CYP4T1, CYP11A, CYP11B, CYP17 and CYP19, and these are mostly associated with xenobiotic metabolism (Hasselberg et al., 2008; Uno et al., 2012).

The CYP1A family is analogous to mammalian CYPs, with similar substrate specificity in rainbow trout, and is involved in phase I metabolism of xenobiotics by exposing or adding a polar group to aid solubility (Whyte et al., 2000). In rainbow trout, CYP1A is induced by exposure to polycyclic aromatic hydrocarbons (PAHs), polychlorinated biphenols (PCBs), tetrachlorodibenzodioxin (TCDD) and other dioxins, polychlorinated dibenzofurans (PCDFs) and other pesticides (Buhler & Wang-

Buhler, 1998). Catalytic measurements of CYP1A induction and inhibition in fish can be quantified using an ethoxyresorufin-*O*-deethly-ase (EROD) assay whereby 7-ethoxyresorufin is converted to fluorescent resorufin. CYP1A can be induced *in vitro* in gill cells by beta-naphthoflavone (BnF) (Carlsson & Pärt, 2001; Carlsson et al., 1999) and inhibited by alpha-naphthoflavone (AnF) (Thibaut et al., 2006). In rainbow trout, propranolol induces CYP1A activity in the liver and gills both *in vivo* and *in vitro* (Bartram et al., 2011).

Benzyloxy-4-trifluoromethylcoumarin-*O*-debenzyloxylase (BFCOD) activity is used to measure CYP3A-like enzymatic activity in fish (Hasselberg et al., 2008; Thibaut et al., 2006). Known mammalian inducers and inhibitors of CYP3 enzymes give inconsistent results in fish. Ketoconazole has been shown to increase CYP3A protein levels 1.5-fold and decrease BFCOD activities in rainbow trout *in vivo* (Hasselberg et al., 2008). Clotrimazole, omeprazole and rifampicin, but not dexamethasone or lithocholic acid, decrease the activity of BFCOD in rainbow trout liver microsomes (Burkina et al., 2013; Wassmur et al., 2010).

1.7 Xenobiotic efflux

Research into the occurrence of multi-drug resistance (MDR) using cancerous cell lines has led to the better understanding of the cellular efflux of drugs (Cole & Deeley, 1998; Leslie et al., 2005) and the mediation of the MDR phenotype. For example, intrinsic or acquired over expression of the membrane transporter P-glycoprotein (Pgp) is associated with the rapid and unspecific efflux of cancer drugs and results in the decreased success of chemotherapy treatment in cancer patients (Takara et al., 2006). This is known as phase 0 of cellular defense, as the drug is eliminated from cells before it can affect the body. Pgp is also present in aquatic organisms (Bard, 2000). Kurelec (1992) coined the term 'multixenobiotic resistance' (MXR) when describing the occurrence of populations of aquatic organisms in polluted water systems, as they are capable of

rapidly pumping out harmful xenobiotics by Pgp transporters and thus inhabiting toxic environments.

Pgp is part of the adenosine triphosphate (ATP) binding cassette (ABC) superfamily of ATP requiring membrane proteins involved in the transport (Fig 1.7C), primarily efflux (Zolnerciks et al., 2011), of peptides, ions, sterols and other endogenous solutes and metabolites as well as exogenous hydrophobic molecules such as xenobiotics (Dean & Annilo, 2005; Dean et al., 2001; Deeley et al., 2006). In humans, 7 subfamilies are encoded by the genes ABCA-ABCG, which transcribe 49 proteins that are highly conserved between species (Dean et al., 2001). Each transporter typically consists of 1-3 hydrophobic transmembrane domains (TMDs) made up of 6-11 alpha helices, which transport the solute, and 1-3 nucleotide binding domains (NBDs), which bind and hydrolyse ATP providing the energy for transport to occur (Dean & Annilo, 2005). Studies isolating and crystallising NBDs have determined the amino acid sequence and binding site of nucleotides. This region is very highly conserved amongst the ABC transporters (Zolnerciks et al., 2011), and is composed of Walker A and B motifs separated by 90-120 amino acids which contain the C motif upstream from Walker B (Deeley et al., 2006; Sturm & Segner, 2005). ABC genes can code for full transporters, or two ABC genes are required for the expression of two half transporters that together form a functional unit (Dean et al., 2001).

The main ABC transporters involved in the efflux of xenobiotics and MXR in aquatic organisms are Pgp and BSEP (ABCB1 and ABCB11), the MRPs (ABCCs) and BCRP (ABCG2) (Dean et al., 2001; Fischer et al., 2011; Lončar et al., 2010). Whilst Pgp is mainly associated with the efflux of unmetabolised xenobiotics (phase 0), others move biotransformed xenobiotics out of cells, such as the MRPs (ABCCs) that transport phase I and II metabolised xenobiotics, particularly glutathione and sulphate conjugates. This is therefore termed phase III of cellular defense (Fischer et al., 2011). The two transporters of the SLC47 family, SLC471 and SLC474, MATE1 and MATE2 (multidrug and toxin extrusion 1 and 2), export toxic endogenous and exogenous substrates out of

cells by H⁺-coupled electroneutral exchange (Otsuka et al., 2005) in humans, primarily in the liver to aid excretion of toxins into bile (Giacomini et al., 2010).

ABC transporters in aquatic species have been documented in sponges, aquatic molluscs, marine worms and bivalves (Bard, 2000; Luckenbach & Epel, 2008; Sturm & Segner, 2005). After preliminary work suggesting the presence of Pgp like proteins in teleosts, Sturm et al. (2001) used primary hepatocyte cells isolated from perfused livers of *O. mykiss* to demonstrate the presence of MDR (ABCB) proteins such as Pgp (ABCB1) through the accumulation of fluorescent Rhodamine-123 in hepatocytes preloaded with Pgp inhibitors, such as verapamil. Pgp and MRP3 (ABCC3) sequences have been characterised to a high degree of homogeny in the topminnow hepatoma cell line PLHC-1 (Zaja et al., 2007). The ABC transporters Pgp, BSEP (bile salt export pump; ABCB11) and MRP2 (ABCC2) are present in primary *O. mykiss* hepatocytes, and their presence and function was confirmed using fluorescent substrate accumulation assays in the presence and absence of inhibitors (Zaja et al., 2008).

Lončar et al. (2010) presented the first thorough insight into the whole body distribution of the 8 MXR ABC transporters in rainbow trout using qRT-PCR. mRNA from whole bodies was isolated and reverse transcribed and specific ABC transporter primers provided the detailed expression levels in the liver, brain, kidney, gills, gonads and proximal and distal intestine. All 8 of the MXR ABC transporters were detected, with Pgp (ABCB1) being expressed ubiquitously in all tissues apart from the gills. However, a study using the rainbow trout gill cell line RTgill-W1 opposed this and found its expression (Fischer et al., 2011). Other MXR ABC transporters expressed preferentially in organs of rainbow trout included BSEP in the liver (like in mammals), MRP1 and MRP2 in the kidney (supporting their role localised in cells for apical cellular transport), MRP3 in most tissues (but mainly intestinal in mammals), MRP4 and MRP5 in gonads and kidneys (similar to mammals) and BCRP in most tissues and the liver (as supported by Zaja et al., 2008). MRP1 and MRP3 are present in the rainbow trout gill cell line, RTgill-W1, (Fischer et al., 2010). A study using 7

permanent cell lines derived from different rainbow trout tissues showed the expression of 9 ABC efflux transporters related to phase 0 and III metabolism associated with MXR (Fischer et al., 2011). However, differences in transcription levels between cell lines and live tissues are commonly reported (Zaja et al., 2008).

1.8 Xenobiotic excretion

The excretion of pharmaceuticals involves the removal of parent and conjugated pharmaceutical compounds, made more soluble and with greater molecular weights from phase I and II metabolism, via the urine and faeces.

In fish, parent compounds and their hydroxylated forms are made more soluble and conjugated typically through glucuronidation to increase their molecular weight (Togunde et al., 2012), which allows concentration into fish bile from the plasma (Ferreira-Leach & Hill, 2001), along with inorganic ions and bile acids. Xenobiotics can be concentrated in the bile to many times higher than in that of the plasma (Statham et al., 1976; Förlin & Haux, 1985), and this bile enters the gut lumen and is excreted in faeces. Pharmaceuticals and their metabolites in fish bile act as biomarkers of the uptake and metabolism of drugs in fish (Vuorinen et al., 2006; Lahti et al., 2011), and these can be used to assess excretion rates. The perfused trout liver has also provided the study of biliary excretion (Nichols et al., 2009). In the bile of wild bream and roach, the presence of 17 different pharmaceuticals, including naproxen, diclofenac and ibuprofen, and six different phase I metabolites were identified (Brozinski et al., 2013). *In vitro*, primary cells of rainbow trout liver S9 fractions and microsomes are metabolically active (Conners et al., 2013; Gomez et al., 2011) and have been used to generate metabolism data for fish (Nichols et al., 2007). Primary liver cells in 2D monoculture and 3D spheroid culture have been shown to be more metabolically active than microsomal fractions (Uchea et al., 2013) the latter being a more representative model of the liver in terms of morphology and biochemical activity (Baron et al., 2012).

1.9   Xenobiotic drug targets

Much drug research focuses on the development of compounds with mammalian drug targets in mind. Many of these systems are highly conserved in rainbow trout with high levels of homogeneity (Huggett et al., 2003; Fischer et al., 2011; Madigou et al., 2000; Nickerson et al., 2001; Zaja et al., 2008; Zou et al., 1999). Therefore, mammalian pharmacology data can be used to assess the potential chronic receptor mediated responses in fish (Bartram et al., 2011; Daughton & Brooks, 2011; Huggett et al., 2003; Owen et al., 2007).

Beta-adrenoceptors are 7-transmembrane receptors coupled with G proteins, involved in the activation of the sympathetic nervous system. The endogenous catecholamines, adrenaline and noradrenaline, are synthesised in the medulla of the adrenal glands and are released in response to stress. They bind to β-adrenoceptors of which there are three types in humans, β1-3. Binding of adrenalin or noradrenaline causes activation of the associated G protein, which in turn stimulates the membrane-bound enzyme adenylyl cyclase. This catalyses the synthesis of cyclic adenosine monophosphate (cAMP), which activates target proteins such as protein kinase A, and enhances the phosphorylation of other membrane channels. In general this increases the likelihood of cellular depolarisation, which in the heart (β1 receptors) causes increased speed and strength of contraction, in the lungs (β2 receptors) causes increased bronchodilation and in adipose tissue (β3 receptors), increased lipolysis to increase energy availability. These are required for the 'flight or flight' response, but can have adverse effects when there is a cardiac problem (Black & Stephenson, 1962). Activation of β-adrenoceptors in these cases cause adverse strain on the cardiac system, hence the development of the beta-adrenergic receptor antagonist drugs (β-blockers) that treat conditions such as angina, high blood pressure and glaucoma, through selective inhibition of one or more of the β receptors.

β-blockers are often detected in WWTP effluents and the environment in the ng-µg L^{-1} range (Johnson et al., 2007; Owen et al., 2007; Owen et al., 2009). As in mammals, the adrenergic system in fish functions using adrenalin and noradrenalin, and the associated β-adrenoceptors, which are highly conserved amongst vertebrates (Owen et al., 2007). Activation of the adrenergic system results in a range of outcomes in fish due to the wide distribution of receptor types. The physiological outcomes of this result in the preparation for the fight or flight response, such as changes in cardiac performance and ventilation rates, metabolic regulation, skeletal muscle performance and melanophore regulation (Owen et al., 2007).

After a 40-day exposure to 10 mg L^{-1} of the β-blocker propranolol, the concentration of propranolol in rainbow trout blood plasma reached 5200 ng mL^{-1} (Owen et al., 2009). In rainbow trout, the expression of β2 receptors is high in the liver and red and white muscle, and less so in the gills, heart, kidney and spleen (Nickerson et al., 2001).

1.10 Aims and objectives

The present study aims to investigate the suitability of the *in vitro* rainbow trout gill as a tool to assess the uptake, efflux and metabolism of xenobiotics such as pharmaceuticals. The study therefore aimed to complete the following objectives

I. The development, optimisation and standardisation of rainbow trout primary gill cell culture.

II. The characterisation of SSI and DSI primary gill cell epithelia, as well as epithelia cultured using the rainbow trout gill cell line RTgill-W1. This involves the monitoring of transepithelial resistance (TER) and potential (TEP) during epithelial development and

during apical freshwater exposure and the quantification of epithelial paracellular permeability.

III.   The investigation into the improvement of RTgill-W1 epithelial preparations by increasing TER and decreasing paracellular permeability through the supplement of culture medium and the co-culture with primary gill cells.

IV.   The investigation into the uptake and efflux of 7 pharmaceuticals across the *in vitro* primary gill cell system, including bidirectional, concentration equilibrated, pH-dependent, and concentration-dependent transport assays, as well as membrane channel inhibitor studies. The uptake rates were compared to *in silico* (Fitzsimmons et al., 2001; Huggett et al., 2003) and *in vivo* data (Owen et al., 2009).

V.   The assessment of the metabolism of pharmaceuticals by the gill epithelia cultured using SSI, DSI techniques, and the cell line RTgill-W1 through metabolic enzyme assays and HPLC analysis of parent compounds and a metabolite.

It is hypothesised that the DSI primary cell culture will most accurately resemble the gill in situ. Uptake and efflux experiments using DSI are hypothesised to show that a combination of both passive and carrier-mediated transport of pharmaceuticals exists at the gill. Furthermore, it is hypothesised that the DSI primary cell cultures will produce metabolic products whilst SSI and RTgill-W1 gill cell cultures may not.

Chapter 2

General Materials and Methods

The body of this chapter is also presented as a film produced as part of the BBSRC Sparking Impact

prize awarded to this project, on a DVD at the back of this thesis.

2.1 Materials

2.1.1   Reagents and suppliers

Leibovitz's L-15 cell culture medium with L-glutamine (2 mM) and without phenol red (L-15),

penicillin-streptomycin (5000 units mL^{-1} penicillin, 5 mg mL^{-1} streptomycin), gentamicin (5 mg mL^{-1})

and 10x 0.5% trypsin-EDTA were purchased from Invitrogen Life Technologies. Fetal bovine serum

(FBS), amphotericin B and Trypan blue were purchased from Sigma Aldrich. Phosphate buffered

saline tablets were purchased from Thermo Scientific. Ethanol absolute was purchased from VWR.

2.1.2   Equipment and suppliers

The laminar flow hood was model number M51424/2 produced by Microflow Biological Safety.

The refrigerated centrifuge was model number 5810R, with rotor A-4-62 by Eppendorf. The vortex

was model number F20220176 by VELP Scientifica. The dissecting equipment used included a large

sharp knife, forceps purchased from SLS, scissors from VWR and scalpels from Swann-Morton. The

portable gyratory shaker was model IKA-VIBRAX-VXR. Pipettes used were adjustable Gilson; P-20,

P-200 and P-1000 with disposable pipette tips from Starlab. The 5, 10 and 25 mL tissue culture

pipettes were purchased from Corning. The inverted phase contrast microscope was model

number TE200 by Nikon Eclipse. The cells were cultured in a cell culture cooling incubator model

number MIR-1554 by Sanyo set to 18°C, without CO_2 atmosphere. The haemocytometer was

purchased from Neubauer. The EVOM™ epithelial voltohmmeter was modified to read TER up to 100,000 Ω cm^2 and purchased from World Precision Instruments with EVOM™ 'chopstick' electrodes number STX-2. Twelve well cell culture inserts with 0.4 µm pore, 0.9 cm^2 effective growth area and made of polyethylene terephthalate (PET) membrane were purchased from BD Falcon. The companion cell culture plates, 12 well with low (notched) evaporation lid, were also purchased from BD Falcon. 25 and 75 cm^2 cell culture flasks were purchased from Nunc. 0.2 µm sterile syringe filters and sterile Petri dishes were purchased from VWR and the cell strainers (100 µm, nylon) and 50 and 14 mL conical tubes were purchased from BD Falcon.

2.1.3   Preparation of reagents

Penicillin-streptomycin was stored in 11 mL aliquots at -20°C. Gentamicin solution was divided into two 50 mL aliquots and stored at room temperature. Amphotericin B was reconstituted in sterile double distilled water according to the manufacturer's instructions to a final concentration of 250 µg mL^{-1} amphotericin B and 250 µg mL^{-1} sodium desoxycholate, then passed through a sterile filter and stored in 1.5 mL aliquots at -20°C in the dark. PBS tablets were dissolved in 100 mL Milli-Q water per tablet, autoclaved, and stored at room temperature. 10x 0.5% trypsin-EDTA was diluted to 0.05% with PBS, sterile filtered and stored in 50 mL aliquots at -20°C.

2.1.4   Cell culture reagents

Cell culture medium with antibiotics and FBS was composed of L-15 with 2% (*v/v*) gentamicin, 2% (*v/v*) penicillin-streptomycin and 5% (*v/v*) FBS. Cell culture medium without antibiotics was composed of L-15 with 5% (*v/v*) FBS. Artificial freshwater is defined as water prepared to the standard used for maintaining fish such as the Organisation for Economic Co-operation and Development (OECD) (OECD$_{305}$, 2012). OECD freshwater (FW) was composed of 2.0 mM CaCl$_2$, 0.5 mM MgSO$_4$, 0.8 mM NaHCO$_3$, 77.1 µM KCl at pH 7.7 and aerated until oxygen saturation was

achieved, then stored for 2 days at 4°C with further aeration before use. L-15 exposure medium was composed of L-15 cell culture medium without any supplementation.

2.1.5 Animal husbandry

Gill cells for the use in primary cultures were obtained from juvenile diploid rainbow trout weighing 50-120 g purchased from a trout farm (in Hampshire, UK). Fish were acclimatised for at least 2 weeks in three 1000 L fiberglass aquaria at King's College London, and maintained at 13-14°C in recirculating aerated city of London tap water ($[Na^+]$ = 0.53 mM, $[Ca^{2+}]$ = 0.92 mM, $[Mg^{2+}]$ = 0.14 mM, $[K^+]$ = 0.066 mM and $[NH_4^+]$ = 0.027 mM) that was passed through carbon, mechanical and biological filters. Photoperiod was maintained at a constant 14 hour light 10 hour dark cycle and fish were fed a daily 1% (*w/w*) ration of fish chow.

2.2 Methods

Methods follow those described in Schnell, Stott, et al. (2016) and in the DVD included at the back of this thesis.

2.2.1 Sterile techniques

Sterile techniques were used throughout all cell culture procedures, which were performed in a laminar flow hood. Equipment, containers and solutions were either autoclaved at 120°C at 15 psi for 20 minutes, or sterile filtered. Dissecting equipment was disinfected with ethanol (70%). Plastic ware was purchased sterile and used once.

2.2.2 Quality assurance

Good laboratory practice (GLP) was followed throughout the laboratory procedures and data analysis. Where appropriate, instruments were routinely checked or calibrated and reagents and materials were certified for cell culture procedures.
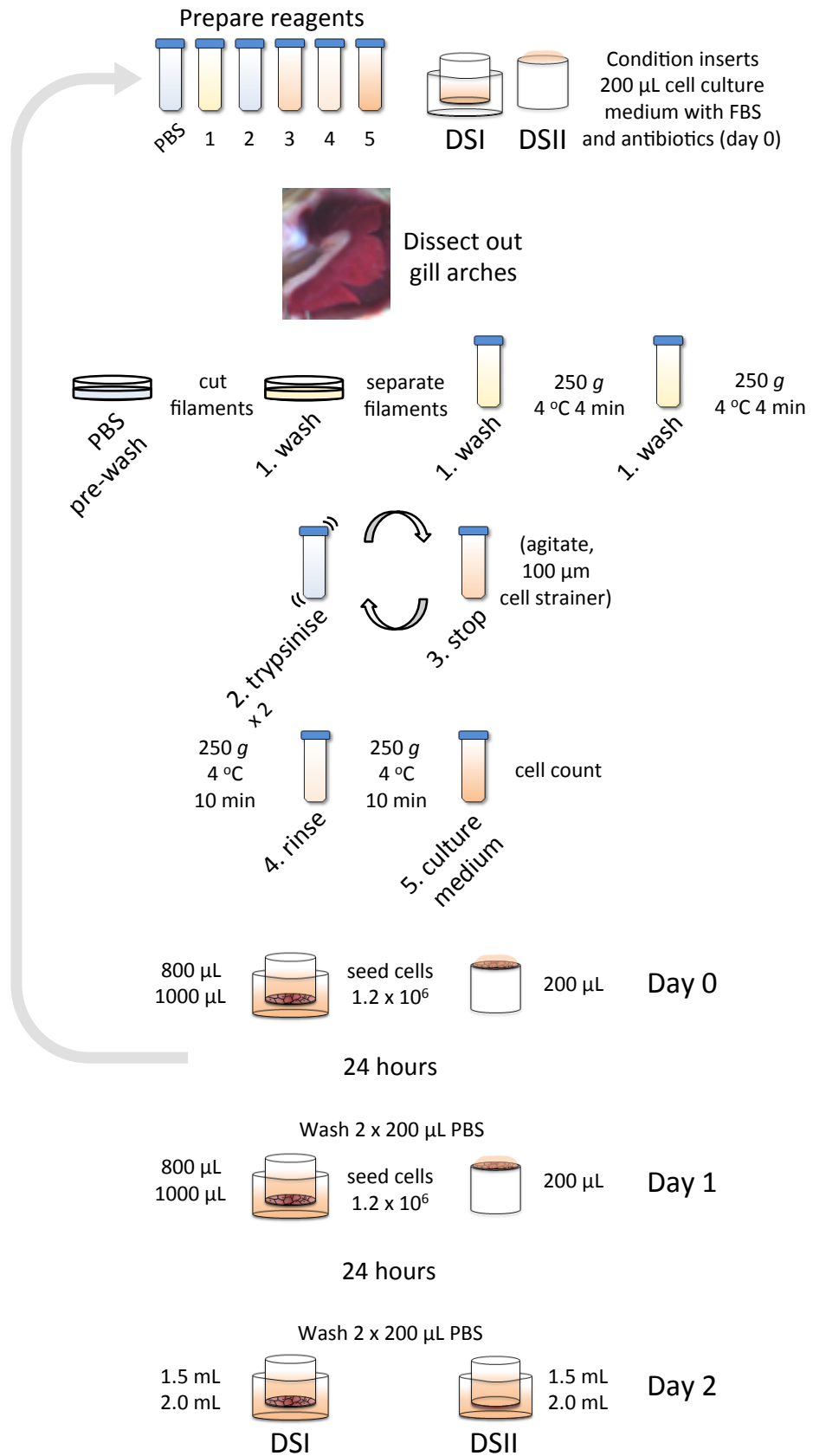
Fig 2.1 Summary of the DSI and DSII (see Chapter 3) cell culture procedures of primary rainbow trout gill cells.

2.2.3 Cell isolation

The gill cell isolation and culture procedure was based on methods previously described by Pärt et al. (1993); Wood & Pärt (1997); Kelly et al. (2000) and Fletcher et al. (2000) and developed by Wood et al. (2002), Walker et al. (2008) and Schnell, Stott et al. (2016). The technique used in our laboratory is described below and summarised (along with the developed double seeded inverted – DSII – technique, see Chapter 3) in Figure 2.1. Firstly, the permeable membrane inserts were placed in a companion well plate and conditioned with 200 µL cell culture medium with FBS and antibiotics in the apical compartment and stored at 18°C. Next, one or two fish (depending on cell numbers required) were randomly isolated from the aquarium and sacrificed using the Schedule 1 technique (Home Office, 1986). Displacing the operculum on one side revealed the first of 4 gill arches (Fig 2.2A). These were removed by cutting the gill arch dorsally and ventrally, blotted carefully to remove gill mucus and placed into 20 mL PBS in a Petri dish (Fig 2.2B). Filaments were cut from the arches (leaving the branchial artery intact on the gill arch) and placed into 10 mL of filament washing solution (solution 1, Fig 2.1), comprised of 4% (*v/v*) penicillin-streptomycin, 4% (*v/v*) gentamicin and 3% (*v/v*) amphotericin B solution in PBS, in another Petri dish. The filaments were teased and cut apart using a scalpel and transferred to a fresh 10 mL of filament washing solution in a 50 mL conical tube and incubated for 10 minutes on ice. The gill filaments were then centrifuged (250 g, 4°C, 5 minutes) and the filament washing solution was aspirated and replaced with a further 10 mL of fresh filament washing solution before incubating for 10 minutes on ice. Centrifugation was repeated (same centrifuge settings) and following aspiration the tryptic digestion followed whereby the filaments were first pretreated with 500 µL 0.05% trypsin-EDTA (solution 2, Fig 2.1), which was immediately removed by centrifuging at the same settings, followed by two rounds of digestion with 5 mL trypsin on an orbital shaker for 12 minutes (325 rpm). After each trypsinisation, the filaments were passed through a 100 µm cell strainer into 20 mL PBS containing an excess of FBS (10% *v/v*) (solution 3, Fig 2.1) to deactivate the trypsin. This

was centrifuged (250 g, 4°C, 10 minutes) and the pellet was resuspended in 2.5% FBS (*v/v*) in PBS

(solution 4, Fig 2.1). After a further centrifugation (same 10 minute centrifuge settings) the pellet

was fiercely dislodged by flicking the conical tube to ensure proper mixing of cells upon addition of

20 mL cell culture medium with antibiotics and FBS (solution 5, Fig 2.1). A total viable gill cell count

was obtained using Trypan blue and a haemocytometer and cells were deemed of acceptable

viability at >80%. The cells were then seeded as below; in flasks or immediately onto cell culture

inserts.
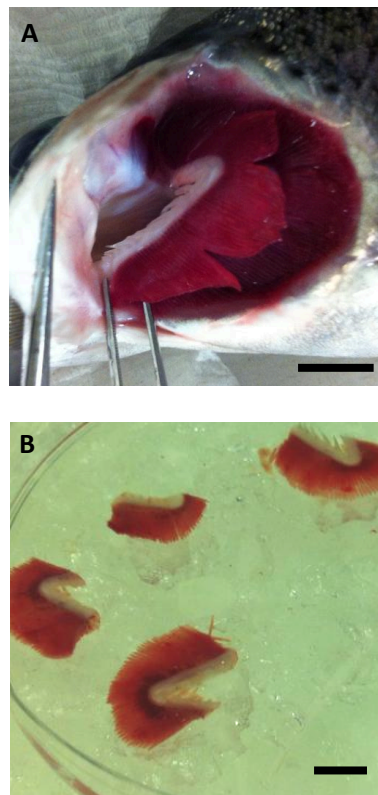
Fig 2.2 Four gill arches are located underneath each operculum (A) on the lateral sides of the rainbow trout head. *Bar* = 1

cm. Gill arches are dissected by cutting the cartilage of the arch and placed into PBS (B). *Bar* = 1 cm.

2.2.4 Seeding in cell culture flasks

For experiments requiring primary gill cells first grown in cell culture flasks ('SSI'), cells were

seeded at a density of 20-25 x 10^6 in 3 mL per 25 cm^2 cell culture flask or 40-60 x 10^6 in 10 mL per

75 cm^2 flask. These flasks were washed 24 hours later with PBS to remove unattached cell debris,

and the media was replaced with 3 or 10 mL (respectively) cell culture medium with FBS and without antibiotics and maintained at 18°C in the dark, with media changes every 2-3 days (Wood & Pärt, 1997). After 6-9 days, when cells appeared confluent, they were trypsinised by applying 200-500 µL 0.05% trypsin-EDTA for 3-5 minutes at room temperature, with gentle agitation. The cells were then collected in cell culture medium with FBS and without antibiotics, counted (as above) and seeded on inserts at a cell density of 0.7 x 10^6 per 1.5 mL per insert. The basolateral compartment contained 2.0 mL of cell culture medium with FBS. The gill cell cultures were then maintained as below. In later chapters, 'SSI' will refer to this culture technique.

2.2.5   Double seeded inserts

For primary gill cells seeded straight onto the permeable membrane inserts, cells were seeded at a density of 1.2 x 10^6 cells in a volume of 600 µL cell culture medium with FBS and antibiotics per cell culture insert (so that with the pre-conditioning step, the final volume in the apical compartment was 800 µL). The basolateral compartment was filled with 1000 µL of cell culture medium with FBS and antibiotics. The low evaporation lid was replaced and the cells were maintained at 18°C in the dark. This was termed 'day 0' (Fig 2.1).

After the first day of cell seeding, the above cell isolation procedures were repeated, resulting in a solution of cells in cell culture medium with FBS and antibiotics. Cells were counted and diluted to 1.2 x 10^6 cells per 800 µL of cell culture medium with FBS and antibiotics, and kept on ice. The medium from the previously seeded inserts was carefully aspirated (basolateral compartment first, then apical compartment to maintain hydrostatic pressure on the apically seeded cells). The cells were then carefully washed twice with 200 µL PBS. 800 µL of the new gill cell solution was applied carefully to the apical compartment, so as not to disturb the cells already attached. The basolateral compartment was refilled with 1000 µL cell culture medium with FBS and antibiotics. The gill cell cultures were then maintained at 18°C in the dark for 24 hours. This was termed 'day

1'. Twenty-four hours later, the cell culture medium was aspirated and the DSI epithelia were washed twice with 200 µL PBS to remove the cell debris from seeding. The cell culture medium with FBS and antibiotics was then replaced with full volumes – 1.5 mL in the apical compartment (applied first to maintain hydrostatic pressure on the cells) and 2.0 mL in the basolateral compartment. This was termed 'day 2'.
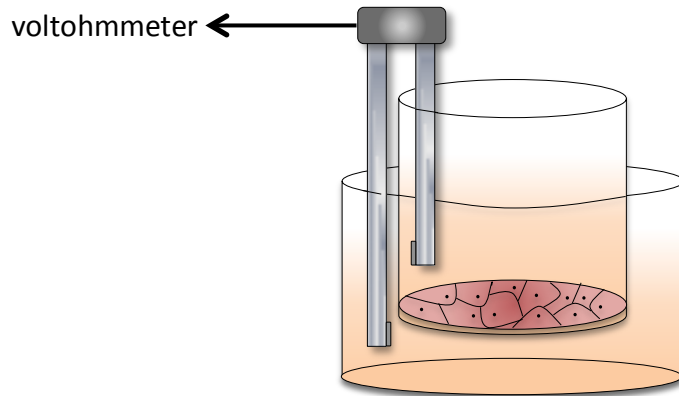
Fig 2.3 Membrane development was monitored by daily transepithelial electrical resistance (TER) measurements using a custom-modified epithelial tissue voltohmmeter fitted with chopstick electrodes. The electrode arms are inserted above and below the gill cell epithelium of each insert, such that one arm of the electrode is in the apical, and the other in the basolateral compartment.

2.3   Maintenance

On day 4, the media was changed to cell culture medium with FBS (1.5 mL in the apical and 2.0 mL in the basolateral), as the cells no longer required antibiotic supplementation. The media could then be changed every 2 or 3 days whilst the DSI gill cell epithelia develop. This development was monitored by daily transepithelial electrical resistance (TER) measurements using a custom-modified epithelial tissue voltohmmeter fitted with chopstick electrodes with the mode selected to '*R*' (the resistance setting). Briefly, the electrode was inserted over the gill cell epithelium of each insert, such that one arm of the electrode is in the apical, and the other in the basolateral compartment (Fig 2.3). Once a current is generated, the voltohmmeter can make a measurement

of transepithelial electrical resistance that corresponds to the tightness of the gill epithelium, and hence its development, without disturbing the epithelia. A 'blank' cell free insert (for 12 well culture plates) gave a value of 180 Ω cm^2, which was subtracted from each measurement. An encouraging development would show TER values in the region of 5000 Ω cm^2 by day 7 (see Chapter 3).

2.4   RTgill-W1

The rainbow trout gill cell line, RTgill-W1, was kindly donated by Prof Kristin Schirmer and maintained in our laboratory by Dr Sabine Schnell according to Bols et al. (1994). Briefly, the cells were routinely cultured at 18°C in 75 cm^2 cell culture flasks in L-15 with 10% (*v/v*) FBS, 2% (*v/v*) gentamicin and 2% (*v/v*) penicillin-streptomycin. The cells were maintained and split once per week. When required, RTgill-W1 cells were trypsinised by applying 200-500 µL 0.05% trypsin-EDTA for 3-5 minutes at room temperature, with gentle agitation. The cells were then collected in cell culture medium with 10% (*v/v*) FBS and without antibiotics, counted and seeded on inserts at a cell density of 0.2 x 10^6 cells per insert, in the same cell culture volumes – 1.5 mL in the apical and 2.0 mL in the basolateral. TER measurements were conducted as outlined above.

2.5   Cell culture exposures

Once gill cell cultures were ready for experimentation, the cell culture medium with FBS was removed, and the epithelia were washed twice with 200 µL PBS and placed in a new companion well plate to insure no traces of FBS remained. The apical surface of the cells could then be exposed to sterile 1.5 mL apical FW, whilst the basolateral remained in L-15 medium without supplementation. Substances (pharmaceuticals, paracellular markers, etc.) could be added to either FW or L-15 accordingly.

2.6   *N* and biological replicates

Throughout, the numbers of individual inserts per condition are denoted as *n*, derived from biological replicates (referring to one set of epithelia derived from 2 fish for DSI) indicating the numbers of fish from which they were isolated. For cells grown in flasks (SSI), these cells will be from at least 2 fish, pooled together and seeded. For the cell line RTgill-W1, the passage number (P) is quoted.

Chapter 3

The characterisation of the primary rainbow trout gill cell system, the cell line RTgill-W1 and the 3D hepatocyte co-culture

3.1 Abstract

Several gill surrogates exist that can be used to investigate the transport of substances over the gill and into fish. The most advanced primary gill cell culture model involves the seeding of cells over two days using the double seeded insert (DSI) technique. This was developed from the single seeded insert (SSI) method. The immortalised gill cell line, RTgill-W1, also exists and was isolated in 1995. This chapter characterised the features of these three systems, SSI, DSI and RTgill-W1. Micrographs showed the different cell morphologies of the primary cells compared to the gill cell line. After days of development, DSI epithelia exhibited the highest transepithelial resistance (TER), to values similar to *in vivo*. All gill cell preparations showed increases in TER, and hence membrane tightness, after apical freshwater application. In DSI, transepithelial potential (TEP) was positive with respect to TER and became negative upon apical freshwater application, as seen *in vivo*. The permeability of DSI rapidly decreased as TER increased, indicating the formation of a tight epithelium that is paracellulary impermeable. DSI had the lowest epithelial permeability of all cell preparations, and RTgill-W1 had the highest. Mitochondria-rich cells (MRCs) can be observed in DSI, as well as the tight junction protein, zonula occludin (ZO-1). ZO-1 was also observed in double seeded inverted (DSII) preparations that were later used in the culture of primary gill epithelial cells and 3D hepatocyte spheroids. The initial characterisation of this showed that the co-culture of these two different cell types resulted in tighter gill epithelium development.

3.2 Introduction

The gills of freshwater teleost fish are a multifunctional organ; comprising multiple cell types performing specific physiological activities. Owing to the differences in osmotic potential between the freshwater environment and that of internal body fluids, the gill maintains a protective barrier to the aquatic environment, as well as controlling the uptake of oxygen and excretion of carbon dioxide and nitrogenous waste.

Fletcher et al. (2000) developed a double seeding technique (DSI) that enables primary gill cells to be cultured on permeable membrane inserts in a two-compartment model. This method was further developed (Walker et al., 2008) and then optimised in our laboratory (Schnell, Stott et al., 2016). This procedure produces a gill epithelium with features akin to the *in vivo* gill tissue (Kelly et al., 2000). These characteristics include a gill epithelium composed of different cell types such as pavement cells (PVC), mitochondria-rich cells (MRC) and mucous cells, high transepithelial resistance (TER), a transepithelial potential (TEP), low paracellular permeability and tight junction proteins including zonula occludin (ZO-1), occludins and claudins (Chasiotis et al., 2012). Importantly, this system is able to tolerate freshwater at the apical surface of the cells and produces a negative transepithelial potential (TEP) (Stott et al., 2015), further simulating the *in vivo* scenario. The tolerance of the *in vitro* gill to freshwater is important if we are to recreate the gill epithelium for bioconcentration and ecotoxicological study.

This chapter will present the full characterisation of the primary gill cell culture system; necessary for its proof of functionality as an *in vitro* gill epithelium with which further experiments in later chapters were based upon. This chapter will focus on the single seed of primary cells (SSI, using cells that were initially cultured in cell culture flasks), double seeds of primary cells (DSI) and the immortalised rainbow trout gill cell line RTgill-W1 (see Chapter 2) in terms of cell morphology, TER, TEP, permeability, tight junctions and cell type.

The DSI technique (Fig 3.1A) was further altered in our laboratory to the double seeded inverted insert (DSII), whereby the cells are grown on the underside of the insert (Fig 3.1B; Schnell, Stott, et al., 2016). Culturing in this way allows the system to be used as a solvent-free dosing system similar to that described by Kramer et al. (2010) and also allows a reduction in the volume of the receiving compartment thus increasing the chemical analytical power necessary for assessing xenobiotic biotransformation. This chapter therefore also presents the initial characterisation of the DSII gill epithelial system and its co-culture for the first time with another cell type, rainbow trout 3D spheroidal hepatocytes.
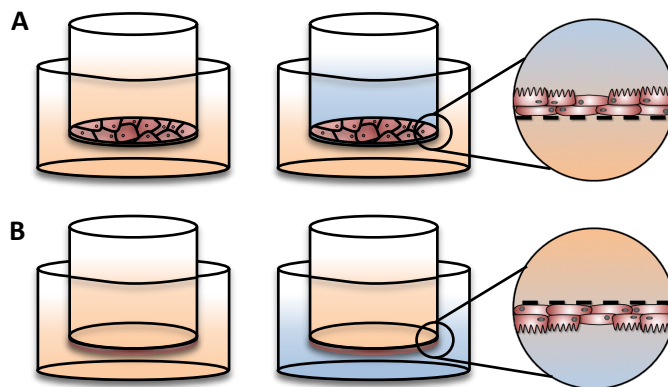
Fig 3.1 Summary of the DSI and DSII cell culture procedures of primary rainbow trout gill cells. Reconstructed as (A) DSI or (B) DSII preparations. The epithelium attaches to the permeable membrane supports and polarises so as to have an apical and basolateral cell surface (right). Epithelia are bathed on both sides with cell culture medium supplemented with FBS and antibiotics during development (left). For experimental purposes, freshwater can replace cell culture medium on the apical surface, whilst the basolateral surface is bathed in L-15 (without FBS or antibiotics) (middle).

3.3 Materials and methods

3.3.1   Reagents and suppliers

Reagents purchased were the same as those outlined in Chapter 2 with the following additions. Rhodamine-123, Hoechst, bovine serum albumin (BSA), poly(2-hydroxyethylmethacrylate) (pHEMA), Trypan blue, ethylenediaminetetraacetic acid (EDTA), sodium bicarbonate ($NaHCO_3$), Triton™ X-100 and crystalline paraformaldehyde were obtained from Sigma Aldrich; the latter was made up according to manufacturer's instructions. Hank's balanced salt solutions (HBSS) with and without calcium and magnesium and Alexa Fluor AF488 were purchased from Invitrogen Life Technologies. Primary zonula occludin (ZO-1) rabbit antibody was purchased from Abcam. Collagenase D was obtained from Roche Scientific. Vectashield was purchased from Vectorlabs. Finally, ^{14}C-mannitol (specific activity 20 Ci $mmol^{-1}$) was purchased from Amersham Biosciences.

3.3.2   Equipment and suppliers

Equipment used was the same as those outlined in Chapter 2 with the following additions. Six well culture plates were purchased from BD Falcon; 23G hypodermic needles and polythene tubing (0.76 mm internal diameter; 1.22 mm external diameter) were purchased from Smiths Medical, UK and the peristaltic pump was produced by Watson Marlow, UK. The gyratory shaker was manufactured by Innova (model number 2000 with a 1.9 cm orbit). The light microscope was an Eclipse TE200 by Nikon with a digital camera (DXM1200, Nikon) and the imaging software was Lucia G by Nikon. The confocal microscope was produced by Leica and the imaging software was Leica Confocal Software by Leica. The liquid scintillation fluid was purchased from Ecolume and the scintillation counter was a Tri Carb 460CD liquid scintillation system by Packard.

3.3.3   Preparation of reagents

Reagents were prepared as outlined in Chapter 2. Hank's Balanced Salt Solution (HBSS) without calcium or magnesium was supplemented with 4.2 mM $NaHCO_3$ and 2.3 mM EDTA. pHEMA was reconstituted in 90% ethanol to 2.5%. Collagenase D was reconstituted in HBSS with calcium and magnesium to 0.1% with 4.2 mM $NaHCO_3$.

3.3.4   Cell culture reagents

The primary gill cell culture and RTgill-W1 culture media was the same as that described in Chapter 2. 3D spheroidal hepatocyte cell culture medium was composed of L-15 with 10% (*v/v*) FBS.

3.3.5   Gill cell culture methods

The general material and methods for the SSI, DSI gill cell culture and RTgill-W1 procedures can be found in Chapter 2. SSI will always refer to primary gill cells first cultured in flasks, then trypsinised and seeded onto cell culture inserts as detailed in Chapter 2. Seeding densities on inserts are 0.7 x 10^6 for SSI, (2 x) 1.2 x 10^6 for DSI and 0.2 x 10^6 for RTgill-W1.

3.3.6   Double seeded inverted inserts

The following method describes the same double seeded insert (DSI) technique, with the amendment of culturing on the underside of the insert, and so is termed the double seeded inverted insert (DSII) technique (Fig 2.1; Fig 3.1B; Schnell, Stott et al., 2016). Firstly, permeable membrane inserts were placed upside down on glass slides (i.e. a flat surface) in a sterile Gilson 'tip box' with damp cotton wool inside to provide a moist environment and reduce evaporation of culture medium. These were preconditioned with 200 µL cell culture medium with FBS and antibiotics on the insert membrane (Fig 2.1, DSII). The previous gill cell isolation procedure then followed (Chapter 2), after which cells were seeded at a density of 1.2 x 10^6 in 200 µL cell culture

medium with FBS and antibiotics. The tip box was carefully shut and the gill cell cultures were maintained on the upside down inserts at 18°C in the dark ('day 0'). After the first day of cell seeding, 24 hours later, the cell isolation procedures were repeated resulting in a new gill cell culture suspension. Cells were counted and diluted to 1.2×10^6 cells per 200 µL of cell culture medium with FBS and antibiotics, and kept on ice. The medium from the previously seeded inserts was removed and the cells were carefully washed twice with 200 µL PBS. 200 µL of the new gill cell solution was then applied carefully to the membrane of the upside down insert, so as not to disturb the cells already attached, the Gilson tip box lid was replaced and cells were maintained at 18°C in the dark for a further 24 hours ('day 1'). On day 2, the inverted inserts could then be washed as previously and turned right-way-up and placed in a companion well plate. Finally, 1.5 mL of cell culture medium with FBS and antibiotics was applied to the apical compartment, with 2.0 mL in the basolateral (where the cells were growing on the underside of the insert). The DSII epithelia were maintained and prepared for experimental procedures in the same way as DSI, but by adding freshwater into the basolateral compartment (the apical cell surface) and cell culture medium in the apical compartment (the basolateral cell surface) (Fig 3.1B).

3.3.7 3D hepatocyte cell culture

For the development and optimisation of the 3D spheroidal hepatocytes culture protocol, the following methods were employed based on those described by Baron et al. (2012).

3.3.8 Rainbow trout dissection

One rainbow trout was randomly isolated from the aquarium and sacrificed using Schedule 1 techniques (Home Office, 1986). Its external surface was sterilised with 70% ethanol and the whole body was placed right-flank down on a dissecting mat in a laminar flow hood. The first incision was a cut at the anus using a scalpel, upwards towards the lateral line (approximately 2 cm, Fig 3.2A). Two horizontal cuts followed, one along the ventral edge towards the pectoral fins,

followed by a further cut along the lateral line to the operculum. The resulting fillet was removed

to expose the body cavity (Fig 3.2B). Carefully pulling back the pyloric caecae revealed the liver

and hepatic portal vein, and cutting the pericardial cavity tissue exposed the heart (Fig 3.3A).
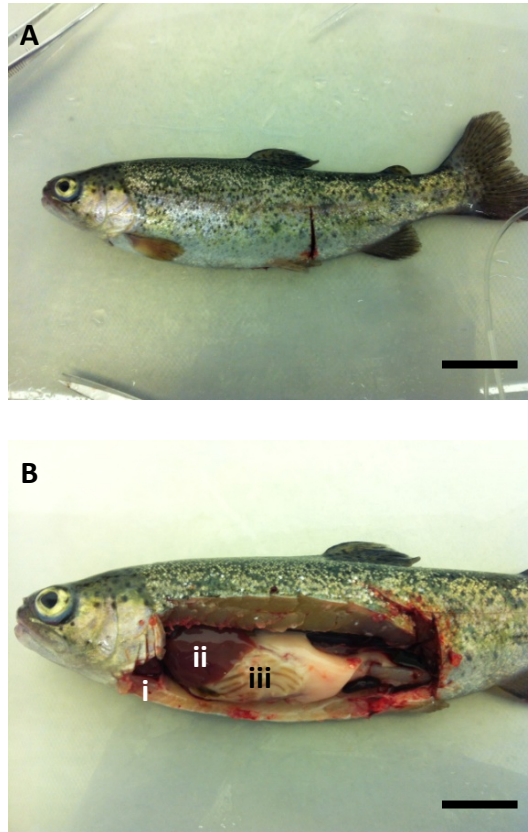
Fig 3.2 Image of a rainbow trout showing (A) the initial cut from the anus to the lateral line. *Bar* = 3 cm. The left lateral

fillet is removed to expose the body cavity (B). The liver (ii) is located next to the heart (i) and underneath the pyloric

cacae (iii). *Bar* = 1.5 cm).

3.3.9 *In situ* liver perfusion

A 23G hypodermic needle inserted into polythene tubing was connected to a calibrated peristaltic

pump and flushed through with 100% ethanol. After running through with HBSS without metals,

the needle was inserted into the hepatic portal vein (Fig 3.3B) and perfusion initiated at a rate of 1

mL min^{-1}. After the initial yellowing of the liver as the blood was displaced (after approximately 1

minute), the heart was cut to allow the perfusate out of the circulatory system, and the perfusion

continued for a further 9 minutes. The liver was kept damp throughout by applying a few mL of L-15. The perfusion then proceeded with 0.1% Collagenase D for a further 15 minutes. During this time, the liver can be observed to shine and mottle as the enzyme digests the internal cellular
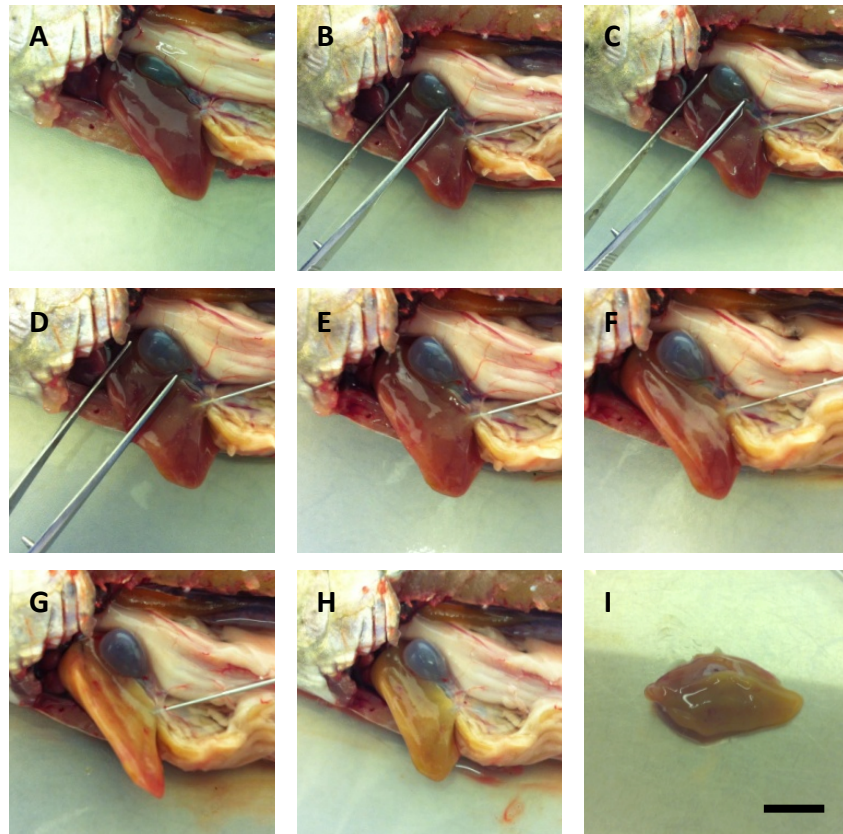
Fig 3.3 Stages of the *in situ* liver perfusion. A needle is inserted into the hepatic portal vein (B) and the cells are disaggregated with Collagenase D. The liver can be observed to yellow and mottle as the internal cellular matrices are digested and the hepatic cells disaggregate. Finally, the liver is dissected intact by severing the hepatic portal vein, veins and arteries, connective tissue and gall bladder (I). *Bar* = 1 cm.

matrices and the hepatic cells disaggregate (Fig 3.3C-H). At this point, the Collagenase D was flushed through with L-15 for approximately 2 minutes. The liver was then dissected by severing the hepatic portal vein, veins and arteries and connective tissue. The gall bladder was removed by severing at the duct to retain the bile within and the liver was placed on a sterile Petri dish (Fig 3.3I).

3.3.10 Hepatocyte isolation and seeding

Approximately 15 mL of L-15 medium was applied to a Petri dish and the liver membrane was cut to expose the disaggregated cells in solution. Any parts having bypassed the perfusion (appearing red from blood) were removed along with the membrane. The resulting cell solution was drawn into a 20 mL syringe and passed through a 100 µL and then 40 µL cell strainer into a sterile 50 mL conical tube, and the volume was adjusted to 20 mL with L-15. The cell suspension was then centrifuged (50 g, 18°C, 3 minutes), aspirated (to remove non-hepatic cells) and resuspended in a further 20 mL of L-15. This was repeated twice more until the final resuspension in 20 mL cell culture medium with FBS. A total viable gill cell count was obtained using Trypan blue and a haemocytometer and cells were deemed of acceptable viability at >80%.

Hepatic cells were seeded at 3.0×10^6 cells mL^{-1} in 3 mL L-15 with 5% FBS per well in a 6 well culture plate pre-coated and dried with 500 µL pHEMA (to discourage cell attachment). Wells were transferred immediately to a gyratory shaker at 70 RPM at room temperature.

3.3.11 Maintenance

After 24 hours, 2 mL of cell culture medium and unattached cell debris was removed from each well and new medium replaced. From that point onwards 2 mL cell culture media was removed and replaced with new every 48 hours until day 7. The spheroids were monitored daily by light microscope observation.

3.3.12 Light microscopy

Different preparations of cells were visualised using a light microscope, digital camera and imaging software as outlined in Chapter 2.

3.3.13   Transepithelial electrical resistance

TER development in SSI, DSI and RTgill-W1 was monitored for 1-7 or 8 days after seeding onto permeable membrane inserts. TER measurements were conducted as described in Chapter 2, using a custom-modified epithelial tissue voltohmmeter fitted with chopstick electrodes in mode '*R*'. The TER was measured in 3 sets of SSI epithelia (n = 30 from 6 fish), 3 sets of DSI epithelia (n = 36 from 1 biological replicate) and RTgill-W1 (n = 6, passage 90) grown in cell culture medium with FBS and antibiotics in both the apical and basolateral compartments.

To monitor the effect of apical FW exposure in epithelia, TER was measured before (from day 1 to day 7, 4 or 9) and in the following days after 1.5 mL FW was added to the apical compartment, whilst the basolateral contained 2.0 mL L-15 in SSI (n = 6 from 6 fish), DSI epithelia (n = 6 from 2 biological replicates) and RTgill-W1 preparations (n = 4, passage 90).

3.3.14   Transepithelial electrical potential

TEP between the two sides of DSI epithelia was measured using the same voltohmmeter with the mode selected to '*V*'. To determine if a relationship between TER and TEP existed, TEP was measured in symmetrical conditions (n = 19) in epithelia at varying degrees of development, with TER values from 1-15 kΩ cm^2. To monitor the effect of FW application on TEP, TEP was monitored before and 6 hours after FW application (n = 8). All TEP measurements are expressed as basal side relative to the apical at 0 mV.

3.3.15   Paracellular permeability

Paracellular epithelial permeability was determined using ^{14}C-mannitol with a molecular weight of 182 Daltons. Using this marker as opposed to conventional polyethylene glycol (PEG) polymers (typically 400-40,000 Daltons) quantifies paracellular transport of molecules with similar molecular weights to mannitol, which is more applicable to the paracellular transport of pharmaceuticals in

later chapters (Hubatsch et al., 2007). To monitor paracellular transport at various points of DSI

epithelial development, DSI epithelia with TER values ranging from 0-15 kΩ cm^2 were exposed to

0.013 µCi (2.2 × 10^5 dpm) ^{14}C-mannitol (*n* = 37 from 4 biological replicates) in 1.5 mL sterile FW in

the apical compartment, whilst the basolateral contained 2.0 mL L-15 (Wood et al., 1998,

Hubatsch et al., 2007). After gentle mixing, aliquots of 100 µL were taken from the apical and basal

compartments at time 0 and 24 h, and placed in 2 mL liquid scintillation fluid and the radioactivity

was measured by beta counting on a scintillation counter. Paracellular flux after 24 h was

calculated using the equation

$$Permeability \ (cm \ s^{-1}) = \frac{[\Delta M]_{BL} \times volume}{M_{AP} \times time \times 3600 \times area}$$

where [ΔM]$_{BL}$ is the change in radioactivity in the basal compartment, M_{AP} is the radioactivity at

the start, time is 24 hours and area is 0.9 cm^2 (Fletcher et al., 2000).

To investigate the paracellular permeability of different cell preparations in symmetrical and

asymmetrical conditions, the TER of RTgill-W1 (*n* = 4 and 3), SSI (*n* = 3 and 4 from 6 fish), and DSI (*n*

= 12 and 10 from 4 biological replicates) was measured and then preparations were exposed. ^{14}C-

mannitol (0.013 µCi; 2.2 × 10^5 dpm) was applied apically to either 1.5 mL L-15 or FW (for

symmetrical or asymmetrical conditions), whilst the basolateral compartment always contained L-

15. Aliquots of 100 µL were taken and counted as above. Cell free inserts were used to calculate

permeability through the PET membrane on which the cells grew in both symmetrical and

asymmetrical conditions (*n* = 4).

3.3.16 Mitochondria-rich cell staining

Approximately 1 x 10^6 freshly isolated cells were resuspended in 1 mL of 5 µM Rhodamine-123 in

PBS and incubated for 15 minutes in the dark at room temperature. To view MRC present in DSI

epithelia, cell cultures that had surpassed a TER of 5000 Ω cm^2 (*n* = 2) were washed twice with 200

µL PBS and detached by applying 400 µL 0.05% trypsin-EDTA in the apical compartment for 2 minutes at room temperature. 400 µL of cell culture medium with FBS was applied to stop tryptic digestion and the cells were carefully scraped from the cell culture membrane using a pipette and collected. The cells were centrifuged (250 g, 4°C, 5 minutes) and resuspended in 500 µL of 5 µM Rhodamine-123 in PBS for 15 minutes in the dark at room temperature. From both preparations of freshly isolated and DSI cells, several 100 µL aliquots were transferred to microscope slides underneath a cover slip, and the cells were visualised using a fluorescent microscope, digital camera, and imaging software.

3.3.17   ZO-1 protein localisation

Two DSI epithelia cultured for 14 days and with TERs of 7730 and 9890 Ω cm^2, were exposed in either symmetrical (L-15 medium both sides of the epithelium), or asymmetrical (apical FW and L-15 in the basolateral compartment) for 24 hours. The epithelia were then washed twice with 200 µL PBS and fixed for 15 minutes using 400 µL of 3.7% (*v/v*) paraformaldehyde in PBS in the apical compartment, and 600 µL in the basolateral. Three 200 µL PBS washes followed, where the PBS was left on the apical surface of the epithelia for 5 minutes each time and shaken at 30 RPM. 400 µL of 0.1% (*v/v*) Triton™ in PBS was applied in the apical compartment, and 600 µL in the basolateral, for 10 minutes at room temperature to permeabilise the epithelia. Afterwards, 400 µL of 3% (*w/v*) bovine serum albumin (BSA) in PBS was applied for 30 minutes at room temperature to block non-specific protein interactions. 0.5% (*v/v*) primary zonula occludin (ZO-1) rabbit antibody was prepared in 3% (*v/v*) BSA in PBS, and 400 µL was added to each apical compartment and incubated at 4°C in a damp box (containing damp tissue to reduce evaporation) overnight. The following day, the epithelia were washed twice with 200 µL PBS and labeled using 400 µL of 0.1% (*v/v*) Alexa Fluor green (AF488) in PBS, applied to the apical surface of each epithelium for 1 hour at room temperature in the dark. Afterwards, epithelia were again washed twice with 200 µL PBS, and 400 µL of 5 µM Hoechst in PBS was applied (to label cell nuclei) and incubated for 15 minutes

at room temperature in the dark. Afterwards, the epithelia were washed 3 x 200 µL PBS, and the cell culture inserts were cut from their plastic holders using a scalpel and placed cell-side-up on a microscope slide. One drop of mounting media was applied under a cover slip, which was then varnished onto the slide. The slides were left to dry overnight in the dark (wrapped in foil) at 4°C before visualisation.

3.3.18   Double seeded inverted inserts

TER, TEP and paracellular permeability were measured in the same way as DSI, previously. DSII epithelia were also stained for ZO-1 as before, but with the amendment that all washes and staining solutions were added to the basolateral compartment (the apical cell surface).

3.3.19   DSII and 3D hepatocyte co-culture

DSII epithelia at 9 days and with a TER > 5000 Ω cm^2 (n = 7) were prepared for experimental procedures as outlined previously. Liver hepatocytes at 9 days and observed to have reached morphological maturity were counted and collected from two 6-well culture plates into a 14 mL conical tube and allowed to settle. The culture medium was aspirated and replaced with 10 mL L-15 to wash, and again the livers were allowed to settle before aspirating. These were finally resuspended in 4.5 mL cell culture medium with FBS and antibiotics. 1.5 mL liver hepatocytes were added to three of the DSII epithelia in the apical compartment, whilst the remaining four DSII had 1.5 mL cell culture medium with FBS and antibiotics added. 2.0 mL cell culture medium with FBS and antibiotics was added to the basolateral compartment of all DSII. Gill epithelial membrane integrity of DSII and DSII co-cultures were then monitored by daily measurements of TER.

3.3.20   Analysis of data and statistics

The relationship between TER and TEP was analysed by ordinary least squares linear regression. An independent samples *t*-test with equal variances assumed was used to test for differences in

TEP before and after FW exposure and statistical significance was accepted when P < 0.05 (SPSS software, SPSS Inc.). Differences of permeability in symmetrical or asymmetrical conditions between cell free inserts and RTgill-W1, SSI or DSI were tested for by a one-way analysis of variance (ANOVA) and post hoc testing using Tukey's honest significance test (HSD). Statistical significance was accepted when P < 0.05 (SPSS software, SPSS Inc.). The paracellular permeability of DSII epithelia in symmetrical and asymmetrical conditions were compared to that of cell free inserts and DSI epithelia using an independent samples *t*-test with equal variances assumed. Differences in the TER of DSII and DSII co-cultured with hepatocytes were tested for using an independent samples *t*-test with equal variances assumed and statistical significance was accepted when P < 0.05 (SPSS software, SPSS Inc.). All graphical illustrations were produced using either Excel (Microsoft Office) or Sigmaplot (Systat Software Inc.).

3.4 Results

3.4.1 Light microscopy

Primary gill cells cultured in cell culture flasks (Fig 3.4A) were visualised adhered to the flask surface, or in globular form preparing for or having undergone mitotic division. Less easily visualised are DSI primary gill cells on membrane inserts, as the microscope views from below through the insert membrane. Nevertheless, cells were observed adhering to the insert membrane (Fig 3.4B). RTgill-W1 cells exhibit different cell morphology (Bols et al., 1994), and successfully attach to the insert membranes, with fewer unattached cells and debris (Lee et al., 2009).

3.4.2 Transepithelial electrical resistance

Epithelial development was monitored by daily measurements of TER in symmetrical conditions. TER in SSI reached 585.2 ± 31.2, 498.0 ± 24.2 and 608.8 ± 62.0 Ω cm^2 after 7 days (*n* = 12, 12 and 6;
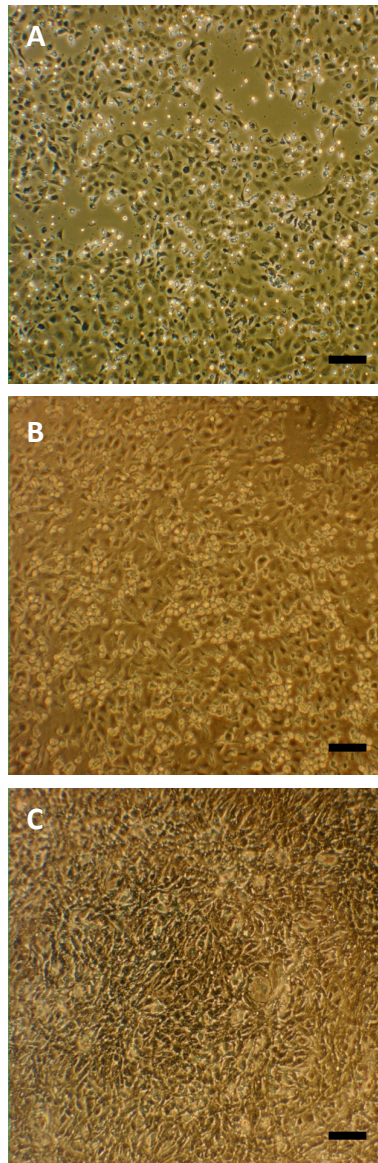
Fig 3.4 Phase contrast micrographs of gill epithelial cells. After isolation, primary gill cells can attach and grow in cell culture flasks with cell culture medium with FBS and with or without antibiotics. These cells can then be seeded onto inserts (SSI) (A). Primary cells can also be seeded directly onto culture inserts (B) using DSI culture techniques. The immortalised rainbow trout gill cell line, RTgill-W1, also successfully attaches and grows in the same cell system set up on cell culture inserts (C). *Bar* = 100 µm.

Fig 3.5A) and typically showed a 70% increase in TER and there were no differences in TER values between different sets of epithelia. After 8 days, the TER of DSI epithelia increased by around 97% and reached 25.5 ± 1.0, 23.0 ± 1.5 and 22.9 ± 2.1 kΩ cm^2 (*n* = 12, 12 and 12; Fig 3.5B), with no difference between sets of epithelia. After 8 days, the TER in RTgill-W1 cells increased by 34% and reached 28.5 ± 3.4 Ω cm^2 (*n* = 4; Fig 3.5C).

In asymmetrical conditions when water is placed on the apical surface on day 7, SSI showed an increase in TER from 0.5 ± 0.0 to 3.8 ± 0.3 kΩ cm^2. TER remained above 3.0 kΩ cm^2 for 24 hours before declining to 0.4 ± 0.0 kΩ cm^2 by day 10 and lower values thereafter (*n* = 30; Fig 3.6A). The TER of DSI epithelia increased from 27.4 ± 0.4 kΩ cm^2 to 33.2 ± 0.1 kΩ cm^2 after 24 hours FW exposure, then decreased to 30.8 ± 0.7 kΩ cm^2 after 48 hours, before decreasing to values below 16.8 ± 2.39 kΩ cm^2 thereafter (*n* = 36; Fig 3.6B). RTgill-W1 TER rose from 24.5 ± 2.9 Ω cm^2 to 45.0 ± 9.1 Ω cm^2 after 24 hours and remained at higher values for the resulting 3 days (*n* = 4; Fig 3.6C).

3.4.3 Transepithelial electrical potential

The mean TEP in symmetrical conditions with L-15 both sides of the epithelia was -0.5 ± 0.1 mV and no relationship between TER and TEP existed during symmetrical conditions (r^2 = 0.046, *n* = 19; Fig 3.7A). After apical freshwater application TEP in the basolateral compartment became significantly more negative (with respect to the apical compartment) from -0.9 ± 0.1 mV to -12.9 ± 2.9 mV after 6 hours apical FW exposure (*P* < 0.05; *n* = 8; Fig 3.7B).

A

B

C
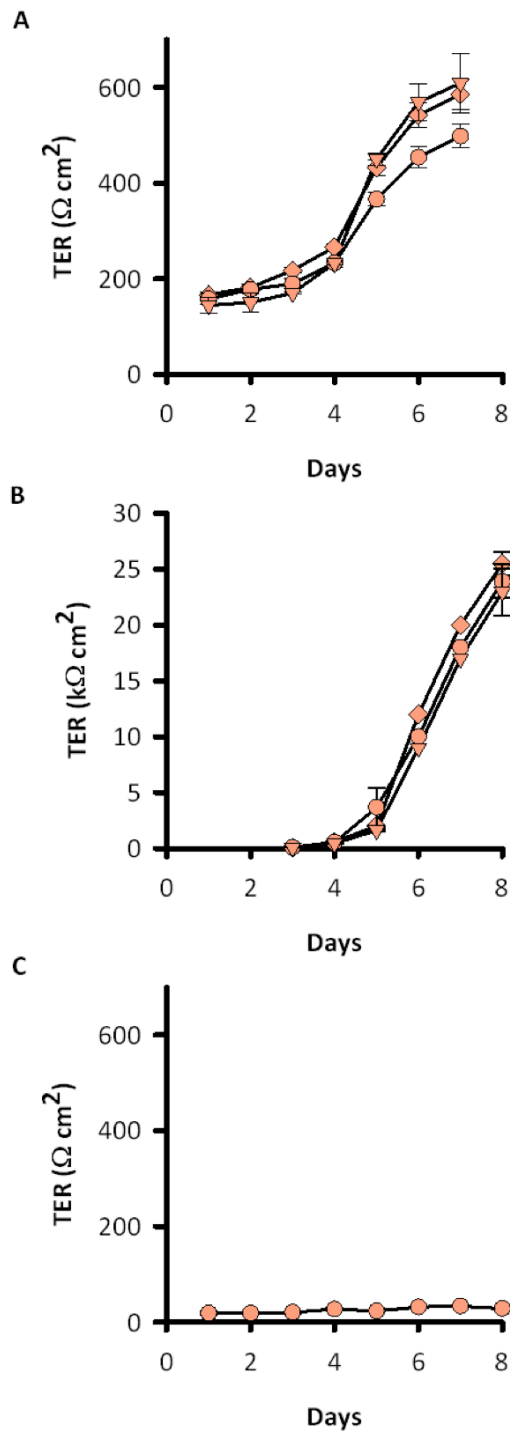
Fig 3.5 The development of TER from 1 or 3 to 8 days in (A) 3 sets of SSI preparations (*n* = 12, 12 and 6 from 6 fish)*,* (B) 3 sets of DSI (*n* = 12, 12 and 12 from 1 biological replicate) (note the axis in kΩ cm^2) and (C) RTgill-W1 cells (*n* = 4, P90) in symmetrical conditions with cell culture medium with FBS and antibiotics both sides of the epithelia. Symbols (circles, diamonds or triangles) represent groups of epithelia from different cell preparations. The values represent mean ± SEM. Error bars are behind data points where none can be seen.
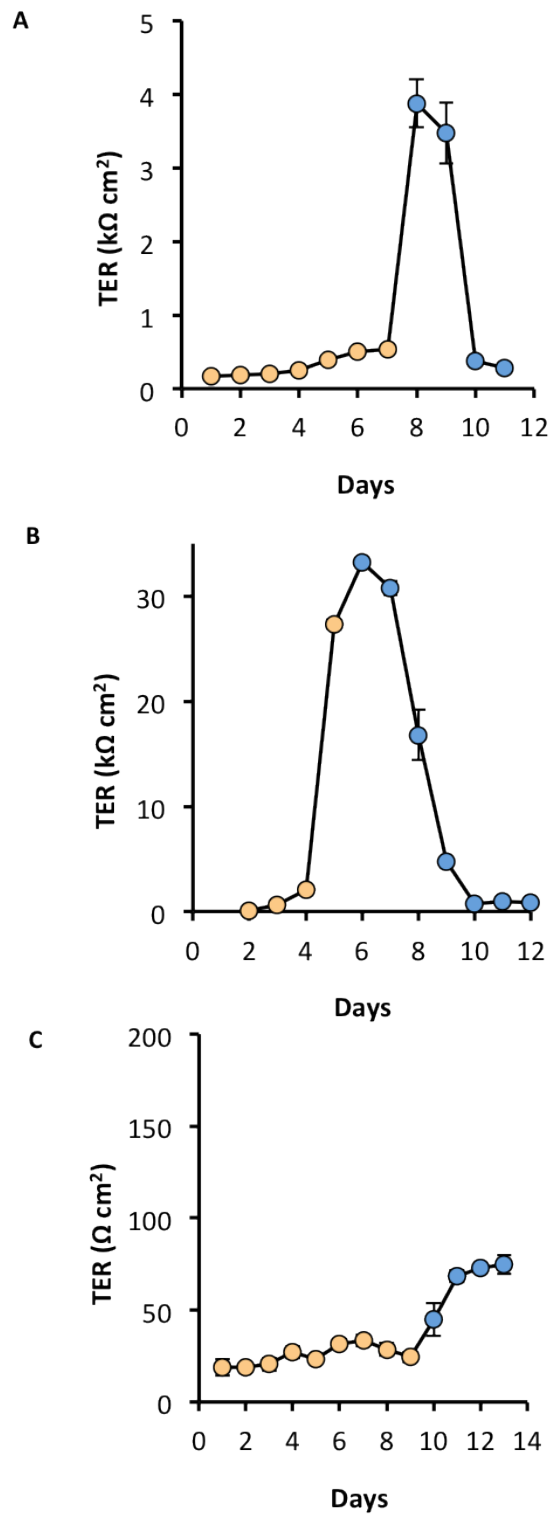
Fig 3.6 TER in symmetrical conditions with cell culture medium with FBS and antibiotics both sides of the epithelia (orange circles), until apical freshwater application with L-15 in the basal compartment (blue circles) in (A) SSI preparations (n = 24), (B) DSI (n = 6) and (C) RTgill-W1 cells (n = 4). Note the axes in (A) and (B) are in kΩ cm^2. The values represent mean ± SEM. Error bars are behind data points where none can be seen.
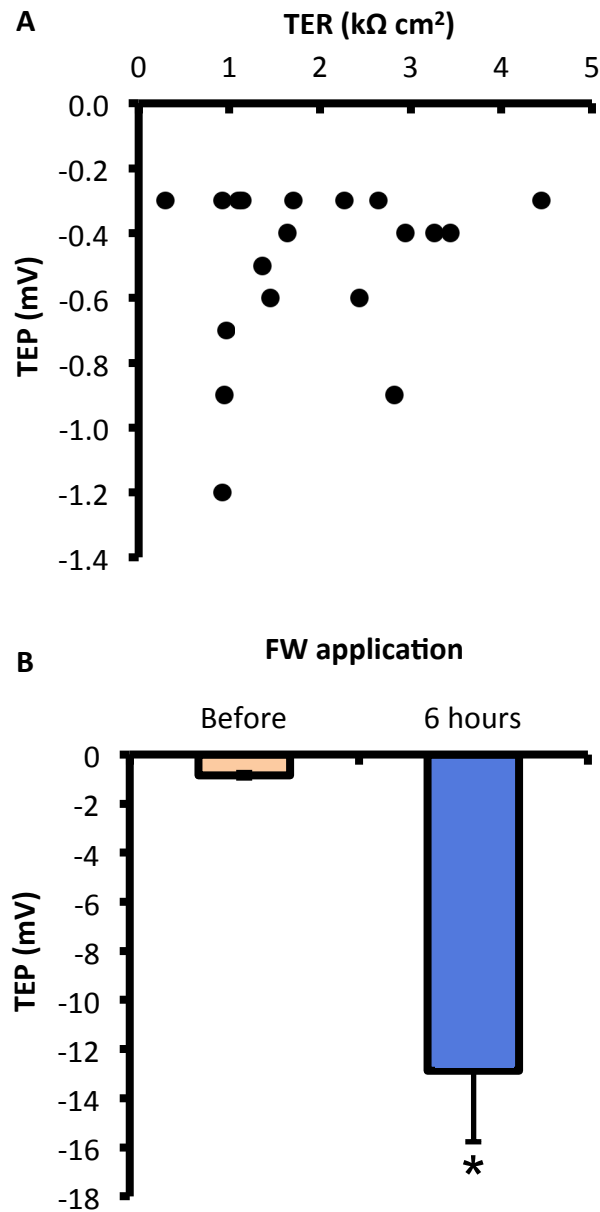
Fig 3.7 (A) The relationship between TEP and TER in DSI epithelia in symmetrical conditions with cell culture medium with FBS and antibiotics both sides of the epithelia *(n = 19, r^2 = 0.046)*. (B) TEP in symmetrical conditions before FW application with L-15 both sides of the epithelia (orange bar) and after FW application to the apical compartment, whilst the basolateral contained L-15 after 6 hours (blue bar) (*n* = 8). Significant differences are indicated by the asterisk (independent samples *t*-test; *P < 0.05). Values are mean ± SEM.

3.4.4   Paracellular permeability

In DSI preparations, small increases in TER resulted in large decreases in paracellular ^{14}C-mannitol influx (Fig 3.8A). A TER of between 200-1000 Ω cm^2 exhibited the highest mannitol permeability of $1.5 \pm 0.2 \times 10^{-6}$ cm s^{-1} (*n* = 9). Those with a TER of 1-2 kΩ cm^2 showed a decreased mannitol permeability of $0.9 \pm 0.1 \times 10^{-6}$ cm s^{-1} (*n* = 11), whilst those > 2 kΩ cm^2 showed the lowest mannitol permeability ($0.1 \pm 0.0 \times 10^{-6}$ cm s^{-1}; *n* = 13), with little variation between epithelia (Fig 3.8A).

No differences in paracellular permeability between symmetrical and asymmetrical conditions existed within different preparations of gill cell epithelia (*P* > 0.05; Table 3.1; Fig 3.8B).

Table 3.1

Summary of the ^{14}C-mannitol permeabilities and TER of gill cell preparations.

	Symmetrical (L-15:L-15)		Asymmetrical (FW:L-15)	
	TER ± SEM (Ω cm^2)	Permeability (x 10^{-6} cm s^{-1})	TER ± SEM (Ω cm^2)	Permeability (x 10^{-6} cm s^{-1})
Cell free	0 ± 0	4.68 ± 0.5	0 ± 0	3.63 ± 0.1
RTgill-W1	34 ± 3	2.85 ± 0.1	36 ± 2	3.01 ± 0.1
SSI	1240 ± 30	0.22 ± 0.0	1252 ± 11	0.17 ± 0.0
DSI	22970 ± 2000	0.01 ± 0.0	16423 ± 1690	0.07 ± 0.0

Values represent average +/- SEM

There was a significant difference in paracellular permeability between all cell preparations in both symmetrical and asymmetrical conditions ($F_{(7,36)}$ = 233.22; *P* = 0.000). All gill cell preparations exhibited significantly lower paracellular permeability than cell free conditions in symmetrical (*P* = 0.000) and asymmetrical conditions (*P* = 0.000) apart from RTgill-W1. Despite large differences in TER between SSI and DSI, both these preparations of primary cells showed a significant decrease in permeability compared to the cell free control (*P* = 0.000; Table 3.1; Fig 3.8B) and the cell line RTgill-W1 (*P* = 0.000; Table 3.1; Fig 3.8B).

A

B
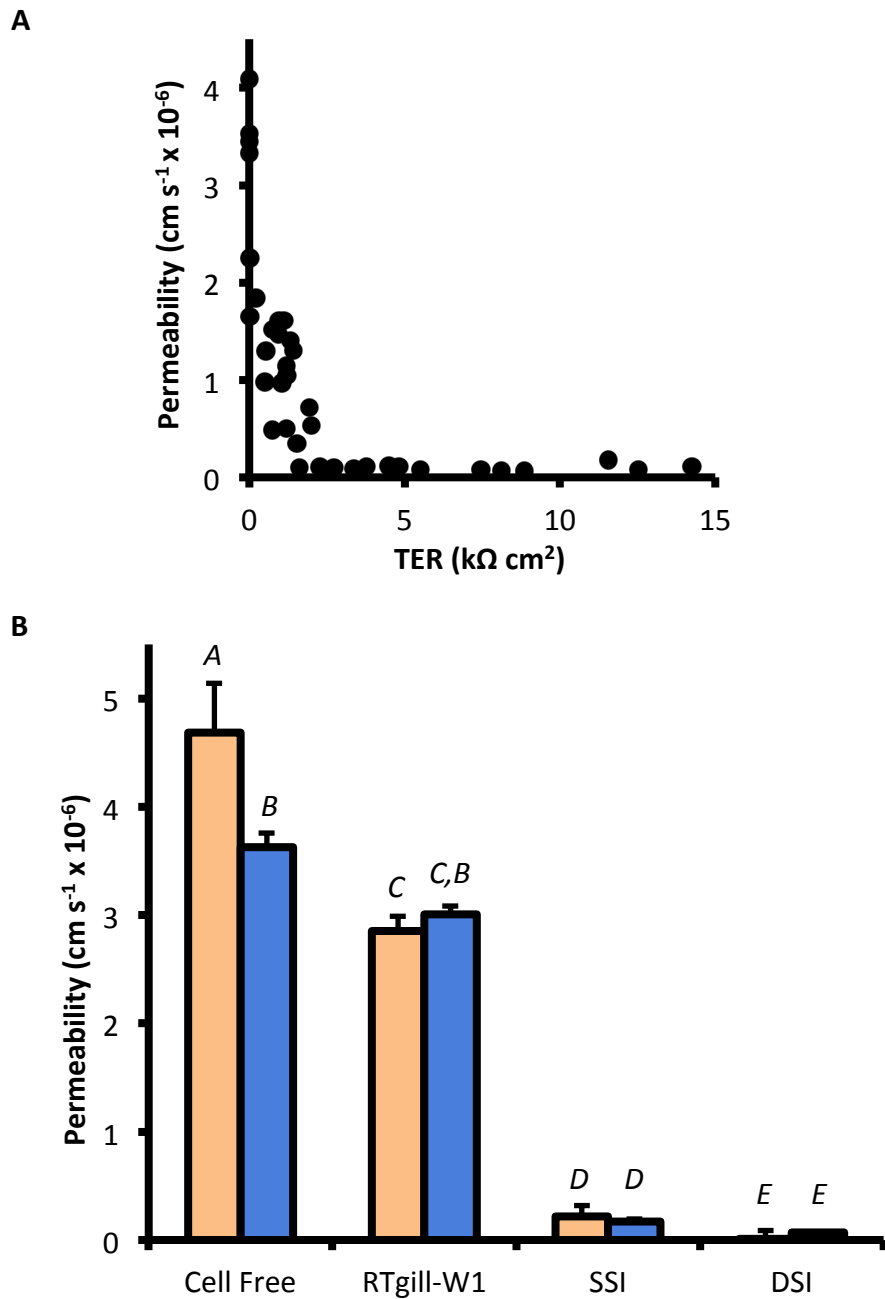
Fig 3.8 ^{14}C-mannitol permeability in gill cell epithelial preparations. ^{14}C-mannitol was applied to the apical compartment and its appearance monitored in the basolateral. (A) shows the relationship between ^{14}C-mannitol permeability (after 24 hours in asymmetrical conditions) and TER in DSI epithelia. Each data point represents one DSI epithelium (n = 37) from 4 biological replicates. (B) shows the reduction in mannitol permeability from the cell free condition in RTgill-W1 cell preparations (n = 4), SSI (n = 4 from 2 biological replicates) and DSI epithelia (n = 10 from 3 biological replicates). Orange bars are symmetrical (L-15:L-15) and blue are asymmetrical (FW:L-15) conditions. Those epithelia that are significantly different from others are indicated by a different capital letter (one-way ANOVA; P < 0.05). Values are mean ± SEM. Error bars are behind bars where none can be seen.
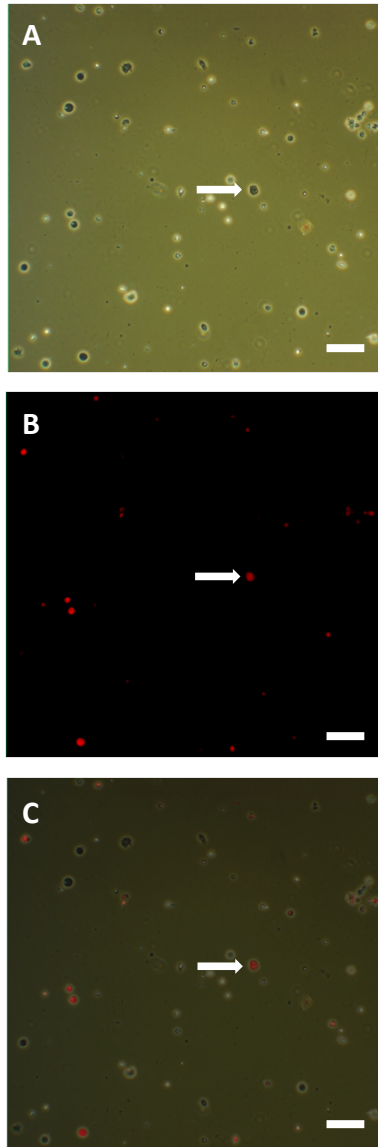
Fig 3.9 Phase contrast microscope images of cells freshly isolated from the rainbow trout gill and stained with Rhodamine-123 in (A) white light and (B) fluorescent light. An overlay of the two pictures identifies those mitochondria-rich cells (MRC) (C); the arrow points to one such example of a cell in all images. *Bar* = 100 μm.

3.4.5   Mitochondria-rich cell staining

The presence of MRCs was observed in preparations of freshly isolated primary rainbow trout gill cells stained with 5 µM Rhodamine-123, confirming their presence after the initial isolation. These can be viewed (e.g. at the arrow) in white light conditions (Fig 3.9A), in fluorescent light (Fig 3.9B), and indeed when the two images are superimposed upon one another (Fig 3.9C). Likewise, MRC cells were observed in DSI epithelia that had surpassed 5000 Ω cm^2 and had been trypsinised and stained with Rhodamine-123 (Fig 3.10).
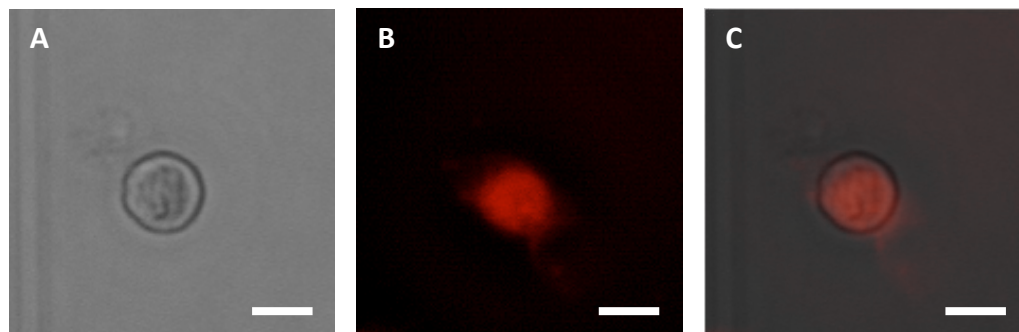
Fig 3.10 Phase contrast microscope images of a cell isolated from a DSI epithelial preparation and stained with 5 µM Rhodamine-123 (red). Light micrograph (A) and fluorescent image (B) of the cell. Overlaying the two images (C) confirms the red fluorescent signal from the DSI cell, identifying it as a mitochondria-rich cell (MRC). *Bar* = 25 µm.

3.4.6   ZO-1 protein localisation

Staining using 5 µM Hoechst allowed visualisation of DSI cell nuclei (blue) in both preparations from symmetrical and asymmetrical exposures (Fig 3.11A; Fig 3.11B). Overlaying of some nuclei can be seen where cells were growing in layers. ZO-1 was successfully visualised (green) around the periphery of cells. In this way, the cell surface morphology can be observed as a typical polygonal 'carpet' of PVCs.
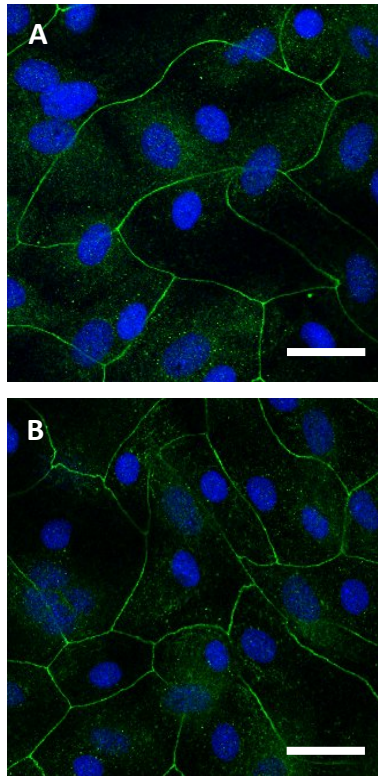
Fig 3.11 Confocal microscope images of DSI epithelia in (A) symmetrical conditions with L-15 media on both sides of the epithelium and (B) in asymmetrical conditions with FW in the apical compartment and L-15 media in the basolateral for 24 hours before cell fixing. Cell nuclei were stained with 5 µM Hoechst (blue) and tight junctions with zonula occludin antibody (green). *Bar* = 50 µm.

3.4.7 Double seeded inverted inserts

Similar to DSI epithelia, the TER of DSII epithelia rose during epithelial development from 54.7 ± 7.7 Ω cm^2 on day 4 to 15.5 ± 3.0 kΩ cm^2 on day 9 (n = 3), showing an increase of 99%. After freshwater exposure to the apical surface of DSII epithelia, TEP became positive with respect to the apical (the basolateral surface), indicating a negative transepithelial potential across the epithelium, like that seen in DSI.

DSII gill epithelia with a TER of 3170 ± 360 Ω cm^2 exhibited a mannitol permeability of 0.1 ± 0.0 x 10^{-6} cm s^{-1} in symmetrical conditions (n = 3). This was significantly different from the cell free control (P = 0.000). In asymmetrical conditions DSII epithelia with a TER of 13.5 ± 1.9 kΩ cm^2

showed a mannitol permeability of $0.1 \pm 0.0 \times 10^{-6}$ cm s^{-1} (n = 8) which was significantly different from the cell free control and not significantly different from the permeability of DSI epithelia (P = 0.000 and P = 0.06).

Staining using 5 μM Hoechst showed cell nuclei (blue) in DSII epithelia in both symmetrical and asymmetrical conditions (Fig 3.12A; Fig 3.12B). Like in DSI, ZO-1 was visualised (green) around the periphery of all cells and the DSII epithelia exhibited the typical polygonal 'carpet' of cells on the apical surface.
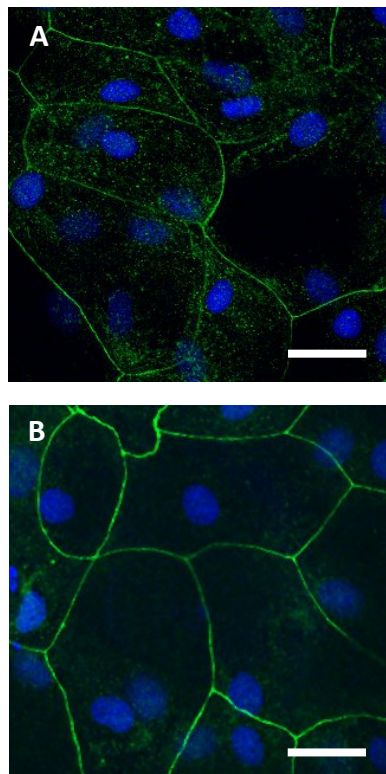
Fig 3.12 Confocal microscope images of DSII epithelia in (A) symmetrical conditions with L-15 media on both sides of the epithelium and (B) in asymmetrical conditions with FW in the apical compartment and L-15 media in the basolateral for 24 hours before cell fixing. Cell nuclei were stained with 5 μM Hoechst (blue) and tight junctions with zonula-occludin antibody (green). *Bar* = 50 μm.

3.4.8   DSII and 3D hepatocyte co-culture

Liver hepatocytes were observed to reach morphological maturity over 9 days in rotational cell culture (Fig 3.13A-F).
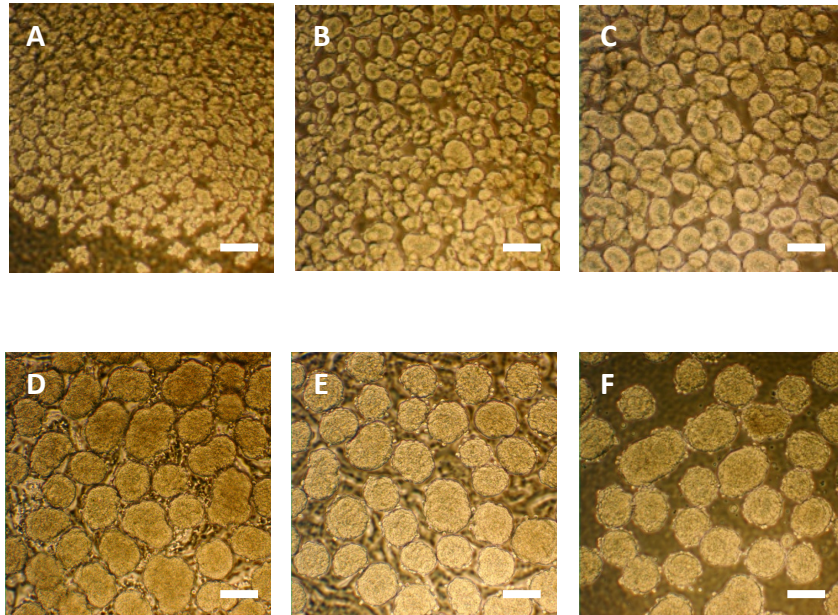
Fig 3.13 Phase contrast micrographs of 3D liver hepatocytes developing through days 2-4 (A-C) and 7-9 (D-F). *Bar* = 100 µm. Spheroids can be observed as small clusters on the second and third day after seeding into 6 well culture plates coated in pHEMA (A and B). By day 4, irregularly shaped immature spheroids have formed (C). The hepatocytes become larger, with defined edges by days 7 and 8 (D and E) before reaching similarly shaped spheroids by day 9 (F).

After the addition of mature hepatocytes to the basolateral surface of DSII epithelia (into the apical chamber) on day 9, the TER is shown to increase to values significantly higher than that of cultures of only DSII on days 9, 10 and 11 ($P < 0.05$; $n = 7$; Fig 3.14), and the spheroids remain morphologically stable during this time.
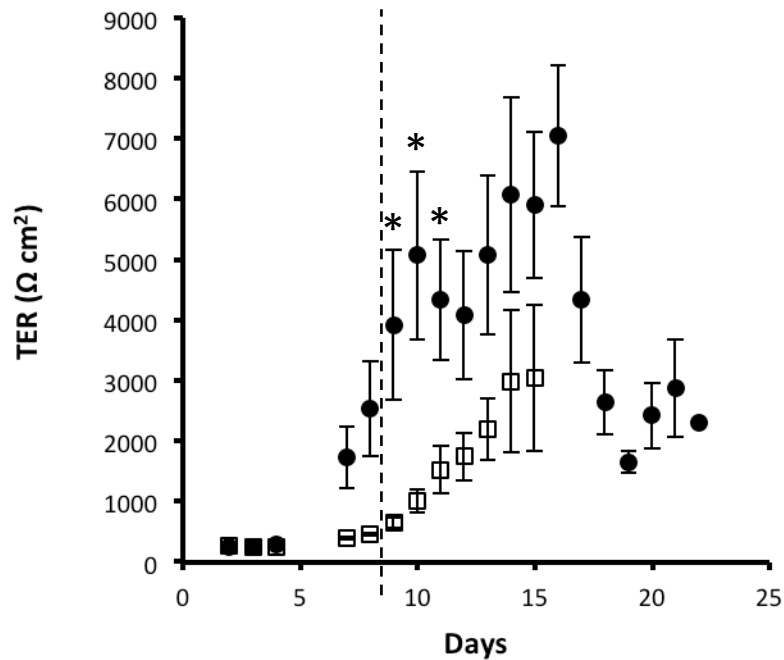
Fig 3.14 The TER from 2 to 22 days of DSII epithelia (□) and DSII epithelia in co-culture with hepatocytes (•) from day 9

(dashed line) in symmetrical conditions with cell culture medium with FBS and antibiotics both sides of the epithelia.

Significant differences are indicated by the asterisk (independent samples *t*-test; *$P < 0.05$). The values represent mean

± SEM. Error bars are behind data points where none can be seen.

3.5 Discussion

The gill epithelial cells freshly isolated from juvenile rainbow trout can be cultured successfully in

cell culture flasks and on permeable membrane inserts using the SSI and DSI techniques. Likewise,

the immortalised rainbow trout gill cell line RTgill-W1 attaches and proliferates on the same cell

culture inserts. Gill epithelia grown from SSI cells are populations of solely PVCs (Wood & Pärt,

1997).

During gill cell epithelial development, SSI cells exhibited increases in TER of 70% over 7 days. DSI

epithelial cells exhibited greater TER development, with values increasing approximately 100-fold

after 8 days. Typically, DSI epithelial development was sigmoidal and reached a plateau of 30,000

Ω cm^2 after 7-14 days, as has been previously documented (Fletcher et al., 2000; Wood et al., 2002). An increase in TER is indicative of the organisation of an epithelial cell layer. Increases in TER are not due to increases in cell number or growth, but rather the increases in tight junction proteins expression and interaction (Wood et al., 2002), especially between PVCs and MRCs (Fletcher et al., 2000), of which the latter are not present in SSI preparations (Wood et al., 1998), and thus may explain their more limited epithelial development in terms of TER. Tight junctions can also be observed in transmission electron micrographs of primary gill cells cultured using the DSI technique (Wood & Pärt, 1997; Fletcher et al., 2000). Mammalian epithelial cells cultured on permeable cell culture inserts form epithelia with TERs of 325 Ω cm^{-2} for Caco-2 (Dickman et al., 2000), <1000 Ω cm^{-2} in blood-brain barrier (BBB) models (Wilhelm et al., 2011) and 173 Ω cm^{-2} in MDCK cells (Irvine et al., 1999). In contrast, the gills present a formidable barrier to paracellular transport and the TER values observed in SSI and DSI confirm these preparations as 'tight' epithelia. The TER of RTgill-W1 cell preparations plateaued at lower values, equivalent to approximately 0.1% of the TER seen in DSI cell cultures. Addition of tetrabromocinnamic acid and cortisol, both stimulators of the development of TER, to RTgill-W1 preparations does cause improvement in RTgill-W1 TER development (Trubitt et al., 2015), but not to the values observed in DSI preparations.

For all cell preparations, application of apical freshwater resulted in the increase of TER, which dropped after 48 hours for DSI and SSI but was maintained in RTgill-W1. The DSI exposed to apical freshwater in this instance had already high TER values around 27 kΩ cm^2, so after 24 hours showed a smaller increase in TER. Typically, the increase in TER observed after freshwater application depended on the TER before FW exposure – DSI epithelia at lower TER values around 5-10 kΩ cm^2 show much greater increases to similar 30 kΩ cm^2 values before declining as before, whilst those at already high values show smaller increases, as they have already appeared to reach their upper limit of TER values. Rapid increases in TER upon freshwater application are brought

about by fast changes in transcellular or paracellular conductance in the epithelium (Wood and Pärt, 1997). The SSI and DSI epithelia show the highest observed TER after 7 days of development and after freshwater application (Fig 3.6; Wood et al., 2002), higher compared to other freshwater gill surrogates such as the killifish opercular epithelium, which increases from 294 to 660 Ω cm^2 after freshwater application (Wood & Marshall, 1994), or the Nile tilapia opercular epithelium, which increases from 169 to 1052 Ω cm^2 (Burgess et al., 1998).

In symmetrical conditions, no relationship between TER and TEP was observed, as the conditions either side of the gill epithelium are the same. In these conditions, TEP is slightly negative and becomes more negative after apical freshwater application (-12.9 ± 2.9 mV; -10.3 ± 0.2 mV, Fletcher et al., 2000) to values similar to that observed *in vivo* (Potts, 1984). The change in membrane potential to basolateral negative generates an electrical gradient that aids cation partitioning across the gill epithelium, specifically the differential permeability of the tight junctions to Na$^+$ compared with Cl$^-$ (Fletcher et al., 2000).

Once a tight epithelium (> 2000 Ω cm^2) has formed, the DSI *in vitro* gill presents a barrier to paracellular transport that is relatively impermeable to the paracellular permeability marker ^{14}C-mannitol (Stott et al., 2015; Fig 3.8A). The paracellular marker PEG4000 also showed the relative impermeability of DSI epithelia (Fletcher et al., 2000). Like increases in TER, this is not due to increases in cell numbers or growth, but to the increases in tight junction proteins that form over time as the epithelium develops (Wood et al., 2002). No differences in paracellular permeability were observed between symmetrical and asymmetrical conditions in all gill cell preparations, indicating that the application of freshwater does not disrupt the tight junctions formed between gill cells, even after 24 hours.

In symmetrical conditions, the mannitol permeability of RTgill-W1 was significantly lower than that of cell free inserts indicating that this epithelial cell line forms an impermeable layer. However,

when freshwater is applied in asymmetrical conditions, no differences exist between the permeability of cell free inserts and RTgill-W1 preparations, indicating that epithelia formed of this cell line are permeable after 24 hours of freshwater exposure. For primary gill cells, the paracellular permeability in SSI and DSI were significantly lower than both the cell free inserts and the RTgill-W1 preparations in symmetrical conditions, and also after 24 hours of freshwater exposure. These primary cells can tolerate freshwater at their apical surface due to their features that are similar to the intact gill (Wood et al., 2002). MRCs contain an abundance of mitochondria employed to synthesise the ATP required for active ionic transport (Perry, 1997). The mitochondrial fluorescent dye Rhodamine-123 identified those cells with abundant mitochondria as MRCs in freshly isolated primary gill cells (Fig 3.9) and cells grown in DSI (Fig 3.10). Previous work has estimated that DSI retain approximately 10-15% MRC, similar to those observed *in vivo* (Walker et al., 2007). The SSI technique yields an epithelium composed of uniform PVCs and so no MRCs can be observed (Wood et al., 2002). MRCs have also been observed in preparations of RTgill-W1 grown on inserts and stained with Rhodamine-123 (Lee et al., 2009).

DSI epithelia exhibited a characteristic polygonal carpet of PVCs with the tight junction protein ZO-1 adjoining cells (Fig 3.11; Walker et al., 2007). ZO-1 and other transmembrane and cytosolic proteins stitch cells together to form tight junctions (Chasiotis et al., 2012) (Fig 1.4). In the teleost gill, tight junction proteins form connections between cells to produce a barrier between the environment and internal milieu of the organism (González-Mariscal et al., 2003). The proteins occludin and claudin are integral to the TJ backbone, as well as cadherins, ZOs and junction adhesion molecules (JAMs) (Bauer et al., 2010; González-Mariscal et al., 2003). Communication between exposed transmembrane proteins between cells and ZO-1 allows information about the external environment to be relayed to the cell nucleus, affecting transcriptional pathways regulating membrane permeability (Chasiotis et al., 2012). The ZO-1 proteins visualised in DSI link the external tight junction proteins such as claudin and occludins to the internal actin

cytoskeleton, whilst also acting to transduce signals to the nucleus about tight junction formation and cell proliferation (Bauer et al., 2010). The DSI tight junction complex is also evident by the high TER measurements documented above. ZO-1 is also present in cultures of SSI and is confined to the apical surface of the epithelium as in DSI, and addition of cortisol caused the deepening of these tight junctions and increased the barrier properties of epithelia (Sandbichler et al., 2011b). ZO-1 mRNA has been detected in RTgill-W1 epithelia grown on inserts, but its level is unaffected by treatments with cortisol, and other hormone treatments such as carp growth hormone and ovine prolactin (Trubitt et al., 2015).

A new double seeded inverted insert (DSII) technique is described. The development of this protocol from the DSI technique was required to reduce the distance between cells of different organ origins during co-culture (as used in the *in vitro* blood brain barrier, BBB; Santaguida et al., 2006), and to reduce the volumes of receiver medium to increase the chemical analytical power necessary for assessing xenobiotic biotransformation (Kramer et al., 2010). Here for the first time, the DSII epithelia are characterised and found to exhibit the same epithelial properties as DSI preparations (Schnell, Stott, et al., 2016). The DSII develop in a similar way to DSI and reach TER values as high as those previously observed. The permeability of DSII was found to not be significantly different from DSI, and so these DSII preparations form a tight epithelial barrier with low paracellular permeability. Furthermore, the ZO-1 protein was identified in DSII preparations, and the epithelia exhibited the same polygonal morphology (Fig 3.12) as that seen in DSI (Fig 3.11).

The 3D spheroidal hepatocyte primary cell culture described here was developed by Baron et al. (2012) and successfully optimised for use in our laboratory such that the spheroids produced (Fig 3.13) morphologically resembled those previously described (Baron et al., 2012). The use of spheroidal hepatocytes is an important advancement in the use of alternative *in vitro* methods (3Rs) to study aquatic ecotoxicology, as the spheroids represent a more organotypic system, and

exhibit properties more akin to the *in vivo* organ such as glucose and albumin production (more so than 2D monolayers) and reduced lactate dehydrogenase (LDH) leakage.

The co-culture of primary DSII gill cell cultures and 3D spheroidal hepatocytes is documented here for the first time. The co-culture of different cell types simulates the *in vivo* environment more accurately than monoculture and allows important cell-to-cell communication (Miki et al., 2012). It is widely used in BBB study, as the co-culture of different cell types promote the development of epithelia with higher TER, deeper tight junctions and cells that display more pronounced structural changes with better functionality than when grown as monocultures (Dehouk et al., 1990; Hurst & Fritz, 1996; Abbott et al., 2006). Here, both the DSII and spheroids remain viable during co-culture, and the TER of DSII in co-culture is shown to be significantly greater than that of DSII in monoculture on the first 3 days after co-culture. This primary rainbow trout *in vitro* cell system can be used to study the uptake of xenobiotics across the gill and the metabolism of xenobiotics in the liver, which may more accurately represent the process *in vivo*.

Chapter 4

The paracellular permeability of gill cell epithelia

4.1 Abstract

There is high demand for developing alternative methods to *in vivo* experimentation. A number of ecotoxicity tests use live fish that have to be carried out due to REACH legislation. Two models currently being investigated to supplement or replace live fish in ecotoxicity testing are primary gill cells and the gill cell line RTgill-W1. The advantage of the former is that it allows the exposure of gill cells to waterborne chemicals, mimicking one of the most critical sites of toxicity of fish, the gill. This ability to form a polarised epithelium capable of tolerating water at the apical surface would be desirable in the gill cell line RTgill-W1 if it were to be used as a replacement for whole fish uptake assays. To assess the ability of RTgill-W1 cells to form a tight epithelium on the cell culture inserts as used in primary gill cell models, a number of culture scenarios were performed. RTgill-W1 was previously cultured in flasks for more than 12 months in cell culture medium (L-15), or medium supplemented with either cortisol (100 ng mL^{-1}) or epithelial growth factor (100 ng mL^{-1}) before being seeded at different densities on culture inserts. In some, primary gill cells (either freshly isolated or cultured previously in flasks) were then seeded on top. For each scenario the transepithelial resistance (TER) was monitored for 7-10 days before water was added to the apical surface for 48 hours. The epithelial permeability of the different preparations was also measured using ^{14}C-mannitol. TER increased in RTgill-W1 cells cultured on permeable supports and supplemented with cortisol. This was observed most in RTgill-W1 cells seeded at the lowest seeding density (0.1 x 10^6) and with 0.7 x 10^6 primary gill cells, previously grown in cell culture flasks, seeded on top. The paracellular permeability of these was also lowest in symmetrical conditions and in asymmetrical conditions after 24 hours of freshwater exposure to the apical surface of the cells. However, the symmetrical paracellular permeability, with cell culture medium both sides of the epithelium, is still higher than that of just single seeded (SSI) primary gill cells. In asymmetrical conditions however, paracellular permeability decreased to values similar to SSI cells.

4.2 Introduction

Advances in primary gill cell culture techniques have provided an *in vitro* model to study the freshwater gill (Bury et al., 2014). This system cultures primary gill cells on a flat permeable cell culture membrane in a two-compartment model that promotes the development of a gill epithelium with an apical and basolateral cell surface. In this way, cells maintain many of the physiological characteristics of the tissue from which they were isolated (Schnell, Stott et al., 2016). However, there are disadvantages in dealing with primary cells in culture; it being labour intensive and producing cell cultures with shorter life spans (Bols et al., 2005). Furthermore, individual differences between animals from which cells are obtained mean there is more likely to be variation between biological replicates, which may lead to difficulties in obtaining data in a reproducible manner.

An alternative to primary rainbow trout cell culture uses immortalised cell lines, the availability of which has increased in recent years and removes the requirement for live fish in line with the reduction, refinement and replacement (3Rs) of animals in scientific procedures. Cell lines are used to assay common cellular responses such as cytotoxicity, cell growth, genotoxicity and xenobiotic metabolism (Bols et al., 2005). Rainbow trout cell lines include populations derived from seven different tissues, including RTL-W1 (Lee et al., 1993) derived from liver; RTG-2 from gonad (Wolf & Quimby, 1962); RTgutGC from intestine (Kawano et al., 2011); RTbrain from brain (Ganassin & Bols, 1997); RTS11 from spleen (Ganassin & Bols, 1998); RTP-2, RTP-91E and RTP-91F from the female and male pituitary (Bols et al., 1995; Tom et al., 2001) and RTgill-W1 from the gill (Bols et al., 1994). Compared to primary gill cells, the gill cell line RTgill-W1 is relatively easy to maintain and handle and can be routinely cultured in the laboratory for many passages (Bols et al., 1994). The repeated culture of cell lines may result in the loss of morphological or physiological characteristics of the original cells or tissue, including the loss of three dimensional structure or

differences in mRNA expression during the stabilisation of cell lines (Fischer et al., 2011). Pavement cells, mitochondria-rich cells and goblet cells have been reported in RTgill-W1 (Lee et al., 2009), although the microridges of PVCs are absent, the numbers of mitochondria in MRCs are fewer and the Golgi complex and cytoplasmic droplets of mucous cells are absent (Bols et al., 1994). Furthermore, a fundamental physiological feature of gill epithelial membrane integrity is high transepithelial resistance (corresponding to low paracellular permeability), which the RTgill-W1 cell line, appears to lack (Trubitt et al., 2015). Once cultured on permeable supports, transepithelial resistance values in RTgill-W1 typically reach 30 Ω cm^2, whilst primary gill cells can surpass values one thousand times that to around 30,000 Ω cm^2 (see Chapter 3). The RTgill-W1 cell line also appears to be deficient in certain metabolic enzymes such as CYP1A (Schirmer et al., 1998). Nonetheless, the removal of the requirement of live fish offers an appealing advantage of using fish cell lines, and their incorporation into regulatory testing legislation has been recommended (Dayeh et al., 2013).

Low paracellular permeability is principle in the functioning of the freshwater gill, due to the osmotic gradient between blood and external freshwater that has to be maintained (González-Mariscal et al., 2003). *In vivo*, this is achieved through the development of tight junctions between cells provided by proteins such as claudin, occludin, cadherin, zonula occludin (ZO-1) and junction adhesion molecules (JAMs) (Chasiotis et al., 2012). Some of these have been characterised in both primary gill cells (Sandbichler et al., 2011a) and RTgill-W1 (Trubitt et al., 2015).

Culturing primary gill cells with cortisol has been shown to improve epithelial development as illustrated by increases in transepithelial resistance and decreases in paracellular permeability (Chasiotis et al., 2010). Furthermore, occludin protein abundance increased dose-dependently with cortisol treatment (Chasiotis et al., 2010). Epidermal growth factor (EGF) binds to the EGF receptor resulting in cell growth proliferation and differentiation. In epidermal cells, this is known to encourage the formation of tighter junctions between cells by concentrating the tight junction

protein ZO-1 at these junctions (González-Mariscal et al., 2003). However application of 10 ng mL^{-1} to primary gill cell medium did not significantly improve either attachment efficiency or cell growth as measured by ^{3}H-thymidine incorporation (Pärt et al., 1993).

In blood brain barrier (BBB) *in vitro* models, cells of different types may be co-cultured together in order to induce certain epithelial characteristics such as higher transepithelial resistance, low paracellular permeability and transporter expression (Wilhelm et al., 2011). Astrocytes are known to stimulate BBB properties in other endothelial cells and so can be co-cultured with cell lines to produce a more accurate BBB model (Gaillard et al., 2001).

In this study, the rainbow trout gill cell line RTgill-W1 was treated with EGF or cortisol to improve epithelial development and membrane integrity in terms of transepithelial resistance and paracellular permeability. Some populations were also co-cultured with primary cells (either freshly isolated or previously seeded in cell culture flasks) in order to further stimulate epithelial membrane development. Transepithelial resistance (TER) was monitored for 7-10 days, after which a mannitol permeability assay was conducted to quantify paracellular permeability.

4.3 Materials and Methods

4.3.1 Reagents and suppliers

Reagents purchased were the same as those outlined in Chapter 2 with the following additions. Epidermal growth factor (EGF) and cortisol were purchased from Sigma Aldrich. ^{14}C-mannitol was obtained from Amersham as before.

4.3.2 Equipment and suppliers

Equipment used was the same as those outlined in Chapter 2.

4.3.3   Preparation of reagents

Reagents were prepared as outlined in Chapter 2.

4.3.4   Cell culture reagents

Cell culture reagents were prepared as outlined in Chapter 2. During culture and maintenance before experimental procedures, EGF or cortisol were added to RTgill-W1 culture medium at a concentration of 100 ng mL^{-1}.

4.3.5   Methods

The general material and methods for the maintenance of RTgill-W1 and the primary cell culture of both SSI (single seeded inserts from primary cells initially cultured in flasks) and DSI (double seeded inserts) are outlined in Chapter 2.

4.3.6   RTgill-W1 cell culture

The rainbow trout gill cell line, RTgill-W1, was maintained according to Bols et al. (1994). At passage P70, the cells were split into 3 cell culture flasks and maintained in normal cell culture media supplemented with antibiotics (L-15) or with additional EGF or cortisol at a concentration of 100 ng mL^{-1} (Pärt et al., 1993; Wood et al., 2002). Dr Sabine Schnell maintained the cells under these conditions for more than 12 months according to the normal maintenance protocol.

4.3.7   Experimental set up

RTgill-W1 cells at passage P90-114 (Fig 4.1) cultured in L-15, EGF or cortisol, were trypsinised by removing the culture medium before applying 500 µL 0.05% trypsin-EDTA for approximately 3 minutes at room temperature. Applying 10 mL of cell culture solution stopped the action of the trypsin and cells were collected in a 50 mL conical tube. RTgill-W1 cells were stained for viability using Trypan blue and diluted in cell culture medium to the appropriate cell concentration. The

cells were then seeded onto permeable membrane inserts at densities of 0.1, 0.2 or 0.5 x 10^6 (n = 24 per seeding density [3], per condition [3], *total n* = 216, Fig 4.1) in 1.5 mL and 2.0 mL cell culture medium (with or without supplementation with EGF or cortisol) in the apical and basal compartments respectively and maintained at 18°C in the dark. The first of these sets (n = 8 per seeding density) was maintained for 7-10 days with a media change every 2-3 days (Fig 4.1A). The second set (n = 8) was seeded the next day with 0.7 x 10^6 primary gill cells that had been grown in flasks for 6-8 days previously (Wood & Pärt, 1997) (Fig 4.1B), and the third set (n = 8) with 1.2 x 10^6 freshly isolated primary rainbow trout gill cells (Chapter 2) (Fig 4.1C). These preparations were also maintained at 18°C in the dark for 7-10 days with a media change every 2-3 days.

4.3.8   Epithelial development and L-15 or freshwater exposure

The development of cells to form electrically tight epithelia was monitored by transepithelial resistance (TER) for 7-10 days following cell seeding using a custom-modified epithelial tissue voltohmmeter fitted with chopstick electrodes. As previously, a 'blank' cell free insert (for 12 well culture plates) gave a value of 180 Ω cm^2, which was subtracted from each measurement. At days 7-10, all inserts were prepared by washing with 2 x 200 µL PBS and 1.5 mL of L-15 without antibiotics or FBS was applied to the apical chamber of half of the epithelia (symmetrical; n = 108), whilst the other half were changed to FW (asymmetrical; n = 108; Fig 4.1). The basolateral compartment always contained 2.0 mL L-15. TER was then again monitored.
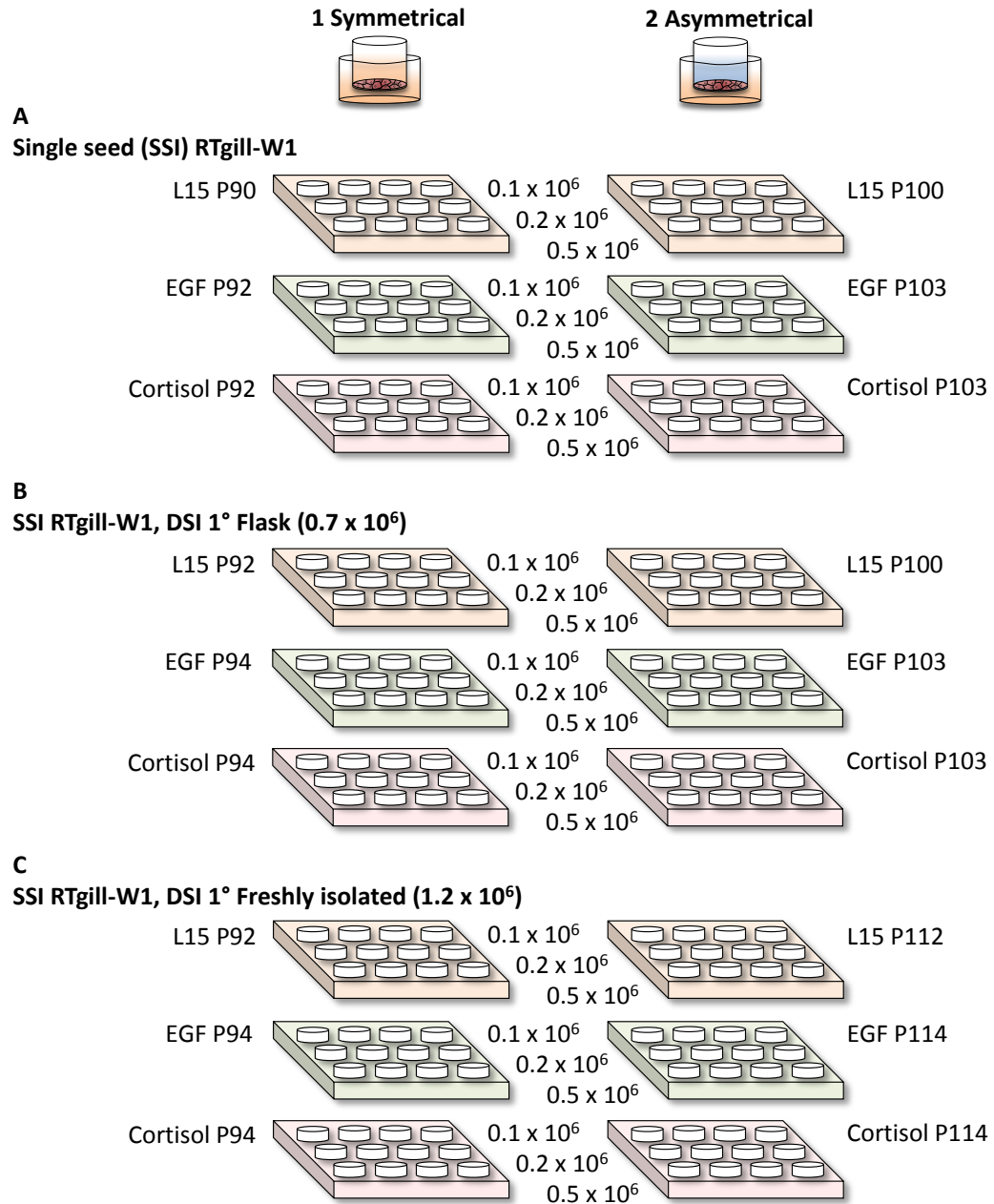
Fig 4.1 Diagram of the experimental set up and passage numbers of RTgill-W1 cells routinely cultured in flasks (> 6 months) in cell culture medium with antibiotics (L15; orange plates), or with supplementation with 100 ng mL^{-1} epidermal growth factor (EGF; green plates) or 100 ng mL^{-1} cortisol (red plates) and seeded at 0.1, 0.2 and 0.5 x10^{6} cells per insert (A). Inserts in (B) were double seeded on top the next day with 0.7 x 10^{6} primary rainbow trout gill cells grown in flasks for the previous 6-9 days, whilst those in (C) were seeded on top with 1.2 x 10^{6} freshly isolated rainbow trout gill cells. The first set (1) were exposed to L-15 in symmetrical conditions for 24 hours whilst those in (2) were exposed to apical freshwater for 24 hours in asymmetrical conditions.

4.3.9 Paracellular permeability

To provide the quantitative assessment of paracellular permeability, the transport of the marker molecule ^{14}C-mannitol across gill epithelia was measured (Petri et al., 2004). This marker has low protein binding affinity and a lower molecular weight than the PEG-4000 commonly used in permeability assays, making it more sensitive so that small changes in permeability between conditions may be detected (Shah et al., 2007).

Twenty-four hours after FW or L-15 exposure, 0.013 µCi (2.2 x 10^5 dpm mL^{-1}) ^{14}C-mannitol was applied to the apical compartment (in either FW or L-15 medium accordingly) and its appearance was monitored in the L-15 medium in the basolateral compartment after 24 hours. From this, the mannitol flux was calculated using the following equation

$$Permeability \; (cm \; s^{-1}) = \frac{[\Delta M]_{BL} \; x \; volume}{M_{AP} \; x \; time \; x \; 3600 \; x \; area}$$

where $[\Delta M]_{BL}$ is the change in radioactivity in the basal compartment, M_{AP} is the radioactivity at the start, time is 24 hours, 3600 converts hours to seconds and area is 0.9 cm^2 (Wood et al., 1998). The rate of flux was then expressed as a percentage of the mannitol flux in the cell free negative control. Data are expressed as means ± SEM, *n* = 3-4 in each condition (Fig 4.1).

4.3.10 Analysis of data and statistics

Differences in the paracellular permeability of gill cell cultures were tested for within a seeding condition for either symmetrical or asymmetrical scenarios – that is within the RTgill-W1 seeded group (Fig 4.2A; Fig 4.3A), the RTgill-W1 with primary flask cells seeded on top (Fig 4.2B; Fig 4.3B) and RTgill-W1 with freshly isolated primary cells (Fig 4.2C; Fig 4.3C). The data were expressed as a percentage of mannitol flux in a cell free control insert and then log transformed, before testing for differences by a two-way ANOVA. Statistical significance was accepted when *P* < 0.05 (SPSS

software v21, SPSS Inc.). All graphical illustrations were produced using either Excel or PowerPoint

(Microsoft Office) or Sigmaplot (Systat Software Inc.).

4.4 Results

4.4.1   Epithelial development

Dr Sabine Schnell completed the TER measurements to monitor epithelial development and so the

data for this is not shown but instead a general summary of results is included.

RTgill-W1 (Fig 4.1A) cultured in L-15 or L-15 supplemented with EGF showed no increases in TER

after 7 days of culture. Those cells cultured with cortisol increased from approximately 20 Ω cm^2

to 65 Ω cm^2.

RTgill-W1 double seeded with primary cells previously grown in flasks (Fig 4.1B) showed no

increases in TER when cultured in L-15 alone. Those co-cultured in L-15 supplemented with EGF

increased to from around 20 to 144, 116 and 64 Ω cm^2 for the 0.1, 0.2 and 0.5 x 10^6 seeding

conditions respectively. Those cultured with 100 ng mL^{-1} cortisol showed the largest increases of

all conditions from around 20 to 354 Ω cm^2 for the 0.1 x 10^6 seeding condition, and values to 130

and 55 Ω cm^2 for the 0.2 and 0.5 x 10^6 RTgill-W1 seeding densities.

RTgill-W1 double seeded with freshly isolated primary cells (Fig 4.1C) showed no changes in TER

when cultured in L-15 alone in all seeding densities. Those cultured in L-15 supplemented with EGF

or cortisol showed increases from 21 to 43 Ω cm^2 and 11 to 29 Ω cm^2 after 7 days of co-culture on

permeable inserts.

4.4.2 Paracellular Permeability

RTgill-W1 cells seeded alone, in symmetrical conditions (with L-15 both side of the epithelium) showed the lowest permeability when not supplemented with EGF or cortisol, in all seeding densities. RTgill-W1 cells seeded at 0.2 x 10^6 had the lowest mannitol permeability of 60.99 ± 2.18% of the cell free control (Table 4.1; Fig 4.2A). RTgill-W1 cells seeded at the lowest density of 0.1 x 10^6 and supplemented with 100 ng mL^{-1} EGF had the highest at 93.92 ± 3.80% cell free control. Here, seeding density and culture condition had a significant effect on permeability ($P <$ 0.001), but not when combined (P = 0.069; Table 4.1; Fig 4.2A).

Table 4.1

Summary of the ^{14}C-mannitol permeabilities of RTgill-W1 treatments, expressed as % of the cell free control.

| | | Permeability (x 10^{-6} cm s^{-1}) | | | | | |
| | | Symmetrical (L-15:L-15) | | | Asymmetrical (FW:L-15) | | |
RTgill-W1 seeding density	**Culture medium condition**	RTgill-W1	RTgill-W1 + DSI Flask	RTgill-W1 + DSI 1°	RTgill-W1	RTgill-W1 + DSI Flask	RTgill-W1 + DSI 1°
0.1	L-15	70.55 ± 3.33	43.11 ± 1.59	61.42 ± 1.26	100.22 ± 3.77	66.83 ± 2.42	75.02 ± 1.05
	EGF	93.92 ± 3.80	48.82 ± 2.46	70.25 ± 5.89	84.49 ± 2.17	44.76 ± 5.83	80.52 ± 0.74
	Cortisol	82.10 ± 1.97	28.05 ± 0.84	59.10 ± 1.66	88.16 ± 0.34	7.09 ± 0.69	86.63 ± 2.85
0.2	L-15	60.99 ± 2.18	54.75 ± 5.53	62.99 ± 3.46	101.11 ± 2.50	70.70 ± 1.21	70.26 ± 1.19
	EGF	76.55 ± 1.91	64.31 ± 2.81	77.55 ± 2.41	79.35 ± 1.40	58.51 ± 5.83	75.36 ± 2.34
	Cortisol	77.43 ± 2.60	38.42 ± 1.55	65.65 ± 6.65	70.25 ± 0.98	25.08 ± 1.91	74.55 ± 5.21
0.5	L-15	63.91 ± 2.84	52.93 ± 2.59	63.29 ± 2.63	86.01 ± 1.37	54.00 ± 0.97	58.96 ± 1.11
	EGF	76.37 ± 1.82	66.43 ± 1.26	71.79 ± 6.42	71.25 ± 0.30	54.55 ± 0.70	59.96 ± 1.38
	Cortisol	70.65 ± 1.50	44.61 ± 2.60	60.99 ± 1.23	64.82 ± 0.68	40.15 ± 4.96	70.40 ± 2.24

Values represent average +/- SEM

All RTgill-W1 cells seeded with primary gill cells previously grown in flasks showed the lowest paracellular permeability, and the seeding density of RTgill-W1 and culture condition had a significant effect on permeability (P < 0.001), but again, not when combined (Table 4.1; Fig 4.2B). RTgill-W1 cells seeded at 0.1 x 10^6 and cultured in L-15 with cortisol, with a seeding of 0.7 x 10^6 primary cells grown in flasks, exhibited the lowest mannitol permeability of all, at 28.05 ± 0.84%

that of the cell free control. The actual flux value obtained was $1.06 \pm 0.03 \times 10^{-6}$ cm s^{-1}, which is still higher than that obtained for a preparation of primary cells grown previously in flasks (SSI) alone ($0.22 \pm 0.00 \times 10^{-6}$ cm s^{-1}).

RTgill-W1 cells cultured with a second seed of freshly isolated primary gill cells exhibited no differences between all flux values in terms of seeding density (Table 4.1; Fig 4.2C). Differences were significant depending on culture medium condition ($P = 0.05$) and the lowest permeability observed was seen in RTgill-W1 cells seeded at 0.5×10^6 and with freshly isolated primary cells, and cultured with 100 ng mL^{-1} cortisol at $59.10 \pm 1.66\%$ of the cell free control.

After 24 hours of freshwater exposure in asymmetrical conditions, RTgill-W1 cells cultured alone on inserts without supplementation of EGF or cortisol in the cell culture medium exhibited high epithelial paracellular permeability – those seeded at 0.1 and 0.2×10^6 showed values the same or higher than that of the cell free control ($>100\%$; Fig 4.3A). Neither seeding density nor culture medium condition significantly affected the permeability.

RTgill-W1 cells cultured with primary cells grown previously in flasks showed the lowest permeability after 24 hours of freshwater exposure. Here, both seeding density and culture condition combined significantly affected mannitol flux ($P < 0.001$; Fig 4.3B). The lowest permeability obtained was $7.09 \pm 0.69\%$ that of the cell free control, and was from RTgill-W1 cells seeded at 0.1×10^6, with 0.7×10^6 flask primary cells on top and supplemented with 100 ng mL^{-1} cortisol. The actual flux value obtained for this was $0.24 \pm 0.02 \times 10^{-6}$ cm s^{-1}, and is similar to the value obtained from flask primary cells seeded alone (SSI) after 24 hours of freshwater exposure ($0.17 \pm 0.03 \times 10^{-6}$ cm s^{-1}).

Finally, the permeability of RTgill-W1 cells seeded with 1.2×10^6 freshly isolated primary gill cells was significantly affected by seeding density ($P < 0.001$) and culture medium condition ($P < 0.001$), although not combined ($P = 0.155$; Fig 4.3C). The lowest permeability obtained here was $58.96 \pm$

1.11% that of the cell free control, and was obtained by seeding RTgill-W1 cells cultured without

supplemented medium and seeded at 0.5 x 10^6 with 1.2 x 10^6 freshly isolated primary cells on top.
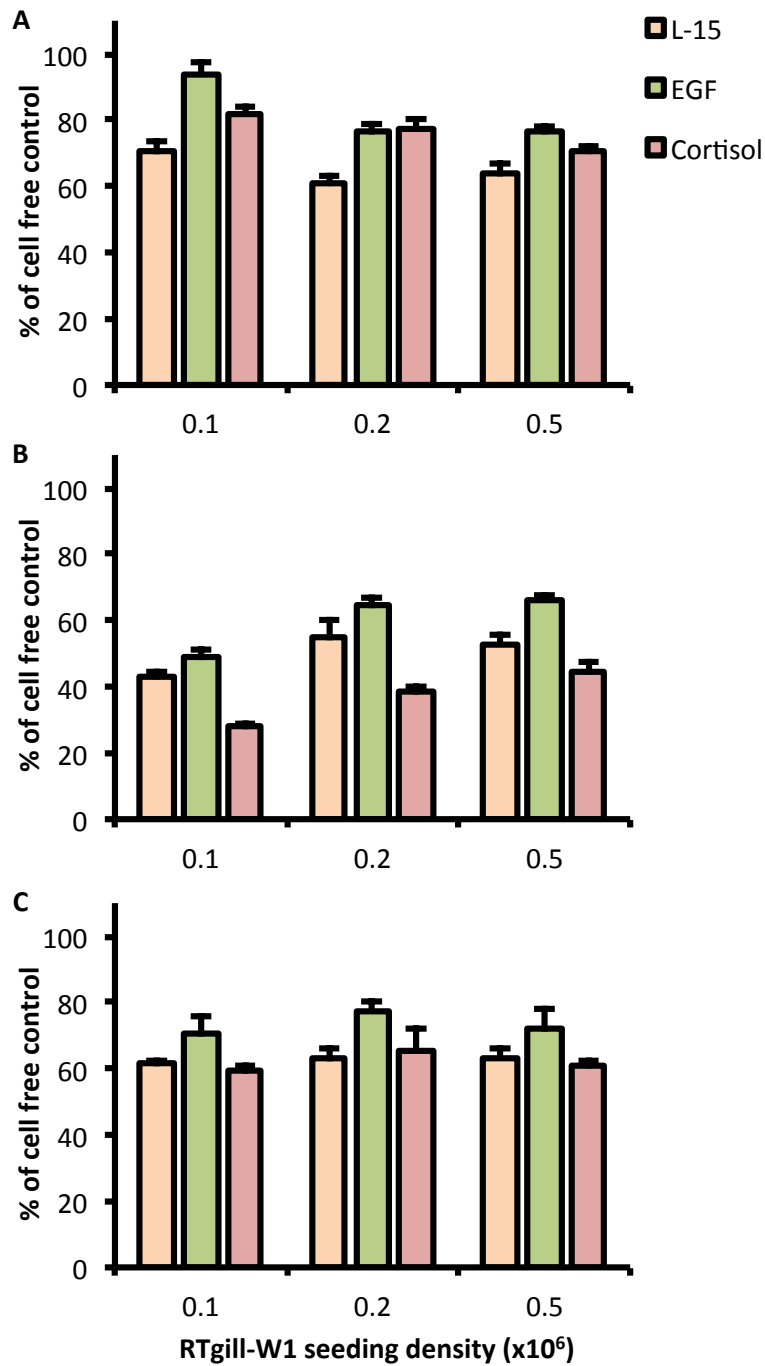
Fig 4.2 The 24 hour ^{14}C-mannitol permeability in symmetrical conditions (L-15 either side of the epithelia) of RTgill-W1 routinely cultured in flasks (> 12 months) in cell culture medium with antibiotics (L-15; orange bars), or with supplementation with 100 ng mL^{-1} epidermal growth factor (EGF; green bars) or 100 ng mL^{-1} cortisol (red bars) and seeded at 0.1, 0.2 and 0.5 x10^{6} cells per insert (A). Inserts in (B) were double seeded on top the next day with 0.7 x 10^{6} primary rainbow trout gill cells grown in flasks for the previous 6-9 days, whilst those in (C) were seeded on top with 1.2 x 10^{6} freshly isolated rainbow trout gill cells. The flux took place after 7-10 days culture and exposure to L-15 (symmetrical conditions) for 24 hours.
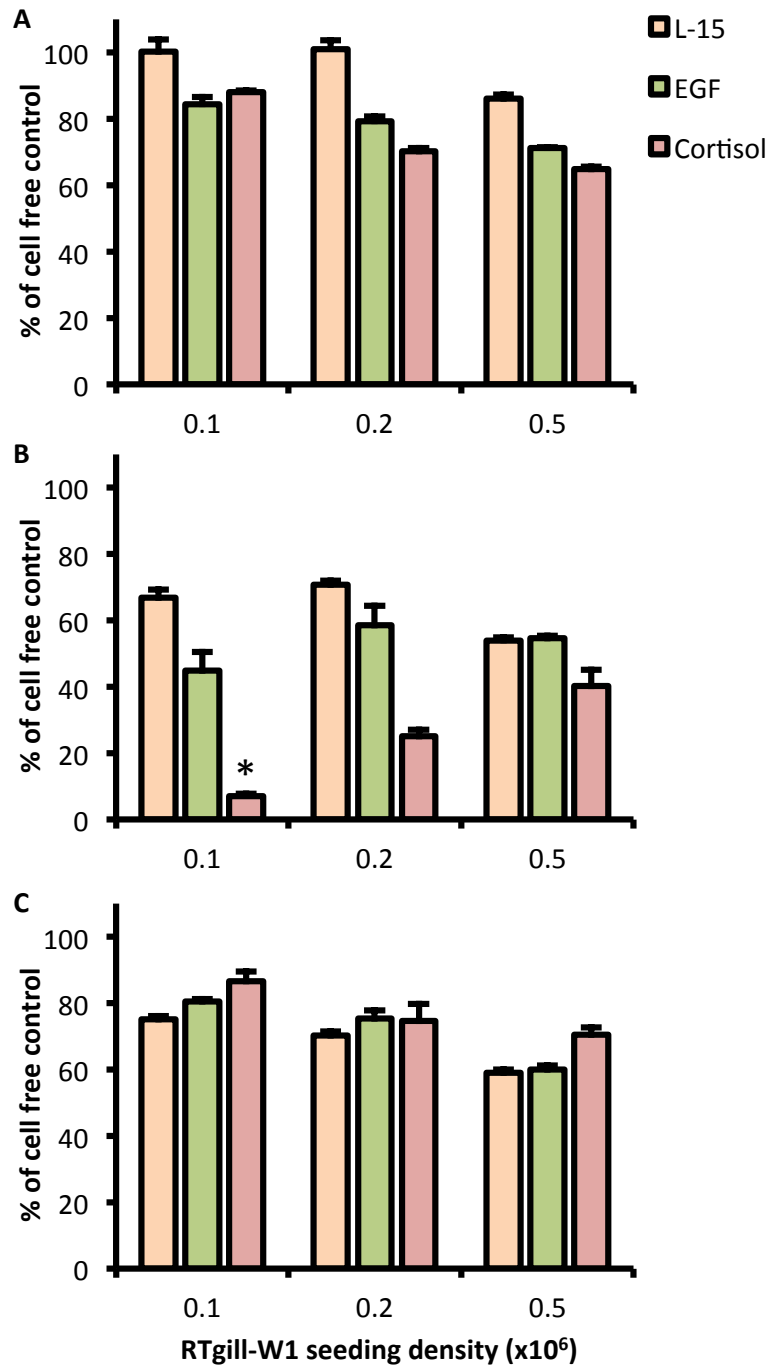
Fig 4.3 The 24 hour ^{14}C-mannitol permeability in asymmetrical conditions (freshwater in the apical compartment) of RTgill-W1 routinely cultured in flasks (> 12 months) in cell culture medium with antibiotics (L-15; orange bars), or with supplementation with 100 ng mL^{-1} epidermal growth factor (EGF; green bars) or 100 ng mL^{-1} cortisol (red bars) and seeded at 0.1, 0.2 and 0.5 x10^{6} cells per insert (A). Inserts in (B) were double seeded on top the next day with 0.7 x 10^{6} primary rainbow trout gill cells grown in flasks for the previous 6-9 days, whilst those in (C) were seeded on top with 1.2 x 10^{6} freshly isolated rainbow trout gill cells. The flux took place after 7-10 days culture and exposure to apical freshwater (asymmetrical conditions) for 24 hours.

4.5 Discussion

The gill is the principle organ used to study the transport of waterborne toxicants into fish. *In situ*, the gills are difficult to study, requiring the mouth, gills and body of the animal to be separated into compartments, which can cause distress to the animal in *in vivo* studies (e.g. Fitzsimmons et al., 2001). The *in vitro* gill provides a worthy system to study the transport properties of the gill (Bury et al., 2014), and both primary cells and immortalised cell lines provide useful tools in this research. Most notably, using these *in vitro* cells reduces the numbers of whole animals used in scientific studies (Scholz et al., 2013), a notion that is supported in the EU (REACH, 2009). Large *n* numbers of groups of cells can be obtained from a single animal, or indeed from stocks of immortalised cell lines (although fish cell lines do not currently form any part of any regulation yet; Schirmer, 2006, but recommendations have been made for their incorporation; Dayeh et al., 2013).

Primary gill cells require more careful handing to isolate and successfully culture (Schnell, Stott et al., 2016) and often produce results with greater variability due to individual differences between animals from which cells are obtained. Furthermore, live fish are necessary in order to isolate primary cells from the gill, which the cell line RTgill-W1 does not require. Using RTgill-W1 offers a useful system in which to study the rainbow trout gill (Fischer et al., 2010; 2011; Kramer et al., 2010; Lee et al., 2006; Lee et al., 2009) and is a valuable complement to whole animal studies (Stadnicka-Michalak et al., 2014). However, certain physiological characteristics of the freshwater gill are lacking in cell cultures of RTgill-W1, including the microridge architecture of PVCs, high numbers of mitochondria in MRCs, the Golgi complex and cytoplasmic droplets of mucous cells (Bols et al., 1994), metabolic enzymes such as CYP1A (Schirmer et al., 1998) and high transepithelial resistance values (Trubitt et al., 2015). In fish, transepithelial resistance indicates a measure of epithelial integrity and tightness in terms of both transcellular and paracellular

pathways (Chasiotis et al., 2012). This study aimed to improve the epithelial characteristics of RTgill-W1 by supplementing culture medium with known promoters of epithelial development, or induce these characteristics by co-culturing with primary gill cells.

Transepithelial resistance increased in RTgill-W1 cells cultured on permeable supports and supplemented with cortisol in cell culture medium. This increase was observed most in RTgill-W1 cells seeded at the lowest seeding density (0.1×10^6) and with 0.7×10^6 primary gill cells, previously grown in cell culture flasks, seeded on top. The paracellular permeability of these was also lowest in symmetrical conditions and in asymmetrical conditions after 24 hours of freshwater exposure to the apical surface of the cells. However, the symmetrical paracellular permeability, with cell culture medium both sides of the epithelium, is still higher than that of just SSI cells, indicating that this epithelial preparation is 'leakier' than just SSI alone. In asymmetrical conditions however, paracellular permeability decreased to values similar to SSI epithelia.

In RTgill-W1, supplementation of culture medium with cortisol elevates TER in a concentration-dependent manner to values over 80 Ω cm^2 (Trubitt et al., 2015), a little more than what was achieved here. Likewise, culturing primary gill cells with cortisol has been shown to improve epithelial development by increasing transepithelial resistance and decreasing paracellular permeability (Chasiotis et al., 2010), which is also reflected in lower unidirectional Na$^+$ and Cl$^-$ fluxes (Kelly & Wood, 2001). Cortisol is thought to act through an inhibition of cell proliferation and mitosis and an increase of the maintenance of total gill cells; suggesting that cortisol reduces cell degeneration (Leguen et al., 2007). Taken together, the improvement in TER and paracellular permeability brought about in this study suggests that cortisol is acting on both RTgill-W1 cells and primary gill cells, of which the latter cultured using SSI – that is, primary gill cells previously grown in cell culture flasks – appears to be more positively affected than primary gill cells freshly isolated and seeded. However, this improvement does not match that seen in primary cells cultured alone with cortisol (Chasiotis et al., 2010), so although it can be concluded that there is a positive effect

of co-culturing RTgill-W1 with primary gill cells, these advantages do not equal those from using primary gill cell cultures such as SSI and DSI alone. The practical significance of this is that RTgill-W1 cell cultures should not be used for xenobiotic uptake studies, as their epithelia are not physiologically tight enough to present a realistic biological barrier that the freshwater gill is. Still, there is scope for the improvement of RTgill-W1 gill preparations through the use of other supplementations such as stem cell growth media.

Chapter 5

The uptake and efflux of pharmaceuticals over the primary gill cell epithelium

5.1 Abstract

The gill is the principle site of xenobiotic transfer to and from the aqueous environment. To replace, refine or reduce (3Rs) the large numbers of fish used in *in vivo* uptake studies an effective *in vitro* model is required that mimics the function of the teleost gill. This study uses a rainbow trout primary gill cell culture system to assess the uptake and efflux of pharmaceuticals across the gill. Bidirectional transport studies in symmetrical conditions (with L-15 both sides of the epithelium) of seven pharmaceuticals showed they were transported transcellularly across the epithelium. However, studies conducted in asymmetrical conditions with water at the apical cell surface showed the enhanced uptake of propranolol, ranitidine and imipramine. Concentration-equilibrated conditions without a concentration gradient suggested that a proportion of the uptake of propranolol and imipramine is via a carrier-mediated process. Further study using propranolol showed that its transport is pH-dependent and at very low, environmentally relevant concentrations (ng L^{-1}), transport deviated from linearity. At higher concentrations, passive uptake dominated. Known inhibitors of drug transport proteins inhibited propranolol uptake, whilst some were without effect. Together this suggests the involvement of some members of SLC and ABC drug transporter families in pharmaceutical transport.

5.2 Introduction

In vivo ecotoxicology testing produces bioconcentration factor (BCF) values that indicate the potential of a compound to bioconcentrate within an organism (OECD$_{305}$, 2012). Highly lipophilic compounds are exposed to fish via the diet, whilst others via the water; the principle being to use the uptake and depuration rates to calculate a compounds propensity to bioconcentrate. Typically, each test can use up to 108 fish per compound and many thousands of fish are used for this test every year (Scholz et al., 2013). Alternative methods can be developed to replace these standardised whole fish studies to recognise and classify environmental hazards (Creton et al., 2013; Wolf et al., 2007). This requires the identification and validation of appropriate *in vitro* systems that could replace such studies (Baron et al., 2012). To find alternatives to the OECD$_{305}$ water exposure it is necessary to identify a suitable fish gill model that mimics the intact organ because the gill, being constantly and continuously exposed to substances in water, is the principle site of xenobiotic uptake (Bury et al., 2014). Consequently, the use of the primary gill cell culture model (described in Chapters 2 and 3) in pharmaceutical uptake and efflux studies was assessed as a compliment to whole fish studies.

The following study investigates the uptake and efflux of 7 pharmaceuticals across the *in vitro* gill. It was hypothesised that both passive transcellular and carrier-mediated transport of xenobiotics (see Chapter 1 for further details) across the gill are likely principle drivers in determining the rate of uptake of waterborne compounds (McKim & Erickson, 1991). Briefly, passive transcellular transport depends on the pH of the solution (changes in pH can change the speciation of pharmaceuticals to ionised forms, which reduce their passive uptake over biological membranes), acid base constants (pKa) and the lipophilicity of the compound, whereas facilitated transport may be via members of the solute carrier (SLC) and ATP-binding casette (ABC) transporter families (Dobson & Kell, 2008). Therefore, to investigate carrier mediated transport for some of these

pharmaceuticals, concentration equilibrated, pH-dependent, and concentration-dependent assays, as well as membrane channel inhibitor studies were conducted. In addition, the uptake of propranolol across the *in vitro* gill model was compared to *in silico* and *in vivo* data (Owen et al., 2009), to demonstrate the use of this model as a predictive tool for pharmaceutical uptake in live fish.

5.3 Materials and methods

5.3.1 Reagents and suppliers

All drugs used in transport assays were at concentration of 1 µg L^{-1} to represent those levels detected in the environment whilst remaining within detectable limits (Table 5.1). These were radiolabeled and re-suspended in ethanol or methanol with a final solvent concentration in assay conditions of <0.0003%, and chosen to demonstrate a range of different classes (β1-, β2- and non-specific β- receptor agonists, a H2- receptor agonist and a tricyclic anti-depressant) with mid-range Log K_{ow} values (see Table 5.1). ^{3}H-propranolol hydrochloride (29.0 Ci mmol^{-1}) was obtained from Amersham Biosciences. ^{3}H-metoprolol (29.7 Ci mmol^{-1}), ^{3}H-formoterol (18.5 Ci mmol^{-1}) and ^{3}H-terbutaline (29.0 Ci mmol^{-1}) were obtained from Vitrax. ^{3}H-atenolol (7.3 Ci mmol^{-1}) and ^{3}H-ranitidine (2.5 Ci mmol^{-1}) were obtained from Moravek Biochemicals, and ^{3}H-imipramine hydrochloride (48.5 Ci mmol^{-1}) from Perkin-Elmer. Propranolol hydrochloride was obtained from Sigma Aldrich.

Table 5.1

Properties of selected pharmaceuticals and the levels at which they are found in the environment.

Pharmaceutical	Use	MW	pK_a	Log K_{ow}[1]	Log K_{ow}[2]	Environmental levels (ng L^{-1})
Propranolol	non-selective β antagonist	259.340	9.4	2.54	1.12 *	33 [3]
Metoprolol	β1 receptor antagonist	267.364	9.6	1.76	-0.90 [#]	410 [3]
Atenolol	β1 receptor antagonist	266.336	9.6	0.67	0.0015 *	940 [3]
Formoterol	long-acting β2 agonist	344.405	7.9 [a] /9.2 [b]	1.93	0.41 *	n/a
Terbutaline	β2-adrenergic receptor agonist	225.284	8.86 [a] /9.76 [b]	1.25	1.29	7 [4]
Ranitidine	H2-receptor antagonist	314.4	8.08	1.47		120 [3]
Imipramine	Tricyclic antidepressant	280.407	9.4	4.39		0.14 [5]

[1] Parameter Client (Tetko et al., 2005)

[2] Environmental Risk Assessment data, experimentally measured values (AstraZeneca, 2012)

[3] Kostich et al. (2014)

[4] Breitholtz et al. (2012)

[5] Giebułtowicz & Nałęcz-Jawecki (2014)

[a] Acidic; [b] basic

*pH 7.4; [#]pH 7

5.3.2 Equipment and suppliers

Equipment used was the same as those outlined in Chapter 2. The pH meter was by Corning.

5.3.3 Preparation of reagents

Reagents were prepared as detailed in Chapter 2.

5.3.4 Cell culture reagents

Cell culture reagents were prepared as outlined in Chapter 2.

5.3.5 Methods

The same standardised procedure for the culture of DSI primary gill cells on permeable inserts, and their preparation for exposure, was used as detailed in Chapter 2. All assays took place at 18°C.

5.3.6 Bidirectional transport assays and apparent permeability coefficients

Bidirectional transport assays (BTA) assess both passive and facilitated transport in a bidirectional manner, from apical to basal (uptake) or vice versa (efflux). In these, concentration gradient conditions exist, whereby total transport is a sum of both passive transcellular and carrier-mediated processes. DSI epithelia were exposed to test compounds in either symmetrical or asymmetrical conditions. Symmetrical contained 1.5 and 2.0 mL L-15 (without FBS) in apical and basal compartments respectively, whilst asymmetrical required the application of 1.5 mL FW in the apical compartment and 2.0 mL L-15 in the basal. The test compound was added to either the apical side (uptake; A:B) or basal compartment (efflux; B:A) at a concentration of 1 µg L^{-1}. Each experimental condition used 3-5 epithelia from 1-2 biological replicates. For all experiments the FW or L-15 from the apical or basal compartment was mixed before taking 100 µL samples at 0, 6, 24, 30 and 48 hours. Each 100 µL aliquot sample was placed into a scintillation vial with scintillation fluid and beta counted, and the drug concentration was calculated from the specific radioactivities. For uptake and efflux BTA, apparent permeability coefficients (P_{app}) at 6 hours were calculated using the following equation.

$$P_{app} \ (cm \ s^{-1}) = \frac{\left(\frac{dQ}{dt} \times \frac{1}{A \times C_0}\right)}{3600}$$

where *dQ/dt* is the flux rate of the drug (pmol L^{-1} h^{-1}), *A* is the surface area of the monolayer (0.9 cm^2) and C_0 is the initial concentration of the drug in the donor compartment (fM) (Petri et al., 2004). Transport ratios (TR) for both uptake and efflux were calculated using the following equations (Schwab et al., 2003).

$$Uptake \ TR = \frac{P_{app \ A:B}}{P_{app \ B:A}}$$

$$Efflux \; TR = \frac{P_{app \; B:A}}{P_{app \; A:B}}$$

An uptake or efflux TR ≥ 1.5 is considered an indicator of active transport (Schwab et al., 2003; Luna-Tortós et al., 2008). For time-dependent BTA, the results were also expressed as the percentage of the initial drug concentration of the donor compartment for uptake (A:B) and efflux (B:A) over 48 hours.

5.3.7 Concentration equilibrated transport assays

Concentration equilibrated transport assays (CETA) examine transport by adding equivalent concentrations on either side of the gill epithelium and assessing the movement of compounds over time to evaluate carrier-mediated uptake or efflux regardless of passive transport processes, as used in blood-brain barrier transport assays (Luna-Tortós et al., 2008). The same experimental procedures for BTA were used (in symmetrical and asymmetrical conditions), but with both apical and basal compartments containing test drugs at the same concentration of 1 µg L^{-1}. The results are expressed as a percentage of the initial concentration in each compartment (apical or basal) over time.

5.3.8 The pH-dependent transport of propranolol

DSI epithelia were exposed in apical FW adjusted to pH 6 (by addition of HCl), pH 8 or pH 9.5 (by addition of NaOH). The basolateral contained 2.0 mL L-15. Radiolabeled propranolol was added at a concentration of 1 µg L^{-1} to either the apical or basal compartments (BTA) to investigate uptake and efflux. At 6 hours a 100 µL sample was collected from the apical and basal compartments and the radioactivity analysed as above. The apparent permeability coefficients (P$_{app}$) were calculated using the equation shown previously.

5.3.9   The concentration-dependent uptake of propranolol

DSI epithelia (*n* = 54) were exposed to 17 concentrations of propranolol ranging from 0.014-10000 µg L^{-1}. Concentrations above 0.1 µg L^{-1} were made using propranolol hydrochloride and radiolabeled propranolol as a marker. Experiments were conducted in asymmetrical conditions with propranolol added to the FW in the apical compartment, thus mimicking the *in vivo* scenario (Owen et al., 2009). Radioactivity was analysed as previously described.

5.3.10   The inhibition of the uptake of propranolol

Epithelia were pre-incubated with an inhibitor at a concentration 100 times higher (400 nM) than that of propranolol. Amantadine, cimetidine, cyclosporine A, MK571, quinidine or verapamil hydrochloride were dissolved in DMSO (0.1% in final solution) and added to the apical (in 0.75 mL FW) or basal (in 1.0 mL L-15 medium). Controls and compartments without inhibitor contained 0.1% DMSO. After 1 hour, volumes were replaced with 1.5 mL FW containing 1 µg L^{-1} (4 nM) propranolol in the apical compartment, and the basal contained 2.0 mL plain L-15, whilst keeping the final concentration of inhibitor at 400 nM throughout. The same sampling procedure as for BTA at time 0, 6 (not for cyclosporine A), 24, 36 and 48 hours proceeded and the uptake P_{app} of propranolol was calculated as previously. The P_{app} in all inhibitor free controls was expressed as a percentage of the mean (100%) and the change in uptake P_{app} (inhibition) in the presence of inhibitors was expressed as a percentage of this mean control.

5.3.11   Analysis of data and statistics

For bidirectional P_{app} comparisons between the uptake and efflux, an independent samples *t*-test with equal variances assumed was used and statistical significance was accepted when *P* < 0.05 (SPSS software, SPSS Inc.). The same statistical analysis was used to test for differences between asymmetrical and symmetrical uptake or efflux P_{app} for each drug to assess the effect of apical FW

application. For the time dependent BTA, significant differences between the uptake and efflux percentage of the donor compartment were tested for by one-way analysis of variance (ANOVA) on log-transformed data (SPSS software, SPSS Inc.). For the time-dependent CETA, statistical significance of differences between each percentage increase or decrease in the apical or basal compartments were also tested for by one-way ANOVA (after log transformation). Differences between the uptake of propranolol at different pHs, and similarly the efflux, were tested for by one-way ANOVA and statistical significance was accepted when *P* < 0.05 (SPSS software, SPSS Inc.). The rate of propranolol flux for each concentration in the dose response was calculated at 6 hours and analysed by ordinary least squares linear regression to describe the best fit, and further analysis of low dose concentrations were analysed by cubic polynomial regression to best describe the relationship (SPSS software, SPSS Inc.). Statistical differences between inhibitor (applied either apically or basally) and the inhibitor free control were tested for by one-way ANOVA (after log transformation) and statistical significance was accepted at *P* < 0.05.

5.3.12   Comparison to predicted and actual plasma concentrations

In vitro propranolol 'internal' concentrations after uptake (A:B) from the dose response study were compared to predicted *in silico* and actual *in vivo* plasma concentrations of propranolol in *O. mykiss*. The predicted partition of propranolol between blood and water can be determined by [plasma] = 0.87 [water] as described by Owen et al. (2009). This was calculated using the mammalian fish leverage model, whereby the predicted plasma concentration can be described by multiplying the environmental concentration by the blood to water partitioning coefficient (Huggett et al., 2004) using the Fitzsimmons model for the partitioning of compounds between blood and water (Fitzsimmons et al., 2001). Actual plasma concentrations of propranolol in *O. mykiss* were obtained from Owen et al. (2009). *In vitro* propranolol concentrations at 6 hours (*n* = 3-6 from 3 biological replicates) were tested for correlation to *in silico* and *in vivo* plasma concentrations by ordinary least squares linear regression (SPSS software, SPSS Inc.).

5.4 Results

5.4.1 Apparent permeability coefficients and transport ratios

In symmetrical conditions with L-15 medium on both sides of the gill cell epithelium, no significant differences between $P_{app\ A:B}$ and $P_{app\ B:A}$ for all 7 pharmaceuticals were observed (Fig 5.1A), yet all permeabilities were higher than that of the paracellular marker mannitol (except for atenolol; $P_{app\ A:B}$: $0.1 \pm 0.03 \times 10^{-6}$ cm s^{-1} and $P_{app\ B:A}$: $0.1 \pm 0.02 \times 10^{-6}$ cm s^{-1} compared to mannitol; $P_{app\ A:B}$: $0.1 \pm 0.01 \times 10^{-6}$ cm s^{-1}, see Chapter 3). In asymmetrical conditions with FW at the apical surface of the gill epithelium, $P_{app\ A:B}$ was significantly higher than $P_{app\ B:A}$ ($P < 0.001$) for propranolol and imipramine, whilst no significant differences existed between uptake and efflux P_{app} of the remaining 5 drugs metoprolol, atenolol, formoterol, terbutaline and ranitidine (Fig 5.1B). For propranolol, the $P_{app\ A:B}$ increased significantly from $1.7 \pm 0.2 \times 10^{-6}$ cm s^{-1} in symmetrical to $2.7 \pm 0.2 \times 10^{-6}$ cm s^{-1} in asymmetrical conditions ($P < 0.05$) and $P_{app\ B:A}$ decreased significantly from 1.1 ± 0.02 to $0.8 \pm 0.1 \times 10^{-6}$ cm s^{-1} ($P < 0.05$) (Fig 5.1A; Fig 5.1B). Similarly for imipramine a significant increase in $P_{app\ A:B}$ from symmetrical ($1.9 \pm 0.2 \times 10^{-6}$ cm s^{-1}) to asymmetrical ($3.0 \pm 0.1 \times 10^{-6}$ cm s^{-1}; $P < 0.05$) and a significant decrease in $P_{app\ B:A}$ (2.2 ± 0.04 to $1.6 \pm 0.1 \times 10^{-6}$ cm s^{-1}; $P < 0.05$) (Fig 5.1A and B) was observed.

Propranolol showed uptake TR values greater than 1.5 in both symmetrical and asymmetrical conditions, whilst for imipramine; this was only observed in asymmetrical conditions. Both metoprolol and atenolol had efflux TR values greater than 1.5 in symmetrical and asymmetrical respectively (Table 5.2).
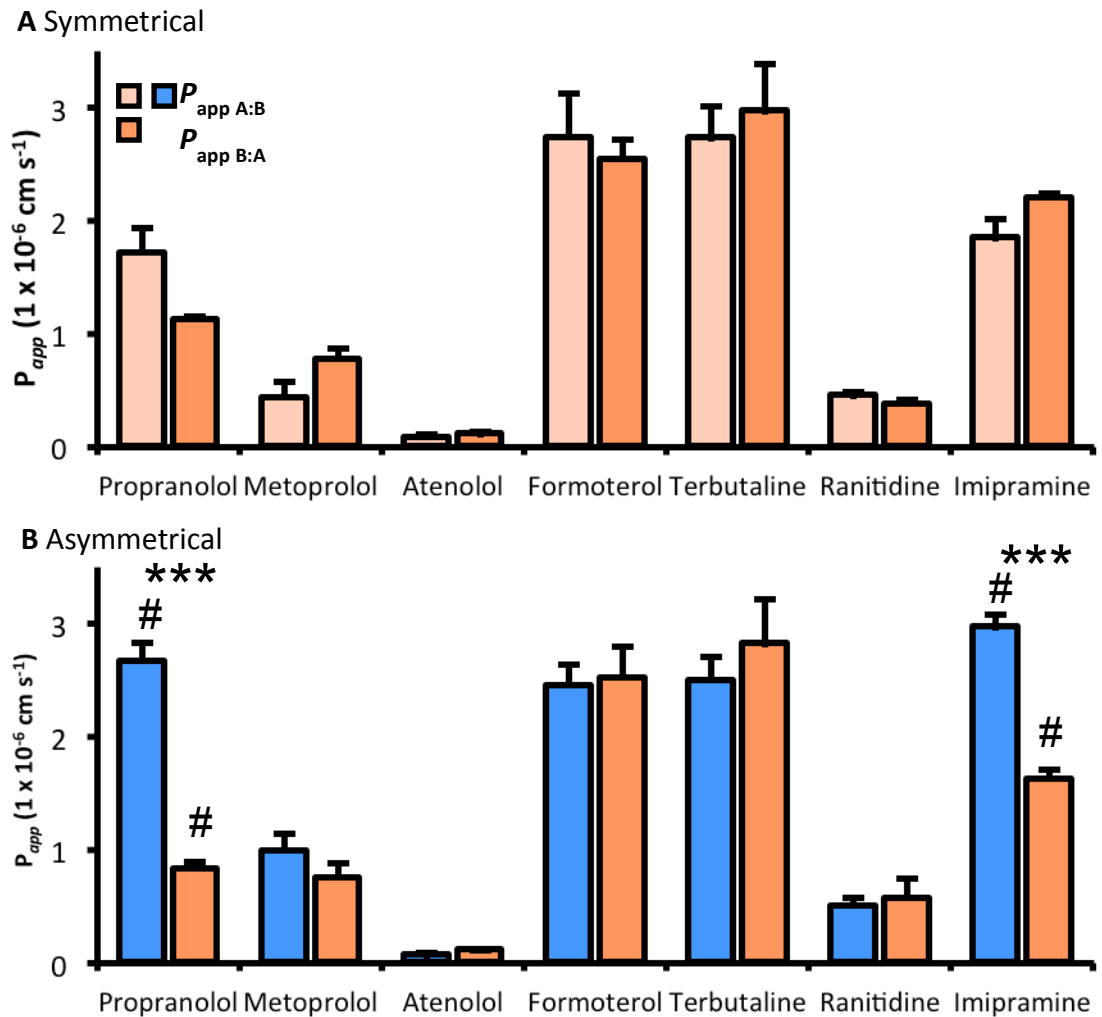
Fig 5.1 The apparent permeability coefficients (P_{app}) for uptake ($P_{app\ A:B}$, peach or blue bars) and efflux ($P_{app\ B:A}$, orange bars) of seven pharmaceuticals (1 µg L^{-1}) across the DSI gill cell epithelium at 6 hours in symmetrical conditions (A) and asymmetrical conditions (B). Significant differences between the $P_{app\ A:B}$ and $P_{app\ B:A}$ for a drug within a condition (symmetrical or asymmetrical) are indicated by asterisk (independent samples *t*-test; *** $P < 0.001$). Significant differences between symmetrical and asymmetrical $P_{app\ A:B}$ or $P_{app\ B:A}$ for each drug are indicated by hash tag in (B) (independent samples *t*-test; #$P < 0.05$). All experiments were performed in triplicate or more (*n* = 3-5) from at least 1 biological replicate and values are shown as means ± SEM.

Table 5.2

The uptake and efflux transport ratios (TR) of 7 drugs in symmetrical and asymmetrical conditions.

	Uptake TR		Efflux TR	
	Symmetrical	Asymmetrical	Symmetrical	Asymmetrical
Propranolol	1.52*	3.21*	0.66	0.31
Metoprolol	0.56	1.32	1.78*	0.76
Atenolol	0.74	0.60	1.34	1.67*
Formoterol	1.08	0.97	0.93	1.03
Terbutaline	0.92	0.89	1.09	1.13
Ranitidine	1.21	0.88	0.83	1.14
Imipramine	0.84	1.83*	1.19	0.55

* indicates values greater than 1.5

5.4.2 Bidirectional transport assays

In symmetrical conditions with L-15 medium on both sides of the epithelium, ranitidine and imipramine exhibited greater efflux transport from the basal to the apical compartments at 24 hours ($P < 0.05$) and at 30 and 48 hours ($P < 0.05$) respectively (Fig 5.2A). In asymmetrical conditions involving the application of FW at the apical surface, more propranolol, ranitidine and imipramine were taken up across the gill cell surface than were effluxed after 48 hours. This was significantly more so at 6 ($P < 0.001$) and 24, 30 and 48 ($P < 0.01$) hours for propranolol, 30 hours ($P < 0.01$) for ranitidine and at all sampling points (6, 24, 30 and 48 hours) for imipramine ($P < 0.001$) (Fig 5.2A). Metoprolol, formoterol and terbutaline showed slightly greater uptake than efflux after 48 hours, and this was significantly more so for formoterol at 48 hours ($P < 0.05$).
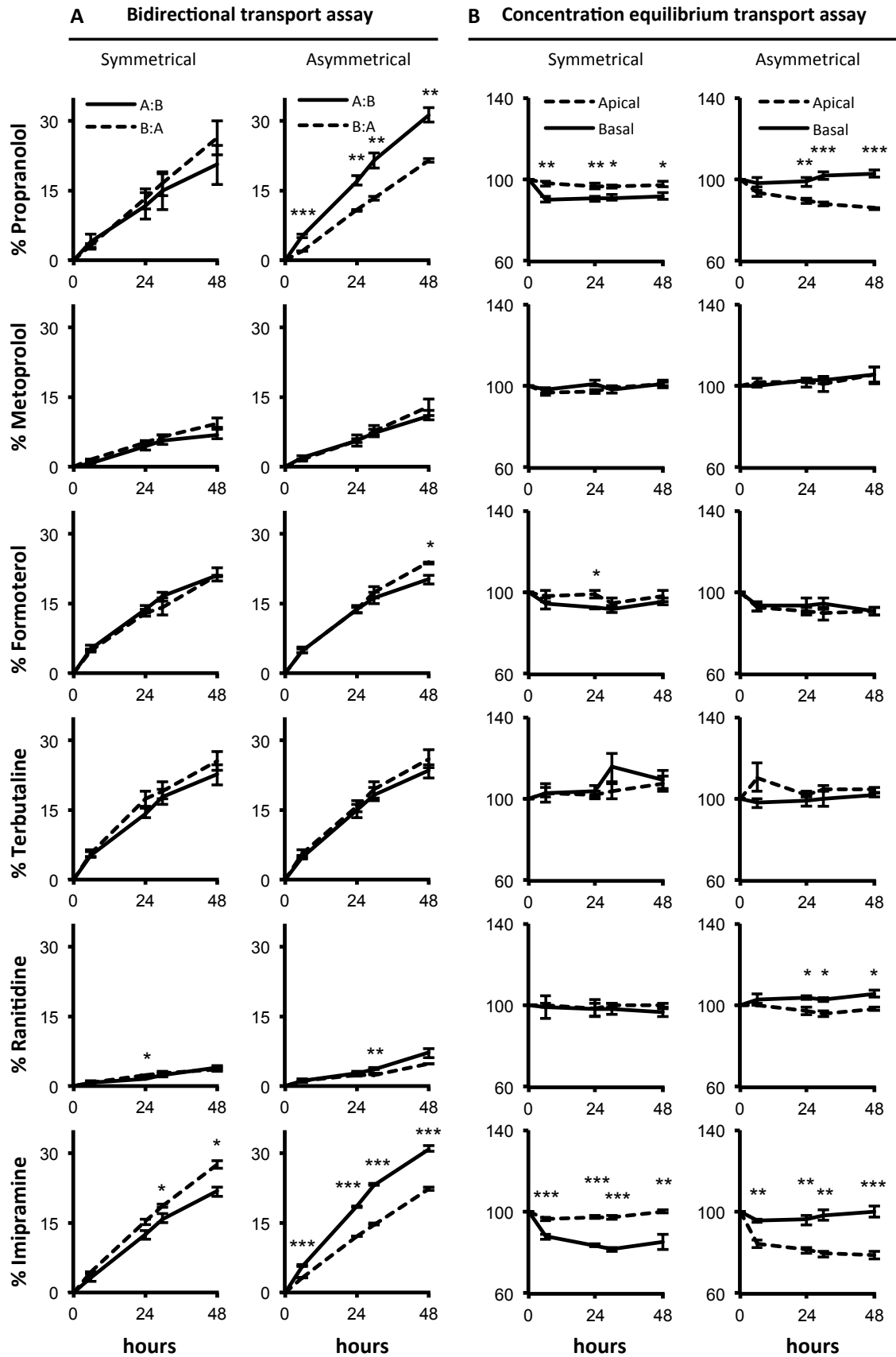
Fig 5.2

Fig 5.2 The transport assays of six pharmaceuticals: propranolol, metoprolol, formoterol, terbutaline, ranitidine and imipramine, in the DSI rainbow trout primary gill cell system over 48 hours under (A) bidirectional transport assays (BTA) and (B) concentration equilibrated transport assays (CETA) conditions. For BTA (A) the drug is applied at a concentration of 1 μg L^{-1} to either the apical (⎯⎯) for apical to basal transport; uptake, A:B or basal compartment (⎯ ⎯ ⎯) for basal to apical transport; efflux, B:A in either symmetrical (L-15 medium in both compartments) or asymmetrical (freshwater in the apical compartment and L-15 medium in the basal) conditions. For this assay, data are shown as a percentage of the initial drug concentration in the donor chamber versus time. For CETA (B), the drug is added to both the apical and basal compartments at the same concentration (1 μg L^{-1}) in both symmetrical and asymmetrical conditions. Data are shown as a percentage of the initial concentration in either the apical or basal versus time. For both assays, significant differences between the two compartments are indicated by asterisk (One-way ANOVA; *P* < 0.05; **P* < 0.01; ***P* < 0.001). All experiments were performed in triplicate or more (*n* = 3-6) from at least 1 biological replicate and values are shown as means ± SEM.

5.4.3   Concentration equilibrated transport assays

In symmetrical conditions with L-15 and test drug on both sides of the epithelium, no significant differences between percentage of the initial drug concentrations in the apical and basal compartments were observed for metoprolol, terbutaline and ranitidine at all time points (Fig 5.2B). The percentage of the initial concentration of formoterol was more in the apical than basal but only significantly so at 24 hours (*P* < 0.05). The percentage of the initial concentration of propranolol in the apical compartment was significantly more than the basal at all sampling points after 0 hours (6 and 24 hours *P* < 0.01 and 30 and 48 hours *P* < 0.05). This was also seen for imipramine, which showed the same increased basal to apical transport (*P* < 0.001 at 6, 24 and 30 hours and *P* < 0.01 at 48 hours). However, in asymmetrical conditions the situation was reversed whereby increased apical to basal transport, indicative of facilitated uptake, resulted in significantly more propranolol and imipramine in the basal compartments (*P* < 0.01 at 24 hours and *P* < 0.001 to 30 and 48 hours for propranolol and *P* < 0.01 at 6, 24 and 30 hours and *P* < 0.001 at 48 hours for imipramine). The same was true for ranitidine in asymmetrical conditions but to a lesser degree (*P* < 0.05 at 24, 30 and 48 hours). Metoprolol, formoterol and terbutaline showed no

signs of facilitated transport across the epithelium as no significant differences were observed (Fig 5.2B).

5.4.4 The pH-dependent transport of propranolol

A decrease in pH from 8 to 6 resulted in the significant reduction in the uptake permeability ($P_{app\ A:B}$) of propranolol from $2.7 \pm 0.2 \times 10^{-6}$ to $0.4 \pm 0.03 \times 10^{-6}$ cm s^{-1} (P < 0.001) in asymmetrical conditions. The effect was opposite for efflux permeability ($P_{app\ B:A}$) with an increase from 0.8 ± 0.1 to $2.8 \pm 0.1 \times 10^{-6}$ cm s^{-1} (P < 0.001; Fig 5.3). An increase in pH from 8 to 9.5 was without significant effect (Fig 5.3).
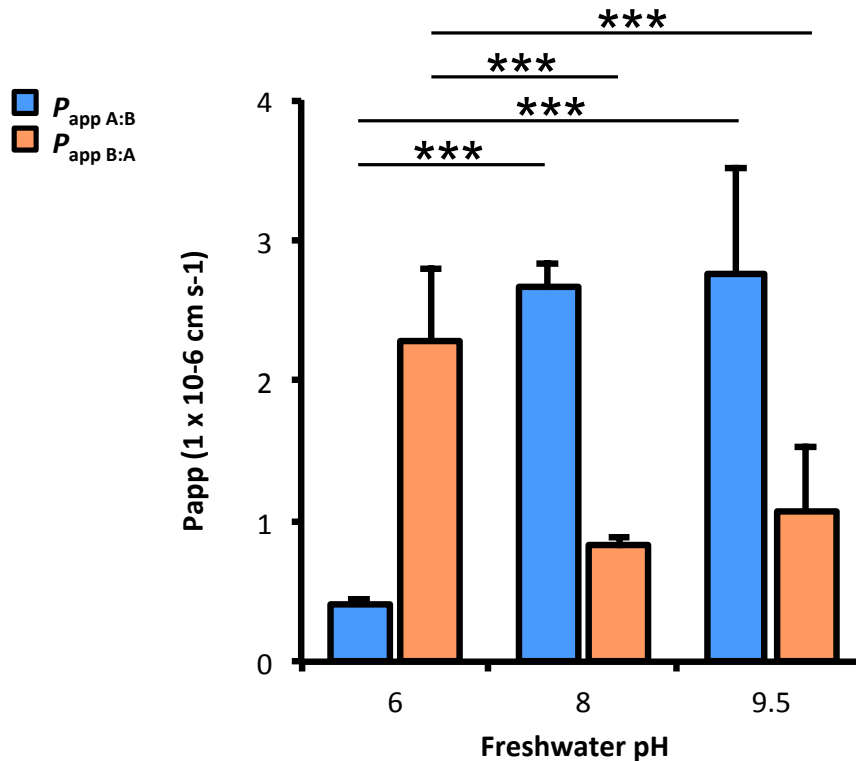
Fig 5.3 The pH dependent uptake of propranolol. Shown are the apparent permeability coefficients (P_{app}) for uptake ($P_{app\ A:B}$, blue bars) and efflux ($P_{app\ B:A}$, orange bars) of propranolol (1 µg L^{-1}) across the DSI gill cell epithelium at 6 hours in asymmetrical conditions at three different pHs. Significant differences between uptake P_{app} or efflux P_{app} are indicated by asterisk (One-way ANOVA; *** P < 0.001). All experiments were performed in triplicate or more (*n* = 3-5) from 2 biological replicates and values are shown as means ± SEM.

5.4.5   The concentration-dependent uptake of propranolol

A positive linear correlation between concentration (0.014-10000 µg L^{-1}) and rate of flux of propranolol was observed with regression line representing the best fit of [rate] = 0.052 [concentration] (n = 54, r^2 = 0.974, Fig 5.4A). However at lower propranolol concentrations (0.014-0.14 µg L^{-1}) a 2nd order polynomial regression best described the concentration response relationship (n = 24, r^2 = 0.927, Fig 5.4B) rather than linear (n = 24, r^2 = 0.908) with line representing the best fit of [rate] = 0.057 [concentration].
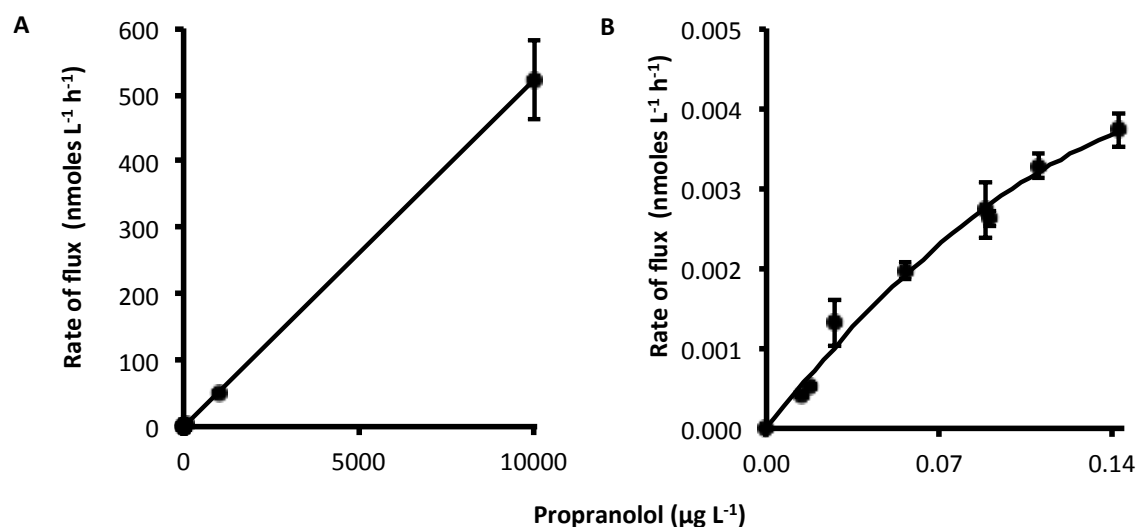
Fig 5.4 The concentration dependent uptake of propranolol (uptake; A:B) at 6 hours after exposure to (A) 17 propranolol concentrations ranging from 0.014 to 10000 µg L^{-1} with the line representing the fit of [rate] = 0.052 [concentration] (n = 54, r^2 = 0.974) (note at lower concentrations that multiple data points are stacked) and (B) low propranolol concentrations (0.014-0.14 µg L^{-1}) with the line representing the fit of [rate] = 0.057 [concentration] (n = 24, r^2 = 0.927). The values represent mean ± SEM from 5 biological replicates.

5.4.6 The inhibition of the uptake of propranolol

Fig 5.5 The inhibition of the uptake of 1 µg L^{-1} (4 nM) propranolol from apical (freshwater) to basal (L-15 medium) using 400 nM of the six inhibitors amantadine (A); cimetidine (B); cyclosporine A (C); MK571 (D); quinidine (E) and verapamil (F), applied either apically, AP (——) or basally, BL (– –). Data are shown as percentage of the mean control, CTL (·····) over time. Significant differences between the apically applied inhibitor and the control are indicated by asterisk (One-way ANOVA; *P < 0.05; **P < 0.01; ***P < 0.001). Significant differences between the basally applied inhibitor and the control are indicated by hash tag ($^{\#}P$ < 0.05; $^{\#\#}P$ < 0.01; $^{\#\#\#}P$ < 0.001). All experiments were performed in triplicate or more (n = 3-6 from at least 1 biological replicate for inhibitor studies; n = 18 from 6 biological replicates for the inhibitor free controls) and values are shown as means ± SEM.

Amantadine and verapamil did not inhibit $P_{app\ A:B}$ of propranolol (Fig 5.5A; Fig 5.5F). Apical and basal cimetidine application significantly inhibited the transport of propranolol at all time points (apart from basal at time 6 hours) by approximately 40% to 61.4% ± 3.4 (apical application) and 55.9% ± 1.3 (basal application) at 48 hours (P < 0.001) (Fig 5.5B). Similarly, cyclosporine A showed

a significant inhibition of propranolol transport after 48 hours to 69.9% (± 3.7) that of the control ($P < 0.01$) for apical application and to 66.3% (± 6.1) ($P < 0.001$) for basal (Fig 5.5C). Application of the inhibitors MK571 and quinidine again showed a significant decrease in propranolol permeability over time by approximately 40% that of the control at 48 hours for both apical and basal applications ($P < 0.001$) (Fig 5.5D; Fig 5.5E).

5.4.7 Comparison to predicted and actual propranolol plasma concentrations

Table 5.3

Propranolol concentrations *in silico* (predicted), *in vivo* and *in vitro* (measured at various external propranolol concentrations).

Nominal propranolol concentration in water (µg L^{-1})	*In silico* (ng mL^{-1}) (Hugget et al., 2004)	*In vivo* (ng mL^{-1}) (Owen et al., 2009)	*In vitro* (ng mL^{-1})
0.1	0.087	n/a	0.04 (± 0.002)
1.0	0.87	0.94* (n/a)	0.10 (± 0.001)
10	8.7	3.3 (± 0.4)	0.72 (± 0.02)
100	87	16 (± 7)	7.5 (± 0.3)
1000	870	280 (± 116)	79.5 (± 7.3)
10000	8700	5200 (± 1333)	812 (± 158)
100000	87000	n/a	5545 (± 313)

*pooled plasma sample

Propranolol is not toxic to primary gill cells at concentrations <10000 µg L^{-1} (based on MTT assays, data not shown). Predicted plasma concentrations were calculated using [plasma] = 0.87 [water] and actual plasma concentrations from Owen et al. (2009) (Table 5.3). A linear correlation between predicted plasma concentration and *in vitro* basal concentrations was obtained and described by [*in vitro*] = 0.063 [predicted] ($n = 21$, $r^2 = 0.995$, Fig 5.6A). Furthermore, a correlation between actual plasma concentrations (Owen et al., 2009) and *in vitro* basal concentrations was obtained and described by [*in vitro*] = 0.155 [actual] ($n = 21$, $r^2 = 0.966$, Fig 5.6B).
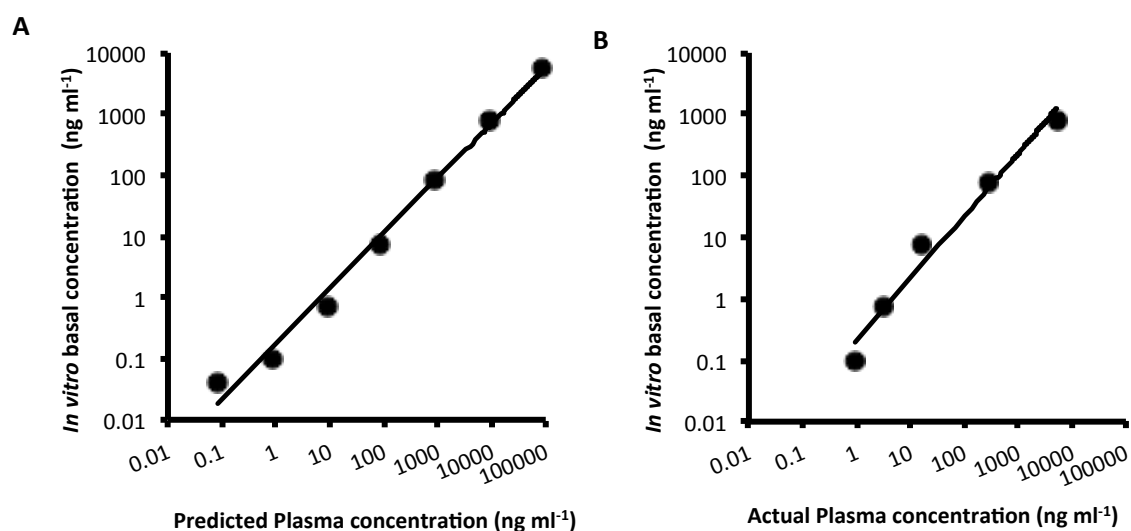
Fig 5.6 Propranolol concentrations in the basal compartment of the primary gill cell model after 6 hours apical exposure

to propranolol in asymmetrical conditions plotted against (A) predicted (see text) *O. mykiss* propranolol plasma

concentrations (0.1-100000 μg L^{-1}) with regression line representing the fit of [*in vitro*] = 0.063 [predicted] (*n* = 21, r^2 =

0.995) or (B) actual *in vivo* plasma concentrations (1-10000 μg L^{-1}) after 40 days exposure (Owen et al., 2009) with the

regression line representing the fit of [*in vitro*] = 0.155 [actual] (*n* = 21, r^2 = 0.966) (table 3). Basal *in vitro* concentrations

were performed in triplicate or more (*n* = 3-5) and represent mean ± SEM from 3 biological replicates.

5.5 Discussion

The development of suitable *in vitro* cellular models to replace, refine and reduce (3Rs) the

numbers of fish used in ecotoxicological studies is an important requirement in current regulatory

testing (Scholz et al., 2013). Pharmaceuticals in the environment are contaminants of emerging

concern and their behavior in water affects uptake into biological systems (Boxall et al., 2012). Log

K_{ow} is often used to determine the bioconcentration potential of a compound, which may not be

relevant to ionisable compounds such as pharmaceuticals (Hermens et al., 2013). The pH-

corrected Log D_{ow} is used to account for the fraction of ionisable and nonionisable species of a

substance at a given pH, but this accounts for partitioning between two liquid phases and does not

include partitioning across a biological membrane. The present study is the first to demonstrate how a primary rainbow trout gill cell culture system can be used to assess pharmaceutical uptake from water across a biological membrane. Therefore, this offers a potential alternative to replace whole organism pharmaceuticals uptake studies at differing water chemistries, such as different pHs, the presence of dissolved organic matter or real water samples from the field.

Once a tight epithelium (>5000 Ω cm^2, see Chapter 3) has formed, the gills present a barrier for paracellular transport that is relatively impermeable to the paracellular permeability marker ^{14}C-mannitol (Fig 3.7A). All pharmaceuticals (except atenolol) were transported across the epithelium in both directions at a rate greater than that of ^{14}C-mannitol, indicating that their transport is via a transcellular or carrier-mediated process, as all exhibit molecular weights greater than that of the marker (Hubatsch et al., 2007; Schwab et al., 2003).

The application of apical freshwater resulted in significantly different drug permeations for propranolol and imipramine where more is taken up across the epithelium from the water than is effluxed from the basolateral compartment (Table 5.2; Fig 5.1B; Fig 5.2A). The uptake of ionisable chemicals such as pharmaceuticals depends on pH and the acid base constant (pK_a) (Lahti et al., 2011). Both propranolol and imipramine are weak bases with pK_a values around 9.5. Using the Henderson-Hasselbalch equation, 99% of propranolol and imipramine exist in their protonated ionised form at pH 7.4 in symmetrical conditions, which then falls to 98% in freshwater at pH 8. Here, at pH 8, more of the natural unionised forms are lipid-soluble, and thus may cross the membrane via passive transcellular routes explaining the enhanced uptake. However, the 1% change in speciation is unlikely to fully account for the difference in uptake observed (Fig 5.1) and other factors are likely to play a role. For example, in symmetrical conditions TEP is positive (1.9 ± 0.2 mV) and becomes negative after apical freshwater application (−10.3 ± 0.2 mV, Fletcher et al., 2000; −12.9 ± 2.9 mV, data not shown), to a value similar to that observed *in vivo* (Potts, 1984). The change in membrane potential to basolateral negative generates an electrical gradient that

aids cation partitioning across the membrane (Fletcher et al., 2000). Alternatively, TR values greater than 1.5 in asymmetrical conditions for propranolol and imipramine in BTA conditions (Table 5.2) indicate that a proportion of the transport is via a carrier-mediated process (Schwab et al., 2003). This observation was substantiated by the concentration equilibrated transport assay (CETA) that eliminates concentration dependent passive transport across the gill epithelium allowing the observation of carrier-mediated processes that drive xenobiotic transport. In CETA the difference in partitioning of radioactivity between the two compartments is not due to disproportional loss of compound adhering to the plastic ware of the apical and basolateral compartments, since in cell free blank insert experiments equal absorption is seen in each compartment (an acid wash recovered less than 1% of the initial radioactivity added in each). Thus, it is possible to conclude that for propranolol and imipramine, facilitated transport makes up approximately 10% of the total transport, and around 5% for ranitidine efflux (Fig 5.2B).

Uptake rates are important for predicting potential internal concentrations and are used to predict effects based on the "read across" hypothesis and Mode of Action (Rand-Weaver et al., 2013). Much of the *in vivo* uptake work used for these predictions expose fish to very high water concentrations and extrapolates back to these lower environmentally relevant values. Propranolol uptake is dose dependent over the whole range of concentrations but in the low, ng L^{-1} range, uptake deviates from linearity (0.014 – 0.14 μg L^{-1}, Fig 5.4). A similar result was obtained for the uptake at very low concentrations of iron across zebrafish gills and was attributable to proton dependent metal transporters (Bury & Grosell, 2003). The facilitated transport of propranolol that occurs at these environmentally relevant concentrations (Kostich et al., 2014) is of interest because it suggests that the predictive models for uptake using data derived for higher doses may underestimate uptake.

The uptake of propranolol is pH dependent up to pH 8, after which further increases do not cause significant effects (Fig 5.3). This again could be attributed to the difference in composition of

ionised and unionised species at different pHs, with a caveat that a proportion of transport is likely via a facilitated process. However, it should be noted that the pH of the apical bulk compartment, and the microclimate at the boundary layer, were not measured after the 6 hour duration of the experiment, and variations in such may account for changes in drug uptake. pH dependent uptake of propranolol has been observed in other epithelia including retina (Kubo et al., 2013), Caco-2 cells (Wang et al., 2010) and kidney MDCK cells (Dudley et al., 2000). In contrast, efflux of propranolol is far greater at pH 6 than uptake (Fig 5.3). This may suggest the export of propranolol or its metabolite is pH dependent. Candidates for drug export are the ABC transporters; however these are not directly regulated by pH changes (Altenberg et al., 1993; Neuhoff et al., 2003). The internal pH of the cells is constant against external pH changes and thus intracellular speciation of the drug is unlikely to explain potential increase in efflux. It is therefore likely that there are other propranolol parent and/or metabolite exporters present on the gill.

Propranolol uptake from water was inhibited by cimetidine, cyclosporine A, MK571 and quinidine. These are inhibitors of a number solute carrier and ABC transporters. Many human SLCs implicated in drug transport (SLC15s, SLCOs, SLC22s and SLC47s [Dobson & Kell, 2008; Giacomini et al., 2010]) are homologous to SLCs found in teleost fish (Verri et al., 2012). Similarly, ATP-binding cassette (ABC) transporters involved in the cellular efflux of toxicants such as ABCBs, ABCCs and ABCG2 (Deeley et al., 2006) are considered highly conserved amongst vertebrates (Dean & Annilo, 2005) and have been documented in rainbow trout cells both *in vivo* and *in vitro* (Fischer et al., 2011; Lončar et al., 2010) but not fully characterised. Recent microarray studies using the primary gill cell culture system have identified the presence of these transcripts for a number of SLCs, ABCs as well as biotransformation enzymes (Schnell, Bury, Kille & Hogstrand, unpublished data). But, the identification of active proteins requires further work.

The application of cimetidine and quinidine, which both interact with organic cation transporter OCT2 (SLC22A2) (Giacomini et al., 2010; Koepsell, 2013) significantly reduce propranolol uptake.

Propranolol transport via OCT2 was observed in renal LLC-PK$_1$ cells transiently transfected with hOCT2-V5, more specifically in the active uptake of its cationic form across the apical membrane (Dudley et al., 2000). Cimetidine is also used as a blocker of cisplatin transport by OCT2 in zebrafish lateral line hair cells (Thomas et al., 2013) and the presence of OCT2-like proteins have been suggested in other teleost fish gill epithelia (Verri et al., 2012). MK571 is an inhibitor of the multidrug resistance protein (MRP) efflux pumps (Deeley et al., 2006) and significantly inhibited propranolol uptake. The main MRP expressed in the gill is MRP3 (ABCC3) (Lončar et al., 2010). P-glycoprotein (Pgp; ABCB1) is implicated in propranolol transport in rabbit conjunctivial epithelial cells (Yang et al., 2000) and Caco-2 cells (Wang et al., 2010) and is present in rainbow trout tissues but at low levels in the gill (Lončar et al., 2010). Whether Pgp is involved in propranolol transport in the gill cell culture system is unclear. In addition to inhibiting OCT2, quinidine also acts as Pgp inhibitor (Giacomini et al., 2010) and cyclosporine A, another Pgp inhibitor, also blocked propranolol transport but this may be via MRP inhibition instead. Application of the Pgp inhibitor verapamil however did not affect propranolol transport (Fig 5.5F). Taken together these observations would suggest that OCT2 and MRP3 may be candidates for propranolol transport across the teleost gill epithelium, but the location (apical or basolateral membrane) of these transporters, and others, needs further assessment.

Owen et al. (2009) showed that predicted plasma concentrations (Fitzsimmons et al., 2001) were good indicators of propranolol uptake over a range of high concentrations. Our data also correlates well with predicted (Fig 5.6A) and measured plasma concentrations (Fig 5.6B). However, *in vitro* propranolol concentrations in the basolateral compartment were an average 6% of the predicted and 16% of actual plasma concentrations, whilst actual plasma concentrations were only 59% of predicted (Owen et al., 2009). *In vivo* bioconcentration studies can involve an uptake phase of 60 days until a steady state is reached (OECD$_{305}$; 2012). Owen et al. (2009) used a 40-day exposure period, and both procedures used a flow through system with a steady-state endpoint.

This *in vitro* assay took place over 6 hours in a static system, which could account for reduced propranolol uptake. Furthermore, actual plasma concentrations may be lower than predicted as a proportion of the drug may bind to proteins or be metabolised by the gill, which prediction models fail to take into account. Nevertheless, the relationships between this *in vitro* system to predicted and actual propranolol plasma concentrations suggest its applicability as a suitable *in vitro* model to investigate the uptake of xenobiotics and when combined with elimination rates, may supplement *in vivo* bioconcentration fish studies. This model provides a rapid and ethically acceptable tool with which to perform a preliminary assessment of compounds of low Log K_{ow}, and as such is ideal for large numbers of pharmaceuticals that typically have a lower propensity to bioaccumulate.

This study shows that as well as the passive uptake and efflux of neutral forms of pharmaceuticals, water enhances drug uptake of ionisable pharmaceuticals via both passive transcellular and carrier mediated processes. Hence, the ability of this system to tolerate freshwater is fundamental if we are to simulate *in vivo* drug uptake across the gill. In addition, the facilitated uptake of propranolol was more evident at low concentrations that are more environmentally relevant; suggesting that in certain situations uptake may be under predicted. Indeed there is significant variation (five-fold) recorded in plasma concentrations of individual fish exposed to pharmaceuticals *in vivo* (Owen et al., 2009), and it could be that individual differences in transporter expression may be a mechanistic explanation for this variance. The use of this system provides an opportunity to reduce the numbers of fish used in regulatory ecotoxicological testing as the primary gill cells cultured from two fish may provide many individual gill cell cultures, and this method bypasses *in vivo* drug exposures and uses much less test compound, thus offering refinement through improved animal welfare methods.

Chapter 6

The metabolism of pharmaceuticals by gill cell epithelia

6.1 Abstract

The metabolism of chemicals after they pass into fish has been attributed to a reason why models used to predict BCF values might be unreliable, as they fail to take this into account. The gill is the primary route of uptake of pharmaceuticals, but whether it metabolises pharmaceuticals has not been fully ascertained. This study utilised an *in vitro* primary rainbow trout gill cell model and the gill cell line RTgill-W1, grown on permeable membrane inserts in a two-compartment model. The primary gill cell culture technique produces epithelia that mimic the intact organ and can withstand apical freshwater application. Thus, environmentally relevant types and concentrations of pharmaceuticals can be added to the apical surface of the gill in the freshwater, like the *in vivo* scenario. This study aimed to show that the gill is metabolically active through cytochrome P450 activity and is a 'first-pass' organ of waterborne xenobiotic metabolism in fish. Cytochrome P450 assays indicated the presence of CYP1A, which may play a role in the metabolism of xenobiotics at the gill organ level. An appropriate solid phase extraction (SPE) method was optimised to analyse freshwater (the apical compartment) and cell culture medium samples (the basolateral compartment) after propranolol exposure at a range of concentrations over 24 hours. High-performance liquid chromatography (HPLC) analysis using a validated method confirmed the xenobiotic metabolic capacity of this primary gill cell culture, as the metabolite of propranolol, 4-hydroxypropranolol, was confirmed in both basal cell medium and apical water samples, indicating the presence of metabolite uptake and efflux, respectively.

6.2 Introduction

Pharmaceuticals enter the aquatic environment through the improper or insufficient removal by wastewater treatment plants (Kostich et al., 2014). Awareness of their effect on aquatic species is increasing (Lajeunesse et al., 2011) and legislation requires the bioconcentration factor (BCF) of chemicals to be determined to evaluate the bioconcentrative properties of the parent compound (OECD$_{305}$, 2012). Many physiological transport and metabolic systems are conserved between taxa (Lukenbach et al., 2014; Schreiber et al., 2011), leading to the suggestion that these parent compounds may also be metabolised by non-target aquatic species (Gunnarsson et al., 2008). Biotransformation of compounds can strongly influence the extent to which metabolites bioconcentrate in fish and so actual BCF values may be under- or over-estimated (Gomez et al., 2010).

Pharmaceuticals are metabolised by cytochrome P450 (CYP) enzymes that typically add hydroxyl groups to aid solubility. There are over 1000 known CYP enzymes identified throughout the vertebrate lineage, approximately 60 have been identified in humans (Anzenbacher & Anzenbacherová, 2001), and of these , CYP1A2, 2C9, 2C8, 2C19, 2D6, and 3A4 gene expression is induced by xenobiotics (Levien & Baker, 2003). Gene expression is not a measure of activity, however, and catalytic alkoxyresorufin-*O*-dealkylase assays are used to detect specific CYP enzyme induction and inhibition in response to xenobiotic exposure by measuring the amount of fluorescent resorufin produced. For example, the activities of ethoxy-, methoxy-resorufin-*O*-dealkylases (EROD and MROD) can quantify CYP1A and CYP1A2 activity, respectively.

To date, CYP enzymes identified in rainbow trout total 10, and some information is known on their induction and inhibition (Table 6.1). The trout CYP1A family is analogous to mammalian CYP1A, with similar substrate specificity that is inducible by beta-naphthoflavone (BnF) (Carlsson et al., 1999; Carlsson & Pärt, 2001; Jönsson et al., 2002) and inhibited by alpha-naphthoflavone (AnF)

(Thibaut et al., 2006). The rainbow trout liver is the principle site of xenobiotic metabolism and primary liver cells have been shown to be metabolically active in S9 fractions (Conners et al., 2013; Gomez et al., 2011), and in 2D monoculture and 3D spheroid culture (Baron et al., 2012; Uchea et al., 2013).

Table 6.1

Rainbow trout CYP isoforms and their proposed inducers, inhibitors and assays.

Family	Symbol	Inducer	Inhibitor	Assay
CYP1	1A	BNF[a]	ANF[a] Clotrimazole[c]	EROD
CYP2	2K		Ketoconazole[b]	(ω-1)- and (ω-2)-Laurate hydroxylase (CYP2K-like)
	2M		Ketoconazole[b]	ω-Laurate hydroxylase (CYP2M-like)
CYP3	3A27	Phenobarbital[*], rifampicin[*] dexamethasone[*]	Clotrimazole[c] Ethynylestradiol[b]	BFCOD (CYP3A-like)
	3A45	Phenobarbital[*], rifampicin[*]	Ethynylestradiol[b]	
CYP4	4T1			
CYP11	11A			
	11B			
CYP17	17			
CYP19	19	Phenobarbital[*], rifampicin[*]		

[*] Mammalian data

[a] Rainbow trout primary *in vitro* gill cells (Carlsson et al., 1999)

[b] Carp liver subcellular fractions (Thibaut et al., 2006)

[c] Rainbow trout hepatic microsomes (Burkina et al., 2013)

In order to reach the liver for detoxification, xenobiotics must first enter the fish via the diet, or over the dermis or gill. The gill is the primary site of oxygen uptake and nitrogenous waste excretion, ion transport (Evans et al., 2005) and xenobiotic uptake (Bury et al., 2014; Stott et al., 2015). *In vitro*, primary gill cell suspensions and S9 fractions are metabolically active; they contain CYP enzymes that are inducible resulting in the depletion of parent compound and the formation of hydroxy-metabolites (Bartram et al., 2011; Gomez et al., 2010; Gomez et al., 2011). We

hypothesise that the rainbow trout gill is a metabolic organ, offering 'first-pass' metabolism of xenobiotics to be excreted or further metabolised.

The non-selective beta-antagonist propranolol has been detected in surface waters in the UK and is present on the Environmental Agency's (EA) targeted monitoring programme for pharmaceuticals in the aquatic environment (Hilton et al., 2003). Propranolol has a BCF value of 160 in mussels (AstraZeneca, 2012) and is known to cross the rainbow trout gill epithelium *in vitro* (Stott et al., 2015). In humans, propranolol is metabolised via three pathways to more than 12 metabolites by three known CYPs, but chiefly by CYP1A2 and CYP2D6 (Fig 6.1; Walle et al., 1983; Walle et al., 1985; Mehvar & Brocks, 2001). In rainbow trout propranolol is metabolised by primary *in vitro* gill cells in suspension or S9 fractions (Bartram et al., 2011; Gomez et al., 2010).

The following study aimed to quantify the metabolism of propranolol at the gill using primary and immortalised *in vitro* gill cells cultured on permeable supports. Primary gill cells cultured first in cell culture flasks (SSI) are known to contain a population solely of pavement cells, the main respiratory cell of the freshwater gill epithelium (Wood et al., 1998). Primary DSI epithelia are the most accurate representation of the rainbow trout gill and contain multiple cell types including PVCs and mitochondria-rich cells (MRCs), the cells responsible for active and ionic transport at the gill (Wood, 2001). The immortalised rainbow trout gill cell line, RTgill-W1, also contains PVCs and MRCs (Lee et al., 2009) but lacks some metabolic enzymes such as CYP1A (Schirmer et al., 1998) and other epithelial physiological characteristics such as high transepithelial resistance. These differences in epithelial characteristics could explain any observed differences in transport and metabolism.
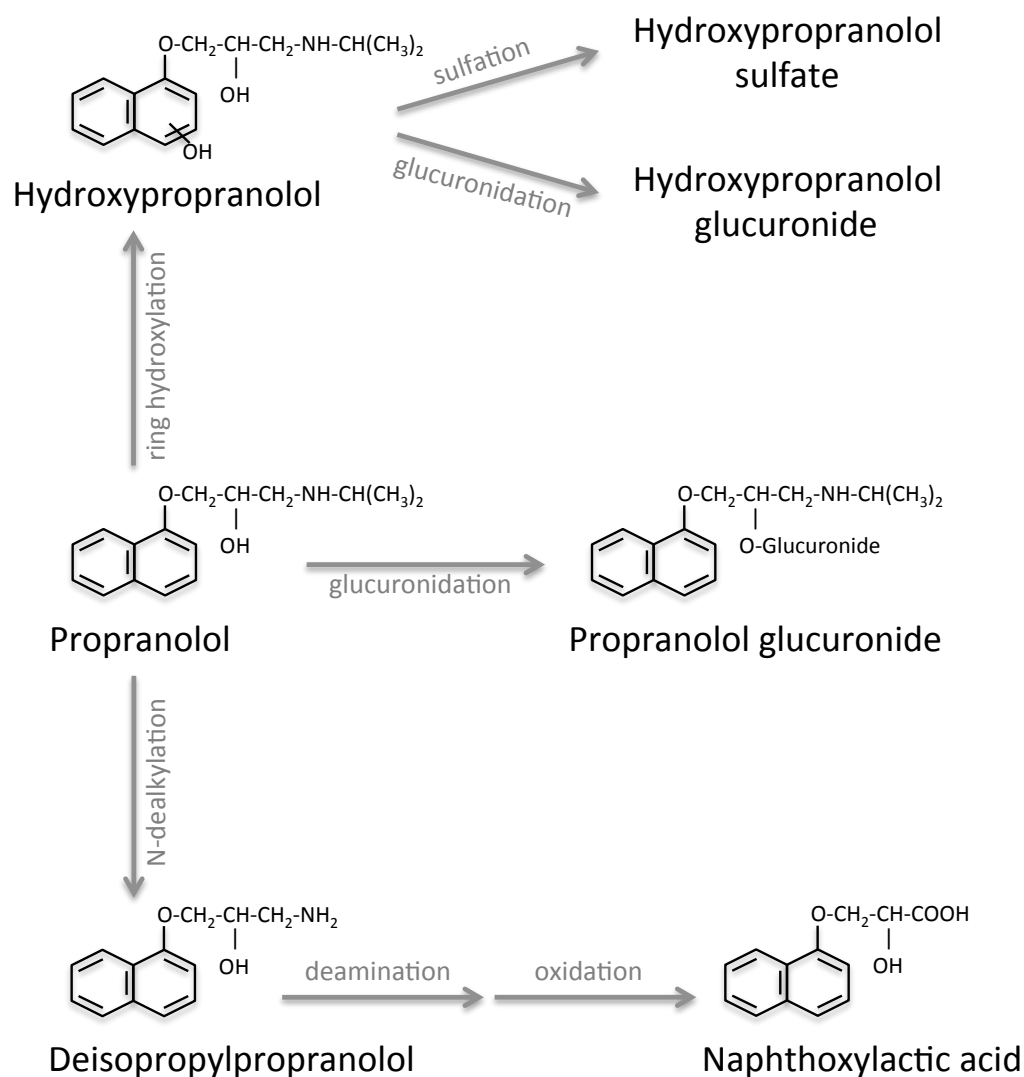
Fig 6.1 The main pathways of propranolol metabolism in humans. Adapted from Mehvar & Brocks (2001).

6.3 Materials and methods

6.3.1 Reagents and suppliers

Propranolol hydrochloride, (±)-4-hydroxypropranolol hydrochloride (of analytical standard), ammonium acetate and ethoxy-resorufin-*O*-dealkylase (EROD) were purchased from Sigma Aldrich. Beta and alpha -naphthoflavone were purchased from Insight Biotechnology. Resorufin

was obtained from Santa Cruz Biotechnology. Bradford dye reagent was purchased from Biorad. Analytical grade methanol, acetonitrile and ultrapure HPLC water were purchased from VWR.

6.3.2 Equipment and suppliers

Equipment used was the same as those outlined in Chapter 2 with the following additions. Oasis HLB cartridges (6 mL, 200 mg) were purchased from Waters Ltd. The 24-port SPE manifold was purchased from Thermo Scientific. The evaporation system was a TurboVap LV produced by Biotage. The Agilent 1200 series HPLC system was equipped with degasser, quaternary pumps, autosampler, column oven and UV detector produced by Agilent Technologies. This was controlled by GINA Star software version 5.8 produced by Raytest. The HPLC system used a Waters SunFire C18 column (3.5 µm, 2.1 mm × 150 mm) (Waters) fitted with a SecurityGuard™ guard column (2.0 mm ID; Phenomenex). HPLC amber-glass vials were purchased from Fisher Scientific. For protein quantification 96 well plates were purchased from Nunc. The multiwall plate reader was produced by Synergy HT and operated using the KC4 program.

6.3.3 Preparation of reagents

Reagents were prepared as detailed in Chapter 2. Standard solutions of propranolol and hydroxypropranolol were diluted from stocks made in ultrapure water into freshwater, L-15 and phase A for standard HPLC calibrations. EROD was reconstituted into 10 mM stock in DMSO and resorufin to a 2 mM stock in DMSO and stored at -20°C in the dark.

6.3.4 Cell culture reagents

Cell culture reagents were prepared as outlined in Chapter 2.

6.3.5   Methods

The general material and methods for the cell culture and maintenance of SSI (from primary gill cells first cultured in cell culture flasks), DSI and RTgill-W1 can be found in Chapter 2. SSI cells were cultured for at least 1 week before exposure after having reached a plateau in TER (Fig 3.2A). DSI epithelia were used once they had passed a TER of 5000 Ω cm^2. RTgill-W1 was cultured for at least 1 week on permeable inserts. Before xenobiotic exposure, cell culture medium was removed and inserts were washed as detailed in Chapter 2 to remove traces of FBS. All assays took place at 18°C.

6.3.6   EROD induction and inhibition

BnF and AnF are hydrophobic and in water have the tendency to adhere to plastic ware, thus lowering exposure concentrations. To reduce this the exposure was performed in L-15 medium (Leguen et al., 2000). BnF and AnF were diluted from a 10 mM stock in DMSO to a final concentration of 10 µM (Carlsson et al., 1999) in L-15 (0.01% DMSO). The control L-15 contained the same concentration of DMSO. For induction assays, 1.5 mL of the BnF solution was applied to the apical cell surface (the apical compartment) of SSI epithelia (*n* = 4 from 3 fish), DSI epithelia (*n* = 3 from 2 fish, 1 biological replicate) and RTgill-W1 epithelia *(n* = 3, Passage number 108) with 2.0 mL L-15 in the basolateral compartment for 24 hours at 18°C. Similarly for inhibition assays, 1.5 mL AnF solution was applied to the apical compartment in the same way.

After 24 hours, the exposure medium was removed (basolateral first, then the apical) and gill cell epithelia were washed twice with 200 µL PBS. 2 µM EROD was made in PBS from a 2 mM stock in DMSO, and 200 µL was applied to the apical cell surface. This was incubated at room temperature in the dark for 20 minutes. The whole 200 µL was then transferred to a black 96 well plate and the florescence of the formed resorufin was read at 544 nm (emission) and 590 nm (excitation) using a

multiwall plate reader. Quantification was made by calibration with a resorufin standard curve (0.02-2 µM in PBS from a 2 mM stock in DMSO) constructed on each plate.

6.3.7   Propranolol exposure

SSI epithelia (*n* = 3 from 3 fish), DSI epithelia (*n* = 3 from 1 biological replicate) and RTgill-W1 epithelia *(n* = 3, P108) were prepared for experimental procedures as previously described (Chapter 2). 1000 µg L^{-1} of propranolol in FW was applied to the apical compartments, whilst the basolateral remained in L-15 for 24 hours at 18°C. After 24 hours, the exposure medium was removed and the EROD assay was carried out exactly as above.

6.3.8   Protein quantification assays

To determine cellular protein content following the EROD assay, gill cell epithelia were again washed twice with 200 µL PBS, exposed to 200 µL Milli-Q water and left at room temperature for 20 minutes, before the whole plate was transferred to -80°C for at least 24 hours. Samples were thawed and three 5 µL samples from each insert was transferred to a clear 96 well plate with 250 µL of Bradford dye and left to incubate at room temperature in the dark for 5 minutes. The absorbance was read at 595 nm using a multiwall plate reader and quantification made by calibration with a protein standard curve (0.13-2 mg mL^{-1} BSA in Milli-Q water) constructed on the same plate. Protein was quantified to express EROD activity per mg of protein.

6.3.9   Propranolol exposure for HPLC analysis

SSI, DSI and RTgill-W1 were cultured, maintained and prepared for experimental procedures as outlined above. Propranolol was applied to either the apical compartment in 1.5 mL FW with L-15 in the basolateral ('uptake') (*n* = 12), or in 2.0 mL L-15 with 1.5 mL FW in the apical ('efflux') (*n* = 12) at a concentration of 10, 100 and 1000 µg L^{-1}. Excess exposure L-15 and FW with and without propranolol (time 0) were stored at -80°C, the same as samples as outlined below.

6.3.10   Sample collection and storage

At each time point, 1, 3, 6 and 24 hours after exposure, the 2.0 mL of L-15 medium was removed from the basolateral well and stored in a 14 mL conical tube, and the 1.5 mL FW was removed from the apical compartment and stored in a 2.0 mL eppendorf. These were immediately transferred to -80°C until samples underwent SPE, when they were thawed, pooled (n = 3, giving a total volume of 6 mL for L-15 samples and 4.5 mL for FW samples) and used immediately.

6.3.11   Solid phase extraction of samples and standard solutions

The same SPE protocol was used for both sample and standard solution (below) preparation. Firstly, Oasis HLB cartridges were conditioned with 6 mL of methanol and rinsed with 6 mL of ultrapure water under a vacuum (20 psi) on a 24-port SPE manifold. The samples or standards (of known propranolol and hydroxypropranolol concentrations), in either 6 mL of L-15 or 4.5 mL FW respectively) were then loaded onto the preconditioned cartridges at a rate of 2 mL min^{-1}. Cartridges were then washed with half the volume previously applied of ultra-pure water (i.e. either 3 mL for L-15 or 2.25 mL for FW samples) and dried for 30 minutes under a vacuum. Sample extracts were then eluted with either 6 mL or 4.5 mL methanol (for L-15 or FW samples, respectively) and dried under pure nitrogen (1.0 bar) whilst heated to 40°C using an evaporation system. Extract residues were reconstituted in either 600 µL (for L-15 samples or standards) or 450 µL (for FW samples or standards) of phase A solvent (see below), achieving a concentration of x10 the original. This was transferred to a 2 mL HPLC amber-glass vial, crimped shut and immediately injected onto the HPLC system.

6.3.12   Standard solutions for HPLC

Individual stock standard solutions (2 mg mL^{-1}) of propranolol and hydroxypropranolol were prepared in HPLC grade ultra-pure water and stored at -80°C. Working standard solutions were

prepared firstly by diluting the two stocks together 50:50 to create a working stock of 1 mg mL^{-1} propranolol and hydroxypropranolol in HPLC grade ultrapure water. Working standard solutions were prepared through appropriate dilutions in either 6 mL L-15 culture media or 4.5 mL FW to obtain concentrations between 100-100000 µg L^{-1}, to be used immediately.

6.3.13 Apparatus and chromatographic conditions

This HPLC method was developed and optimised on an Agilent 1200 series HPLC system. Analytes ran at a flow rate of 0.2 mL min^{-1} using automatic injection at a volume of 20 µL. Mobile phases were 90:10 (*v/v*) 10 mM ammonium acetate in water:acetonitrile (phase A) and 20:80 (*v/v*) 10 mM ammonium acetate in water:acetonitrile (phase B). The profile used an isocratic mobile phase B at 30% for 10 minutes with a column oven temperature of 45°C. Detection of the analytes was carried out at 254 nm and quantification was carried out by calculating the peak area using GINA Star software. Confirmation of the analytes was achieved using the retention time of the analytical standard (Fig 6.4).

6.3.14 Method validation using standard solutions

Instrumental linearity was determined by measuring the peak area of propranolol and hydroxypropranolol at 6 concentrations (from 500-100000 µg L^{-1}) in ultra-pure HPLC grade water (*n* = 3). Method linearity was determined by measuring the peak area of propranolol and hydroxypropranolol at 6 concentrations (from 500-10000 µg L^{-1}) made in either L-15 or FW and after having undergone SPE and reconstituted in mobile phase A. Limits of detection (LOD) and quantification (LOQ) were determined for both propranolol and hydroxypropranolol in either L-15 or FW after SPE from the linear calibration of the method, calculated using the equations

$$LOD = \frac{3SD_a}{b}$$

$$LOQ = \frac{10SD_a}{b}$$

where SD_a is the standard deviation of the lowest measured analyte and *b* is the slope of the regression line (Shrivastava & Gupta, 2011). The percentage recoveries were calculated by comparing peak area of analytes spiked with 3 concentrations (1, 5, 10 mg L^{-1}) of propranolol and hydroxypropranolol in either L-15 or FW before and after (with the expected concentrations) SPE (*n* = 3). Instrumental retention times for propranolol and hydroxypropranolol in either FW or L-15 were determined in all standards (*n* = 15) to calculate the mean value (±SD) for analyte identification from samples. Intraday reliability was determined for 3 concentrations (1, 5, 10 mg L^{-1}) of propranolol and hydroxypropranolol in both L-15 and FW after SPE (*n* = 3). The same was repeated for 2 further days to calculate interday reliability. Method precision was determined for propranolol and hydroxypropranolol in both L-15 and FW after SPE at 3 concentrations (1, 5, 10 mg L^{-1}) (*n* = 6). Control samples containing no propranolol or hydroxypropranolol were also analysed for background correction purposes. Finally, mobile phase A was injected between batches of samples (FW or L-15) to minimise the possibility of carry over. None of the analytes were detected in any of the mobile phases or ultra-pure water used in this study.

6.3.15 Analysis of data and statistics

EROD activity was expressed as the mass of resorufin produced per min per mg of protein. Results of the EROD assays are expressed as means ± SEM for each condition. To test for significant increases or decreases in EROD activity levels compared to the control baseline values, an independent samples *t*-test with equal variances assumed was used and statistical significance was accepted when *P* < 0.05 (SPSS software, SPSS Inc.). Likewise, for significant differences between normal EROD activity and those values from exposure to 1000 μg L^{-1} propranolol, an independent samples *t*-test with equal variances assumed was again used and statistical significance was accepted when *P* < 0.05 (SPSS software, SPSS Inc.).

Samples (n = 3) for HPLC analysis were pooled to increase to concentrations that were identifiable. Quantification of the analytes in apical FW and basolateral L-15 was made based on their peak areas relative to the calibration curve made from the standard solutions. The values were then expressed as a percentage of the initial concentration of propranolol at time 0 for all time points. Because samples were pooled, these samples were not statistically compared to one another. All graphical illustrations were produced using either Excel (Microsoft Office) or Sigmaplot (Systat Software Inc.).

6.4 Results

6.4.1 EROD induction and inhibition

EROD activity in SSI epithelia was 16.04 ± 2.97 pmol resorufin min^{-1} mg protein^{-1} and was not induced by 10 µM BnF or inhibited by 10 µM AnF (Fig 6.2A). Baseline EROD activity in DSI epithelia was at a similar rate of 17.78 ± 0.47 pmol resorufin min^{-1} mg protein^{-1}. This was significantly induced by 10 µM BnF to 33.77 ± 0.93 pmol resorufin min^{-1} mg protein^{-1} (P < 0.001) and significantly inhibited by 10 µM AnF to 10.84 ± 3.17 pmol resorufin min^{-1} mg protein^{-1} (P < 0.001; Fig 6.2B). RTgill-W1 epithelia had the lowest EROD activity of 0.08 ± 0.00 pmol resorufin min^{-1} mg protein^{-1} that was not significantly induced nor inhibited (Fig 6.2C).

6.4.2 EROD activity from propranolol exposure

After 24 hours exposure to 1000 µg L^{-1} propranolol, SSI epithelia showed no significant increases or decreases in EROD activity (Fig 6.3A). DSI epithelia showed a significant inhibition of EROD activity, from 7.09 ± 0.86 in control cells to 3.68 ± 0.78 pmol resorufin min^{-1} mg protein^{-1} (P < 0.05; Fig 6.3B). RTgill-W1 cells also showed no significant differences in EROD activity (Fig 6.3C).
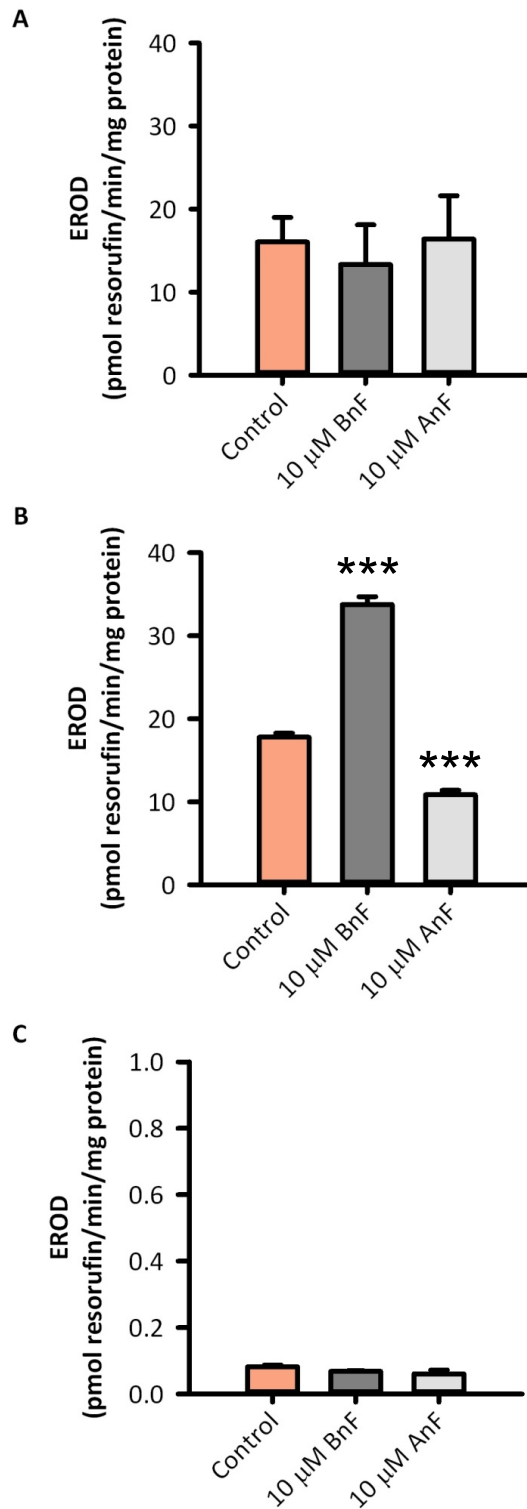
Fig 6.2. Baseline control 7-ethoxyresorufin *O*-deethylase (EROD) activity levels (orange bars), induced activity (dark grey bars) from 24 hours exposure to 10 µM *β*-naphthoflavone and inhibited activity (light grey bars) from 24 hour exposure to 10 µM *α*-naphthoflavone in (A) SSI (*n* = 4 from 3 fish) (B) DSI (*n* = 3 from 2 fish, 1 biological replicate) and (C) RTgill-W1 *(n* = 3, P108). Significant differences from the control are indicated by the asterisk (independent samples *t*-test; ****P <* 0.001) and values are means ± SEM.
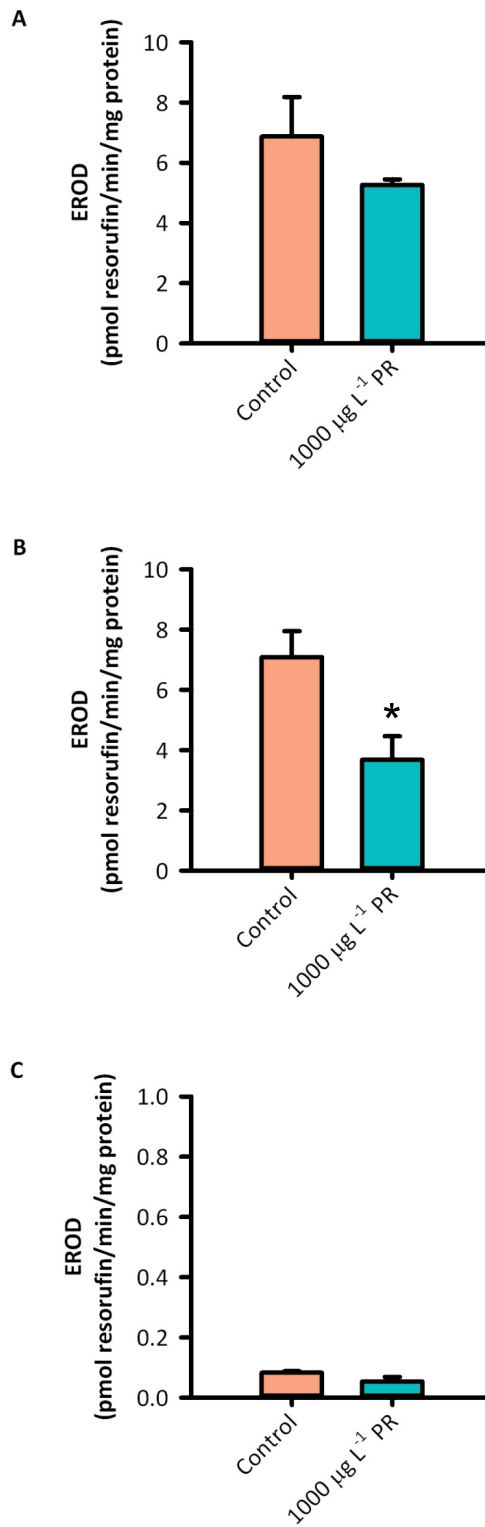
Fig 6.3. Baseline control 7-ethoxyresorufin *O*-deethylase (EROD) activity levels (orange bars) and EROD activity after 24 hours exposure to 1000 µg L^{-1} propranolol in freshwater (PR; green bars) in (A) SSI (*n* = 3 from 3 fish) (B) DSI (*n* = 3 from 1 biological replicate) and (C) RTgill-W1 *(n* = 3, P108). Significant differences from the control are indicated by the asterisk (independent samples *t*-test; *P* < 0.05) and values are means ± SEM.

6.4.3   Optimisation of HPLC conditions

The mobile phase used, a mixture of 10 mM ammonium acetate with water and acetonitrile, was found to be suitable for the separation of the two analytes, propranolol and hydroxypropranolol. A column oven temperature of 45°C further aided separation. The UV region that gave a shared absorption for both compounds was scanned and 254 nm was found to be the optimum for simultaneous determination during the 10 minute run. Figure 6.4 shows the separation of analytes in freshwater (Fig 6.4A) and L-15 medium (Fig 6.4B) (with satisfactorily separated peak of L-15 solutes; Fig 6.4B*) obtained using this method.

6.4.4   Method performance characteristics

The development of appropriate SPE and an HPLC method for the extraction of propranolol and hydroxypropranolol from both freshwater and L-15 medium produced analyte peaks that were detectable and quantifiable (Fig 6.4) and a method that was validated as summarised in Table 6.2. Instrumental linearity produced good fits for both propranolol and hydroxypropranolol, achieving R^2 values of 1 and 0.9997 respectively over the concentration range 500-10000 µg L^{-1} (n = 3). Limits of detection for propranolol extracted from FW and L-15 were 49.72 and 6.46 µg L^{-1}, whilst those for hydroxypropranolol were higher at 105.26 and 72.20 µg L^{-1}. Limits of quantification were 165.74 and 21.54 µg L^{-1} for propranolol in FW and L-15, and 350.88 and 240.66 µg L^{-1} for hydroxypropranolol. Correlation coefficients of R^2 > 0.99 were achieved for the method linearities for all compounds. Mean absolute recoveries for propranolol ranged from 80-91% and 23-74% for hydroxypropranolol.
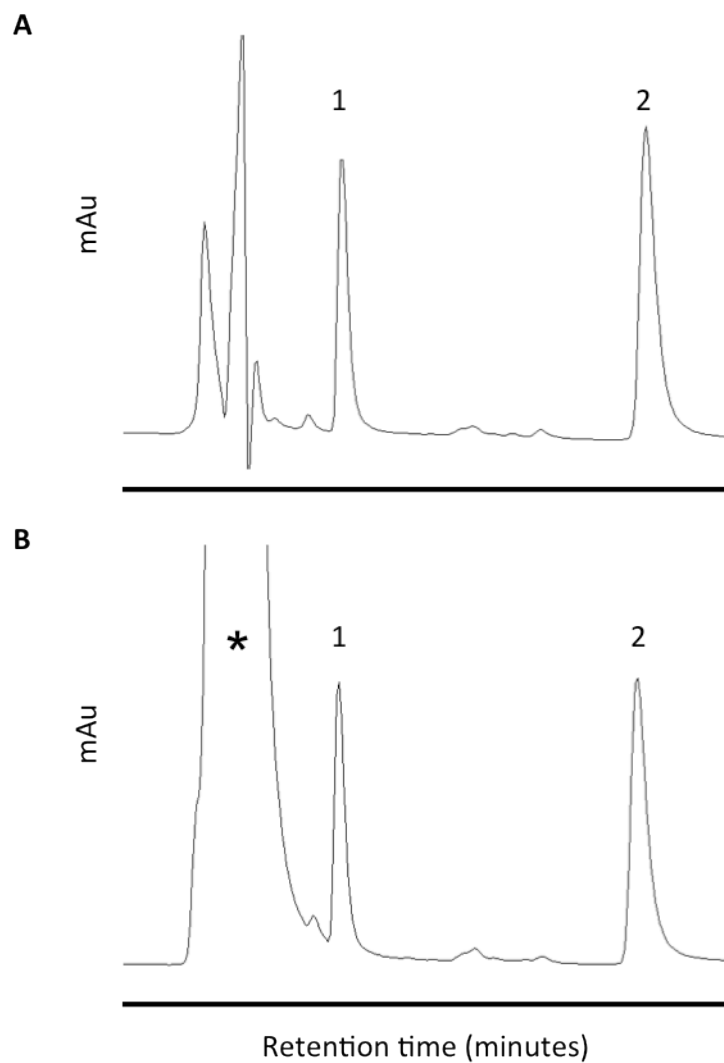
Fig 6.4. Typical chromatograms of the standard retention times and intensities of hydroxypropranolol (1) and propranolol (2) obtained from a freshwater (FW) standard (A) and an L-15 cell culture medium standard (B), both pre-spiked and having undergone SPE. The peak of inorganic salts and amino acids present in L-15 is separated from the analytes (*).

Table 6.2

HPLC method performance characteristics.

Medium	Compound	t_R[a] ± SD[b]	R^2	Concen-tration	Intra-day accuracy ± SD	Inter-day accuracy ± SD	Absolute recovery ± intra-day precision
		(min)		(µg L^{-1})	(%)	(%)	(%)
		$n = 15$	$n = 5$				$n = 3$
FW	Propranolol	8.38 ± 0.18	0.9982	1000	100 ± 1.5	100 ± 5.3	92 ± 1.3
				5000	101 ± 11.8	101 ± 9.4	80 ± 9.0
				10000	100 ± 6.8	100 ± 5.4	82 ± 5.3
	Hydroxy-propranolol	3.67 ± 0.07	0.9972	1000	100 ± 4.9	101 ± 7.5	23 ± 3.2
				5000	102 ± 18.3	101 ± 11.8	56 ± 10.8
				10000	100 ± 5.3	100 ± 3.2	60 ± 3.3
L-15	Propranolol	8.44 ± 0.11	0.9988	1000	102 ± 15.2	101 ± 7.8	85 ± 15.4
				5000	100 ± 5.0	100 ± 6.2	82 ± 4.1
				10000	100 ± 2.1	100 ± 4.7	83 ± 1.8
	Hydroxy-propranolol	3.66 ± 0.07	0.9980	1000	100 ± 4.4	100 ± 5.6	46 ± 4.7
				5000	100 ± 5.4	100 ± 6.3	63 ± 4.0
				10000	100 ± 1.2	100 ± 4.3	74 ± 0.9

[a] retention time

[b] standard deviation

6.4.5   HPLC analysis

The epithelia exposed to 10 and 100 µg L^{-1} propranolol resulted in peaks of analytes that were far lower than the detectable limits and so quantification using this HPLC method and could not be used.

SSI epithelia exposed to 1000 µg L^{-1} propranolol in FW (the apical compartment; uptake) or in L-15 (the basolateral compartment; efflux) contained 100% propranolol in these donor compartments at time 0 hours (Fig 6.5A; Fig 6.5B). In uptake assays, the concentration of propranolol in FW remained at 100% of the initial until 24 hours when it dropped to 89.71% due to its appearance in the basolateral compartment (Fig 6.5A). In efflux assays, the appearance of propranolol in the

basolateral receiving compartment occurred sooner, after 1 hour, reaching 4.10% that of the initial concentration of the donor (Fig 6.5B). Hydroxypropranolol was not detected in any of the samples.

In uptake assays using DSI epithelia, the amount of propranolol declined from 100% of the initial at time 1, 3 and 6 hours to 89.22% after 24 hours (Fig 6.5C). In the basolateral compartment, propranolol was detected at 24 hours only (Fig 6.5C), at 8.78% of the initial concentration of the donor compartment. Hydroxypropranolol was detected in the apical donor compartment after 1 hour, and remained at approximately 40 µg L^{-1} for the remaining time up to 24 hours (Fig 6.5C). No hydroxypropranolol was measured in the basolateral L-15 receiver compartment. In efflux assays, the amount of propranolol declined more quickly from 100% to 89% after 6 hours (Fig 6.5D). This was observed to appear in the receiving apical compartment after just 1 hour, resulting in 8.72% of the initial concentration after 24 hours (Fig 6.5D). Hydroxypropranolol was again detected in the apical compartment after 1 hour, and remained at 28-37 µg L^{-1} for the remaining time up to 24 hours (Fig 6.5D). Again, no hydroxypropranolol was detected in the basolateral L-15 compartment.

Assays using the rainbow trout gill cell line RTgill-W1 showed results similar to those obtained from SSI gill cell cultures. The concentration of propranolol in the apical compartment remained at 100% until 24 hours when it had declined to 91.31% of the initial concentration (Fig 6.5E). This resulted in the appearance of propranolol in the receiving basolateral compartment of 8.68% at 24 hours (Fig 6.5E). In efflux assays, the concentration of propranolol decreased sooner, after 3 hours, and appeared in the receiving apical compartment at 1% the initial concentration, reaching a maximum of 6.38% of the initial concentration after 24 hours (Fig 6.5F). Hydroxypropranolol was not detected in any of the samples.
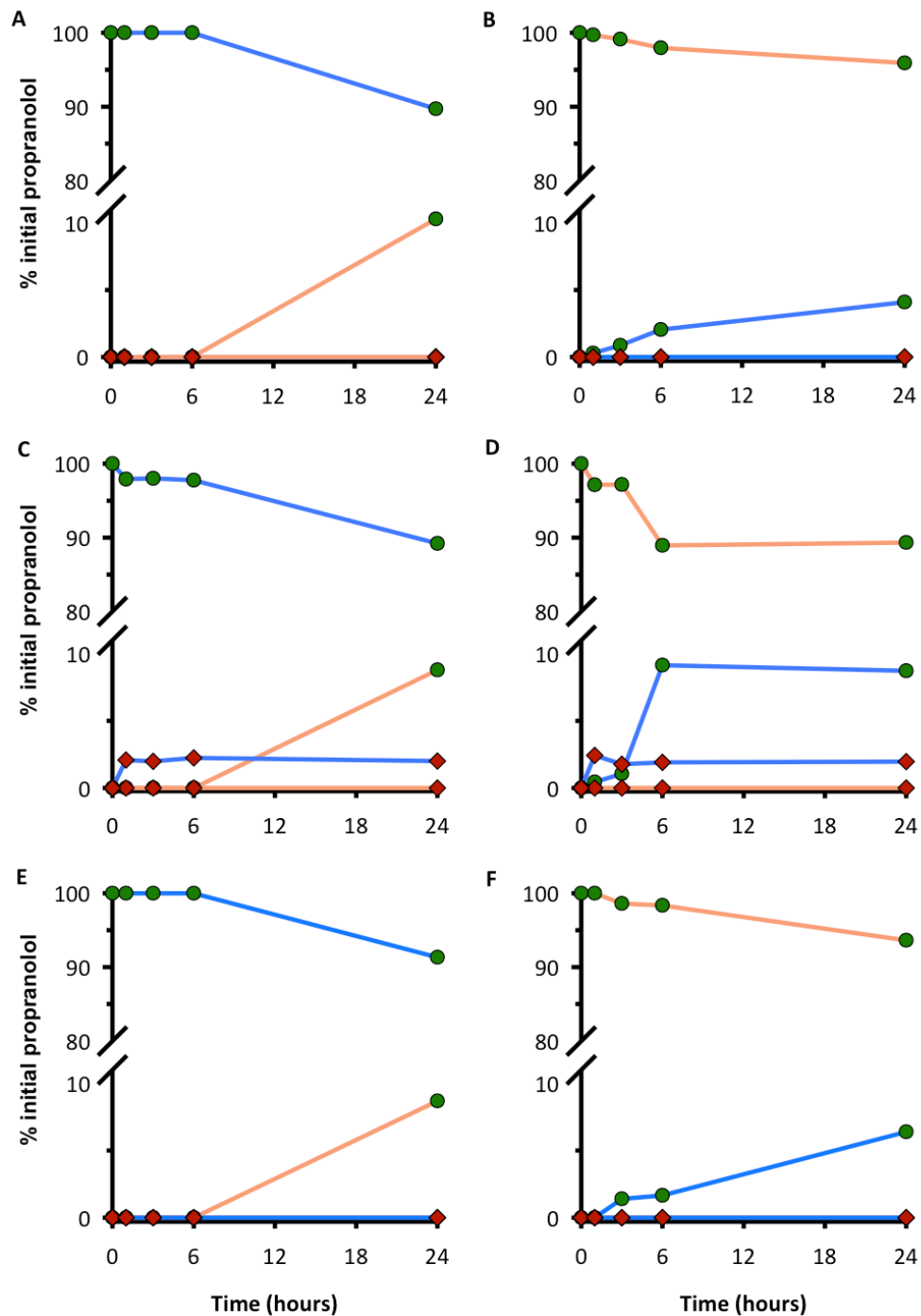
Fig 6.5. The transport of propranolol across the SSI (A & B) or DSI (C & D) primary rainbow trout primary gill cell epithelium, or RTgill-W1 epithelia (E & F) over 24 hours. Propranolol is applied at a concentration of 1000 µg L^{-1} to either the apical (A, C, E) for apical to basal transport; uptake, or basal compartment (B, D, F) for basal to apical transport; efflux, in asymmetrical (freshwater in the apical compartment and L-15 medium in the basal) conditions. Orange lines represent L-15 and blue lines water samples. The green circles represent propranolol and the red diamonds represent hydroxypropranolol. Data are shown as a percentage of the initial propranolol concentration versus time.

6.5 Discussion

These SPE and HPLC methods are the first documentation of the extraction of a pharmaceutical and its metabolite from aqueous samples obtained from the exposure of primary and immortalised gill cell cultures cultured on permeable membrane inserts. Analysis using HPLC first required the development of a SPE method that produced a sample with high enough concentrations of parent compounds and metabolites for analysis. This was achieved in three ways. Firstly, the loading volumes onto SPE cartridges were from pooled samples to either 6 mL for L-15 or 4.5 mL for FW. This provided a high enough concentration of propranolol and hydroxypropranolol to be retained on the SPE cartridge, but unfortunately meant that three samples were pooled, thus reducing the *n* number of samples to 1 and eliminating the option of statistical analysis. Loading of smaller volumes resulted in the elution of compounds at concentrations below detectable limits. Secondly, analytes stored on SPE cartridges after being dried down were reconstituted in volumes ten times less the original volume loaded onto the cartridge (600 µL for L-15 samples or standards and 450 µL for FW samples or standards in phase A solvent). This brought these concentrations up to detectable and quantifiable limits. Thirdly, it was found that samples of L-15 contained a number of solutes that needed to be removed. Leibovitz's L-15 cell culture medium without phenol red contained 17 amino acids with molecular weights less than 204 and at concentrations less than 500 mg L^{-1}, 8 vitamins with molecular weights less than 478 and at concentrations less than 2 mg L^{-1}, 7 inorganic salts with molecular weights less than 142 and at concentrations less than 400 mg L^{-1} (except sodium chloride at 8 g L^{-1}), as well as D-(+)-galactose and sodium pyruvate. During method development, L-15 samples produced a large peak of these salts and vitamins that distorted the view of any analyte peaks. Therefore, a method was developed that washed the SPE cartridges of these solutes, whilst allowing the propranolol and hydroxypropranolol to remain adhered to the cartridge. Similarly, the mobile phase and column temperature further aided this separation (Fig 6.4B*). In this way, we obtained good absolute

recoveries for propranolol ranging from 80-91% and fair recoveries for hydroxypropranolol of 23-74% (only two of these were below 50%; 23 and 43%). This again resulted in analytes that were able to be detected for HPLC analysis, but only for experiments run at 1000 µg L^{-1}, those at 10 and 100 µg L^{-1} were disregarded for analysis using HPLC.

CYP1A-catalysed *O*-deethylation of ethoxyresorufin (EROD) is widely used as a biomarker for aryl hydrocarbon receptor (AhR) agonist exposure in wild populations of fish (Whyte et al., 2001). In rainbow trout, EROD can be induced in gill filaments (Jönsson et al., 2002), branchial microsomes (Lindström-Seppä & Oikari, 1990), gill S9 fractions (Bartram et al., 2011) and in primary gill cell cultures (Carlsson et al., 1999; Carlsson & Pärt, 2001). Through an optimised EROD assay method, this study showed CYP1A activity as measured in an EROD induction and inhibition in primary rainbow trout gill cells in SSI and DSI (Fig 6.2A; Fig 6.2B). Exposure to BnF at 10 µM failed to induce EROD activity in SSI to values higher than that of the control. Previously, it was found that EROD could be induced in SSI by BnF in a concentration dependent manner, which peaked at 0.1 µM BnF to approximately 36 pmol resorufin min^{-1} mg protein^{-1}, and declined to control levels at higher concentrations, for which the highest tested was 1 µM BnF (producing approximately 14 pmol resorufin min^{-1} mg protein^{-1}) (Carlsson & Pärt, 2001). This is similar to the SSI EROD vales obtained here (16.04 ± 2.97 pmol resorufin min^{-1} mg protein^{-1}) for a 10 µM BnF exposure. This is the first time rainbow trout DSI epithelia have been shown to contain inducible and inhibitable EROD activities. DSI epithelia cultured from the gills of tilapia have previously been shown to significantly induce EROD activity in response to benzo(a)pyrene (BaP) (Zhou et al., 2006), but to activities that are five times lower than those obtained here. Similarly, baseline values were reported as <1 pmol resorufin min^{-1} mg protein^{-1} (Zhou et al., 2006), whereas those measured in our rainbow trout control DSI epithelia was 17.78 ± 0.47 pmol resorufin min^{-1} mg protein^{-1}. These differences could be due to differences between EROD activity in the gills of tilapia and rainbow trout or differences

between EROD assay protocols. EROD has not been induced in RTgill-W1 (Schirmer et al., 1998) and CYP1A activity remained undetected in this cell line in this study.

The extensive metabolism of propranolol is well documented in both humans and mammals (Masubuchi et al., 1994; Walle et al., 1983; Walle et al., 1985). This metabolism is brought about by oxidative reactions initially performed by cytochrome P450 involving side-chain glucuronidation, ring hydroxylation and side-chain *N*-desisopropylation (Fig 6.1; Masubuchi et al., 1994). In human liver microsomes, propranolol 4- and 5-hydroxylation is catalysed mainly by CYP2D6, whilst CYP1A2 catalyses the side chain *N*-desisopropylation of propranolol (Masubuchi et al., 1994). "Reading across" to fish, one might expect some aspect of the latter pathway to be present in fish due to the CYP1A-like activities of piscine CYP1A (Uno et al., 2012). Indeed, propranolol has been shown to induce CYP1A as shown by increased EROD activity *in vivo* in both rainbow trout liver hepatocytes (Laville et al., 2004), gill samples from whole fish exposure (producing 5.7 pmol resorufin min^{-1} mg protein^{-1} from a 400 µg L^{-1} exposure, Bartram et al., 2011) and *in vitro* in primary gill cell suspensions which produced 2.1-6.1 pmol resorufin min^{-1} mg protein^{-1} from a 200 µg L^{-1} exposure (Bartram et al., 2011). In the current study however, propranolol significantly inhibited EROD activity in DSI after a 24 hour exposure to 1000 µg L^{-1}. Another study investigated the inhibitory effects of polycyclic aromatic hydrocarbons, flavones and coumarins on CYP1A1 and A2, and likewise found xenobiotics such as propranolol to be potent inhibitors of CYP1A1 and A2 in cDNA-expressed enzymes and human liver microsomes (Tassaneeyakul et al., 1993). Propranolol did not appear to induce or inhibit EROD activity in SSI, nor RTgill-W1, and EROD activity remained near baseline values after exposure to 1000 µg L^{-1} in freshwater.

Propranolol is metabolised in both liver and gill S9 fractions prepared from rainbow trout, as shown by a 70% and 25% (respectively) loss of parent compound over 90 minutes (Gomez et al., 2010). The gills show intrinsic clearance rates of propranolol that are significantly lower than that

of the liver (Gomez et al., 2010) probably because the metabolic activity in rainbow trout gill cells is 7-60 times less than isolated hepatocytes (and substrate dependent) (Leguen et al., 2000). Substrate depletion assays show the significant metabolism of propranolol in rainbow trout liver S9 fractions and CYP1A is the likely enzyme catalysing its metabolism in fish (Conners et al., 2013). Up to 10 phase I metabolites of propranolol have also been documented (some remain unidentified) in 2D primary trout hepatocyte cell cultures and 7 of these are also found in human 2D hepatic cultures (Dr Stewart Owen, personal communication). Propranolol is passively and actively taken up over the trout gill epithelium *in vitro* (Stott et al., 2015) and we again show here its transport from donor to receiver compartments in SSI, DSI and RTgill-W1 and uptake and efflux rates appear to be comparable, with similar amounts of propranolol appearing in receiver compartments. We know that for DSI, a proportion of this uptake is active; whilst concentration equilibrated transport assays (CETA) using SSI show this is not the case (Stott et al., unpublished data). This is perhaps owing to the absence of mitochondria-rich cells (MRCs) in SSI (Wood et al., 1998), the main sites of active and ionic transport in the rainbow trout gill (Wood, 2001).

In DSI epithelia, hydroxypropranolol was identified and measured in apical water samples in both apical and basolateral propranolol exposures. Hydroxypropranolol was not detected in basolateral L-15 samples, which could be due to its absence entirely at the basolateral surface of gill epithelia, or a distortion of its peak from the large salt and vitamin peak obtained from L-15 samples (Fig 6.4B*), and a more sensitive method of identification (and quantification), such as ultra-high performance liquid chromatography-tandem mass spectrometry (UPLC/MS), could be used. SSI or RTgill-W1 did not produce hydroxypropranolol and it was undetected in all samples. We could assume that its formation is due to the presence of MRCs in DSI, as this cell type is absent in SSI, but MRCs appear to be present in RTgill-W1 (Lee et al., 2009) although at much fewer numbers (Bols et al., 1994) and metabolic enzymes such as CYP1A are lacking (Schirmer et al., 1998). The only study to date investigating the metabolism of propranolol in whole fish (crucian carp,

Carassius carassius) reports the formation of five metabolites by the liver (Ding et al., 2015). These are *N*-desisopropylated propranolol, propranolol glucuronic acid, monohydroxylated propranolol, hydroxypropranolol glucuronide and dihydroxypropranolol glucuronide, formed by the same three processes present in mammals – side chain glucuronidation, aromatic ring hydroxylation and side chain *N*-desisopropylation (Masubuchi et al., 1994). This suggests that hepatic metabolism may be the primary elimination mechanism once propranolol is absorbed in to fish (via the diet or gills), and hence there is no need to absorb hydroxypropranolol, initially produced here at the gill, and it is rapidly effluxed as a primary efflux mechanism (Fig 6.5C & D).

This study presents the first evidence for the metabolism of propranolol at the *in vitro* rainbow trout gill epithelium. This is important as it suggests that less propranolol may be taken up into the organism over the gill, as a small proportion of it appears to be rapidly metabolised and effluxed out of the gill. The DSI primary gill cell epithelium represents the most accurate *in vitro* model to study these processes (Bury et al., 2014). Using such *in vitro* models can provide information on metabolites to be incorporated in environmental risk assessments of human pharmaceuticals as suggested in guidelines issued by the European Agency for the Evaluation of Medicinal Products (EMEA) (EMEA, 2006).

Chapter 7

General Discussion

When new products containing chemicals are bought to the market, their safety and that of their active components are determined so that the potential environmental risk can be assessed. In Europe, the safety of chemicals is assessed by directives such as REACH (The Registration, Evaluation, Authorisation & Restriction of Chemicals, REACH, 2009) for the evaluation of industrial chemicals, the EMEA (European Agency for the Evaluation of Medicinal Products) for medicines and specific European Union (EU) directives for plant protection products (PPP) and biocidal products (BioP) (e.g. EU, 2013 and EU, 2012, respectively). In the US similar directives such as The Federal Insecticide, Fungicide, and Rodenticide Act (FIFRA) and The Toxic Substances Control Act (TSCA) exist. Most of these bodies accept the use of testing guidelines provided by the Organisation of Economic Co-operation and Development (OECD) to assess a chemicals safety, which reduces the variation of testing methods between laboratories and harmonises the data produced.

To evaluate a compound's environmental risk, a specific OECD test guideline will be used depending on the route of exposure and the environmental compartment to which it is added. For example, owing to their application to plants, all PPP and some BioP require testing in birds using the Avian Acute Toxicity Test (OECD$_{223}$, 2010). The test guideline Bioaccumulation in Fish: Aqueous and Dietary Exposure (OECD$_{305}$, 2012) is required in many instances for chemicals that may enter water systems. These include industrial chemicals produced or imported in over 100 tons per year and with a Log K_{ow} > 3, all plant protection products with Log K_{ow} > 3, all anti-fouling agents and

detergents used as biocidal products, some human and veterinary medicinal products and certain food and cosmetic drugs (OECD, 2012). Each test on one compound uses at least 108 fish (Scholz et al., 2013), and so it is estimated that millions of fish are used in this test worldwide each year.

Within the OECD there is scope for the implementation of alternative methods where appropriate, in line with the OECD's commitment to the 3Rs – the replacement, reduction and refinement of the use of animals in scientific research (OECD, 2012). Furthermore, the Fish Toxicity Testing Framework put together by the OECD in 2012 (OECD, 2012), provided a review of existing fish toxicity test guidelines and suggested where reductions in the numbers of animals used could be made. Test OECD$_{305}$ was advised to be improved to minimise animal use by reducing the number of test concentrations per compound, by refining the number of sampling points during a test and refining the numbers of animals sampled at each point (OECD, 2012).

Furthermore, legislative directives such as REACH and the EMEA, as well as in many similar Asian and North American regulatory bodies, have also committed to the adoption of the 3Rs principle. There have been many advances in mammalian animal alternatives, especially in the cosmetic industry (e.g. skin corrosion tests) (Leist et al., 2012), but much less so in aquatic toxicology – perhaps owing to the ease at which aquatic species can be dosed via the water. One of the main reasons for the so few alternative methods is not due to their lacking in numbers, but the lack of acceptance of the method to provide applicable results (Lillicrap et al., 2016). In order to replace animal tests with *in vitro* alternatives, the most physiologically realistic cellular models need to be validated and proven to show results similar to *in vivo* in terms of toxicity (Tanneberger et al., 2013) or growth (Stadnicka-Michalak et al., 2015).

Many now argue for the stronger push to incorporate *in vitro* alternatives into aquatic regulatory testing (Lillicrap et al., 2016), such as the use of fish-derived cell lines in the assessment of environmental contaminants (Bols et al., 2005; Dayeh et al., 2013; Lee et al., 2009). Using cell lines

as an *in vitro* alternative system to whole animal studies has its advantages, one such being that they produce results with better reproducibility as individual differences are removed. There are also reductions in time, costs and space when using cell models as opposed to housing populations of fish in laboratories. As in Chapter 3, the rainbow trout gill cell line RTgill-W1 is easy to obtain, maintain and handle and can be routinely cultured in the laboratory for many passages (Bols et al., 1994), although it also exhibits the loss of certain physiological features of the original tissue (see Chapter 4). Furthermore, fish cell lines typically underestimate *in vivo* toxicity by 3 orders of magnitude (Tanneberger et al., 2013). It was proposed that this difference can be reduced in three ways: 1) by using cells derived from the specific tissue where the mode of action of a chemical occurs, 2) modifying the culture environment to like that of the *in vivo* and 3) by increasing the amount of chemical exposed by fraction to cells (Schirmer, 2006). This study using the primary gill cell system has accomplished these. Firstly, by directly isolating the cells of the gill, the cells of the primary site of xenobiotic uptake are used. Furthermore, this process also allows the culture environment to be as close to that of the *in vivo* scenario, as test concentrations of drugs can be added to the apical surface of gill cells in freshwater (see Chapters 5 & 6) as opposed to culture medium as is often required by fish cell lines, that may contain solutes that alter processes such as transporter expression (Fischer et al., 2011). Lastly, rather than scaling up the dosing concentrations to initiate a cellular response, this system has exposed cells to much more environmentally relevant and therefore realistic concentrations.

Here, the present study is the first to demonstrate how a primary gill cell system can be cultured (Schnell, Stott, et al., 2016) and used to assess the uptake and efflux (Stott et al., 2015) and metabolism (Stott et al., *in preparation*) of pharmaceuticals across and within an *in vitro* biological membrane, which can provide data that can complement BCF tests. Here, the more relevant morphological, physiological, transport and metabolic characteristics of primary gill cells when cultured using the DSI technique is shown (Schnell, Stott et al., 2016).
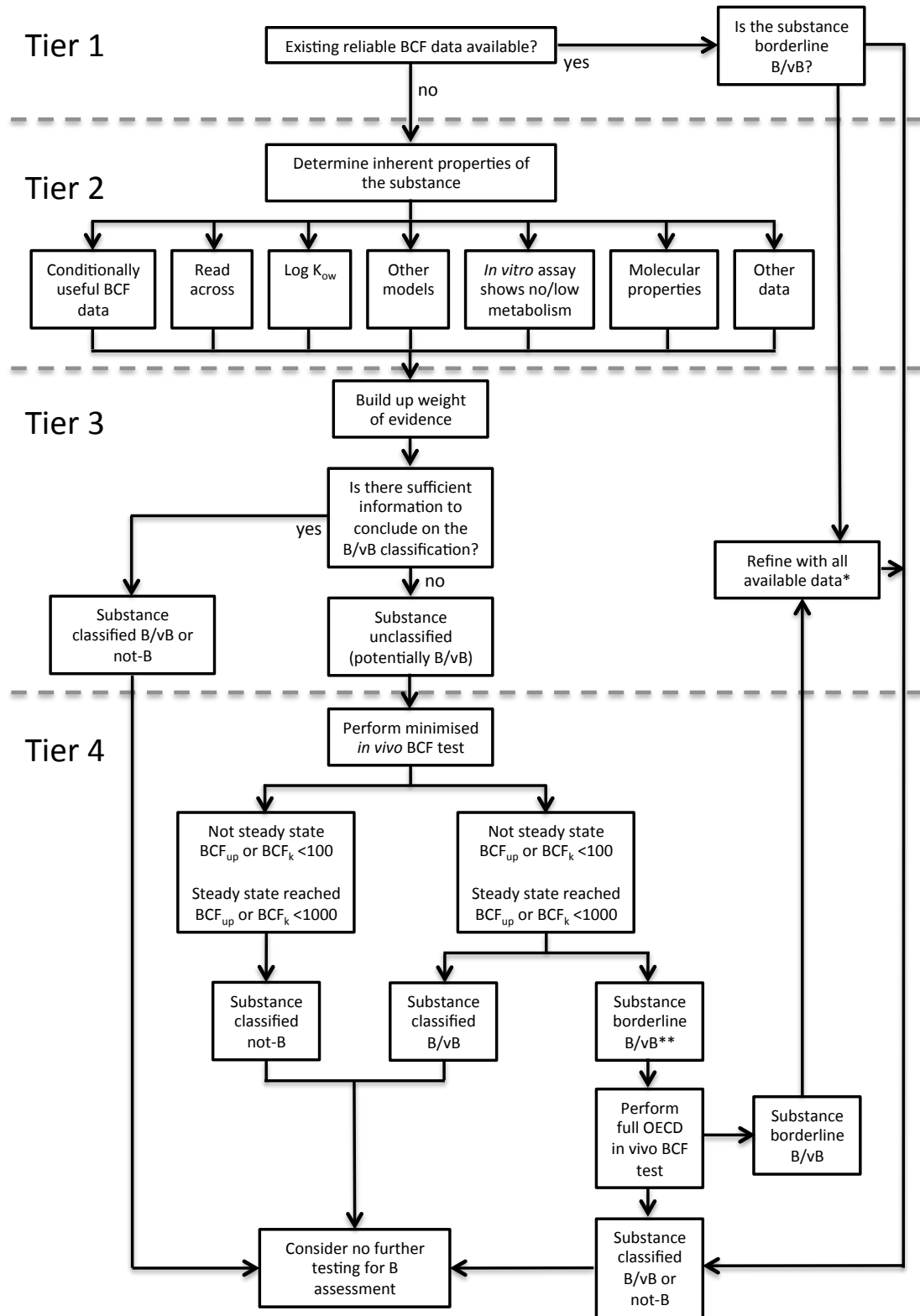
Fig 7.1 Proposed tiered assessment strategy for evaluating bioaccumulation data adapted from Lillicrap et al., 2016. (B: Bioaccumulative; vB: very Bioaccumulative. *A refined BCF could be considered if any data, such as is detailed in Tier 2, are available, ** a minimised test, with a BCF that is borderline B/vB could also be refined in Tier 3).

Primary gill DSI have the potential for many varied applications. Toxicity testing using different endpoints such as cell viability and transcriptomics will provide information on *in vivo* rainbow trout toxicity. Indeed, DSI expressed metallothionein, a protein that binds heavy metals, as a predictor of zinc and silver toxicity with similar sensitivity to that of *in vivo* (Walker et al., 2008). The primary DSI also have potential to be used as a biomonitoring tool, as freshwater collected from the environment can be directly added onto cells (Minghetti et al., 2014; Schnell et al., 2015) and the resulting cell viability and changes in transcription levels of responsive genes can be measured.

The use of this system is not limited to investigate pharmaceutical uptake, efflux and metabolism in freshwater fish. A range of contaminants with different modes of entry can be applied and could include dioxins, metals and polychlorinated biphenyls. Indeed, preliminary work has begun using this system to investigate the uptake and metabolism of a range of other classes of pharmaceuticals including warfarin, ibuprofen and gemfibrozil (Chang et al., *in preparation*).

What currently remains is the challenge of incorporating alternative assessment strategies like this into regulatory testing for evaluating bioaccumulation data. Lillicrap et al. (2016) propose a tiered assessment strategy that incorporates information for evaluating fish bioaccumulation data (Fig 7.1). In this way, they present guidance on how to build up a 'Weight of Evidence' in Tier 2, including using 'Read Across', and already existing BCF information and data generated from *in vitro* models, with the intention to bypass the need for so many tests using live fish. This work offers the preliminary validation of an alternative *in vitro* method that can be incorporated into Tier 2 to assess the bioconcentrative potential of compounds. Furthermore, this system shows the potential of compounds to be metabolised, and perhaps can so further when this system is used in combination with hepatic spheroids (Fig 7.2), and so it has the potential to offer a powerful tool to consider the major metabolic routes in a fish (Lillicrap et al., 2016).

Future directions

Tissue specific *in vitro* models provide a portion of information on the total metabolism of xenobiotics by an organism. Combining cells of different tissues from an organism and exposing to xenobiotics will provide a more accurate and detailed representation of the *in vivo* response and allow the 'crosstalk' of different cell types. The DSII system with the co-culture of liver spheroids (Fig 7.2A), as outlined in Chapter 3, has the potential to provide this information. In this way, there is scope for the co-culture of other epithelial tissues, such as the gut, using the same cell culture inverted technique, with liver spheroids (Fig 7.2B). This information gathered together can be collated together to produce a 'virtual fish' to predict the outcomes of ecotoxicological uptake, efflux and metabolism studies in live fish.
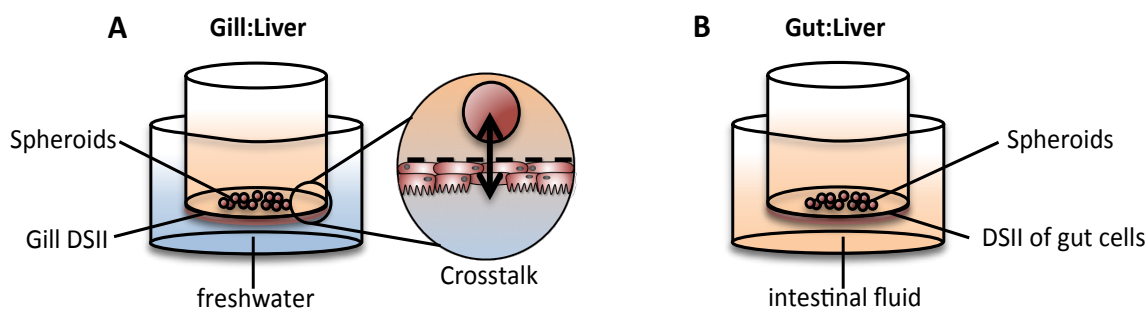
Fig 7.2 Development of the 'virtual fish' cellular models that combine cultures of different organs such as (A) gill DSII epithelia and liver spheroids and (B) gut DSII epithelia and liver spheroids.

VII. References

Abbott, N.J., Rönnbäck, L. & Hansson, E., 2006. Astrocyte-endothelial interactions at the blood-brain barrier. *Nature Reviews Neuroscience* 7; 41–53.

Altenberg, G.A., Young, G., Horton, J.K., Glass, D., Belli, J.A. & Reuss, L., 1993. Changes in intra- or extra-cellular pH do not mediate P-glycoprotein-dependent multidrug resistance. *Proceedings of the National Acadamy of Sciences* 90; 9735–38.

Andersson, T. & Förlin, L., 1992. Regulation of the cytochrome P450 enzyme system in fish. *Aquatic Toxicology* 24; 1–20.

Anzenbacher, P. & Anzenbacherová, E., 2001. Cytochromes P450 and metabolism of xenobiotics. *Cellular and Molecular Life Sciences* 58; 737–47.

Ashton, D., Hilton, M., Thomas, K.V., 2004. Investigating the environmental transport of human pharmaceuticals to streams in the United Kingdom. *Science of the Total Environment* 333; 167–84.

Aslamkhan, A.G., Thompson, D.M., Perry, J.L., Bleasby, K., Wolff, N.A., Barros, S., Miller, D.S. & Pritchard, J.B., 2006. The flounder organic anion transporter fOat has sequence, function, and substrate specificity similarity to both mammalian Oat1 and Oat3. *American Journal of Physiology – Regulatory, Integrative and Comparative Physiology* 291; 1773–80.

AstraZeneca, 2012. Environmental risk assessment data. http://www.astrazeneca.com/Responsibility/The-environment/Pharmaceuticals-in-the-environment/era-data-2012. Accessed 26th January 2015.

Bard, S., 2000. Multixenobiotic resistance as a cellular defense mechanism in aquatic organisms. *Aquatic Toxicology* 48(4); 357–89.

Baron, M.G., Purcell, W.M., Jackson, S.K., Owen, S.F. & Jha, A.N., 2012. Towards a more representative *in vitro* method for fish ecotoxicology: morphological and biochemical characterisation of three-dimensional spheroidal hepatocytes. *Ecotoxicology* 21(8); 2419–29.

Bartram, A.E., Winter, M.J., Huggett, D.B., McCormack, P., Constantine, L.A., Hetheridge, M.J., Hutchinson, T.H., Kinter, L.B., Ericson, J.F., Sumpter, J.P. & Owen, S.F., 2011. *In vivo* and *in vitro* liver and gill EROD activity in rainbow trout (*Oncorhynchus mykiss*) exposed to the beta-blocker propranolol. *Environmental Toxicology* 27(10); 573–82.

Bauer, H., Zweimueller-Mayer, J., Steinbacher, P., Lametschwandtner, A. & Bauer, H.C., 2010. The dual role of Zonula Occludens (ZO) proteins. *Journal of Biomedicine and Biotechnology* 2010; 1–11.

Bioparadigms, 2015. Genomic Transporter Database – SLC series, SLC tables. http://slc.bioparadigms.org/ Accessed 15th December 2015.

Black, J.W. & Stephenson, J.S., 1962. Pharmacology of a new adrenergic beta-receptor-blocking compound (Nethalide). *The Lancet* 280(7251); 311–14.

Bols, N., Barlain, A., Chirnio-Trejo, M., Caldwell, S.J., Goegan, P. & Lee, L.E.J., 1994. Development of a cell line from primary cultures of rainbow trout, *Oncorhynchus mykiss* (Walbaum), gills. *Journal of Fish Diseases* 17(6); 601–11.

Bols, N.C., Yang, B-Y., Lee, L.E.J., Chen, T.T., 1995. Development of a rainbow trout pituitary cell line that expresses growth hormone, prolactin, and somatolactin. *Molecular Marine Biology and Biotechnology* 4(2); 154–63.

Bols, N.C., Dayeh, V.R., Lee, L.E.J. & Schirmer, K., 2005. Use of fish cell lines in the toxicology and ecotoxicology of fish. Piscine cell lines in environmental toxicology. In *Biochemistry and Molecular Biology of Fishes, vol. 6* (Mommsen, T.P & Moon, T.W. Eds.). Elsevier Science, Amsterdam, Netherlands, pp. 43–84.

Boxall, A.B.A, Rudd, M., Brooks, B.W., Caldwell, D.J., Choi, K., Hickmann, S., Innes, E., Ostapyk, K., Staveley, J.P., Verslycke, T. Ankley, G.T., Beazley, K.F., Belanger, S.E., Berninger, J.P., Carriquiriborde, P., Coors, A., DeLeo, P.C., Dyer, S.D., Ericson, J.F., Gagné, F., Giesy, J.P., Gouin, T., Hallstrom, L., Karlsson, M.V., Larsson, D.G.J., Lazorchak, J.M., Mastrocco, F., McLaughlin, A., McMaster, M.E., Meyerhoff, R.D., Moore, R., Parrott, J.L., Snape, J.R., Murray-Smith, R., Servos, M.R., Sibley, P.K., Straub, J.O., Szabo, N.D., Topp, E., Tetreault, G.R., Trudeau, V.L. & and Van Der Kraak, G., 2012. Pharmaceuticals and personal care products in the environment: what are the big questions? *Environmental Health Perspectives* 120; 1221–29.

Breitholtz, M., Näslund, M., Stråe, D., Borg, H., Grabic, R. & Fick, J., 2012. An evaluation of free water surface wetlands as tertiary sewage water treatment of micro-pollutants. *Ecotoxicology & Environmental Safety* 78; 63–71.

Brozinski, J.M., Lahti, M., Meierjohann, A. Oikari, A. & Kronberg, L., 2013. The anti-inflammatory drugs diclofenac, naproxen and ibuprofen are found in the bile of wild fish caught downstream of a wastewater treatment plant. *Environmental Science and Toxicology* 47(1); 342–48.

Buhler, D. & Wang-Buhler, J., 1998. Rainbow trout cytochrome P450s: purification, molecular aspects, metabolic activity, induction and role in environmental monitoring. *Comparative Biochemistry and Physiology. Part C, Pharmacology, Toxicology & Endocrinology* 121; 107–37.

Burgess, D.W., Marshall, W.S. & Wood, C.M., 1998. Ionic transport by the opercular epithelia of freshwater acclimated tilapia (*Oreochromis niloticus*) and killifish (*Fundulus heteroclitus*). *Comparative Biochemistry and Physiology. Part A, Molecular and Integrative Physiology* 121; 155–64.

Burkina, V., Zlabek, V. & Zamaratskaia, G., 2013. Clotrimazole, but not dexamethasone, is a potent *in vitro* inhibitor of cytochrome P450 isoforms CYP1A and CYP3A in rainbow trout. *Chemosphere* 92(9); 1099–1104.

Bury, N.R. & Grosell, M., 2003. Waterborne iron acquisition by a freshwater teleost fish, zebrafish *Danio rerio*. *The Journal of Experimental Biology* 206(19); 3529–35.

Bury N.R., Schnell, S. & Hogstrand, C., 2014. Gill cell culture systems as models for aquatic environmental monitoring. *The Journal of Experimental Biology* 217(5); 639–50.

Carlsson, C., Pärt, P. & Brunström, B., 1999. 7-Ethoxyresorufin O-deethylase induction in cultured gill epithelial cells from rainbow trout. *Aquatic Toxicology* 47; 117–28.

Carlsson, C., Pärt, P., 2001. 7-Ethoxyresorufin O-deethylase induction in rainbow trout gill epithelium cultured on permeable supports: asymmetrical distribution of substrate metabolites. *Aquatic Toxicology* 54; 29–38.

Chasiotis, H., Wood, C. & Kelly, S., 2010. Cortisol reduces paracellular permeability and increases occludin abundance in cultured trout gill epithelia. *Molecular and Cellular Endocrinology* 323(2); 232–38.

Chasiotis, H. & Kelly, S., 2011. Effect of cortisol on permeability and tight junction protein transcript abundance in primary cultured gill epithelia from stenohaline goldfish and euryhaline trout. *General and Comparative Endocrinology* 172(3); 494–504.

Chasiotis, H., Kolosov, D., Bui, P. & Kelly, S.P., 2012. Tight junctions, tight junction proteins and paracellular permeability across the gill epithelium of fishes: A review. *Respiratory Physiology & Neurobiology* 184(3); 269–81.

Cole, S. & Deeley, R., 1998. Multidrug resistance mediated by the ATP-binding cassette transporter protein MRP. *BioEssays* 20(11); 931–40.

Connors, K., Du, B., Fitzsimmons, P.N., Hoffman, A.D., Chambliss, C.K. & Nichols, J.W. 2013. Comparative pharmaceutical metabolism by rainbow trout (*Oncorhynchus mykiss*) liver S9 fractions. *Environmental Toxicology and Chemistry* 32(8); 1810–18.

Creton, S., Weltje, L., Hobson, H. & Wheeler, J.R., 2013. Reducing the number of fish in bioconcentration studies for plant protection products by reducing the number of test concentrations. *Chemosphere* 90(3); 1300–04.

Daniel, H. & Kottra, G., 2004. The proton oligopeptide cotransporter family SLC15 in physiology and pharmacology. *Pflügers Archiv: European Journal of Physiology* 447; 610–18.

Daughton, C.G., & Brooks, B.W., 2011. Active pharmaceutical ingredients and aquatic organisms. In *Environmental Contaminants in Biota: Interpreting Tissue Concentrations*, 2nd ed. (Bayer, W.N., Meador, J.P., Eds.). Taylor and Francis, Boca Raton, FL, USA, pp. 287–347.

Daughton, C.G., & Ternes, T.A., 1999. Pharmaceuticals and personal care products in the environment: Agents of subtle change? *Environmental Health Perspectives* 107(6); 907–38.

Dayeh, V.R., Bols, N.C., Tanneberger, K., Schirmer, K. & Lee, L.E.J., 2013. The Use of fish-derived cell lines for investigation of environmental contaminants: an update following OECD's fish toxicity testing framework No. 171. *Current Protocols in Toxicology* 56; 1.5.1–1.5.20.

Dean, M. & Annilo, T., 2005. Evolution of the ATP-binding cassette (ABC) transporter superfamily in vertebrates. *Annual Review of Genomics and Human Genetics* 6; 123–42.

Dean, M., Rzhetsky, A. & Allikmets, R., 2001. The human ATP-binding cassette (ABC) transporter superfamily. *Genome Research* 11; 1156–66.

Deeley, R.G., Westlake, C. & Cole, S.P.C., 2006. Transmembrane transport of endo- and exo-xenobiotics by mammalian ATP-binding cassette multidrug resistance proteins. *Physiological Review* 86; 849–99.

Dehouck, M.P., Méresse, S., Delorme, P., Fruchart, J.-C. & Cecchelli, R., 1990. An easier, reproducible, and mass-production method to study the blood-brain barrier *in vitro*. *Journal of Neurochemistry* 54(5); 1798–1801.

Dickman, K.G., Hempson, S.J., Anderson, J., Lippe, S., Zhau, L., Burakoff, R. & Shaw, R., 2000. Rotavirus alters paracellular permeability and energy metabolism in Caco-2 cells. *American Journal of Physiology – Gastrointestinal Liver Physiology* 279; 757–66.

Ding, J., Lu, G., Li, S., Nie, Y. & Liu, J., 2015. Biological fate and effects of propranolol in an experimental aquatic food chain. *Science of the Total Environment* 53; 31–39.

Dobson, P. & Kell, D., 2008. Carrier-mediated cellular uptake of pharmaceutical drugs: an exception or the rule? *Nature Reviews Drug Discovery* 7; 205–20.

Dudley, A.J., Bleasby, K. & Brown, C.D., 2000. The organic cation transporter OCT2 mediates the uptake of beta-adrenoceptor antagonists across the apical membrane of renal LLC-PK1 cell monolayers. British Journal of Pharmacology 131(1); 71–9.

EU, 2013. Commission Regulation (EU) No 283/2013 of 1 March 2013 setting out the data requirements for active substances, in accordance with Regulation (EC) No 1107/2009 of the European Parliament and of the Council concerning the placing of plant protection products on the market. OJ. European Union L93, 1– 84.

EU, 2012. Regulation (EU) No 528/2012 of the European Parliament and of the Council of 22 May 2012 concerning the making available on the market and use of biocidal products. OJ. European Union L761, 1– 123.

EMEA, 2006. European Agency for the Evaluation of Medicinal Products. Guideline on the environmental risk assessment of medicinal products for human use. http://www. emea.europa.eu/pdfs/human/swp/444700en.pdf. Accessed 18th December 2015.

Evans, H.H., Piermarini, P.M. & Choe, K.P., 2005. The multifunctional fish gill: dominant site of gas exchange, osmoregulation, acid-Base regulation, and excretion of nitrogenous waste. *Physiological Review* 85; 97–177.

Ferreira-Leach, A.M.R. & Hill, E.M., 2001. Bioconcentration and distribution of 4-*tert*-octylphenol residues in tissues of the rainbow trout (*Oncorhynchus mykiss*). *Marine Environmental Research* 51; 75–89.

Fischer, S., Pietsch, M., Schirmer, K. & Luckenback, T., 2010. Identification of multi-drug resistance associated proteins MRP1 (ABCC1) and MRP3 (ABCC3) from rainbow trout (*Oncorhynchus mykiss*). *Marine Environmental Research* 69; S7–S10.

Fischer, S., Lončar, J., Zaja, R., Schnell, S., Schirmer, K., Smital, T. & Luckenbach, T., 2011. Constitutive mRNA expression and protein activity levels of nine ABC efflux transporters in seven permanent cell lines derived from different tissues of rainbow trout (*Oncorhynchus mykiss*). *Aquatic Toxicology* 101; 438–46.

Fitzsimmons, P.N., Fernandez, J.D., Hoffman, A.D., Butterworth, B.C. & Nichols, J.W., 2001. Branchial elimination of superhydrophobic organic compounds by rainbow trout (*Oncorhynchus mykiss*). *Aquatic Toxicology* 55; 23–34.

Fletcher, M., Kelly, S.P., Pãrt, P., O'Donnell, M.J. & Wood, C., 2000. Transport properties of cultured branchial epithelia from freshwater rainbow trout: a novel preparation with mitochondria-rich cells. *The Journal of Experimental Biology* 203; 1523–37.

Förlin, L. & Haux, C., 1985. Increased excretion in the bile of 17β-[^{3}H]estradiol-derived radioactivity in rainbow trout treated with β-naphthoflavone. *Aquatic Toxicology* 6; 197–208.

Galinis-Luciani, D., Nguyen, L. & Yazdanian, M., 2007. Is PAMPA a useful tool for discovery? *Journal of Pharmaceutical Sciences* 96(11); 2886–92.

Gaillard, P.J., Voorwinden, L.H., Nielsen, J.L., Ivanov, A., Atsumi, R., Engman, H., Ringbom, C., de Boer, A.G., Breimer, D.D., 2001. Establishment and functional characterization of an *in vitro* model of the blood–brain barrier, comprising a co-culture of brain capillary endothelial cells and astrocytes. *European Journal of Pharmaceutical Sciences* 12; 215–222.

Ganassin, R.C. & Bols, N.C., 1997. Development and growth of cell lines from fish: rainbow trout *Oncorhynchus mykiss.* In *Cell & Tissue Culture: Laboratory Procedures* (Griffiths, J.J., Doyle, A., & Newell D.G., Eds.). John Wiley & Sons Limited, Wiltshire, UK, pp. 1.1–1.9.

Ganassin, R.C. & Bols, N.C., 1998. Development of a monocyte/macrophage-like cell line, RTS11, from rainbow trout spleen. *Fish and Shellfish Immunology* 8; 457–476.

Giacomini, K.M., Huang, S., Tweedie, D.J., Benet, L.Z., Brouwer, K.L.R., Chu, X., Dahlin, A., Evers, R., Fischer, V., Hillgren, K.M. Hoffmaster, K.A., Ishikawa, T., Keppler, D., Kim, R.B., Lee, C.A., Niemi, M., Polli, J.W., Sugiyama, Y., Swaan, P.W., Ware, J.A., Wright, S.H., Wah Yee, S., Zamek-Gliszczynski, M.J & Zhang, L., 2010. Membrane transporters in drug development. *Nature Reviews Drug Discovery* 9; 215–36.

Giebułtowicz, J. & Nałęcz-Jawecki, G., 2014. Occurrence of antidepressant residues in the sewage-impacted Vistula and Utrata rivers and in tap water in Warsaw (Poland). *Ecotoxicology and Environmental Safety* 104; 103–109.

Gobas, F.A.P.C., 1993. A model for predicting the bioaccumulation of hydrophobic organic chemicals in aquatic food-webs: application to Lake Ontario. *Ecological Modelling* 69; 1–17.

Gomez, C.F., Constantine, L. & Huggett, D.B., 2010. The influence of gill and liver metabolism on the predicted bioconcentration of three pharmaceuticals in fish. *Chemosphere* 81; 1189–95.

Gomez, C.F., Constantine, L., Moen, M., Vaz, A. Wang, W. & Huggett, D.B., 2011. Ibuprofen metabolism in the liver and gill of rainbow trout, *Oncorhynchus mykiss*. *Bulletin of Environmental Contamination and Toxicology* 86(3); 247–51.

González-Mariscal, L., Betanzos, A., Nava, P. & Jaramillo, B.E., 2003. Tight junction proteins. *Progress in Biophysics and Molecular Biology* 81; 1–44.

Gov.UK, 2014. New plan will work to reduce use of animals in research. https://www.gov.uk/government/news/new-plan-will-work-to-reduce-use-of-animals-in-research. Accessed 18th May 2016.

Gunnarsson, L., Jauhiainen, A., Kristiansson, E., Nerman, O. & Larsson, D.G.J., 2008. Evolutionary conservation of human drug targets in organisms used for environmental risk assessments. *Environmental Science & Technology* 42(15); 5807–13.

Hagenbuch, B. & Meier, P.J., 2003. Organic anion transporting polypeptides of the OATP/SLC21 family: phylogenetic classification as OATP/SLCO superfamily, new nomenclature and molecular/functional properties. *Pflügers Archiv: European Journal of Physiology* 447; 653–65.

Hansch, C., Hoekman, D., Leo, A., Zhang, L. & Li, P., 1995. The expanding role of quantitative structure-activity relationships (QSAR) in toxicology. *Toxicology Letters* 79; 45–53.

Hasselberg, L., Westerberg, S., Wassmur, B. & Celander, M.C., 2008. Ketoconazole, an antifungal imidazole, increases the sensitivity of rainbow trout to 17alpha-ethynylestradiol exposure. *Aquatic Toxicology* 86; 256–64.

Hediger, M.A., Romero, M.F., Peng, J., Rolfs, A., Takanaga, H. & Bruford, E.A., 2004. The ABCs of solute carriers: physiological, pathological and therapeutic implications of human membrane transport proteins. *European Journal of Physiology* 447; 465–8.

Hermens, J.L.M., de Bruijn, J.H.M. & Brooke, D.N., 2013. The octanol-water partition coefficient: strengths and limitations. *Environmental Toxicology and Chemistry* 32(4); 732–3.

Hilton, M.J., Thomas, K.V. & Ashton, D., 2003. Targeted monitoring programme for pharmaceuticals in the aquatic environment. R&D Technical Report P6-012/06/TR, Environment Agency, Bristol, U.K.

Home Office, 1986. The Humane Killing of Animals under Schedule 1 to the Animals (Scientific Procedures) Act 1986 – Code of Practice, 1997. https://www.gov.uk/government/uploads/system /uploads/attachment_data/file/229022/0193.pdf. Accessed 9th May 2016.

Hubatsch, I., Ragnarsson, E.G.E. & Artursson, P., 2007. Determination of drug permeability and prediction of drug absorption in Caco-2 monolayers. *Nature Protocols* 2(9); 2111–9.

Huggett, D., Cook, J.C., Ericson, J.F. & Williams, R.T., 2003. A theoretical model for utilizing mammalian pharmacology and safety data to prioritize potential impacts of human pharmaceuticals to fish. *Human and Ecological Risk Assessment* 9; 1789–99.

Hurst, R.D. & Fritz, I.B., 1996. Properties of an immortalised vascular endothelial/glioma cell co-culture model of the blood-brain barrier. *Journal of Cell Physiology* 167; 81–88.

Irvine, J.D., Takahashi, L., Lockhart, K., Cheong, J., Tolan, J.W., Selick, H.E. & Grove, J.R., 1999. MDCK (Madin-Darby canine kidney) cells: A tool for membrane permeability screening. *Journal of Pharmaceutical Sciences* 88; 28–33.

Jobling, M., 1995. Osmotic and ionic regulation – water and salt balance. In *Environmental Biology of Fishes* 2nd ed. (Jobling, M., ed.). Chapman & Hall, London, UK, pp. 211–49.

Johnson, A.C., Keller, V., Williams, R.J. & Young, A., 2007. A practical demonstration in modelling diclofenac and propranolol river water concentrations using a GIS hydrology model in a rural UK catchment. *Environmental Pollution* 146; 155–65.

Jönsson, E.M., Brandt, I. & Brunström, B., 2002. Gill filament-based EROD assay for monitoring waterborne dioxin-like pollutants in fish. *Environmental Science & Technology* 36(15); 3340–44.

Kawano, A., Haiduk, C., Schirmer, K., Hanner, R., Lee, L.E.J., Dixon, B. & Bols, N.C., 2011. Development of a rainbow trout intestinal epithelial cell line and its response to lipopolysaccharide. *Aquatic Nutrition* 17; e241–52.

Kelly, S.P., Fletcher, M., Pärt, P. & Wood. C.M., 2000. Procedures for the preparation and culture of 'reconstructed' rainbow trout branchial epithelia. *Methods in Cell Science* 22; 153–63.

Kelly, S.P. & Wood, C.M., 2001. Effect of cortisol on the physiology of cultured pavement cell epithelia from freshwater trout gills. *American Journal of Physiology – Regulatory, Integrative and Comparative Physiology* 281; R811–20.

Keys, A. & Willmer, E.N., 1932. "Chloride secreting cells" in the gills of fishes, with special reference to the common eel. *Journal of Fish Physiology* 73; 368–78.

Khetan, S.K. & Collins, T.J., 2007. Human pharmaceuticals in the aquatic environment: a challenge to green chemistry. *Chemical Reviews* 107; 2319–64.

Koepsell, H. & Endou, H., 2004. The SLC22 drug transporter family. *Pflügers Archiv: European Journal of Physiology* 447; 666–76.

Koepsell, H., 2013. The SLC22 family with transporters of organic cations, anions and zwitterions. *Molecular Aspects of Medicine* 34(2-3); 413–35.

Kostich, M.S., Batt, A.L. & Lazorchak, J.M., 2014. Concentrations of prioritized pharmaceuticals in effluent from 50 large wastewater treatment plants in the US and implications for risk estimation. *Environmental Pollution* 184; 354–359.

Kramer, N.I., Busser, F.J.M., Oosterwijk, M.T.T., Schirmer, K., Escher, B.I. & Hermens, J.L.M., 2010. Development of a partition-controlled dosing system for cell assays. *Chemical Research in Toxicology* 23(11); 1806–14.

Kubo, Y., Shimizu, Y., Kusagawa, Y., Akanuma, S.-I. & Hosoya, K.-I., 2013. Propranolol transport across the inner blood-retina barrier: potential involvement of a novel organic cation transporter. *Journal of Pharmaceutical Sciences* 102(9); 3332–3342.

Kümmerer, K., 2008. Pharmaceuticals in the environment – a brief summary. In *Pharmaceuticals in the Environment: Sources, Fate, Effects and Risks* (Kümmerer, K. Ed.)*.* Springer-Verlag Berlin Heidelberg, pp. 3–21.

Kurelec, B., 1992. The multixenobiotic resistance mechanism in aquatic organisms. *Critical Reviews in Toxicology* 22(1); 23–43.

Lahti, M., Brozinski, J.-M., Jylhä, A., Kronberg, L. & Oikari, A., 2011. Uptake from water, biotransformation, and biliary excretion of pharmaceuticals by Rainbow Trout. *Environmental Toxicology and Chemistry* 30(6); 1403–11.

Lajeunesse, A., Gagnon, C., Gagné, F., Louis, S., Čejka, P. & Sauvé, S., 2011. Distribution of antidepressants and their metabolites in brook trout exposed to municipal wastewaters before and after ozone treatment - evidence of biological effects. *Chemosphere* 83(4); 564–71.

Laurent, P. & Perry, S., 1991. Environmental effects on fish gill morphology. *Physiological Zoology* 64(1); 4–25.

Laville, N., Aït-Aïssa, S., Gomez, E., Casellas, C. & Porcher, J.M., 2004. Effects of human pharmaceuticals on cytotoxicity, EROD activity and ROS production in fish hepatocytes. *Toxicology* 196; 41–55.

Lee, L.E.J., Clemons, J.H., Bechtel, D.G., Caldwell, S.J., Han, K.B., Pasitschniak-Arts, M., Mosser, D.D. & Bols, N.C., 1993. Development and characterization of a rainbow trout liver cell line expressing cytochrome P450-dependent monooxygenase activity. Cell Biology and Toxicology 9(3); 279–294.

Lee, L.E.J., Van Es, S.J., Walsh, S.K., Rainnie, D.J., Donay, N., Summerfield, R., Cawthorn, R.J., 2006. High yield and rapid growth of *Neoparamoeba pemaquidensis* in co-culture with a rainbow trout gill derived cell line RTgill-W1. *Journal of Fish Diseases* 29(8); 467–80.

Lee, L.E.J., Dayeh, V.R., Schirmer, K. & Bols, N.C., 2009. Applications and potential uses of fish gill cell lines: examples with RTgill-W1. *In Vitro Cellular & Developmental Biology – Animal* 45; 127–34.

Leguen, I., Carlsson, C., Perdu-Durand, E., Prunet, P., Pärt, P. & Cravedi, J.P., 2000. Xenobiotic and steroid biotransformation activities in rainbow trout gill epithelial cells in culture. *Aquatic Toxicology* 48; 165–76.

Leguen, I., Cravedi, J.P., Pisam, M. & Prunet, P., 2001. Biological functions of trout pavement-like gill cells in primary culture on solid support: pH$_i$ regulation, cell volume regulation and xenobiotic

biotransformation. *Comparative Biochemistry and Physiology. Part A, Molecular & Integrative Physiology* 128(2); 207–22.

Leguen, I., Cauty, C., Odjo, N., Corlu, A. & Prunet, P., 2007. Trout gill cells in primary culture on solid and permeable supports. *Comparative Biochemistry and Physiology. Part A, Molecular & Integrative Physiology* 148; 903–12.

Leist, M., Hasiwa, N., Daneshian, M. & Hartung, T., 2012. Validation and quality control of replacement alternatives – current status and future challenges. *Toxicology Research* 1; 8–22.

Leslie, E.M., Deeley, R.G. & Cole, S.P.C., 2005. Multidrug resistance proteins: role of P-glycoprotein, MRP1, MRP2, and BCRP (ABCG2) in tissue defense. *Toxicology and Applied Pharmacology* 204(3); 216–37.

Levien, T.L. & Baker, D.E., 2003. Cytochrome P450 drug interactions. *Pharmacist's letter* Document #150400; 1–4.

Lillicrap, A., Springer, T. & Tyler, C.R., 2016. A tiered assessment strategy for more effective evaluation of bioaccumulation of chemicals in fish. *Regulatory Toxicology and Pharmacology* 75, 20–26.

Lindström-Seppä, P. & Oikari, A., 1990. Biotransformation and other toxicological and physiological responses in rainbow trout (*Salmo gairdneri* Richardson) caged in a lake receiving effluents of pulp and paper industry. *Aquatic Toxicology* 16; 187–204.

Lončar, J., Popović, M., Zaja, R. & Smital, T., 2010. Gene expression analysis of the ABC efflux transporters in Rainbow Trout (*Oncorhynchus mykiss*). *Comparative Biochemistry and Physiology. Part C, Pharmacology, Toxicology & Endocrinology* 151(2), 209–15.

Luckenbach, T. & Epel, D., 2008. ABCB- and ABCC-type transporters confer multixenobiotic resistance and form an environment-tissue barrier in bivalve gills. *American Journal of Physiology – Regulatory, Integrative and Comparative Physiology* 294(6); R1919–29.

Luckenbach, T., Fischer, S. & Sturm, A., 2014. Current advances on ABC drug transporters in fish. *Comparative Biochemistry and Physiology. Part C, Pharmacology, Toxicology & Endocrinology* 165, 28–32.

Luna-Tortós, C., Fedrowitz, M. & Löscher, W., 2008. Several major antiepileptic drugs are substrates for human P-glycoprotein. *Neuropharmacology* 55(8); 1364–75.

Madigou, T., Mañanos-Sanchez, E., Hulshof, S., Anglade, I., Zanuy, S. & Kah, O., 2000. Cloning, tissue distribution, and central expression of the gonadotropin-releasing hormone receptor in the rainbow trout (*Oncorhynchus mykiss*). *Biology of Reproduction* 63; 1857–66.

Masubuchi, Y., Hosokawa, S., Horie, T., Suzuki, T., Ohmori, S., Kitada, M. & Narimatsu, S., 1994. Cytochrome P450 isozymes involved in propranolol metabolism in human liver microsomes. *The American Journal for Pharmacology and Experimental Therapeutics* 22(6); 909–15.

McDonald, M.D & Wood, C.M, 2004. Evidence for facilitated diffusion of urea across the gill basolateral membrane of the rainbow trout (*Oncorhynchus mykiss*). *Biochimica et Biophysica Acta* 1663; 89–96.

McKim, J.M. & Erickson, R.J., 1991. Environmental impacts on the physiological mechanisms controlling xenobiotic transfer across fish gills. *Physiological Zoology* 64(1); 39–67.

Mehvar, R. & Brocks, D.R., 2001. Stereospecific pharmacokinetics and pharmacodynamics of beta-adrenergic blockers in humans. *Journal of Pharmacy & Pharmaceutical Sciences* 4(2); 185–200.

Meunier, B., de Visser, S.P & Shaik, S., 2004. Mechanism of oxidation reactions catalyzed by Cytochrome P450 enzymes. *Chemical Reviews* 104(9); 3947–80.

Miki, Y., Ono, K., Hata, S., Suzuki, T., Kumamoto, H. & Sasano, H., 2012. The advantages of co-culture over mono cell culture in simulating *in vivo* environment. *Journal of Steroid Biochemistry and Molecular Biology* 131; 68–75.

Minghetti, M., Schnell, S., Chadwick, M., Hogstrand, C. & Bury, N.R., 2014. A primary FIsh Gill Cell System (FIGCS) for environmental monitoring of river waters. *Aquatic Toxicology* 154; 184–92.

Murer, H. & Kinne, R., 1980. The use of isolated membrane vesicles to study epithelial transport processes. *The Journal of Membrane Biology* 55; 81–95.

Neuhoff, S., Ungell, A.L., Zamora, I. & Artursson, P., 2003. pH-dependent bidirectional transport of weakly basic drugs across Caco-2 monolayers: Implications for drug-drug interactions. *Pharmaceutical Research* 20; 1141–1148.

Nichols, J.W., Hoffman, A.D. & Fitzsimmons, P.N., 2009. Optimization of an isolated perfused rainbow trout liver model: Clearance studies with 7-ethoxycoumarin. *Aquatic Toxicology* 95; 182–94.

Nickerson, J.G, Dugan, S.G., Drouin, G. & Moon, T.W., 2001. A putative β2-adrenoceptor from the rainbow trout (*Oncorhynuchus mykiss*). *European Journal of Biochemistry* 268(24); 6465–72.

OECD, 2012. Fish Toxicity Testing Framework. *OECD Environment, Health and Safety Publications Series on Testing and Assessment* No. 171.

OECD$_{107}$, 1995. Test No. 107. Partition Coefficient (n-octanol/water): Shake Flask Method. OECD Guidelines for the Testing of Chemicals Section 1: Physical Chemical Properties. OECD Publishing.

OECD$_{223}$, 2010. Test No. Avian Acute Oral Toxicity Test. OECD Guidelines for the Testing of Chemicals Section 2:Effects on Biotic Systems. OECD Publishing.

OECD$_{305}$, 2012. Test No. 305. Bioaccumulation in Fish: Aqueous and Dietary Exposure. OECD Guidelines for the Testing of Chemicals Section 3: Degradation and Accumulation. OECD Publishing.

Otsuka, M., Matsumoto, T., Morimoto, R., Arioka, S., Omote, H. & Moriyama, Y., 2005. A human transporter protein that mediates the final excretion step for toxic cations. *Proceedings of the National Academy of Sciences of the United States of America* 102(50); 17923–28.

Owen, S.F, Giltrow, E., Huggett, D.B., Hutchinson, T.H., Saye, J. & Winter, M.J., 2007. Comparative physiology, pharmacology and toxicology of β-blockers: mammals versus fish. *Aquatic Toxicology* 82(3); 145–62.

Owen, S.F., Huggett, D.B., Hutchinson, T.H., Hetheridge, M.J., Kinter, L.B., Ericson, J.F. & Sumpter, J.P., 2009. Uptake of propranolol, a cardiovascular pharmaceutical, from water into fish plasma and its effects on growth and organ biometry. *Aquatic Toxicology* 93(4), 217–24.

Pärt, P., Norrgren, L., Bergström, E. & Sjöberg, P., 1993. Primary cultures of epithelial cells from rainbow trout gills. *Journal of Experimental Biology* 175; 219–32.

Penrice, W.S. & Eddy, F.B., 1993. Spatial arrangement of fish gill secondary lamellar cells in intact and dissociated tissues from rainbow trout (*Onchorhynchus mykiss*) and Atlantic salmon (*Salmo salar*). *The Journal of Fish Biology* 42; 845–50.

Perry, S.F., 1997. The chloride cell: structure and function in the gills of freshwater fishes. *Annual Review of Physiology* 59; 325–47.

Petri, N., Tannergren, C., Rungstad, D. & Lennernäs, H., 2004. Transport characteristics of fexofenadine in the Caco-2 cell model. *Pharmaceutical Research* 21(8); 1398–404.

Popovic, M., Zaja, R. & Smital, T., 2010. Organic anion transporting polypeptides (OATP) in zebrafish (*Danio rerio*): Phylogenetic analysis and tissue distribution. *Comparative Biochemistry and Physiology. Part A, Molecular and Integrative Physiology* 155(33); 327–35.

Potts, W.T.W., 1984. Transepithelial potentials in fish gills. In *Fish Physiology, vol. 6, Gills, part B, Ion and Water Transfer* (Hoar, W.S. & Randall, D.J., Eds.). Orlando Academic Press, pp. 105–128.

Rand-Weaver, M., Margiotta-Casaluci, L., Patel, A., Panter, G.H., Owen, S.F. & Sumpter, J.P., 2013. The read-across hypothesis and environmental risk assessment of pharmaceuticals. *Environmental Science & Technology* 47(20); 11384–95.

REACH, 2009. Regulation (EC) No 1907/2006 of the European Parliament and of the Council of 18 December 2006. Legislation concerning the registration, evaluation, authorisation and restriction of chemicals. http://eurlex.europa.eu/LexUriServ/LexUri Serv.do?uri=OJ:L:2009:309:00010050:EN: PDF. Accessed 18th June 2015.

Romano, A., Amilcare, B., Storelli, C. & Verri, T., 2014. Teleost fish models in membrane transport research: the PEPT1 (SLC15A1) H^{+}-oligopeptide transporter as a case study. *Journal of Physiology* 592(5); 881–97.

Sandbichler, A.M., Egg, M., Schwerte, T. & Pelster, B., 2011a. Claudin 28b and F-actin are involved in rainbow trout gill pavement cell tight junction remodeling under osmotic stress. *Journal of Experimental Biology* 214; 1473–87.

Sandbichler, A.M., Farkas, J. Salvenmoser, W., Pelster, B., 2011b. Cortisol affects tight junction morphology between pavement cells of rainbow trout gills in single-seeded insert culture. *Journal of Comparative Physiology* 181(8); 1023–34.

Santaguida, S., Janigro, D., Hossain, M., Oby, E., Rapp, E. & Cucullo, L., 2006. Side by side comparison between dynamic versus static models of blood-brain barrier *in vitro*: a permeability study. *Brain Research* 1109; 1–13.

Schirmer, K., Dixon, D.G., Greenberg, B.M. & Bols, N.C., 1998. Ability of 16 priority PAHs to be directly cytotoxic to a cell line from the rainbow trout gill. *Toxicology* 127; 129–41.

Schirmer, K., 2006. Proposal to improve vertebrate cell cultures to establish them as substitutes for the regulatory testing of chemicals and effluents using fish. *Toxicology* 224(3); 163–83.

Schnell, S., Stott L.C., Hogstrand, C., Wood, C.M., Kelly, S.P., Pärt, P., Owen, S.F. & Bury, N.R., 2016. Procedures for the reconstruction, primary culture and experimental use of rainbow trout gill epithelia. *Nature Protocols* 11; 490–98.

Schnell, S., Bawa-Allah, K., Otitoloju, A., Hogstrand, C., Miller, T.H., Barron, L.P. & Bury, N.R., 2015. Environmental monitoring of urban streams using a primary fish gill cell culture system (FIGCS). *Ecotoxicology and Environmental Safety* 120; 279–85.

Scholz, S., Sela, E., Blaha, L., Braunbeck, T., Galay-Burgos, M., García-Franco, M., Guinea, J., Klüver, N., Schirmer, K., Tanneberger, K., Tobor-Kapłon, M., Witters, H., Belanger, S., Benfenati, E., Creton, S., Cronin, M.T.D., Eggen, R.I.L., Embry, M., Ekman, D., Gourmelon, A., Halder, M., Hardy, B., Hartung, T., Hubesch, B., Jungmann, D., Lampi, M.A., Lee, L., Léonard, M., Küster, E., Lillicrap, A., Luckenbach, T., Murk, A.J., Navas, J.M., Peijnenburg, W., Repetto, G., Salinas, E., Schüürmann, G., Spielmann, H., Tollefsen, K.E., Walter-Rohde, S., Whale, G., Wheeler, J.R. & Winter, M.J., 2013. A European perspective on alternatives to animal testing for environmental hazard identification and risk assessment. *Regulatory Toxicology and Pharmacol*ogy 67; 506–30.

Schreiber, R., Gündel, U., Franz, S., Küster, A., Rechenberg, B. & Altenburger, R., 2011. Using the fish plasma model for comparative hazard identification for pharmaceuticals in the environment by extrapolation from human therapeutic data. Regulatory Toxicology and Pharmacology 61; 261–75.

Schwab, D., Fischer, H., Tabatabaei, A., Poli, S. & Huwyler, J., 2003. Comparison of *in vitro* P-glycoprotein screening assays: recommendations for their use in drug discovery. *Journal of Medicinal Chemistry* 46(9); 1716–25.

Shah, P.J., Jogania, V.V., Mishrab, P., Mishrab, A.K., Bagchic, T. & Misraa, A.R., 2007. Role of 99mTc-mannitol and 99mTc-PEG in the assessment of paracellular integrity of cell monolayers. *Nuclear Medicine Communications* 28(8); 653–9.

Shrivastava, A. & Gupta, V.B. 2011. Methods for the determination of limit of detection and limit of quantification of the analytical methods. *Chronicles of Young Scientists* 2; 21–25.

Stadnicka-Michalak, J., Tanneberger, K., Schirmer, K. & Ashauer, R., 2014. Measured and modeled toxicokinetics in cultured fish cells and application to *in vitro - in vivo* toxicity extrapolation. *PloS one* 9(3); e92303.

Stadnicka-Michalak, J., Schirmer, K. & Ashauer, R., 2015. Toxicology across scales: Cell population growth *in vitro* predicts reduced fish growth. *Science Advances* 1:e1500302.

Statham, C.N., Melancon Jr, M.J. & Lech, J.J., 1976. Bioconcentration of xenobiotics in trout bile: a proposed monitoring aid for some waterborne chemicals. *Science* 193(4254); 680–81.

Stott, L.C., Schnell, S., Hogstrand, C., Owen, S.F. & Bury, N.R., 2015. A primary fish gill cell culture model to assess pharmaceutical uptake and efflux: Evidence for passive and facilitated transport. *Aquatic Toxicology* 159; 127–37.

Sturm, A., Ziemann, C., Hirsch-Ernst, K.I. & Segner, H., 2001. Expression and functional activity of P-glycoprotein in cultured hepatocytes from *Oncorhynchus mykiss*. *American Journal of Physiology – Regulatory, Integrative and Comparative Physiology* 281(4); 1119–26.

Sturm, A. & Segner, H., 2005. P-glycoproteins and xenobiotic efflux transport in fish. *Biochemistry and Molecular Biology of Fishes* 6; 495–534.

Sugano, K., Kansy, M., Artursson, P., Avdeef, A., Bendels, S., Di, L., Ecker, G. F., Faller, B., Fischer, H., Gerebtzoff, G., Lennernaes, H. & Senner, F., 2010. Coexistence of passive and carrier-mediated processes in drug transport. *Nature Reviews Drug Discovery* 9(8); 597–614.

Sumpter, J.P. & Jobling, S., 2012. The occurrence, causes, and consequences of estrogens in the aquatic environment. *Environmental Toxicology and Chemistry* 32(2); 249–51.

Takara, K., Sakaeda, T. & Okumura, K., 2006. An Update on Overcoming MDR1-Mediated Multidrug Resistance in Cancer Chemotherapy. *Current Pharmaceutical Design* 12(3); 276–86.

Tassaneeyakul, W., Birkett, D.J., Veronese, M.E., McManus, M.E., Tukey, R.H., Quattrochi, L.C., Gelboin, H.V. & Miners, J.O. 1993. Specificity of substrate and inhibitor probes for human cytochromes P450 1A1 and 1A2. *Journal of Pharmacology & Experimental Therapeutics* 265 (1); 401–407.

Tanneberger, K., Knöbel, M., Busser, F.J.M., Sinnige, T.L., Hermens, J.L.M. & Schirmer, K., 2013. Predicting fish acute toxicity using a fish gill cell line-based toxicity assay. *Environmental Toxicology and Chemistry* 47; 1110–19.

Tetko, I.V., Gasteiger, J., Todeschini, R., Mauri, A., Livingstone, D., Ertl, P., Palyulin, V.A., Radchenko, E.V., Zefirov, N.S., Makarenko, A.S., Tanchuk, V.Y. & Prokopenko, V.V., 2005. Virtual computational chemistry laboratory - design and description. *Journal of Computor-Aided Molecular Design* 19; 453–63.

Thibaut, R., Schnell, S. & Porte, C., 2006. The interference of pharmaceuticals with endogenous and xenobiotic metabolizing enzymes in carp liver: an *in-vitro* study. *Environmental Science and Technology* 40(16); 5154–60.

Thomas, A.J., Hailey, D.W., Stawicki, T.M., Wu, P., Coffin, A.B., Rubel, E.W., Raible, D.W., Simon, J.A. & Ou, H.C., 2013. Functional mechanotransduction is required for cisplatin-induced hair cell death in the zebrafish lateral line. *Journal of Neuroscience* 33(10), 4405–14.

Thomas, M.A. & Klaper, R.D., 2012. Psychoactive pharmaceuticals induce fish gene expression profiles associated with human idiopathic autism. *PLoS ONE* 7(6); e32917.

Timbrell, J., 2000. Factors Affecting Toxic Responses: Metabolism. In *Principles of biochemical toxicology,* 3rd ed. (Timbrell, J. Ed.) Taylor & Francis, London, UK, pp. 65–110.

Togunde, O.P., Oakes, K.D., Servos, M.R. & Pawliszyn, J., 2012. Determination of pharmaceutical residues in fish bile by solid-phase microextraction couple with liquid chromatography-tandem mass spectrometry (LC/MS/MS). *Environmental Science and Technology* 46(10); 5302–09.

Tom, D.J., Lee, L.E.J., Lew, J. & Bols, N.C. 2001. Induction of 7-ethoxyresorufin-*O*-deethylase activity by planar chlorinated hydrocarbons and polycyclic aromatic hydrocarbons in cell lines from the rainbow trout. *Comparative Biochemistry and Physiology. Part A, Molecular and Integrative Physiology* 128; 185–98.

Trubitt, T.R., Rabenecka, D.B., Bujaka, J.K., Bossusa, M.C., Madsena, S.S. & Tipsmarka, C.K., 2015. Transepithelial resistance and claudin expression in trout RTgill-W1 cell line: Effects of osmoregulatory hormones. *Comparative Biochemistry and Physiology, Part A, Molecular and Integrative Physiology* 182; 45–52.

Uchea, C., Sarda, S., Schulz-Utermoehl, T., Owen, S. & Chipman, K.J., 2013. *In vitro* models of xenobiotic metabolism in trout for use in environmental bioaccumulation studies. *Xenobiotica* 43(5); 421–31.

Uno, T., Ishizuka, M. & Itakura, T., 2012. Cytochrome P450 (CYP) in fish. *Environmental Toxicology and Pharmacology* 34(1); 1–13.

van der Oost, R., Beyer, J. & Vermeulen, N.P.E., 2003. Fish bioaccumulation and biomarkers in environmental risk assessment: a review. *Environmental Toxicology and Pharmacology* 13(2); 57–149.

Verri, T., Terova, G., Romano, A., Barca, A., Pisani, P., Storelli, C. & Saroglia, M., 2012. The Solute Carrier (SLC) family series in teleost fish. In *Functional Genomics in Aquaculture* (Saroglia, M. & Liu, Z., Eds.). John Wiley and Sons, Inc. pp. 219–320.

Vuorinen, P.J., Keinänen, M., Vuontisjärvi, H., Baršiene, J., Broeg, K., Förlin, L., Gercken, J., Kopecka, J., Köhler, A., Parkkonen, J., Pempkowiak, J. & Schiedek, D., 2006. Use of biliary PAH metabolites as a biomarker of pollution in fish from the Baltic Sea. *Marine Pollution Bulletin* 53; 479–87.

Walker, P.A., Bury, N.R. & Hogstrand, C., 2007. Influence of culture conditions on metal-induced responses in a cultured rainbow trout gill epithelium. *Environmental Science & Technology* 41(18); 6505–13.

Walker, P.A., Kille, P., Hurley, A., Bury, N.R. & Hogstrand, C., 2008. An *in vitro* method to assess toxicity of waterborne metals to fish. *Toxicology and Applied Pharmacology* 230; 67–77.

Walle, T., Walle, U.K., Knapp, D.R., Conradi, E.C. & Bargar, E.M., 1983. Identification of major sulphate conjugates in the metabolism of propranolol in dog and man. *The American Society for Pharmacology and Experimental Therapeutics* 11(4); 344–49.

Walle, T., Walle, U.K. & Olanoff, L.S., 1985. Quantitative account of propranolol metabolism in urine of normal man. *The American Society for Pharmacology and Experimental Therapeutics* 13(2); 204–09.

Wang, Y.I., Cao, J., Wang, X. & Zeng, S.U., 2010. Stereoselective transport and uptake of propranolol across human intestinal Caco-2 cell monolayers. *Chirality* 22; 361–368.

Wassmur, B., Gräns, J., Kling, P. & Celander, M. C., 2010. Interactions of pharmaceuticals and other xenobiotics on hepatic pregnane X receptor and cytochrome P450 3A signaling pathway in rainbow trout (*Oncorhynchus mykiss*). *Aquatic Toxicology* 100(1); 91–100.

Whyte, J.J. Jung, R.E. Schmitt, C.J. & Tillitt, D.E., 2000. Ethoxyresorufin-*O*-deethylase (EROD) activity in fish as a biomarker of chemical exposure. *Critical Reviews in Toxicology* 30(4); 347–570.

Wilhelm, I., Fazakas, C. & Krizbai, I.A., 2011. *In vitro* models of the blood-brain barrier. *Acta Neurobiologiae Experimentalis* 71; 113–28.

Wolf, K. & Quimby, M.C., 1962. Established eurythermic line of fish cells *in vitro*. *Science* 135, 1065–1066.

Wolf, W.D, Comber, M., Douben, P., Gimeno, S., Holt, M., Léonard, M., Lillicrap, A., Sijm, D., van Egmond, R., Weisbrod, A. & Whale, G., 2007. Animal use Replacement, Reduction, and Refinement: Development of an integrated testing strategy for bioconcentration of chemicals in fish. *Integrated Environmental Assessment and Management* 3(1), 3–17.

Wood, C.M. & Marshall, W.S., 1994. Ion balance, acid-base regulation, and chloride cell function in the common killifish, *Fundulus heteroclitus* – a euryhaline estuarine teleost. *Estuaries* 17(1); 34–52.

Wood C.M. & Pärt, P., 1997. Cultured branchial epithelia from freshwater fish gills. *The Journal of Experimental Biology* 200; 1047–59.

Wood, C.M., Gilmour, K.M. & Pärt, P., 1998. Passive and active transport properties of a gill model, the cultured branchial epithelium of the freshwater rainbow trout (*Oncorhynchus mykiss*). *Comparative Biochemistry and Physiology. Part A, Molecular and Integrative Physiology* 119(1); 87–96.

Wood, C.M., 2001. Toxic responses of the gill. In *Target Organ Toxicity in Marine and Freshwater Teleosts* (Schlenk, D. & Benson, W.H., Eds.). Taylor & Francis, London, UK, pp. 1–101.

Wood, C.M., Kelly, S.P., Zhou, B., Fletcher, M., O'Donnell, M., Eletti, B. & Pärt, P., 2002. Cultured gill epithelia as models for the freshwater fish gill. *Biochimica & Biophysica Acta* 1566; 72–83.

Wright, P.A. & Wood, C.M., 2009. A new paradigm for ammonia excretion in aquatic animals: role of Rhesus (Rh) glycoproteins. *The Journal of Experimental Biology* 212; 2303–12.

Xu, C., Li, C.Y.-T. & Kong, A.-N. T., 2005. Induction of phase I, II and III drug metabolism/transport by xenobiotics. *Archives of Pharmacal Research* 28(3); 249–68.

Yang, J.J., Kim, K.J. & Lee, V.H., 2000. Role of P-glycoprotein in restricting propranolol transport in cultured rabbit conjunctival epithelial cell layers. *Pharmaceutical Research* 17(5); 533–8.

Yonezawa, A. & Inui, K., 2013. Novel riboflavin transporter family RFVT/SLC52: identification, nomenclature, functional characterization and genetic diseases of RFVT/SLC52. *Molecular Aspects of Medicine* 34(2-3); 693–701.

Zaja, R., Klobucar, R.S. & Smital, T., 2007. Detection and functional characterization of Pgp1 (ABCB1) and MRP3 (ABCC3) efflux transporters in the PLHC-1 fish hepatoma cell line. *Aquatic Toxicology* 81(4); 365–76.

Zaja, R., Munić, V., Klobucar, R.S., Ambriović-Ristov, A. & Smital, T., 2008. Cloning and molecular characterization of apical efflux transporters (ABCB1, ABCB11 and ABCC2) in rainbow trout (*Oncorhynchus mykiss*) hepatocytes. *Aquatic Toxicology* 90(4); 322–32.

Zhou, B., Kelly, S.P., Ianowski, J.P. & Wood, C.M., 2003. Effects of cortisol and prolactin on Na^+ and Cl^- transport in cultured branchial epithelia from FW rainbow trout. *American Journal of Physiology – Regulatory, Integrative and Comparative Physiology* 285; R1305–16.

Zhou, B., Liu, C., Wang, J., Lam, P.K.S. & Wu, R.S.S., 2006. Primary cultured cells as sensitive *in vitro* model for assessment of toxicants - comparison to hepatocytes and gill epithelia. *Aquatic Toxicology* 80(2); 109–18.

Zolnerciks, J.K., Booth-Genthe, C.L., Gupta, A., Harris, J. & Unadkat, J.D., 2011. Substrate- and species-dependent inhibition of p-glycoprotein-mediated transport: implications for predicting *in vivo* drug interactions. *Journal of Pharmaceutical Sciences* 100(8); 3055–61.

Zou, J., Neumann, N.F., Holland, J.W. Belosevic, M., Cunningham, C., Secombes, C.J. & Rowley, A.F., 1999. Fish macrophages express a cyclo-oxygenase-2 homologue after activation. *The Biochemical Journal* 340; 153–59.

VIII. Appendices

Appendix I: List of Publications

(from this thesis)

Stott, L.C., Schnell, S., Hogstrand, C., Owen, S., Bury, N. Primary gill cell culture representing organ functionality: the first evidence of xenobiotic metabolism. (*In preparation for* Aquatic Toxicology).

Schnell, S., **Stott, L.C**., Bury, N., Hogstrand, C. The paracellular permeability of gill cell epithelia. (*In preparation for* Comparative Biochemistry & Physiology Part A).

Schnell*, S., **Stott* L.C**., Hogstrand, C., Wood, C.M., Kelly, S.P., Pärt, P., Owen, S.F. & Bury, N.R., 2016. Procedures for the reconstruction, primary culture and experimental use of rainbow trout gill epithelia. *Nature Protocols* 11; 490–498**.**

Stott, L.C., Schnell, S., Hogstrand, C., Owen, S.F. & Bury, N.R., 2015. A primary fish gill cell culture model to assess pharmaceutical uptake and efflux: Evidence for passive and facilitated transport. *Aquatic Toxicology* 159; 127–37.

Appendix II: Oral presentations

SETAC Europe 25th Annual Meeting, Barcelona, Spain, 3-7th May 2015. **L. C. Stott**, S. Schnell, C. Hogstrand, S. Owen, N. Bury. Primary gill cell culture representing organ functionality: Uptake, efflux and the first evidence of xenobiotic metabolism.

ICBF 11th International Congress on the Biology of Fish, Edinburgh, UK, 3-7th August 2014. **L. C. Stott**, S. Schnell, C. Hogstrand, S. Owen, N. Bury. The passive and facilitated transport of pharmaceuticals by a primary fish gill cell culture model.

HESI Bioaccumulation Project Committee *in vitro* webinar, Online, 20th May 2014. Passive and facilitated uptake of pharmaceuticals by a primary fish gill cell culture model. **L. C. Stott**, S. Schnell, C. Hogstrand, S. Owen, N. Bury.

SETAC Europe 24th Annual Meeting, Basel, Switzerland, 11-15th May 2014. **L. C. Stott**, S. Schnell, C. Hogstrand, S. Owen, N. Bury. Passive and facilitated uptake and efflux of pharmaceuticals by a primary gill cell culture model.

British Society of Parasitology, Bristol, UK, 8-11th April 2013. R. C. Tinsley, **L. C. Stott**, and M. C. Tinsley. Experimental analysis of factors influencing helminth reproduction.

AstraZeneca Science Forum, Brixham, UK, 19th Sept. 2012. **L. C. Stott**, S. Schnell, C. Hogstrand, S. Owen, N. Bury. Xenobiotic uptake by fish: better understanding bioaccumulation.

Appendix III: Poster presentations

SETAC North America 35th Annual Meeting, Vancouver, USA, 9-13th Nov. 2014. **L. C. Stott**, S. Schnell, C. Hogstrand, S. Owen, N. Bury. Uptake, efflux and metabolism of pharmaceuticals at the gill: A primary gill cell culture model.

EUROTOX 50th Congress of the Europeans Societies of Toxicology, Edinburgh, UK, 7-10th September 2014. **L. C. Stott**, S. Schnell, C. Hogstrand, S. Owen, N. Bury. A primary fish gill cell model to assess xenobiotic transport and bioconcentration in fish.

AstraZeneca and BBSRC Forum, Alderley Park, Cheshire, 6th June 2014. **L. C. Stott**, S. Schnell, C. Hogstrand, S. Owen, N. Bury. The Virtual Fish: An *in vitro* gill to compliment *in vivo* pharmaceutical testing in ecotoxicology.

Diabetes and Nutritional Sciences Research Symposium, King's College, London, 21st May 2014. **L. C. Stott**, S. Schnell, C. Hogstrand, S. Owen, N. Bury. The Virtual Fish: An *in vitro* gill to compliment *in vivo* pharmaceutical testing in ecotoxicology.

SETAC UK Meeting, Plymouth, UK, 9-10th Sept. 2013. **L. C. Stott**, S. Schnell, C. Hogstrand, S. Owen, N. Bury. Xenobiotic uptake by fish: an *in vitro* gill model to better under-stand bioaccumulation in ecotoxicology.

Diabetes and Nutritional Sciences Research Symposium, King's College, London, 22nd May 2013. **L. C. Stott**, S. Schnell, C. Hogstrand, S. Owen, N. Bury. Xenobiotic uptake by fish: an *in vitro* gill model to better under-stand bioaccumulation in ecotoxicology.

SETAC Europe 23rd Annual Meeting, Glasgow, UK, 12-16th May 2013. **L. C. Stott**, S. Schnell, C. Hogstrand, S. Owen, N. Bury. Xenobiotic uptake by fish: an *in vitro* gill model to better under-stand bioaccumulation in ecotoxicology.

Diabetes and Nutritional Sciences Research Symposium, King's College, London, 23rd May 2012. **L. C. Stott**, S. Schnell, C. Hogstrand, S. Owen, N. Bury. Xenobiotic uptake by fish: better understanding bioaccumulation.

Appendix IV: Awards

BBSRC Sparking Impact Award 2015 – (£10,000) Awarded to my project proposal developing and improving the routes of dissemination of the cell techniques used in my current project for industry. This produced a video instructional resource (on DVD at the back of this thesis and at https://www.youtube.com/watch?v=ai84eQ5Mktg) with over 300 views to date, a website (http://www.burylabs.co.uk) and received media attention from KCL, BBSRC, NC3Rs and Phys.Org.

Grants – SETAC travel & registration (2014, £500), EUROTOX registration (2014, £250), KCL Graduate School (2013, £100 & 2014, £500), Company of Biologists (2013, £150).

Prizes – AstraZeneca UK 3Rs poster winner (2013), AstraZeneca Global 3Rs poster 2nd prize (2013), KCL departmental seminar 1st year poster winner (2012, £100).
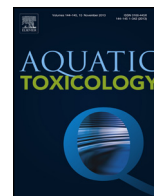
A primary fish gill cell culture model to assess pharmaceutical uptake and efflux: Evidence for passive and facilitated transport

Lucy C. Stott [a,b], Sabine Schnell [a], Christer Hogstrand [a], Stewart F. Owen [b], Nic R. Bury [a,*]

[a] *Division of Diabetes and Nutritional Sciences, King's College London, Franklin-Wilkins Building, 150 Stamford Street, London SE1 9NH, United Kingdom*
[b] *AstraZeneca, Alderley Park, Macclesfield, Cheshire SK10 4TF, United Kingdom*

A B S T R A C T

The gill is the principle site of xenobiotic transfer to and from the aqueous environment. To replace, refine or reduce (3Rs) the large numbers of fish used in *in vivo* uptake studies an effective *in vitro* screen is required that mimics the function of the teleost gill. This study uses a rainbow trout (*Oncorhynchus mykiss*) primary gill cell culture system grown on permeable inserts, which tolerates apical freshwater thus mimicking the intact organ, to assess the uptake and efflux of pharmaceuticals across the gill. Bidirectional transport studies in media of seven pharmaceuticals (propranolol, metoprolol, atenolol, formoterol, terbutaline, ranitidine and imipramine) showed they were transported transcellularly across the epithelium. However, studies conducted in water showed enhanced uptake of propranolol, ranitidine and imipramine. Concentration-equilibrated conditions without a concentration gradient suggested that a proportion of the uptake of propranolol and imipramine is *via* a carrier-mediated process. Further study using propranolol showed that its transport is pH-dependent and at very low environmentally relevant concentrations (ng L^{-1}), transport deviated from linearity. At higher concentrations, passive uptake dominated. Known inhibitors of drug transport proteins; cimetidine, MK571, cyclosporine A and quinidine inhibited propranolol uptake, whilst amantadine and verapamil were without effect. Together this suggests the involvement of specific members of SLC and ABC drug transporter families in pharmaceutical transport.

© 2014 The Authors. Published by Elsevier B.V. This is an open access article under the CC BY license (http://creativecommons.org/licenses/by/4.0/).

1. Introduction

There are currently over 140,000 compounds that are being reassessed for their bioconcentrative properties as a part of the EU Registration, Evaluation, Authorization & Restriction of Chemicals (REACH) initiative (REACH, 2009). Conventionally, the main determinant used for assessing bioconcentration of a compound is the octanol–water partitioning coefficient (K_{ow}), a measure of

hydrophobicity that drives sorption and accumulation, and a main input parameter in quantitative structure–activity relationships (QSARs) (Hansch, 1969). However, this may not be fully applicable to pharmaceuticals, many of which are polar and ionizable (Hermens et al., 2013). In this case, the pH-corrected octanol–water partitioning coefficient, D_{ow}, may be used, but this fails to take into account other major interactions such as hydrogen bonding and van der Waals forces, as well as uptake *via* carrier-mediated processes (Dobson and Kell, 2008; Sugano et al., 2010).

In vivo ecotoxicology testing produces bioconcentration factor (BCF) values that indicate the potential of a compound to bioconcentrate within an organism (OECD$_{305}$, 2012). Fish are exposed to highly lipophilic compounds *via* the diet, whilst to others *via* the water; the principle being to use the uptake and depuration rates to calculate the propensity of a compound to bioconcentrate. Typically, each test can use up to 108 fish per compound and many thousands of fish are used for this test every year (Scholz et al., 2013). There is currently a desire to develop alternative methods to replace these standardized whole fish studies to recognize and classify environmental hazards (Creton et al., 2013; Wolf et al., 2007). This requires the identification and validation of appropriate *in vitro*

systems that could replace such studies (Baron et al., 2012; Uchea et al., 2013). To find alternatives to the OECD$_{305}$ water exposure it is necessary to identify a suitable fish gill model that mimics the intact organ because the gill, being constantly and continuously exposed to substances in water, is the principle site of xenobiotic uptake (Bury et al., 2014).

Fletcher et al. (2000) developed a double-seeding technique that enables primary gill cells to be cultured on permeable membrane inserts in a two-compartment model. This cultured epithelium comprises the different cell types (mitochondrial rich cells, respiratory cells and mucus cells) found in the gill and produces high transepithelial resistance (reviewed by Bury et al., 2014). Importantly, the system is able to tolerate apical freshwater and produces a negative transepithelial potential, further simulating the in vivo scenario. This is crucial when investigating the transport of ionizable compounds such as pharmaceuticals that may behave differently in culture medium and water. Furthermore, the gill cells from two fish can be used to create up to 72 individual gill epithelial inserts for assaying, thus potentially reducing numbers of fish in in vivo testing.

The present study thus aims to use the in vitro gill to investigate the uptake and efflux of seven pharmaceuticals representing a range of classes. We hypothesize that both passive transcellular and carrier-mediated transport of xenobiotics across the gill are likely principle drivers in determining the rate of uptake of waterborne compounds (Mckim and Erickson, 1991). Passive transcellular transport depends on the pH of the solution, acid–base constants (pK_a) and the lipophilicity of the compound, whereas facilitated transport may be via members of the solute carrier (SLC) and ATP-binding casette (ABC) transporter families (Dobson and Kell, 2008). Therefore, to investigate carrier-mediated transport for some of these pharmaceuticals, concentration-equilibrated, pH-dependent, and concentration-dependent assays, as well as membrane channel inhibitor studies were conducted. In the context of this work, paracellular transport refers to the movement of compounds over membranes between cells and passive transport refers to concentration-dependent transcellular processes, whereas facilitated transport indicates concentration-independent carrier-mediated transport via membrane channel proteins. In addition, the uptake of propranolol across the in vitro gill model was compared to in silico and in vivo data (Owen et al., 2009), to demonstrate the use of this model as a predictive tool for pharmaceutical uptake.

2. Materials and methods

2.1. Animal husbandry

Gill cells for the use in primary cultures were obtained from juvenile diploid rainbow trout weighing 50–120 g purchased from a trout farm (Hampshire, UK). Fish were acclimatized in three 1000 L fiberglass aquaria at King's College, London, and maintained at 13–14 °C in recirculating aerated city of London tap water ([Na$^+$] = 0.53 mM, [Ca^{2+}] = 0.92 mM, [Mg^{2+}] = 0.14 mM, [K$^+$] = 0.066 mM and [NH$_4^+$] = 0.027 mM), which was passed through carbon, mechanical and biological filters. Photoperiod was maintained at a constant 14 h light/10 h dark cycle and fish were fed a daily 1% (w/w) ration of fish chow.

2.2. Gill cell culture

Sterile techniques were used throughout all cell culture procedures. Equipment, containers and solutions were autoclaved or sterile filtered (0.2 μm, Corning). The gill cell isolation procedure was based on methods previously documented (Fletcher et al.,

2000) and the cell culture double-seeded insert (DSI) technique as described by Walker et al. (2008) and Wood et al. (2002). Briefly, primary gill cells are isolated, washed and resuspended in L-15 medium (Invitrogen) supplemented with FBS (5% (v/v)) (Sigma) and seeded onto a permeable polyethylene terephthalate (PET) membrane inserts with 0.4 μm pores with an area of 0.9 cm^2 and maintained at 18 °C. This Transwell system (Corning) has an apical compartment above and a basal compartment below.

The development of an intact and electrically tight gill epithelium was monitored daily through 'blank'-corrected measurements of transepithelial resistance (TER) using a custom-modified epithelial tissue voltohmeter (EVOMX; World Precision Instruments) fitted with chopstick electrodes (STX-2). The same device was used to measure transepithelial potential (TEP) before and after freshwater application. DSI epithelia that reached a TER of ≥5 kΩ cm^2 were considered developed and electrically 'tight' for experimental procedures. In this instance, DSI preparations were washed twice with PBS (to remove any media supplemented with FBS) and exposed to radiolabeled pharmaceuticals apically in either L-15 medium (without FBS) or freshwater (2.0 mM CaCl$_2$, 0.5 mM MgSO$_4$, 0.8 mM NaHCO$_3$, 77.1 μM KCl at pH 7.7), or basally, always in L-15 medium. L-15 medium has an osmolarity of 300–320 mOsm kg^{-1} (Invitrogen) and that of freshwater is around 15 mOsm kg^{-1}. All experiments and exposures are based on individual inserts (n) derived from at least one biological replicate. Due to the seeding procedure over two days, one biological replicate is derived from two fish.

2.3. Membrane permeability

Paracellular permeability was measured using the paracellular marker ^{14}C-mannitol (20 Ci mmol^{-1}, Amersham Biosciences, CAS no. 88404-24-4). Thirty-seven DSI epithelia with TER values ranging from 0 to 14 kΩ cm^2 were exposed to 0.013 μCi (2.2 × 10^5 dpm) ^{14}C-mannitol in 1.5 mL sterile freshwater in the apical compartment, with 2.0 mL L-15 medium in the basal (Hubatsch et al., 2007). From this, a TER value at which paracellular transport is at its most minimal can be deduced as a threshold for when epithelia are ready for transport assays (≥5 kΩ cm^2). Aliquots of 100 μL were taken from the apical and basal compartments at time 0 and 24 h, and placed in 2 mL liquid scintillation fluid (Ecolume) and radioactivity measured by beta counting (Tri Carb 460CD liquid scintillation system; Packard). Mannitol flux after 24 h was calculated using Eq. (1):

$$\text{Permeability (cm s}^{-1}) = \frac{[\Delta M]_{BL} \times \text{volume}}{M_{AP} \times \text{time} \times 3600 \times \text{area}} \qquad (1)$$

where $[\Delta M]_{BL}$ is the change in radioactivity in the basal compartment, M_{AP} is the radioactivity at the start, time is 24 h and area is 0.9 cm^2 (Fletcher et al., 2000).

2.4. Radiolabeled pharmaceuticals

All drugs used in transport assays were at a concentration of 1 μg L^{-1} to represent the levels detected in the environment whilst remaining within detectable limits (Table 1). These were purchased radiolabeled and re-suspended in ethanol or methanol with a final solvent concentration in assay conditions of <0.0003%, and chosen to demonstrate a range of different classes (β$_1$-, β$_2$- and non-specific β-receptor agonists, a H$_2$-receptor agonist and a tricyclic anti-depressant) with mid-range logK_{ow} values (see Table 1). This method of using labeled compounds allows for the recovery of label during cell-free conditions to calculate the amount that sticks to plastic ware. Furthermore, the label may be detected as either the parent compound or biotransformed products. ^{3}H-propranolol hydrochloride (29.0 Ci mmol^{-1},

Table 1
Properties of selected pharmaceuticals and the levels at which they are found in the environment.

Pharmaceutical	Use	MW	pK_a	$\log K_{ow}$ [1]	$\log K_{ow}$ [2]	Environmental levels (ng L^{-1})
Propranolol	Non-selective β antagonist	259.340	9.4	2.54	1.12[*]	33[3]
Metoprolol	β1 receptor antagonist	267.364	9.6	1.76	−0.90[#]	410[3]
Atenolol	β1 receptor antagonist	266.336	9.6	0.67	0.0015[*]	940[3]
Formoterol	Long-acting β2 agonist	344.405	7.9[a]/9.2[b]	1.93	0.41[*]	n/a
Terbutaline	β2-Adrenergic receptor agonist	225.284	8.86[a]/9.76[b]	1.25	1.29	7[4]
Ranitidine	H2-receptor antagonist	314.4	8.08	1.47		120[3]
Imipramine	Tricyclic antidepressant	280.407	9.4	4.39		0.14[5]

[1] Parameter Client (Tetko et al., 2005).
[2] Environmental Risk Assessment data, experimentally measured values (AstraZeneca, 2014).
[3] Kostich et al. (2014).
[4] Breitholtz et al. (2012).
[5] Giebułtowicz and Nałęcz-Jawecki (2014).
[a] Acidic.
[b] Basic.
[*] pH 7.4.
[#] pH 7.

CAS no. 152588-63-93) was obtained from Amersham Biosciences. ^{3}H-metoprolol (29.7 Ci mmol^{-1}), ^{3}H-formoterol (18.5 Ci mmol^{-1}) and ^{3}H-terbutaline (29.0 Ci mmol^{-1}) were obtained from Vitrax. ^{3}H-Atenolol (7.3 Ci mmol^{-1}) and ^{3}H-ranitidine (2.5 Ci mmol^{-1}) were obtained from Moravek Biochemicals, and ^{3}H-imipramine hydrochloride (48.5 Ci mmol^{-1}, CAS no. 113-52-0) from Perkin-Elmer.

2.5. Bidirectional transport assays and apparent permeability coefficients

Bidirectional transport assays (BTA) assess both passive and facilitated transport in a bidirectional manner, from apical to basal (uptake) or *vice versa* (efflux). In these, concentration gradient conditions exist, whereby total transport is a sum of both passive transcellular and carrier-mediated processes. DSI epithelia with a TER > 5 kΩ cm^2 with low paracellular transport rates were exposed to test compounds in either symmetrical or asymmetrical conditions. Symmetrical contained 1.5 and 2.0 mL L-15 (without FBS) in apical and basal compartments respectively, whilst asymmetrical required the application of 1.5 mL freshwater in the apical compartment and 2.0 mL L-15 in the basal. The test compound was added to either the apical side (uptake; A:B) or basal compartment (efflux; B:A) at a concentration of 1 μg L^{-1}. Each experimental condition used 3–5 epithelial inserts from 1 to 2 biological replicates. For all experiments the water or media from the apical or basal compartment was mixed before taking 100 μL samples at 0, 6, 24, 30 and 48 h. Each 100 μL aliquot sample was placed into scintillation vials with scintillation fluid and beta-counted, and the drug concentration was calculated from the specific radioactivities. For uptake and efflux BTA, apparent permeability coefficients (P_{app}) at 6 h were calculated using Eq. (2):

$$P_{app}(\text{cm s}^{-1}) = \frac{(dQ/dt \times 1/(A \times C_0))}{3600} \quad (2)$$

where dQ/dt is the flux rate of the drug (pmol L^{-1} h^{-1}), A is the surface area of the monolayer (0.9 cm^2) and C_0 is the initial concentration of the drug in the donor compartment (fM) (Petri et al., 2004). Transport ratios (TR) for both uptake and efflux were calculated using Eqs. (3) and (4) (Schwab et al., 2003).

$$\text{Uptake TR} = \frac{P_{app\,A:B}}{P_{app\,B:A}} \quad (3)$$

$$\text{Efflux TR} = \frac{P_{app\,B:A}}{P_{app\,A:B}} \quad (4)$$

An uptake or efflux TR ≥ 1.5 is considered an indicator of active transport (Schwab et al., 2003; Luna-Tortós et al., 2008). For

time-dependent BTA, the results were also expressed as the percentage of the initial drug concentration of the donor compartment for uptake (A:B) and efflux (B:A) over 48 h.

2.6. Concentration equilibrium transport assays

Concentration equilibrium transport assays (CETA) examine transport by adding equivalent concentrations on either side of the gill epithelium and assessing the movement of compounds over time to evaluate carrier-mediated uptake or efflux regardless of passive transport processes, as used in blood–brain barrier transport assays (Luna-Tortós et al., 2008). The same experimental procedures for BTA were used (in symmetrical and asymmetrical conditions), but with both apical and basal compartments containing test drugs at the same concentration of 1 μg L^{-1}. The results are expressed as a percentage of the initial concentration in each compartment (apical or basal) over time.

2.7. The pH-dependent transport of propranolol

DSI epithelia were exposed in apical freshwater adjusted to pH 6 (by addition of HCl), pH 8 or pH 9.5 (by addition of NaOH; Corning pH meter 140). Radiolabeled propranolol was added at a concentration of 1 μg L^{-1} to either the apical or basal compartments (BTA) to investigate uptake and efflux. At 6 h a 100 μL sample was collected from the apical and basal compartments and radioactivity analyzed as above, and apparent permeability coefficients (P_{app}) calculated using Eq. (2).

2.8. The concentration-dependent uptake of propranolol

DSI epithelia (n = 54) were exposed to 17 concentrations of propranolol ranging from 0.014 to 10,000 μg L^{-1}. Concentrations above 0.1 μg L^{-1} were made using propranolol hydrochloride (Sigma, CAS no. 318-98-9) and radiolabeled propranolol as a marker. Experiments were conducted in asymmetrical conditions with propranolol added to the water in the apical compartment, thus mimicking the *in vivo* scenario (Owen et al., 2009). Radioactivity was analyzed as previously described in Section 2.3.

2.9. The inhibition of the uptake of propranolol

Cells were pre-incubated with inhibitor at a concentration 100 times higher (400 nM) than that of propranolol to competitively inhibit the membrane channel. Amantadine (Sigma, CAS no.

768-94-5), cimetidine (ICN, CAS no. 51481-61-9), cyclosporine A (Fluka, CAS no. 59865-13-3), MK571 (Tocris Biosciences, CAS no. 115104-28-4), quinidine (Sigma, CAS no. 56-54-2) or verapamil hydrochloride (Fluka, CAS no. 152-11-4) were dissolved in DMSO (0.1% in final solution) and added to the apical (in 0.75 mL freshwater) or basal (in 1.0 mL L-15 medium). Controls and compartments without inhibitor contained 0.1% DMSO. After 1 h, volumes were replaced with 1.5 mL freshwater containing $1 \mu g L^{-1}$ (4 nM) propranolol apically and 2.0 mL L-15 basally, whilst keeping the final concentration of inhibitor at 400 nM throughout. The same sampling procedure as for BTA at time 0, 6 (not for cyclosporine A), 24, 36 and 48 h proceeded and the uptake P_{app} of propranolol was calculated using Eq. (2). The P_{app} in all inhibitor-free controls were expressed as a percentage of the mean (100%) and the change in uptake P_{app} (inhibition) in the presence of inhibitors was expressed as a percentage of this mean control.

2.10. Analysis of data and statistics

For bidirectional P_{app} comparisons between the uptake and efflux, an independent samples t-test with equal variances assumed was used and statistical significance was accepted when $P < 0.05$ (SPSS software, SPSS Inc.). The same statistical analysis was used to test for differences between asymmetrical and symmetrical uptake or efflux P_{app} for each drug to assess the effect of apical freshwater application. For the time-dependent BTA significant differences between the uptake and efflux percentage of the donor compartment were tested for by one-way analysis of variance (ANOVA) on log-transformed data (SPSS software, SPSS Inc.). For the time-dependent CETA the statistical significance of differences between each percentage increase or decrease in the apical or basal compartments were also tested for by one-way ANOVA (after log transformation). Differences between the uptake of propranolol at different pHs, and similarly the efflux, were tested for by ANOVA and statistical significance was accepted when $P < 0.05$ (SPSS software, SPSS Inc.). The propranolol flux for each concentration in the concentration–response evaluation was calculated at 6 h and analyzed by ordinary least squares linear regression to describe the best fit, and further analysis of low concentrations was done by cubic polynomial regression to best describe the relationship (SPSS software, SPSS Inc.). Statistical differences between inhibitor (applied either apically or basally) and the inhibitor-free control were tested for by one-way ANOVA (after log transformation) and the statistical significance was set to $P < 0.05$.

2.11. Comparison to predicted and actual plasma concentrations

In vitro propranolol 'internal' concentrations after uptake (A:B) from the concentration–response study were compared to predicted in silico and actual in vivo plasma concentrations of propranolol in Oncorhynchus mykiss. The predicted partition of propranolol between blood and water can be determined by [plasma] = 0.87 [water] as described by Owen et al. (2009). This was calculated using the mammalian fish leverage model, whereby the predicted plasma concentration can be described by multiplying the environmental concentration by the blood to water partitioning coefficient (Huggett et al., 2004) using the Fitzsimmons model for the partitioning of compounds between blood and water (Fitzsimmons et al., 2001). Actual plasma concentrations of propranolol in O. mykiss were obtained from Owen et al. (2009). In vitro propranolol concentrations at 6 h ($n = 3$–6 from 3 biological replicates) were tested for correlation to in silico and in vivo plasma concentrations by ordinary least squares linear regression (SPSS software, SPSS Inc.)
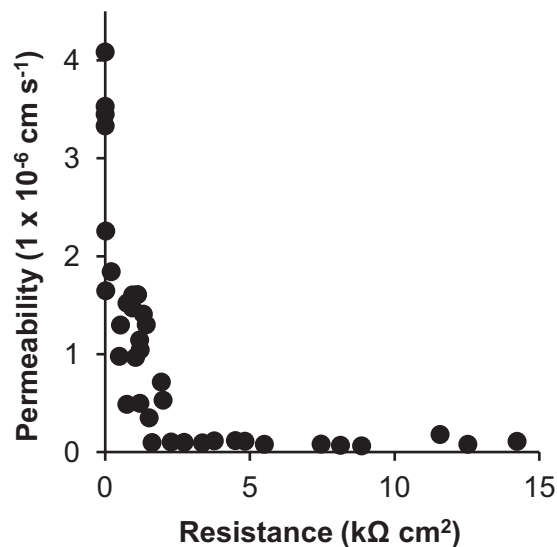

Fig. 1. The relationship between ^{14}C-mannitol permeability (after 24 h) and transepithelial electrical resistance (TER) in 37 cultured rainbow trout gill epithelia derived from four biological replicates. ^{14}C-mannitol was applied to the apical compartment in freshwater, with L-15 medium in the basal compartment. Each data point represents one DSI epithelium ($n = 37$) from four biological replicates.

3. Results

3.1. Epithelium membrane characteristics

DSI epithelial development was monitored through daily measurements of TER in symmetrical conditions, which after 8 days reached $18.1 \pm 1.3 \, k\Omega \, cm^2$ ($n = 24$). After apical freshwater application TEP became increasingly negative from $-0.9 \pm 0.15 \, mV$ to $-12.9 \pm 2.9 \, mV$ ($n = 8$). The permeability of the paracellular marker ^{14}C-mannitol produces a measure of the rate of paracellular transport for compounds with similar molecular weights via this route. Mannitol flux in cell free inserts with a TER of $0 \, \Omega \, cm^2$ (blanked) was $3.6 \pm 0.2 \times 10^{-6} \, cm \, s^{-1}$ ($n = 4$, Fig. 1). DSI gill epithelia with TER of 200–$1000 \, \Omega \, cm^2$ exhibited a mannitol permeability of $1.1 \pm 1.1 \times 10^{-6} \, cm \, s^{-1}$, whilst those $> 2 \, k\Omega \, cm^2$ showed the lowest mannitol permeability of $0.1 \pm 0.01 \times 10^{-6} \, cm \, s^{-1}$, with little variation between epithelia (Fig. 1).

3.2. Apparent permeability coefficients and transport ratios

In symmetrical conditions with L-15 medium on both sides of the gill cell epithelium no significant differences between $P_{app \, A:B}$ and $P_{app \, B:A}$ for all 7 pharmaceuticals was observed (Fig. 2A), yet all permeabilities were higher than that of the paracellular marker mannitol (except for atenolol; $P_{app \, A:B}$: $0.1 \pm 0.03 \times 10^{-6} \, cm \, s^{-1}$ and $P_{app \, B:A}$: $0.1 \pm 0.02 \times 10^{-6} \, cm \, s^{-1}$ compared to mannitol; $P_{app \, A:B}$: $0.1 \pm 0.01 \times 10^{-6} \, cm \, s^{-1}$). In asymmetrical conditions with freshwater at the apical surface of the gill epithelium, $P_{app \, A:B}$ was significantly higher than $P_{app \, B:A}$ ($P < 0.001$) for propranolol and imipramine, whilst no significant differences existed between uptake and efflux P_{app} of the remaining five drugs metoprolol, atenolol, formoterol, terbutaline and ranitidine (Fig. 2B). For propranolol, the $P_{app \, A:B}$ increased significantly from $1.7 \pm 0.2 \times 10^{-6} \, cm \, s^{-1}$ in symmetrical to $2.7 \pm 0.2 \times 10^{-6} \, cm \, s^{-1}$ in asymmetrical conditions ($P < 0.05$) and $P_{app \, B:A}$ decreased significantly from 1.1 ± 0.02 to $0.8 \pm 0.1 \times 10^{-6} \, cm \, s^{-1}$ ($P < 0.05$) (Fig. 2A and B). Similarly for imipramine a significant increase in $P_{app \, A:B}$ from symmetrical ($1.9 \pm 0.2 \times 10^{-6} \, cm \, s^{-1}$) to asymmetrical ($3.0 \pm 0.1 \times 10^{-6} \, cm \, s^{-1}$; $P < 0.05$) and a significant decrease in P_{app}

	Uptake TR		Efflux TR	
	Symmetrical	Asymmetrical	Symmetrical	Asymmetrical
Propranolol	1.52*	3.21*	0.66	0.31
Metoprolol	0.56	1.32	1.78*	0.76
Atenolol	0.74	0.60	1.34	1.67*
Formoterol	1.08	0.97	0.93	1.03
Terbutaline	0.92	0.89	1.09	1.13
Ranitidine	1.21	0.88	0.83	1.14
Imipramine	0.84	1.83*	1.19	0.55

* represents TR $\geq$ 1.5.

$_{B:A}$ (2.2 ± 0.04 to $1.6 \pm 0.1 \times 10^{-6}$ cm s^{-1}; $P < 0.05$) (Fig. 2A and B) was observed.

Propranolol showed uptake TR values greater than 1.5 in both symmetrical and asymmetrical conditions, whilst for imipramine; this was only observed in asymmetrical conditions. Both metoprolol and atenolol had efflux TR values greater than 1.5 in symmetrical and asymmetrical conditions, respectively (Table 2).

3.3. Bidirectional transport assays

In symmetrical conditions with L-15 medium on both sides of the epithelium, ranitidine and imipramine exhibited greater efflux transport from the basal to the apical compartments at 24 h ($P < 0.05$) and at 30 and 48 h ($P < 0.05$) respectively. In asymmetrical conditions involving the application of freshwater at the apical surface, more propranolol, ranitidine and imipramine were taken up across the gill cell surface than effluxed after 48 h. This was significantly more so at 6 h ($P < 0.001$) and 24, 30 and 48 h ($P < 0.01$) for propranolol, 30 h ($P < 0.01$) for ranitidine and at all sampling

A: Symmetrical

B: Asymmetrical

Fig. 2. The apparent permeability coefficients (P_{app}) for uptake ($P_{app \ A:B}$, white bars) and efflux ($P_{app \ B:A}$, gray bars) of seven pharmaceuticals ($1 \mu g L^{-1}$) across the DSI gill cell epithelium at 6 h in symmetrical conditions (A) and asymmetrical conditions (B). Significant differences between the $P_{app \ A:B}$ and $P_{app \ B:A}$ for a drug within a condition (symmetrical or asymmetrical) are indicated by asterisk (independent samples t-test; ***$P < 0.001$). Significant differences between symmetrical and asymmetrical $P_{app \ A:B}$ or $P_{app \ B:A}$ for each drug are indicated by hash tag in (B) (independent samples t-test; #$P < 0.05$). All experiments were performed in triplicate or more ($n = 3$–5) from at least one biological replicate and values are shown as means $\pm$ SEM.

points (6, 24, 30 and 48 h) for imipramine ($P < 0.001$). Metoprolol, formoterol and terbutaline showed slightly greater uptake than efflux after 48 h, and this was significantly more so for formoterol at 48 h ($P < 0.05$).

3.4. Concentration-equilibrated transport assays

In symmetrical conditions with L-15 media and test drug on both sides of the epithelium no significant differences between percentage of the initial drug concentrations in the apical and basal compartments were observed for metoprolol, terbutaline and ranitidine at any time point (Fig. 3B). The percentage of the initial concentration of formoterol was more in the apical than basal but only significantly so at 24 h ($P < 0.05$). The percentage of the initial concentration of propranolol in the apical compartment was significantly more than the basal at all sampling points after 0 h (6 and 24 h $P < 0.01$ and 30 and 48 h $P < 0.05$). This was also seen for imipramine, which showed the same increased basal to apical facilitated transport ($P < 0.001$ at 6, 24 and 30 h and $P < 0.01$ at 48 h). However, in asymmetrical conditions the situation was reversed whereby increased apical to basal transport, indicative of facilitated uptake, resulted in significantly more propranolol and imipramine in the basal compartments ($P < 0.01$ at 24 h and $P < 0.001$ to 30 and 48 h for propranolol and $P < 0.01$ at 6, 24 and 30 h and $P < 0.001$ at 48 h for imipramine). The same was true for ranitidine in asymmetrical conditions but to a lesser degree ($P < 0.05$ at 24, 30 and 48 h). Metoprolol, formoterol and terbutaline showed no signs of facilitated transport across the epithelium as no significant differences were observed (Fig. 3B).

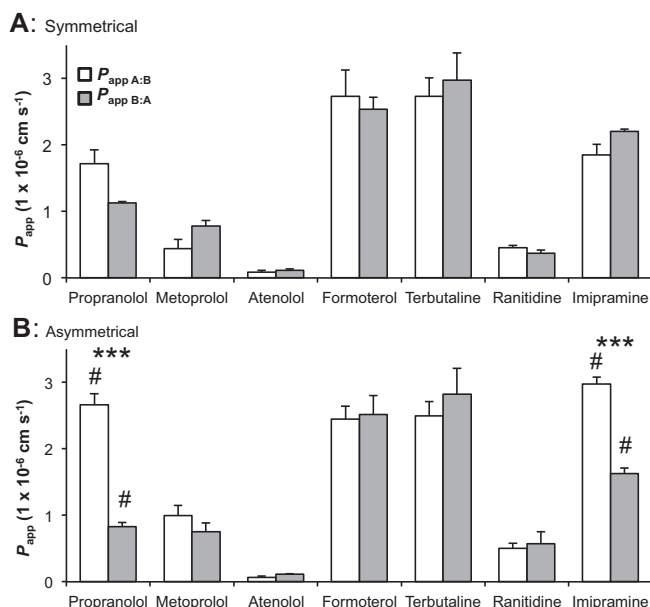### 3.5. The pH-dependent transport of propranolol

A decrease in pH from 8 to 6 resulted in a significant reduction in the uptake permeability ($P_{app \ A:B}$) of propranolol from $2.7 \pm 0.2 \times 10^{-6}$ to $0.4 \pm 0.03 \times 10^{-6}$ cm s^{-1} ($P < 0.001$) in asymmetrical conditions. The effect was opposite for efflux permeability ($P_{app \ B:A}$) with an increase from 0.8 ± 0.1 to $2.8 \pm 0.1 \times 10^{-6}$ cm s^{-1} ($P < 0.001$; Fig. 4). An increase in pH from 8 to 9.5 was without significant effect (Fig. 4).
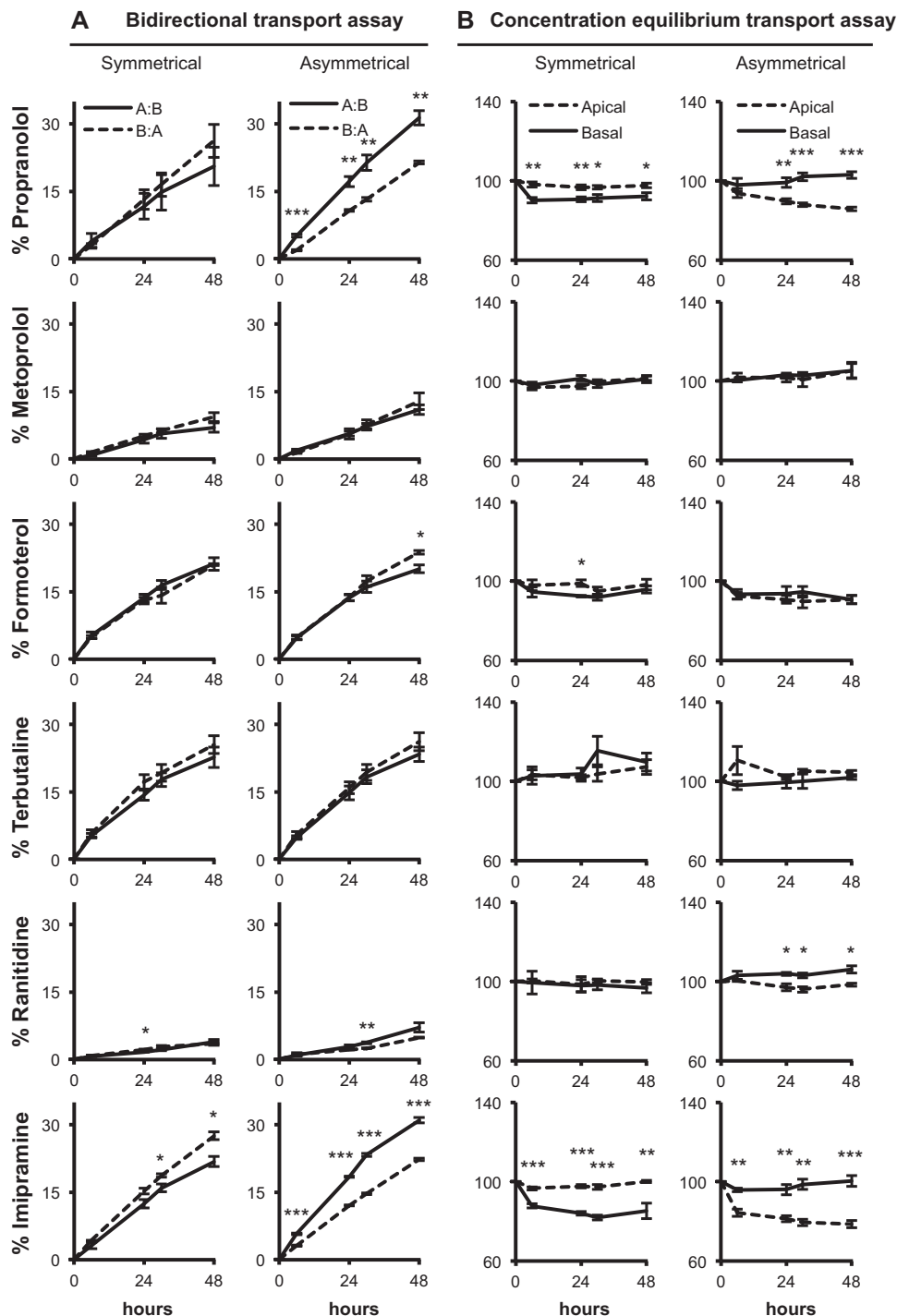
3.6. The concentration-dependent uptake of propranolol

A positive linear correlation between concentration (0.014–$10,000 \mu g L^{-1}$) and flux of propranolol was observed with regression line representing the best fit of [rate] = 0.052 [concentration] ($n = 54$, $r^2 = 0.974$, Fig. 5A). However, at lower propranolol concentrations (0.014–$0.14 \mu g L^{-1}$) a 2nd order polynomial regression best described the concentration–response relationship ($n = 24$, $r^2 = 0.927$, Fig. 5B) rather than linear ($n = 24$, $r^2 = 0.908$) with line representing the best fit of [rate] = 0.057 [concentration].

3.7. The inhibition of the uptake of propranolol

Amantadine and verapamil did not inhibit $P_{app \ A:B}$ of propranolol (Fig. 6A and F). Apical and basal cimetidine application significantly inhibited the transport of propranolol at all time points (apart from basal at time 6 h) by approximately 40–$61.4\% \pm 3.4$ (apical application) and $55.9\% \pm 1.3$ (basal application) at 48 h ($P < 0.001$) (Fig. 6B). Similarly, cyclosporine A showed a significant inhibition of propranolol transport after 48 h to 69.9% (± 3.7) of that in the control ($P < 0.01$) for apical application and to 66.3% (± 6.1) ($P < 0.001$)

Fig. 3. The transport assays of six pharmaceuticals: propranolol, metoprolol, formoterol, terbutaline, ranitidine and imipramine, in the DSI rainbow trout primary gill cell system over 48 h under (A) bidirectional transport assays (BTA) and (B) concentration equilibrium transport assays (CETA) conditions. For BTA (A) the drug is applied at a concentration of $1 \mu g L^{-1}$ to either the apical (− − −) for apical to basal transport; uptake, A:B or basal compartment (− − −) for basal to apical transport; efflux, B:A in either symmetrical (L-15 medium in both compartments) or asymmetrical (freshwater in the apical compartment and L-15 medium in the basal) conditions. For this assay, data are shown as a percentage of the initial drug concentration in the donor chamber *versus* time. For CETA (B), the drug is added to both the apical and basal compartments at the same concentration ($1 \mu g L^{-1}$) in both symmetrical and asymmetrical conditions. Data are shown as a percentage of the initial concentration in either the apical or basal *versus* time. For both assays, significant differences between the two compartments are indicated by asterisk (one-way ANOVA; *$P < 0.05$; **$P < 0.01$; ***$P < 0.001$). All experiments were performed in triplicate or more ($n = 3$–6) from at least one biological replicate and values are shown as means ± SEM.

for basal one (Fig. 6C). Application of the inhibitors MK571 and quinidine again caused a significant decrease in propranolol permeability over time by approximately 40% compared to the control at 48 h for both apical and basal applications ($P < 0.001$) (Fig. 6D and E).
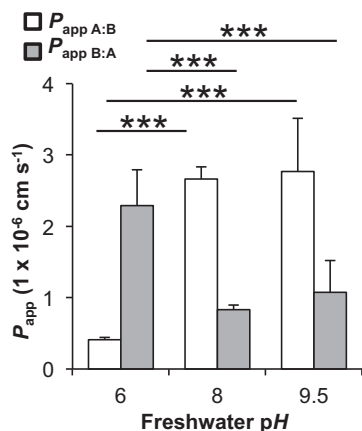
3.8. Comparison to predicted and actual propranolol plasma concentrations

Predicted plasma concentrations were calculated using [plasma] = 0.87 [water] and actual plasma concentrations from

Table 3
Propranolol concentration *in silico* (predicted), *in vivo* and *in vitro* (measured at various external propranolol concentrations).

Nominal propranolol concentration in water (μg L^{-1})	In silico (ng mL^{-1}) (Huggett et al., 2004)	In vivo (ng mL^{-1}) (Owen et al., 2009)	In vitro (ng mL^{-1})
0.1	0.087	n/a	0.04 ($\pm$0.002)
1.0	0.87	0.94[*] (n/a)	0.10 ($\pm$0.001)
10	8.7	3.3 ($\pm$0.4)	0.72 ($\pm$0.02)
100	87	16 ($\pm$7)	7.5 ($\pm$0.3)
1000	870	280 ($\pm$116)	79.5 ($\pm$7.3)
10,000	8700	5200 ($\pm$1333)	812 ($\pm$158)
100,000	87,000	n/a	5545 ($\pm$313)

[*] Pooled plasma sample.

Fig. 4. The pH-dependent uptake of propranolol. Shown are the apparent permeability coefficients (P_{app}) for uptake ($P_{app\ A:B}$, white bars) and efflux ($P_{app\ B:A}$, gray bars) of propranolol (1 μg L^{-1}) across the DSI gill cell epithelium at 6 h in asymmetrical conditions at three different pHs. Significant differences between uptake P_{app} or efflux P_{app} are indicated by asterisk (one-way ANOVA; ***$P < 0.001$). All experiments were performed in triplicate or more ($n = 3$–5) from two biological replicates and values are shown as means $\pm$ SEM.

Owen et al. (2009) (Table 3). A linear correlation between predicted plasma concentration and *in vitro* basal concentrations was obtained and described by [*in vitro*] = 0.063 [predicted] ($n = 21$, $r^2 = 0.995$, Fig. 7). Furthermore, a correlation between actual plasma concentrations (Owen et al., 2009) and *in vitro* basal concentrations was obtained and described by [*in vitro*] = 0.155 [actual] ($n = 21$, $r^2 = 0.966$, Fig. 7).

4. Discussion

The development of suitable *in vitro* cellular models to replace, refine and reduce (3Rs) the numbers of fish used in ecotoxicological studies is an important requirement in current regulatory testing (Scholz et al., 2013). Pharmaceuticals in the environment are contaminants of emerging concern and their behavior in water affects uptake into biological systems (Boxall et al., 2012). Log K_{ow} is often used to determine the bioconcentration potential of a compound which may not be relevant to ionizable compounds such as pharmaceuticals (Hermens et al., 2013). The pH-corrected log D_{ow} is used to account for the fraction of ionizable and nonionisable species of a substance at a given pH, but this accounts for partitioning between two liquid phases and does not include partitioning across a biological membrane. The present study is the first to demonstrate how a primary rainbow trout gill cell culture system can be used to assess pharmaceutical uptake from water across a biological membrane. Therefore, this offers a potential alternative to replace whole organism pharmaceutical uptake studies at differing water chemistries, such as different pHs, the presence of dissolved organic matter or real water samples from the field.

Once a tight epithelium (>5 kΩ cm^2) has formed, the gills present a barrier for paracellular transport that is relatively impermeable to the paracellular permeability marker ^{14}C-mannitol (Fig. 1). All pharmaceuticals (except atenolol) were transported across the epithelium in both directions at a rate greater than that of ^{14}C-mannitol, indicating that their transport is *via* a transcellular or carrier-mediated process, as all exhibit molecular weights greater than that of the marker (Hubatsch et al., 2007; Schwab et al., 2003).

The application of apical freshwater resulted in significantly different drug permeations for propranolol and imipramine where more is taken up across the epithelium from the water than effluxed
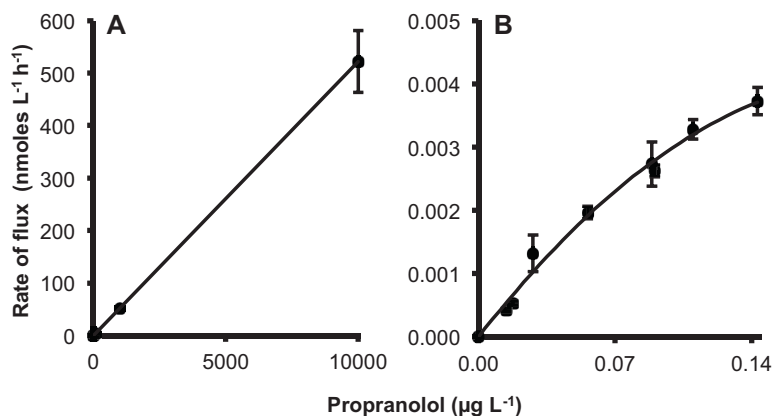
Fig. 5. The concentration dependent uptake of propranolol (uptake; A:B) at 6 h after exposure to (A) 17 propranolol concentrations ranging from 0.014 to 10,000 μg L^{-1} with the line representing the fit of [rate] = 0.052 [concentration] ($n = 54$, $r^2 = 0.974$) (note at lower concentrations that multiple data points are stacked) and (B) low propranolol concentrations (0.014–0.14 μg L^{-1}) with the line representing the fit of [rate] = 0.057 [concentration] ($n = 24$, $r^2 = 0.927$). The values represent mean $\pm$ SEM from five biological replicates.
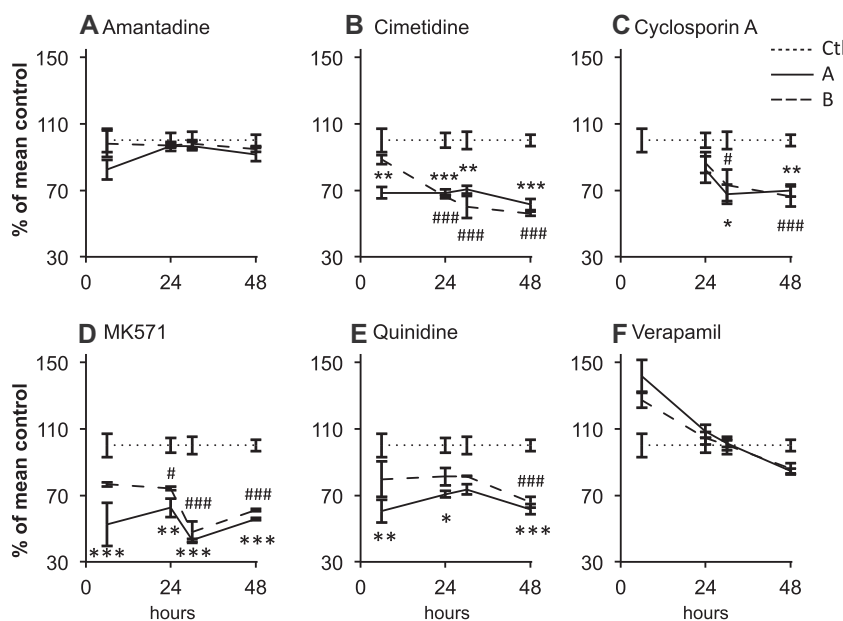
Fig. 6. The inhibition of the uptake of $1\,\mu g\,L^{-1}$ (4 nM) propranolol from apical (freshwater) to basal (L-15 medium) using 400 nM of the six inhibitors amantadine (A); cimetidine (B); cyclosporine A (C); MK571 (D); quinidine (E) and verapamil (F), applied either apically, AP (–––) or basally, BL (– – –). Data are shown as percentage of the mean control, CTL (·····) over time. Significant differences between the apically applied inhibitor and the control are indicated by asterisk (one-way ANOVA; $^*P < 0.05$; $^{**}P < 0.01$; $^{***}P < 0.001$). Significant differences between the basally applied inhibitor and the control are indicated by hash tag ($^{\#}P < 0.05$; $^{\#\#}P < 0.01$; $^{\#\#\#}P < 0.001$). All experiments were performed in triplicate or more ($n = 3$–6 from at least one biological replicate for inhibitor studies; $n = 18$ from six biological replicates for the inhibitor free controls) and values are shown as means ± SEM.

from the basolateral compartment (Table 2; Figs. 2B and 3A). The uptake of ionizable chemicals such as pharmaceuticals depends on pH and the acid base constant (pK_a) (Lahti et al., 2011). Both propranolol and imipramine are weak bases with pK_a values around 9.5. Using the Henderson–Hasselbalch equation, 99% of propranolol and imipramine exist in their protonated ionized form at pH 7.4 in symmetrical conditions, which then falls to only 98% in freshwater at pH 8. Here, at pH 8, more of the natural unionized forms are lipid-soluble, and thus may cross the membrane *via* passive transcellular routes explaining the enhanced uptake. However, the 1% change in speciation is unlikely to fully account for the difference in uptake observed (Fig. 2) and other factors are likely to play a role. For example, in symmetrical conditions TEP is positive (1.9 ± 0.2 mV) and becomes negative after apical freshwater application (-10.3 ± 0.2 mV, Fletcher et al., 2000; -12.9 ± 2.9 mV, data not shown), to a value similar to that observed *in vivo* (Potts, 1984). The change in membrane potential to basolateral negative generates an electrical gradient that aids cation partitioning across the membrane (Fletcher et al., 2000). Alternatively, the TR values greater than 1.5 in asymmetrical conditions for propranolol and imipramine in BTA conditions (Table 2) indicate that a proportion of the transport is *via* an carrier-mediated process (Schwab et al., 2003). This observation was substantiated by the concentration equilibrium transport assay (CETA) that eliminates concentration-dependent passive transport across the gill epithelium allowing the observation of carrier-mediated processes that drive xenobiotic transport. In CETA the difference in partitioning of radioactivity between the two compartments is not due to disproportional loss of compound adhering to the plastic ware of the apical and basolateral compartments, since in cell free blank insert experiments an equal percentage of the initial concentration added was absorbed to each compartment and an 80% recovery was obtained after 48 h (data not shown). Thus, it is possible to conclude that for propranolol and imipramine, facilitated transport makes up approximately 10% of the total transport, and around 5% for ranitidine efflux (Fig. 3B).

Uptake rates are important for predicting potential internal concentrations and are used to predict effects based on the "read

across" hypothesis and Mode of Action (Rand-Weaver et al., 2013). Much of the *in vivo* uptake work used for these predictions expose fish to very high water concentrations and extrapolates back to these lower environmentally relevant values. Propranolol uptake is concentration-dependent over the whole range of concentrations but in the low, $ng\,L^{-1}$ range, uptake deviates from linearity (0.014–$0.14\,\mu g\,L^{-1}$, Fig. 5). A similar result was obtained for the uptake at very low concentrations of iron across zebrafish gills and was attributable to proton-dependent metal transporters (Bury and Grosell, 2003). The facilitated transport of propranolol that occurs in these environmentally relevant concentrations (Kostich et al., 2014) is of interest because it suggests that the predictive models for uptake using data derived for higher concentrations may underestimate uptake.

The uptake of propranolol is pH dependent up to pH 8, after which further increases do not cause significant effects (Fig. 4). This again could be attributed to the difference in composition of ionized and unionized species at different pHs, with a caveat that a proportion of transport is likely *via* a facilitated process. However, it should be noted that the pH of the apical bulk compartment, and the microclimate at the boundary layer, were not measured after the 6 h duration of the experiment, and variations in such may account for changes in drug uptake. pH-dependent uptake of propranolol has been observed in other epithelia including retina (Kubo et al., 2013), Caco-2 cells (Wang et al., 2010) and kidney MDCK cells (Dudley et al., 2000). In contrast, efflux of propranolol is far greater at pH 6 than uptake (Fig. 4). This may suggest the export of propranolol or its metabolite is pH-dependent. Candidates for drug export are the ABC transporters; however these are not directly regulated by pH changes (Altenberg et al., 1993; Neuhoff et al., 2003). The internal pH of the cells is constant against external pH changes and thus intracellular speciation of the drug is unlikely to explain potential increase in efflux. It is likely that there are other propranolol parent and/or metabolite exporters present on the gill.

Propranolol uptake from water was inhibited by cimetidine, cyclosporine A, MK571 and quinidine. These are inhibitors of a
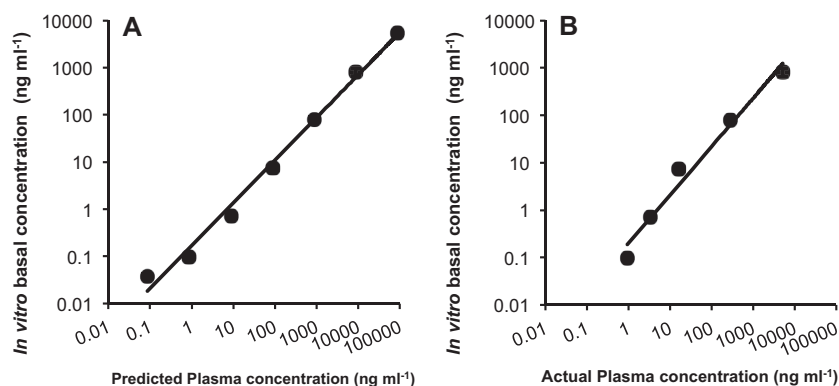
Fig. 7. Propranolol concentrations in the basal compartment of the primary gill cell model after 6 h apical exposure to propranolol in asymmetrical conditions plotted against (A) predicted (see text) *Oncorhynchus mykiss* propranolol plasma concentrations (0.1–100,000 μg L^{-1}) with regression line representing the fit of [*in vitro*] = 0.063 [predicted] ($n = 21$, $r^2 = 0.995$) or (B) actual *in vivo* plasma concentrations (1–10,000 μg L^{-1}) after 40 days exposure (Owen et al., 2009) with the regression line representing the fit of [*in vitro*] = 0.155 [actual] ($n = 21$, $r^2 = 0.966$) (Table 3). Basal *in vitro* concentrations were performed in triplicate or more ($n = 3$–5) and represent mean ± SEM from three biological replicates.

number solute carrier and ABC transporters. A number of human SLCs implicated in drug transport (SLC15s, SLCOs, SLC22s and SLC47s [Dobson and Kell, 2008; Giacomini et al., 2010]) are homologous to SLCs found in teleost fish (Verri et al., 2012). Similarly, ATP-binding cassette (ABC) transporters involved in the cellular efflux of toxicants such as ABCBs, ABCCs and ABCG2 (Deeley et al., 2006) are considered highly conserved amongst vertebrates (Dean and Annilo, 2005) and have been documented in rainbow trout cells both *in vivo* and *in vitro* (Fischer et al., 2011; Lončar et al., 2010) but not fully characterized. Recent microarray studies using the primary gill cell culture system have indentified the presence of transcripts for genes encoding a number of SLCs, ABCs as well as biotransformation enzymes (Schnell, Bury, Kille and Hogstrand, unpublished data). But, the identification of active proteins requires further work.

The application of cimetidine and quinidine, which both interact with organic cation transporter OCT2 (SLC22A2) (Giacomini et al., 2010; Koepsell, 2013) significantly reduce propranolol uptake. Propranolol transport *via* OCT2 was observed in renal LLC-PK$_1$ cells transiently transfected with hOCT2-V5, more specifically in the active uptake of its cationic form across the apical membrane (Dudley et al., 2000). Cimetidine is also used as a blocker of cisplatin transport by OCT2 in zebrafish lateral line hair cells (Thomas et al., 2013) and the presence of OCT2-like proteins have been suggested in other teleost fish gill epithelia (Verri et al., 2012). MK571 is an inhibitor of the multidrug resistance protein (MRP) efflux pumps (Deeley et al., 2006) and significantly inhibited propranolol uptake. The main MRP expressed in the gill is MRP3 (ABCC3) (Lončar et al., 2010). P-glycoprotein (Pgp; ABCB1) is implicated in propranolol transport in rabbit conjunctivial epithelial cells (Yang et al., 2000) and Caco-2 cells (Wang et al., 2010) and is present in rainbow trout tissues but at low levels in the gill (Lončar et al., 2010). Whether Pgp is involved in propranolol transport in the gill cell culture system is unclear. In addition to inhibiting OCT2, quinidine also acts as Pgp inhibitor (Giacomini et al., 2010) and cyclosporine A, another Pgp inhibitor, also blocked propranolol transport but this may be *via* MRP inhibition instead. Application of the Pgp inhibitor verapamil, however, did not affect propranolol transport (Fig. 6F). Taken together these observations would suggest that OCT2 and MRP3 may be candidates for propranolol transport across the teleost gill epithelium, but the location (apical or basolateral membrane) of these transporters, and others, needs further assessment.

Owen et al. (2009) showed that predicted plasma concentrations (Fitzsimmons et al., 2001) were good indicators of propranolol uptake over a range of high concentrations. Our data also correlates well with predicted (Fig. 7A) and measured plasma concentrations (Fig. 7B). However, *in vitro* propranolol concentrations in the basolateral compartment were an average 6% of the predicted and 16% of actual plasma concentrations, whilst actual plasma concentrations were only 59% of predicted (Owen et al., 2009). *In vivo* bioconcentration studies can involve an uptake phase of 60 days until a steady state is reached (OECD$_{305}$; OECD, 2012). Owen et al. (2009) used a 40-day exposure period, and both procedures use a flow through system with a steady-state endpoint. Our *in vitro* assay took place over 6 h in a static system, which could account for reduced propranolol uptake. Furthermore, actual plasma concentrations may be lower than predicted as a proportion of the drug may bind to proteins or be metabolized by the gill (as suggested by Bartram et al., 2011), which prediction models fail to take into account. Nevertheless, the relationships between this *in vitro* system to predicted and actual propranolol plasma concentrations suggest its applicability as a suitable *in vitro* model to investigate the uptake of xenobiotics and when combined with elimination rates, may supplement *in vivo* bioconcentration fish studies. These model pharmaceuticals used do not bioaccumulate; however, they may be taken into a fish, and or excreted. This functional primary gill model facilitates our better understanding of these processes. Currently legislation requires assessment for compounds of log K_{ow} higher than 3. This is an arbitrary value and we suspect that this value may be conservative with little prospect of significant bioaccumulation for compounds lower than log K_{ow} 4. This model provides a rapid and ethically acceptable tool with which to perform a preliminary assessment of compounds of low log K_{ow}, and as such ideal for large numbers of pharmaceuticals that typically have a lower propensity to bioaccumulate.

The study shows that as well as the passive uptake and efflux of neutral forms of pharmaceuticals, water enhances drug uptake of ionizable pharmaceuticals *via* both passive transcellular and carrier mediated processes. Hence, the ability of this system to tolerate freshwater is fundamental if we are to simulate *in vivo* drug uptake across the gill. In addition, the facilitated uptake of propranolol was more evident at low concentrations that are more environmentally relevant; suggesting that in certain situations uptake may be under predicted. Indeed there is significant variation (five-fold) recorded in plasma concentrations of individual fish exposed to pharmaceuticals *in vivo* (Owen et al., 2009), and it could be that individual difference in transporter expression may be a mechanistic explanation for this variance. The use of this system provides an opportunity to reduce the numbers of fish used in regulatory ecotoxicological testing as the primary gill cells cultured from two fish

may provide up to 72 individual gill cell cultures, and this method bypasses *in vivo* drug exposures and uses much less test compound, thus offering refinement through improved animal welfare methods.

Conflict of interest statement

The authors declare no financial conflict of interest.

Acknowledgements

References

Altenberg, G.A., Young, G., Horton, J.K., Glass, D., Belli, J.A., Reuss, L., 1993. Changes in intra- or extra-cellular pH do not mediate P-glycoprotein-dependent multidrug resistance. Proc Natl. Acad. Sci. USA 90, 9735–9738.

AstraZeneca, 2014. Environmental risk assessment data. http://www.astrazeneca.com/Responsibility/The-environment/Pharmaceuticals-in-the-environment/era-data-2012

Baron, M.G., Purcell, W.M., Jackson, S.K., Owen, S.F., Jha, A.N., 2012. Towards a more representative *in vitro* method for fish ecotoxicology: morphological and biochemical characterisation of three-dimensional spheroidal hepatocytes. Ecotoxicology 21 (8), 2419–2429.

Bartram, A.E., Winter, M.J., Huggett, D.B., McCormack, P., Constantine, L.A., Hetheridge, M.J., Hutchinson, T.H., Kinter, L.B., Ericson, J.F., Sumpter, J., Owen, P.S.F., 2011. *In vivo* and *in vitro* liver and gill EROD activity in rainbow trout (*Oncorhynchus mykiss*) exposed to the beta-blocker propranolol. Environ. Toxicol. 27 (10), 573–582.

Boxall, A.B., Rudd, M., Brooks, B.W., Caldwell, D., Choi, K., Hickmann, S., Innes, E., Ostapyk, K., Staveley, J.P., Verslycke, T., 2012. Pharmaceuticals and personal care products in the environment: what are the big questions? Environ. Health. Perspect. 120, 1221–1229.

Breitholtz, M., Näslund, M., Stråe, D., Borg, H., Grabic, R., Fick, J., 2012. An evaluation of free water surface wetlands as tertiary sewage water treatment of micro-pollutants. Ecotoxicol. Environ. Safe 78, 63–71.

Bury, N.R., Grosell, M., 2003. Waterborne iron acquisition by a freshwater teleost fish, zebrafish *Danio rerio*. J. Exp. Biol. 206 (19), 3529–3535.

Bury, N.R., Schnell, S., Hogstrand, C., 2014. Gill cell culture systems as models for aquatic environmental monitoring. J. Exp. Biol. 217, 639–650.

Creton, S., Weltje, L., Hobson, H., Wheeler, J.R., 2013. Reducing the number of fish in bioconcentration studies for plant protection products by reducing the number of test concentrations. Chemosphere 90 (3), 1300–1304.

Dean, M., Annilo, T., 2005. Evolution of the ATP-binding cassette (ABC) transporter superfamily in vertebrates. Annu. Rev. Genom. Human Genet. 6, 123–142.

Deeley, R.G., Westlake, C., Cole, S.P.C., 2006. Transmembrane transport of endo- and xenobiotics by mammalian ATP-binding cassette multidrug resistance proteins. Physiol. Rev. 86, 849–899.

Dobson, P.D., Kell, D.B., 2008. Carrier-mediated cellular uptake of pharmaceutical drugs: an exception or the rule? Nat. Rev. Drug Discov. 7 (3), 205–220.

Dudley, A.J., Bleasby, K., Brown, C.D., 2000. The organic cation transporter OCT2 mediates the uptake of beta-adrenoceptor antagonists across the apical membrane of renal LLC-PK1 cell monolayers. Br. J. Pharmacol. 131 (1), 71–79.

Fischer, S., Lončar, J., Zaja, R., Schnell, S., Schirmer, K., Smital, T., Luckenbach, T., 2011. Constitutive mRNA expression and protein activity levels of nine ABC efflux transporters in seven permanent cell lines derived from different tissues of Rainbow Trout (*Oncorhynchus mykiss*). Aquat. Toxicol. 101, 438–446.

Fitzsimmons, P.N., Fernandez, J.D., Hoffman, A.D., Butterworth, B.C., Nichols, J.W., 2001. Branchial elimination of superhydrophobic organic compounds by rainbow trout (*Oncorhynchus mykiss*). Aquat. Toxicol. 55, 23–34.

Fletcher, M., Kelly, S.P., Pärt, P., O'Donnell, M.J., Wood, C.M., 2000. Transport properties of cultured branchial epithelia from freshwater rainbow trout: a novel preparation with mitochondria-rich cells. J. Exp. Biol. 203, 1523–1537.

Giacomini, K.M., Huang, S., Tweedie, D.J., Benet, L.Z., Brouwer, K.L.R., Chu, X., Dahlin, A., Evers, R., Fischer, V., Hillgren, K.M., et al., 2010. Membrane transporters in drug development. Nat. Rev. Drug Discov. 9 (3), 215–236.

Giebułtowicz, J., Nałęcz-Jawecki, G., 2014. Occurrence of antidepressant residues in the sewage-impacted Vistula and Utrata rivers and in tap water in Warsaw (Poland). Ecotoxicol. Environ. Safe 104, 103–109.

Hansch, C., 1969. A quantitative approach to biochemical structure–activity relationships. Acc. Chem. Res. 2, 232–239.

Hermens, J.L.M., de Bruijn, J.H.M., Brooke, D.N., 2013. The octanol–water partition coefficient: strengths and limitations. Environ. Toxicol. Chem. 32 (4), 732–733.

Hubatsch, I., Ragnarsson, E.G.E., Artursson, P., 2007. Determination of drug permeability and prediction of drug absorption in Caco-2 monolayers. Nat. Protoc. 2 (9), 2111–2119.

Huggett, D.B., Ericson, J.F., Cook, J.C., Williams, R.T., 2004. Plasma concentrations of human pharmaceuticals as predictors of pharmacological responses in fish. In: Kümmerer, K. (Ed.), Pharmaceuticals in the Environment. , 2nd ed. Springer-Verlag, Berlin, pp. 373–386.

Kostich, M.S., Batt, A.L., Lazorchak, J.M., 2014. Concentrations of prioritized pharmaceuticals in effluent from 50 large wastewater treatment plants in the US and implications for risk estimation. Environ. Pollut. 184, 354–359.

Koepsell, H., 2013. The SLC22 family with transporters of organic cations, anions and zwitterions. Mol. Aspects Med. 34 (2–3), 413–435.

Kubo, Y., Shimizu, Y., Kusagawa, Y., Akanuma, S.-I., Hosoya, K.-I., 2013. Propranolol transport across the inner blood–retina barrier: potential involvement of a novel organic cation transporter. J. Pharmacol. Sci. 102 (9), 3332–3342.

Lahti, M., Brozinski, J.-M., Jylhä, A., Kronberg, L., Oikari, A., 2011. Uptake from water, biotransformation, and biliary excretion of pharmaceuticals by rainbow trout. Environ. Toxicol. Chem. 30 (6), 1403–1411.

Lončar, J., Popović, M., Zaja, R., Smital, T., 2010. Gene expression analysis of the ABC efflux transporters in rainbow trout (*Oncorhynchus mykiss*). Comp. Biochem. Physiol. 151C (2), 209–215.

Luna-Tortós, C., Fedrowitz, M., Löscher, W., 2008. Several major antiepileptic drugs are substrates for human P-glycoprotein. Neuropharmacology 55 (8), 1364–1375.

Mckim, J.M., Erickson, R.J., 1991. Environmental impacts on the physiological mechanisms controlling xenobiotic transfer across fish gills. Physiol. Zool. 64 (1), 39–67.

Neuhoff, S., Ungell, A.L., Zamora, I., Artursson, P., 2003. pH-dependent bidirectional transport of weakly basic drugs across Caco-2 monolayers: implications for drug–drug interactions. Pharmaceut. Res. 20, 1141–1148.

Owen, S.F., Huggett, D.B., Hutchinson, T.H., Hetheridge, M.J., Kinter, L.B., Ericson, J.F., Sumpter, J.P., 2009. Uptake of propranolol, a cardiovascular pharmaceutical, from water into fish plasma and its effects on growth and organ biometry. Aquat. Toxicol. 93 (4), 217–224.

OECD, 2012. Test No 305. Bioaccumulation in Fish: Aqueous and Dietary Exposure. OECD Guidelines for the Testing of Chemicals, Section 3. OECD Publishing.

Petri, N., Tannergren, C., Rungstad, D., Lennernäs, H., 2004. Transport characteristics of fexofenadine in the Caco-2 cell model. Pharmaceut. Res. 21 (8), 1398–1404.

Potts, W.T.W., 1984. Transepithelial potentials in fish gills. In: Hoar, W.S., Randall, D.J. (Eds.), Fish Physiology. Gills, part B Ion and Water Transfer, vol. 6. Academic Press, Orlando, pp. 105–128.

Rand-Weaver, M., Margiotta-Casaluci, L., Patel, A., Panter, G.H., Owen, S.F., Sumpter, J.P., 2013. The read-across hypothesis and environmental risk assessment of pharmaceuticals. Environ. Sci. Technol. 47 (20), 11384–11395.

REACH, 2009. Regulation (EC) No 1907/2006 of the European Parliament and of the Council of 18 December 2006. Legislation concerning the registration, evaluation, authorisation and restriction of chemicals. http://eurlex.europa.eu/LexUriServ/LexUriServ.do?uri=OJ:L:2009:309:0001:0050:EN:PDF

Scholz, S., Sela, E., Blaha, L., Braunbeck, T., Galay-Burgos, M., García-Franco, M., Guinea, J., Klüver, N., Schirmer, K., Tanneberger, K., et al., 2013. A European perspective on alternatives to animal testing for environmental hazard identification and risk assessment. Regul. Toxicol. Pharmacol. 67, 506–530.

Schwab, D., Fischer, H., Tabatabaei, A., Poli, S., Huwyler, J., 2003. Comparison of *in vitro* P-glycoprotein screening assays: recommendations for their use in drug discovery. J. Med. Chem. 46 (9), 1716–1725.

Sugano, K., Kansy, M., Artursson, P., Avdeef, A., Bendels, S., Di, L., Ecker, G.F., Faller, B., Fischer, H., Gerebtzoff, G., Lennernaes, H., Senner, F., 2010. Coexistence of passive and carrier-mediated processes in drug transport. Nat. Rev. Drug Discov. 9 (8), 597–614.

Tetko, I.V., Gasteiger, J., Todeschini, R., Mauri, A., Livingstone, D., Ertl, P., Palyulin, V.A., Radchenko, E.V., Zefirov, N.S., Makarenko, A.S., Tanchuk, V.Y., Prokopenko, V.V., 2005. Virtual computational chemistry laboratory – design and description. J. Comput. Aid. Mol. Des. 19, 453–463.

Thomas, A.J., Hailey, D.W., Stawicki, T.M., Wu, P., Coffin, A.B., Rubel, E.W., Raible, D.W., Simon, J.A., Ou, H.C., 2013. Functional mechanotransduction is required for cisplatin-induced hair cell death in the zebrafish lateral line. J. Neurosci. 33 (10), 4405–4414.

Uchea, C., Sarda, S., Schulz-Utermoehl, T., Owen, S., Chipman, K.J., 2013. *In vitro* models of xenobiotic metabolism in trout for use in environmental bioaccumulation studies. Xenobiotica 43 (5), 421–431.

Verri, T., Terova, G., Romano, A., Barca, A., Pisani, P., Storelli, C., Saroglia, M., 2012. The solute carrier (SLC) family series in teleost fish. In: Saroglia, M., Liu, Z. (Eds.), Functional Genomics in Aquaculture. John Wiley and Sons, Inc., pp. 219–320.

Walker, P.A., Kille, P., Hurley, A., Bury, N.R., Hogstrand, C., 2008. An *in vitro* method to assess toxicity of waterborne metals to fish. Toxicol. Appl. Pharmacol. 230 (1), 67–77.

Wang, Y.I., Cao, J., Wang, X., Zeng, S.U., 2010. Stereoselective transport and uptake of propranolol across human intestinal Caco-2 cell monolayers. Chirality 22, 361–368.

Wolf, W., De Comber, M., Douben, P., Gimeno, S., Holt, M., Léonard, M., Lillicrap, A., Sijm, D., van Egmond, R., Weisbrod, A., Whale, G., 2007. Animal use replacement, reduction, and refinement: development of an integrated testing strategy for bioconcentration of chemicals in fish. Integr. Environ. Assess. Manag. 3 (1), 3–17.

Wood, C.M., Kelly, S.P., Zhou, B., Fletcher, M., O'Donnell, M., Eletti, B., Pärt, P., 2002. Cultured gill epithelia as models for the freshwater fish gill. Biochim. Biophys. Acta 1566, 72–83.

Yang, J.J., Kim, K.J., Lee, V.H., 2000. Role of P-glycoprotein in restricting propranolol transport in cultured rabbit conjunctival epithelial cell layers. Pharmaceut. Res. 17 (5), 533–538.

Procedures for the reconstruction, primary culture and experimental use of rainbow trout gill epithelia

Sabine Schnell[1,6], Lucy C Stott[1,6], Christer Hogstrand[1], Chris M Wood[2], Scott P Kelly[3], Peter Pärt[4], Stewart F Owen[5] & Nic R Bury[1]

[1]Division of Diabetes and Nutritional Sciences, Metal Metabolism Group, Faculty of Life Sciences and Medicine, King's College London, London, UK. [2]Department of Zoology, University of British Columbia, Vancouver, British Columbia, Canada. [3]Department of Biology, York University, Toronto, Canada. [4]European Commission, Joint Research Centre, Institute of Environment and Sustainability, Ispra (Varese), Italy. [5]Global Safety Health and Environment, AstraZeneca, Alderley Park, Macclesfield, Cheshire, UK. [6]These authors contributed equally to this work. Correspondence should be addressed to S.S. (sabine.schnell@kcl.ac.uk), C.H. (christer.hogstrand@kcl.ac.uk) or N.R.B. (nic.bury@kcl.ac.uk).

This protocol describes how to reconstruct and culture the freshwater rainbow trout gill epithelium on flat permeable membrane supports within cell culture inserts. The protocol describes gill cell isolation, cultured gill epithelium formation, maintenance, monitoring and preparation for use in experimental procedures. To produce a heterogeneous gill epithelium, as seen *in vivo*, seeding of isolated gill cells twice over a 2-d period is required. As a consequence, this is termed the double-seeded insert technique. Approximately 5–12 d after cell isolation and seeding, preparations develop electrically tight gill epithelia that can withstand freshwater on the apical cell surface. The system can be used to study freshwater gill physiology, and it is a humane alternative for toxicity testing, bioaccumulation studies and environmental water quality monitoring.

INTRODUCTION

The freshwater fish gill is a multifunctional organ, and it is the site of gas exchange, osmoregulation, trace metal transport, nitrogenous waste excretion and xenobiotic uptake[1–4]. Fish are commonly used as indicator species to identify environmental hazards and, as their gills are constantly in contact with water, the gill epithelium is a focal point for countless studies that seek to understand deleterious effects of environmental toxicants[2]. Whole-animal studies can use millions of fish worldwide each year, and efforts are focusing on refining, reducing and replacing (3Rs) these numbers[5]. Alternative animal-free methods used in fish toxicology include the use of immortalized cell lines, as well as primary cultures of cells from fish organs. In the present article, we describe a protocol for the primary culture of a freshwater rainbow trout gill epithelium on a flat permeable membrane, via a repeated gill cell seeding protocol. This double-seeded insert (DSI) technique produces a heterogeneous epithelium similar to that found *in vivo*, and it was first described in Fletcher et al.[6]. We have used the DSI for studies investigating gill physiology and environmental monitoring[7–20].

Development of the DSI technique

Primary culture of a rainbow trout gill epithelium was pioneered by Pärt et al.[21]. Wood and Pärt[22] subsequently developed the single-seeded insert (SSI technique), in which isolated gill cells were cultured on permeable membrane inserts for the first time. This provided a two-chamber system that allowed the cells to grow into a polarized epithelium with an apical (water-facing) and basolateral (blood- or medium-facing) surface. The preparation exhibited barrier properties that were similar to those of the gill epithelium, and it tolerated apical water exposure for limited time periods. However, the epithelium comprised only a cell population of pavement cells (PVCs), which are the respiratory cells of the gill epithelium.

This technique was further developed into the DSI technique[6] whereby primary cells are seeded on inserts over 2 d, producing a gill epithelium of multiple cell layers and types that includes PVCs and mitochondrion-rich cells (MRCs); the latter is associated with the

transport of a number of ions and compounds across the fish gill[1]. The DSI procedure produces tight epithelia with transepithelial resistance (TER) values of up to 34,000 Ω cm[2], which are much higher than that of SSI (typically 1,000–5,000 Ω cm[2])[23]. The preparation expresses tight junction (TJ) proteins such as occludin, claudins, zonula occludens[7,8,24] and tricellulin[9]. The preparation also exhibits ion movement between the apical and basolateral compartments[10–12]. Active Ca^{2+} transport in the cell culture system resembles that of the intact fish[10,12], although so far it has not been possible to produce the net uptake of Na^+ and Cl^- ions present in freshwater fish in cell culture.

Applications of the protocol

Primary cultured gill epithelia have been used to assess how hormones and environmental conditions influence TJ protein expression and regulate epithelial permeability[7,8]. Further applications of the gill cell culture technique include studies on cytochrome *P*450 activity[14], lipid metabolism[15], ammonia transport[16], cytotoxicity[25] and metal-binding characteristics[17]. A recent study also used the DSI preparation to analyze the transport of pharmaceuticals across the gill, and found that, for some, facilitated transport processes may have a role at environmentally relevant concentrations[18]. It has also been used as an environmental water monitoring tool of urban streams[13] and in metal-polluted rivers[19]. However, these monitoring studies are restricted to a limited time frame, because the cultures can only withstand water exposure of up to 48 h. Thus, there is scope for future development of the cell culture technique to improve both active ion transport characteristics and extended water tolerance.

Generation of reliable *in vitro* cell assay results as an alternative to whole-animal tests for hydrophobic and volatile compounds has been proven to be difficult. This is because these compounds adhere to the plastic and/or are volatized, which results in exposure concentrations in the small volumes used in *in vitro* assays that deviate substantially from the nominal concentrations. In addition, these hydrophobic compounds do not readily dissolve in medium, and to

Figure 1 | Diagram of the primary cultured rainbow trout epithelium. (**a,b**) Reconstructed as DSI (**a**) or DSII (**b**) preparations. The epithelium attaches to the permeable membrane supports and polarizes so as to have an apical and basolateral cell surface (right). Epithelia are bathed on both sides with cell culture medium supplemented with FBS and antibiotics during development (left). For experimental purposes, freshwater can replace cell culture medium on the apical surface, whereas the basolateral surface is bathed in L-15 (without FBS or antibiotics).

increase solubility they are administered with co-solvents that may also exert a cellular response in the assay system. Kramer *et al.*[26] described a solvent-free dosing system for hydrophobic compounds in which the immortalized rainbow trout gill cell line RTgill-W1 was grown on the underside of the membrane of an insert. This allows a polydimethylsiloxane membrane preloaded with test compound to be placed on the bottom of the wells in close proximity to but not touching the cells, which in turn allows for a constant dosing concentration[26]. This technique is termed the double-seeded inverted insert (DSII) technique, and it can therefore be used in the development of a partition-controlled dosing system for hydrophobic compounds. We describe a modification to the method used by Kramer *et al.*[26] in which primary gill cells are cultured on an inverted insert. Characterization of the resulting primary gill epithelium growing in the DSII configuration is shown in **Supplementary Figure 1** and was carried out as described in the **Supplementary Methods**. The advantage of the DSII system is that the cultured epithelia resembles that of the intact gill (**Supplementary Fig. 1**),
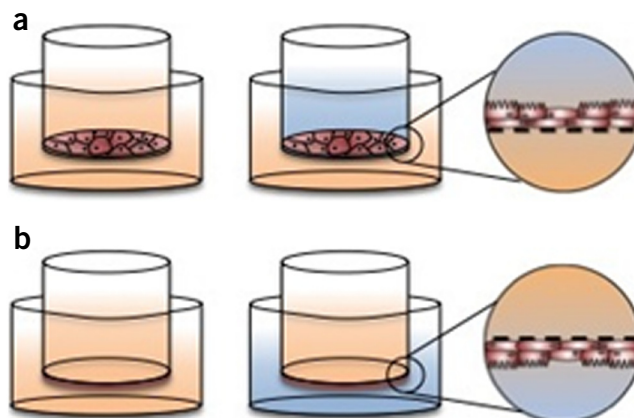
and it can be used in a similar way to the RTgill-W1 cell line when grown on inverted inserts for solvent-free dosing of hydrophobic compounds. However, given that we have only obtained preliminary data to date using the primary cultured epithelium in the DSII configuration, this method may require further optimization to ensure that it is optimally set up as required for specific experiments.

Comparison with other techniques

Bols *et al.*[27] described the isolation of the RTgill-W1 rainbow trout gill cell line. The main difference between using the cell line and the primary gill cell culture is that when using the primary gill cell culture, both the DSI and DSII contain the different cell types present in the *in vivo* gill. The epithelium is polarized and electrically tight, with TER values of >20 kΩ cm^2 compared with TER values in the range of ~200 Ω cm^2 when RTgill W1 cells are used. Importantly, the DSI and DSII tolerate the application of freshwater on the apical surface, which means that these primary cell cultures are better suited for gill physiology and functional studies than the cell line. However, the RTgill-W1 cell line viability[28] and cell growth[29] have been shown to correlate, in most cases, to both whole fish mortality and growth on exposure to pollutants. Thus, the RTgill-W1 cell line shows promise as a replacement for fish in toxicity testing.

In a number of countries, fish are used in whole effluent toxicity testing as part of environmental monitoring programs. The DSI can be used to assist in environmental monitoring because in addition to tolerating the application of freshwater in the laboratory, the DSI also tolerates the application of river water, as shown in two studies[13,19]. In one of these studies[19], we used the knowledge that the DSI responds to metals (assessed via the
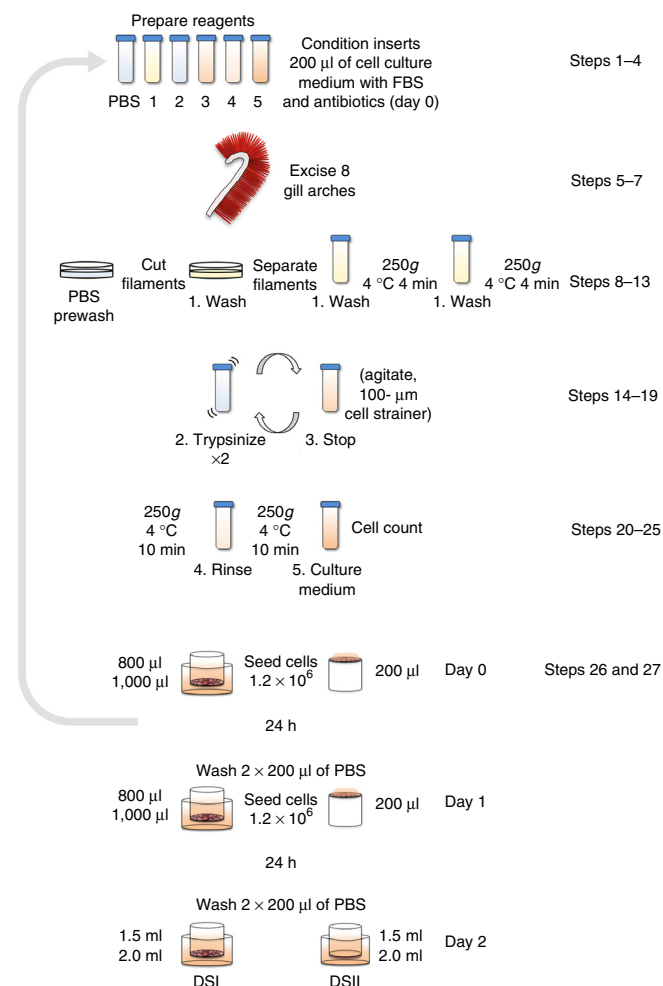
Figure 2 | Summarized flow diagram of rainbow trout gill cell isolation and seeding procedures. The reagents are prepared (see Reagent Setup) before excision of the gills; the filaments are teased apart and washed in PBS (PROCEDURE Steps 1–10). The filaments are centrifuged and washed before being treated with a trypsin solution to isolate cells (PROCEDURE Steps 11–16). The isolated cells are passed through a 100-µm strainer into a stop solution (see Reagent Setup; PROCEDURE Steps 17–21). The cell suspension is centrifuged and resuspended in cell culture medium containing FBS and antibiotics, and the cell density is determined (PROCEDURE Steps 18–25). The cells are seeded onto inserts for the double-seeded insert protocol (PROCEDURE Step 26A(i)) or onto inverted inserts for the double-seeded inverted insert protocol (PROCEDURE Step 26B(i)); this is termed day 0. The gill cell isolation procedure is repeated on day 1, and the inserts from the first seeding are washed with PBS before a second seed is placed on top (PROCEDURE Step 26A(ii–viii), 26B(ii–vii)). On day 2, the cells are washed and for the DSII protocol the insert is placed in the companion wells.

measurement of an increase in expression of the metal-responsive gene encoding metallothionein), mimics the physiological effect of metals on whole organisms in the laboratory[20] and conducted a trial whereby the DSI were exposed to natural metal contaminated water in the field[19]. The field trial study indicated that the DSI responded to metals in this complex matrix (river water), thereby showing that it is able to detect bioreactive metals. However, further experiments are required to assess the response of the DSI to other contaminants in more complex contaminant mixtures[13] and to determine its versatility for environmental monitoring.

Experimental design

The gill cells from two (~80 g) fish provide ~40 individual culture inserts, but this can increase to 72 depending on the success of the cell isolation, and thus this technique has the potential to reduce the number of organisms used in experiments. Therefore, at a practical level, in order to allow the comparison of toxicological data from different aquatic ecotoxicology and physiological

studies, a standardized procedure for DSI and DSII production is required. Here we present the most current and readily available standardized DSI technique (**Fig. 1a**), as well as the development of a DSII (**Fig. 1b**) technique. The protocols for the DSI and DSII techniques are summarized in a flow diagram (**Fig. 2**), and typical characteristics of the cultured epithelia are described in the ANTICIPATED RESULTS section. The controls for an experiment using DSI and DSII will depend on their intended use. For a typical experiment in which the cells are to be exposed to a compound in water[13,18–20], a set of control inserts that are exposed to either medium or water without the test compound should be set up. By comparing results, such as expression of a gene of interest, between the test and controls, it is possible to determine whether the response is due to the effect of exposure to water, or to water and the test compound. To perform experiments that provide statistical rigor, it is recommended that the experiment include inserts derived from several different preparations—i.e., biological replicates.

MATERIALS

REAGENTS

- Juvenile rainbow trout (<100 g) should be acclimatized for at least 2 weeks and maintained according to relevant governmental and institutional guidelines at 13–14 °C in good-quality water with constant 14-h light and 10-h dark photoperiods ▲ CRITICAL The fish must be kept in optimum conditions. The water must be well aerated and of good quality, and fish should eat well and not show signs of stress. ! CAUTION Experiments must conform to relevant institutional and governmental regulations.
- Leibovitz's L-15 medium, no phenol red, with L-glutamine (Invitrogen, cat. no. 21083-027) ▲ CRITICAL We recommend using Leibovitz's L-15 medium without phenol red, because there has been reports that phenol red may contain estrogenic activity that may influence physiological or toxicological responses[30].
- FBS (Sigma-Aldrich, cat. no. F7524)
- Penicillin-streptomycin (5,000 units ml^{-1} penicillin and 5 mg ml^{-1} streptomycin; Invitrogen, cat. no. 15070063)
- Gentamicin solution (10 mg ml^{-1}; Invitrogen, cat. no. 15710049)
- Fungizone (100 mg; Sigma-Aldrich, cat. no. A9528)
- Trypsin-EDTA, 0.5% (wt/vol), ×10 (Invitrogen, cat. no. 15400054)
- PBS (used as prewash solution)
- Ethanol (VWR International, cat. no. 20821.321)
- Calcium chloride dihydrate (Sigma-Aldrich, cat. no. 223506)
- Magnesium sulfate heptahydrate (Sigma-Aldrich, cat. no. 230391)
- Sodium bicarbonate (Sigma-Aldrich, cat. no. S6014)
- Potassium chloride (Sigma-Aldrich, cat. no. P9333)

EQUIPMENT

- Laminar flow hood, model no. M51424/2 (Microflow biological safety cabinet)
- Centrifuge, refrigerated, 5810R, rotor A-4-62 (Eppendorf)
- Vortex, F20220176 (VELP Scientifica)
- Dissecting equipment; large sharp knife, forceps (SLS, cat. no. INS4291; 00:SA), scissors (VWR International, cat. no. INS4808; INS4854) and scalpels (Swann-Morton, cat. no. 0501) ▲ CRITICAL All equipment must be autoclaved or sterilized using 70% (vol/vol) ethanol.
- Portable gyratory shaker, model IKA-VIBRAX-VXR
- Adjustable pipettes: P-20 (Gilson, cat. no. FA10003M), P-200 (Gilson, cat. no. FA10005M) and P-1000 (Gilson, cat. no. F123602)
- Pipette tips: 20 µl (Starlab, cat. no. S1120-1810), 200 µl (Starlab, cat. no. S1120-8810) and 1,000 µl (Starlab, cat. no. S1122-1830)
- Tissue culture pipettes: 5 ml (Corning, cat. no. CORN4051), 10 ml (Corning, cat. no. CORN4101) and 25 ml (Corning, cat. no. CORN4250)
- Inverted phase-contrast microscope, TE200, Nikon Eclipse
- Cell culture cooling incubator, MIR-1554, Sanyo, 18 °C, no CO$_2$ atmosphere required
- Hemocytometer (Neubauer)

- EVOM epithelial voltohmmeter modified by the manufacturer to read TER up to 100,000 Ω cm^{-2} (World Precision Instruments)
- EVOM 'chopstick' electrodes, no. STX-2 (World Precision Instruments)
- Inserts, 12-well, 0.4 µm, 0.9 cm^2 effective growth area, polyethylene terephthalate (PET) membrane (BD Falcon, cat. no. 353180)
- Companion cell culture plates, 12-well with low evaporation lid, notched (BD Falcon, cat. no. 353503)
- Sterile tip box with damp cotton wool and glass slides inside
- Sterile syringe filter, 0.2 µm (VWR International, cat. no. 194-2520)
- Cell strainers, 100 µm, Nylon (BD Falcon, cat. no. 352360)
- Falcon 50-ml conical tubes (BD Falcon, cat. no. 352070)
- Sterile Petri dishes (VWR International, cat. no. 25382-166)

REAGENT SETUP

PBS PBS is 137 mM sodium chloride (Sigma-Aldrich, cat. no. 746398), 2.7 mM potassium chloride (Sigma-Aldrich, cat. no. P9333), 10 mM disodium hydrogen phosphate (Sigma-Aldrich, cat. no. 255793) and 1.8 mM potassium dihydrogen phosphate (Sigma-Aldrich, cat. no. P0662). It is prepared in dH$_2$O and autoclaved. This can be stored for 1 month at room temperature (~20 °C). Before use, place it on ice.

Ethanol, 70% Prepare a 70% (vol/vol) solution of ethanol in dH$_2$O.

Fungizone Prepare a 10 mg ml^{-1} solution and store it in 1-ml aliquots at −20 °C until further use.

Wash solution Add 1.2 ml of penicillin-streptomycin, 1.2 ml of gentamicin and 90 µl of Fungizone solution to a final volume of 30 ml of PBS. Prepare the solution at room temperature in sterile conditions in a tissue culture hood on the day of cell isolation. Before use, place it on ice.

Trypsin solution Dilute 0.5% (wt/vol) trypsin-EDTA to 0.05% by pipetting 650 µl into a conical centrifuge tube and by bringing the volume up to 6.5 ml with PBS. Prepare the solution at room temperature in sterile conditions in a tissue culture hood on the day of cell isolation.

Stop solution Pipette 2 ml of FBS into a conical centrifuge tube with 18 ml of PBS. Prepare it at room temperature in sterile conditions in a tissue culture hood on the day of cell isolation. Before use, place it on ice.

Rinse solution Add 0.5 ml of FBS in a tube, and make up the final volume to 19.5 ml with PBS. Prepare this solution at room temperature in sterile conditions in a tissue culture hood on the day of cell isolation. Before use, place it on ice.

Cell culture medium with antibiotics and FBS (medium A) Pipette 27 ml of FBS, 11 ml of penicillin-streptomycin and 11 ml of gentamicin, all sterile filtered, to 500 ml of L-15 medium. This can be made in advance and stored at 4 °C for up to 1 month.

Cell culture medium with FBS (medium B) Pipette 27 ml of FBS, sterile filtered, to 500 ml of L-15 medium. This can be made in advance and stored at 4 °C for up to 1 month.

Exposure cell culture medium L-15 without any supplementation can be stored at 4 °C for up to 1 month.
Artificial freshwater Freshwater is defined as water prepared to the standard used for maintaining fish, such as that recommended by the Organisation for Economic Co-operation and Development (OECD) and the International Organization for Standardization (ISO). To make up OECD freshwater, prepare the following four solutions (40× stocks). Solution 1: dissolve 11.76 g of $CaCl_2.2H_2O$ in dH_2O, and adjust the volume to 1 liter with dH_2O (0.08 M). Solution 2: dissolve 4.93 g of $MgSO_4.7H_2O$ in dH_2O,

and adjust the volume to 1 liter with dH_2O (0.02 M). Solution 3: dissolve 2.59 g of $NaHCO_3$ in dH_2O, and adjust the volume to 1 liter with dH_2O (0.03 M). Solution 4: dissolve 0.23 g of KCl in dH_2O, and adjust the volume to 1 liter (0.003 M). Once all the solutions are prepared, mix 25 ml of each solution, and the total volume is made up to 1 liter with dH_2O. Aerate the dilution water until oxygen saturation is achieved, and then store it for about 2 d with further aeration before use[23].
Natural freshwater Filter natural freshwater samples using a 0.2-μm sterile syringe filter before exposure to the cell culture.

PROCEDURE
Preparation of solutions and culture inserts ● **TIMING** 1 h, plus 1.5 h of incubation to condition the membrane
▲ **CRITICAL** The recommended volumes in this section are appropriate for one cell isolation procedure.
1| Prepare the two types of cell culture media with antibiotics (medium A) and without antibiotics (medium B; see Reagent Setup). Take a 50-ml aliquot of each and keep them on ice.

2| Prepare the prewash solution (18 ml), wash solution, trypsin solution, stop solution and rinse solution, and keep them on ice.

3| In the cell culture hood, remove the permeable membrane inserts and companion cell culture plates from their packaging. For the DSI technique, place inserts in the wells of cell culture plates and place the lid on top. For DSII, turn the inserts upside down in a humidified chamber. To generate the humidified chamber, we use a sterile pipette tip box with damp sterile cotton wool.
▲ **CRITICAL STEP** For DSI, the flanges of the inserts rest between the notches of the well to minimize medium wicking and to assure the proper fitting of the plate with the lid.
▲ **CRITICAL STEP** For DSII, microscope slides can be placed on top of the cotton wool in the tip box to create a stable and flat surface on which to place the upside-down inserts. This prevents the medium from spilling over the edge of the inverted insert.

4| Condition permeable membrane inserts by applying cell culture medium with FBS and antibiotics (A) to the surface of the insert on which the cells will be seeded. For DSI preparations, add 200 μl of cell culture medium with FBS and antibiotics (A) in the upper compartment. For DSII, add 200 μl of cell culture medium with FBS and antibiotics (A) onto the top of the upside-down insert. Close the systems and keep them at 18 °C in a cell culture incubator for at least 1.5 h.

Rainbow trout dissection and gill cell isolation ● **TIMING** 3 h
5| Euthanize one rainbow trout.
! **CAUTION** Euthanize rainbow trout according to national and institutional guidelines. We follow UK Home Office Schedule 1 procedures in which the fish is euthanized via the destruction of the brain, which is achieved by a blow to the cranium and the use of a sharp probe.

6| Remove the head behind the operculum with a sharp knife.
▲ **CRITICAL STEP** It is important to perform this procedure quickly so as to reduce the extent of gill hemorrhaging and to avoid excessive bleeding and clotting on the filaments, which will reduce the quality of the gill cells obtained.

7| With dissecting scissors and forceps, remove the operculum (**Fig. 3a**) and excise out the intact gill arches by cutting the dorsal and ventral cartilage of each gill arch. Place the gill arches into 10 ml of prewash solution in a Petri dish (**Fig. 3b**).
▲ **CRITICAL STEP** Avoid damage to the filaments by holding the cartilage of the arch and not the filaments.

8| Remove mucus by carefully blotting each gill arch onto tissue paper, and then cut the filaments from the arches and place the filaments into 10 ml of wash solution (prepared in Reagent Setup) in a Petri dish.
▲ **CRITICAL STEP** Do not cut the filaments too close to the cartilage of the gill arch, as this will contaminate the cell culture with fibroblasts.

9| Tease the filaments apart using forceps, and cut them with a scalpel. This should result in filaments separated in bundles of 1–5. This increases the surface areas, which facilitates the action of the trypsin solution later.

10| Pour away this wash solution, and add the filaments to a 10-ml aliquot of wash solution in a 50-ml conical centrifuge tube, and place the tube on ice. Incubate the tube for 10 min.
▲ **CRITICAL STEP** From this step onward, sterile culture technique must be used, and the procedures should therefore take place in a laminar flow hood.

PROTOCOL

Figure 3 | Dissection of the gills and isolation of the cells. (**a**) Four gill arches are located underneath each operculum on the lateral sides of the rainbow trout head. Scale bar, 0.5 cm. (**b**) Gill arches are excised by cutting the cartilage of the arch, and these are placed into 20 ml of prewash solution (PBS). Scale bar, 1 cm. (**c,d**) The gill cell pellet is obtained after centrifugation in Step 21 (**c**) and Step 22 (**d**). Trapped red blood cells give the red color. Scale bars, 1 cm.
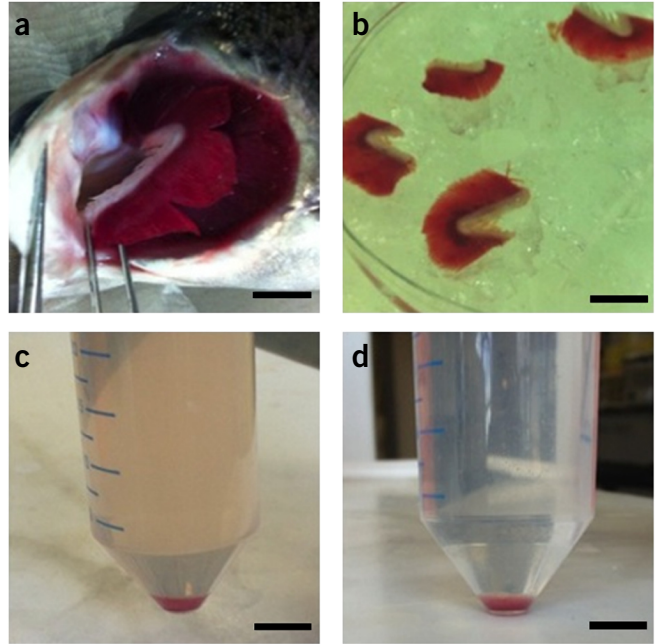
11| Centrifuge the tube for 4 min at 250g at 4 °C to collect the filaments. Aspirate and discard the supernatant.

12| Add the last remaining 10 ml of wash solution and moderately mix to dislodge the filaments. Incubate the tube on ice for a further 10 min.

13| Centrifuge again for 4 min at 250g at 4 °C, and then aspirate and discard the supernatant.

14| Add 500 µl of trypsin solution to the pelleted filaments, and agitate to remove any remaining wash solution. Centrifuge the tube for 4 min at 250g at 4 °C, and then aspirate and discard the supernatant.

15| Add 3 ml of trypsin solution to begin tryptic digestion, and shake for 12 min at 200 r.p.m. at room temperature.

16| To mechanically agitate the cut gill filaments and to improve cell yield, pass the filaments in trypsin solution repeatedly through a wide-bore pipette tip immediately after the 12-min trypsinization period. A wide-bore pipette tip can be prepared by removing the tip of a 1,000-µl pipette tip, so that the bore of the pipette aperture is ~2 mm. Sterilize by storing the cut pipette tip in 70% (vol/vol) ethanol. Before use, blot the wide-bore tip on tissue to remove residual ethanol, and pass the filaments/trypsin solution up and down at least 50 times.

17| Place the 100-µm cell strainer onto the 50-ml conical centrifuge tube containing 20 ml of stop solution (prepared in Reagent Setup) on ice. Pipette the filament/trypsin solution into the strainer, and agitate it to facilitate the collection of gill cells as a single-cell suspension in stop solution.
▲ CRITICAL STEP After collection of cells, gently invert the conical centrifuge tube to mix the gill cells with the stop solution.

18| Remove the filaments from the strainer and replace them back into their original conical centrifuge tube. Repeat tryptic digestion by adding the remaining 3 ml of trypsin solution and by shaking for a further 12 min at 200 r.p.m. at room temperature.

19| Place a new 100-µm cell strainer onto the same 50-ml conical centrifuge tube containing the stop solution and the previously trypsinized cells, and repeat the gill cell isolation as in Step 13.

20| Centrifuge the cell suspension for 10 min at 250g at 4 °C. A red pellet should be obtained (**Fig. 3c**). Aspirate and discard the supernatant.
? TROUBLESHOOTING

21| Resuspend the red pellet in 2 ml of rinse solution (prepared in Reagent Setup), and then add the remaining 18 ml; agitate the mixture briefly and centrifuge it for 10 min at 250g at 4 °C. This should result in another red-colored pellet (**Fig. 3d**). Aspirate and discard the supernatant.

22| Resuspend the red pellet initially in 2 ml of cell culture medium with FBS and antibiotics (medium A), and flick the tube to dislodge the pellet many times; next, resuspend in 8 ml (for a total of 10 ml) and mix it well.

23| Add 10 µl of cell suspension to 90 µl of trypan blue solution in a 0.5-ml bullet centrifuge tube, and mix thoroughly using a vortex.

24| Count the viable cells using a hemocytometer on the basis of the trypan blue exclusion criterion.
▲ CRITICAL STEP Exclude blood cells from the cell count. These appear as ellipsoidal cells, which are smaller than the gill cells.

25| Determine the concentration of cells and adjust cell counts of cell suspension from Step 21 to required seeding density detailed in the following steps.
? TROUBLESHOOTING
■ **PAUSE POINT** Cells can be left up to 2 h on ice.

Cell seeding
26| Follow option A to seed the cells for a DSI experiment, and follow option B to seed cells for a DSII experiment.
(A) DSI cell seeding ● **TIMING** 30 min
  (i) Aspirate the medium conditioning the cell culture inserts (from Step 4) before cell seeding. Seed 1.2×10^6 cells in 800 μl of cell culture medium with FBS and antibiotics (medium A) per insert. In addition, set up three blank inserts (no cells) for TER measurements. Place 1 ml of cell culture medium with FBS and antibiotics (medium A) into the basolateral compartment. This is termed 'day 0'.
    ▲ **CRITICAL STEP** It is recommended that when establishing the protocol an insert seeding density gradient be performed to determine the optimum seeding density for producing inserts with consistently tight epithelia[10].
  (ii) Incubate the cells at 18 °C overnight.
  (iii) After the overnight incubation, begin a new gill cell preparation using another fish, by repeating Steps 5–25.
  (iv) To prepare the previously seeded inserts ('day 0') for double-seeding (from Step 26A(i)), aspirate the medium first from the lower compartment and then carefully from the upper compartment. Wash the surface of the inserts by slowly applying 200 μl of PBS down the side of the insert (not directly onto the attached cells to avoid disruption), and tap the edge of the insert gently at this wash stage to dislodge dead cells and mucus.
    ▲ **CRITICAL STEP** When you are removing or changing the medium, always aspirate the lower compartment first, and then the upper one. This maintains the hydrostatic pressure onto the cells and it prevents them from lifting off.
  (v) Repeat the wash as described in Step 26A(iv), with 200 μl of PBS.
    ? TROUBLESHOOTING
  (vi) Carefully apply the new gill cell preparation (obtained in Step 26A(iii)) directly on top of the previously seeded cells. Seed 1.2×10^6 cells in 800 μl of cell culture medium with FBS and antibiotics (medium A), and add 1 ml in the lower compartment afterward. Also apply medium to your blank insert controls. This is termed 'day 1'. Incubate the cells at 18 °C.
  (vii) After 24 h, wash the inserts again, as described in Step 26A(iv,v).
  (viii) Add maintenance volumes of culture medium; 1.5-ml cell culture medium with FBS and antibiotics (medium A) in the upper compartment and then 2.0 ml in the lower compartment. This is termed 'day 2'. Incubate the cells at 18 °C.
**(B) DSII cell seeding** ● **TIMING** 30 min
  (i) Aspirate the conditioning medium from the inverted cell culture inserts (from Step 4) before seeding. Seed 1.2×10^6 cells in 200 μl of cell culture medium with FBS and antibiotics (medium A) per inverted insert, and leave them at 18 °C in the sterile tip box. Also set up three blank inserts (no cells) for blank TER measurements. This is termed day 0.
    ▲ **CRITICAL STEP** It is recommended that when establishing the protocol an insert seeding density gradient be performed to determine the optimum seeding density to produce inserts with consistently tight epithelia[10].
  (ii) Incubate the cells at 18 °C overnight.
  (iii) After the overnight incubation and 24 h after Step 26B(i), begin a new gill cell preparation using another fish, by repeating Steps 5–25.
  (iv) To prepare the previously seeded inserts ('day 0') for double-seeding, wash the inverted inserts by aspirating the medium and by carefully and slowly applying 200 μl of PBS.
  (v) Repeat another 200-μl PBS wash.
    ? TROUBLESHOOTING
  (vi) Carefully apply the new gill cell preparation (obtained in Step 26B(iii)) directly on top of the previously seeded cells. Seed 1.2×10^6 cells in 200 μl of cell culture medium with FBS and antibiotics (medium A), and leave them in the sterile pipette tip box overnight at 18 °C. This is termed 'day 1'.
  (vii) Twenty-four hours later, wash the inserts again, as described in Step 26B(iv,v). The inserts can now be placed the right way up in companion wells. Replace it with maintenance volumes of culture medium: 1.5 ml of cell culture medium with FBS and antibiotics (medium A) in the upper compartment and then 2.0 ml in the lower compartment. Incubate the inserts at 18 °C. This is termed 'day 2'.

Maintenance ● **TIMING** 5–12 d
27| Incubate the inserts until day 4. On day 4, remove the medium and replace it with cell culture medium with FBS (medium B) without antibiotics. Continue to incubate cells at 18 °C, replacing the medium every 48 h. Monitor appropriate growth of the epithelia under a light microscope (**Fig. 4**). Cell culture inserts should be observed on a daily basis to

Figure 4 | Images of the double-seeded insert epithelium. (**a**) Phase-contrast micrograph of DSI gill epithelial cells. Scale bar, 100 µm. (**b**) Transmission electron micrograph of DSI gill epithelia showing the characteristic microridges on the apical surface. Scale bar, 200 nm. (**c**,**d**) Confocal microscope images of DSI epithelia in which 24 h before cell fixing, epithelia were exposed to symmetrical conditions with L-15 medium on both sides of the epithelium (**c**) or asymmetrical conditions with freshwater in the upper compartment and L-15 medium in the companion well (**d**), and cell nuclei were stained with 5 µM Hoechst (blue) and tight junctions with zonula occludens 1 antibody (green). Scale bars, 50 µm. (See **Supplementary Methods** for details of how we stained tight junctions using zonula occluden 1–specific antibodies.)
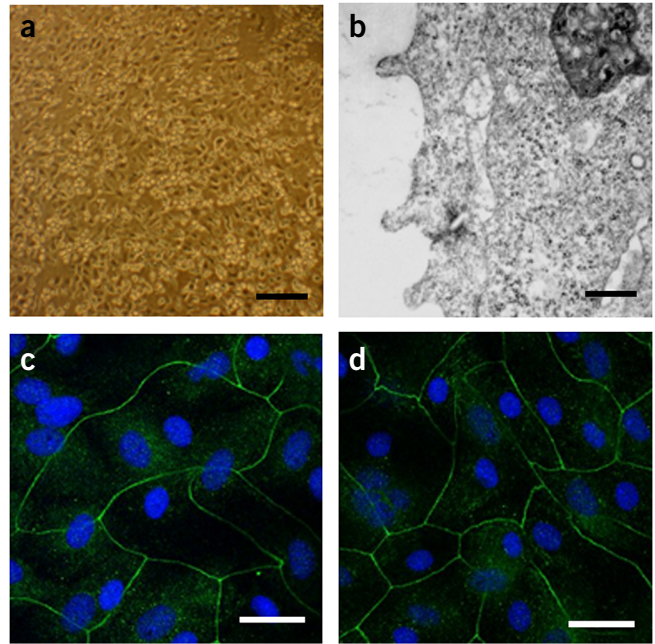
check for (bacterial) contamination. Any contaminated cell culture inserts should be immediately removed, and the associated plate well should be rinsed with 70% (vol/vol) ethanol. From day 4 onward, TER can be monitored daily if desired, as described in the following section.
▲ **CRITICAL STEP** Careful and thorough observation of culture preparations should take place before measuring TER (see following section) or changing the medium. Therefore, if one insert is found to be contaminated, it can be removed without cross-contaminating other epithelia.

Monitoring TER ● TIMING 10 min
▲ **CRITICAL** From day 4 onward, a daily measurement of TER can be made using a custom-modified (see Equipment) epithelial tissue voltohmmeter fitted with chopstick electrodes, as described in this section.
28| Sterilize the electrodes in 70% (vol/vol) ethanol and rinse them in PBS.

29| Confirm that the cells are not contaminated. If the cells are showing no signs of contamination, insert the electrode over the gill cell epithelium of each insert, such that the shorter arm of the electrode is in the upper compartment and the longer is in the lower compartment (**Fig. 5a**), and measure TER.

30| Calculate the net TER by subtracting the average TER of the blank insert (no cells; Step 26A(i) for DSI and Step 26B(i) for DSII) from the experimental value. Obtain final resistance-area values (Ω cm^2) by multiplying the net TER by the effective growth area (0.9 cm^2 for 12-well inserts). During days 7–14, DSI and DSII inserts should show TER values of ~5,000–30,000 Ω cm^2 (**Fig. 5b** and **Supplementary Fig. 1a**). Once a TER value of 5,000 Ω cm^2 or above is obtained, if desired you can proceed to assaying freshwater, as described in the next section.
? TROUBLESHOOTING
■ **PAUSE POINT** Epithelia can be stored with medium A in both the apical and basolateral compartments for later use by maintaining them at 4 °C for up to 2 weeks[31].

Experimental assay ● TIMING 30 min
31| Remove the medium from the lower compartment, followed by the upper compartment.

32| To wash and remove traces of FBS, apply 800 µl of PBS in the upper compartment, and then apply 1,000 µl to the lower compartment.

33| Aspirate the lower compartment and wash a further two times before the final aspiration.

a

Voltohmmeter

b
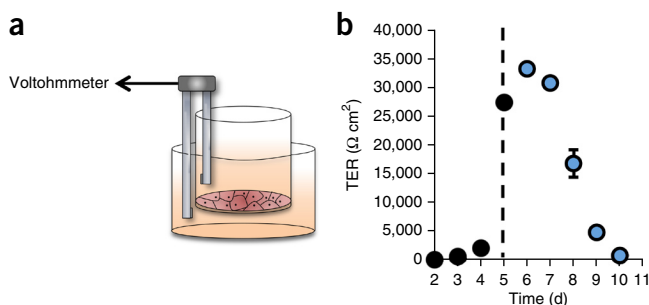
Figure 5 | Membrane development can be monitored by daily TER measurements. (**a**) A custom-modified epithelial tissue voltohmmeter is fitted with chopstick electrodes. The electrode arms are inserted above and below the gill cell epithelium of each insert, such that one arm of the electrode is in the upper compartment and the other arm is in the lower (bottom) compartment. (**b**) Measurements of TER in developing DSI. Freshwater (blue points) was added (after the dotted line) to the companion well compartment (the apical cell surface, while the insert contained L-15 medium) on day 4, resulting in an increase in TER still evident 24 h later on day 5 ($n = 6$). Values are means ± s.e.m.

34| Apply the solution of interest, e.g., freshwater, to the test compartment. For DSI, apply 1.5 ml of freshwater into the upper compartment, while leaving the lower compartment in 2.0 ml of L-15 medium. Depending on the experimental design, FBS can be removed from the medium. For DSII, apply 1.5 ml of L-15 medium without FBS into the upper compartment; 2.0 ml of freshwater can now be applied to the lower compartment. The volume in the upper compartment can be reduced if required. Application of freshwater should cause a rise in TER (**Supplementary Fig. 1a**). After freshwater application, inserts around 5,000 Ω cm^2 may rise to 30,000 Ω cm^2, whereas those already around 25,000–30,000 Ω cm^2 may not rise by as much. After freshwater application, TER values should remain above 5,000 Ω cm^2 for up to 48 h.

? TROUBLESHOOTING
Troubleshooting advice can be found in **Table 1**.

TABLE 1 | Troubleshooting table.

Step	Problem	Possible reason	Solution
20	Pellet is not red	Excessive trypsinization	Check the trypsin concentration and batch, and reduce the trypsinization time
		Trypsin digestion has not stopped	Check the FBS, and if it is out of date, remake the stop solution
25	Low cell viability	Excessive trypsinization	Decrease the trypsinization time
		Low donor quality	Check the health of stock fish
	Low cell number	Slow work pace	Perform the procedure faster
		Low EDTA concentrations in trypsin solution (Reagent Setup)	Increase EDTA concentration to 5 mM in the trypsin solution (Reagent Setup)
26A(v), 26B(v)	Extra mucus on cells	Fish health–related problem	Perform an additional PBS wash
30	Low TER	Contamination	Discard the cells
		Seeding density	Perform a seeding-density assay
		Fish health–related problem	Check the health of stock fish and water quality of the fish tank
		Slow development	Keep monitoring, and discard it if TER is <5,000 Ω cm^2 by day 14

● **TIMING**
Steps 1–4, preparation of solutions and cell culture inserts: 1 h; inserts also need to be left to condition for at least 1.5 h
Steps 5–25, rainbow trout dissection and gill cell isolation: 3 h
Step 26, DSI/DSII cell seeding: 30 min
Steps 27–30, maintenance and monitoring: this will depend on the number of inserts, and it can take between 30 min and 2 h on the day of medium changes; cell preparation reaches maturity over 5–12 d
Steps 31–34, experimental assay: 30 min

ANTICIPATED RESULTS
The epithelia should have distinct apical and basolateral surface consisting of irregularly shaped epithelial (pavement) cells with microridges and plasma membranes (**Fig. 4b** and **Supplementary Fig. 1c,d**) interspersed with MRCs (**Supplementary Fig. 1e**) typically from day 5 onward while growing in both the DSI and DSII configurations. Both preparations should develop an electrically tight epithelium showing the presence of the TJ proteins, such as zonula occludens (**Fig. 4c,d** and **Supplementary Fig. 1f,g**), typically from day 5 onward. The DSI can withstand water applied to the apical surface, but it does not tolerate water when exposed via the basolateral compartment[31], and these traits are also evident in the DSII preparations (**Supplementary Fig. 1b**). On the basis of rhodamine 123 staining[6], the epithelium should consist of between 10 and 15% MRCs, which is consistent with observations of the intact fish gill epithelium; however, PVCs make up the bulk of the epithelium, as is also seen *in vivo*[1].

Note: Any Supplementary Information and Source Data files are available in the online version of the paper.

1. Evans, D.H., Piermarini, P.M. & Choe, K.P The multifunctional fish gill: dominant site of gas exchange, osmoregulation, acid-base regulation, and excretion of nitrogenous waste. *Physiol. Rev.* **85**, 97–177 (2005).
2. Wood, C.M. Toxic responses of the gill. in: *Target Organ Toxicity in Marine and Freshwater Teleosts*, Vol. 1 (eds. Schlenk, D.W. & Benson, W.H.) 1–89 (Taylor & Francis, 2001).
3. Mckim, J.M. & Erickson, R.J. Environmental impacts on the physiological mechanisms controlling xenobiotic transfer across fish gills. *Physiol. Zool.* **64**, 39–67 (1991).
4. Bury, N.R., Walker, P.A & Glover, C.N. Nutritive metal uptake in teleost fish. *J. Exp. Biol.* **206**, 11–23 (2002).
5. Scholz, S. *et al.* A European perspective on alternatives to animal testing for environmental hazard identification and risk assessment. *Regul. Toxicol. Pharmacol.* **67**, 506–530 (2013).
6. Fletcher, M., Kelly, S.P., Pärt, P., O'Donnell, M.J. & Wood, C.M Transport properties of cultured branchial epithelia from freshwater rainbow trout: a novel preparation with mitochondria-rich cells. *J. Exp. Biol.* **203**, 1523–1537 (2000).
7. Kolosov, D., Chasiotis, H. & Kelly, S.P. Tight junction protein gene expression patterns and changes in transcript abundance during development of model fish gill epithelia. *J. Exp. Biol.* **217**, 1667–1681 (2014).
8. Chasiotis, H., Wood, C.M. & Kelly, S.P. Cortisol reduces paracellular permeability and increases occludin abundance in cultured trout gill epithelia. *Mol. Cell. Endocrinol.* **323**, 232–238 (2010).
9. Kolosov, D. & Kelly, S.P. A role for tricellulin in the regulation of gill epithelium permeability. *Am. J. Physiol.* **304**, R1139–R1148 (2013).
10. Walker, P.A., Bury, N.R. & Hogstrand, C. Influence of culture conditions on metal-induced responses in a cultured rainbow trout gill epithelium. *Environ. Sci. Technol.* **41**, 6505–6513 (2007).
11. Zhou, B., Kelly, S.P., Ianowski, J.P. & Wood, C.M. Effects of cortisol and prolactin on Na+ and Cl− transport in cultured branchial epithelia from FW rainbow trout. *Am. J. Physiol.* **285**, R1305–R1316 (2003).
12. Kelly, S.P. & Wood, C.M. Cortisol stimulates calcium transport across cultured gill epithelia from freshwater rainbow trout. *In Vitro Cell. Dev. Biol. Anim.* **44**, 96–104 (2008).
13. Schnell, S. *et al.* Environmental monitoring of urban streams using a primary fish gill cell culture system (FIGCS). *Ecotoxicol. Environ. Saf.* **120**, 279–285 (2015).
14. Carlsson, C. & Pärt, P. 7-Ethoxyresorufin *O*-deethylase induction in rainbow trout gill epithelium cultured on permeable supports: asymmetrical distribution of substrate metabolites. *Aquat. Toxicol.* **54**, 29–38 (2001).
15. Hansen, H.J.M., Kelly, S.P., Grosell, M. & Wood, C.M. Studies on lipid metabolism in trout (*Oncorhynchus mykiss*) branchial cultures. *J. Exp. Zool.* **293**, 683–692 (2002).
16. Kelly, S.P. & Wood, C.M. The cultured branchial epithelium of the rainbow trout as a model for diffusive fluxes of ammonia across the fish gill. *J. Exp. Biol.* **204**, 4115–4124 (2001).
17. Zhou, B., Nichols, J., Playle, R.C. & Wood, C.M. An *in vitro* biotic ligand model (BLM) for silver binding to cultured gill epithelia of freshwater rainbow trout (*Oncorhynchus mykiss*). *Toxicol. Appl. Pharmacol.* **202**, 25–37 (2005).
18. Stott, L.C., Schnell, S., Hogstrand, C., Owen, S.F. & Bury, N.R. A primary fish cell culture model to assess pharmaceutical uptake and efflux: evidence for passive and facilitated transport. *Aquat. Toxicol.* **159**, 127–137 (2015).
19. Minghetti, M., Schnell, S., Chadwick, M.A., Hogstrand, C. & Bury, N.R. A primary Fish Gill Cell System (FIGCS) for environmental monitoring of river waters. *Aquat. Toxicol.* **154**, 184–192 (2014).
20. Walker, P.A., Kille, P., Scott, A., Bury, N.R. & Hogstrand, C. An *in vitro* method to assess toxicity of waterborne metals to fish Toxicol. **30**, 67–77 (2008).
21. Pärt, P., Norrgren, L., Bergström, B. & Sjöberg, P. Primary culture of epithelial cells from rainbow trout gills. *J. Exp. Biol.* **175**, 219–232 (1993).
22. Wood, C.M. & Pärt, P. Cultured branchial epithelia from freshwater fish gills. *J. Exp. Biol.* **200**, 1047–1059 (1997).
23. Kelly, S.P., Fletcher, M., Pärt, P. & Wood, C.M. Procedures for the preparation and culture of 'reconstructed' rainbow trout branchial epithelia. *Methods Cell Sci.* **22**, 153–163 (2000).
24. Sandbichler, A.M., Egg, M., Schwerte, T. & Pelster, B. Claudin 28b and F-actin are involved in rainbow trout gill pavement cell tight junction remodelling under osmotic stress. *J. Exp. Biol.* **214**, 1473–1487 (2011).
25. Sandbacka, M., Pärt, P. & Isomaa, B. Gill epithelial cells as tools for toxicity screening—comparison between primary cultures, cells in suspension and epithelia on filters. *Aquat. Toxicol.* **46**, 23–32 (1999).
26. Kramer, N.I. *et al.* Development of a partition-controlled dosing system for cell assays. *Chem. Res. Toxicol.* **23**, 1806–1814 (2010).
27. Bols, N.C. *et al.* Development of a cell-line from primary cultures of rainbow trout, *Oncorhynchus mykiss* (Walbaum), gill. *J. Fish Dis.* **6**, 601–611 (1994).
28. Tanneberger, K. *et al.* Predicting fish acute toxicity using a fish gill cell line-based toxicity assay. *Environ. Sci. Technol.* **47**, 1110–1119 (2013).
29. Stadnicka-Michalak, J., Schirmer, K. & Ashauer, R. Toxicology across scales: cell population growth *in vitro* predicts reduced fish growth. *Sci. Adv.* **1**, e1500302 (2015).
30. Berthios, Y., Katzenellenbogen, J.A. & Katzenellenbogen, B.S. Phenol red in tissue culture media is a weak estrogen: implications concerning the study of estrogen-responsive cells in culture. *Proc. Natl. Acad. Sci. USA* **86**, 2496–2500 (1986).
31. Wood, C.M., Eletti, B. & Pärt, P. New methods for the primary culture of gill epithelia from freshwater rainbow trout. *Fish Physiol. Biochem.* **26**, 329–344 (2002).